

Magnetohydrodynamic/steam system dynamic modeling and control
by John Donald Aspnes

A thesis submitted in partial fulfillment of the requirements for the degree of DOCTOR OF PHILOSOPHY in Electrical Engineering
Montana State University
© Copyright by John Donald Aspnes (1976)

Abstract:
Three dynamic computer models of an overall magnetohydro-dynamic/steam electrical power generating plant are developed. Time domain solutions to the three sets of system equations are given.

The three models are generated in an increasing order of complexity. Several control configurations are applied to the systems and their effects on system dynamic response are presented. The most detailed model, system model III, utilizes an input-output characterization of the Combustor/Nozzle/Channel/Diffuser developed from polynomial approximations of data resulting from the solution of energy balance, state, and continuity equations for the combustor, and the quasi one-dimensional MHD equations for the channel and diffuser. The. boiler and turbine valve model has turbine valve area and power available to generate steam as inputs, and throttle pressure, power to the turbine, and boiler and stack losses as outputs. The effect of regenerative air preheater cycling is modeled, and the effect of an air preheat temperature controller is given.

# MAGNETOHYDRODYNAMIC/STEAM SYSTEM DYNAMIC MODELING AND CONTROL

by

JOHN DONALD ASPNES

A thesis submitted in partial fulfillment
of the requirements for the degree

of

DOCTOR OF PHILOSOPHY

in

Electrical Engineering

Approved:

Donald A. Pierre
Chairperson, Graduate Committee

Paul B. Schluch
Head, Major Department

Henry L. Parsons
Graduate Dean

MONTANA STATE UNIVERSITY
Bozeman, Montana

August, 1976

# ACKNOWLEDGMENTS

I wish to thank Professor Donald A. Pierre, who, as Chairman of my graduate committee and Principal Investigator of the MHD Cycle Analysis and Control project, continues to be an invaluable source of inspiration and guidance. Credit is due Professor Donald A. Rudberg for many fruitful discussions on several aspects of system modeling. Professor Roy M. Johnson and Dr. Teodoro C. Robles were sources of information on overall system properties.

Financial support essential to the completion of this work was obtained from a National Science Foundation Science Faculty Fellowship and the Montana Energy and MHD Research and Development Institute under Task H III, Cycle Analysis and Control, of contract No. E(49-18) - 1811 with the Energy Research and Development Administration.

I would also like to acknowledge the contributions of Mr. William Crane, who adapted computer programs to solve the system equations of Models I and II, and wrote the plotting routines used to produce the graphs of Chapters III, IV, and V, and Mr. Robert Uhlrich, who revised the computer routines for solving the system equations of Model III. Mr. Chad A. Groth did an excellent job on the final art work of all the block diagrams. The typing was expertly and efficiently done by Mrs. Jean Julian. Mr. Ray Babcock provided high-quality listings of computer programs.

TABLE OF CONTENTS


| | Page |
|---|---|
| VITA | ii |
| ACKNOWLEDGMENTS | iii |
| TABLE OF CONTENTS | iv |
| LIST OF TABLES | viii |
| LIST OF FIGURES | ix |
| ABSTRACT | xv |
| CHAPTER | |
| I. INTRODUCTION | 1 |
| 1.1 Problem Background | 1 |
| 1.2 Research Objectives | 9 |
| 1.3 Scope of This Work | 11 |
| II. LITERATURE REVIEW | 13 |
| 2.1 Introduction | 13 |
| 2.2 Overall MHD/Steam System Description; Systems Analysis | 13 |
| 2.3 MHD Generators and Combustor/Nozzle/Channel/ Diffuser Modeling | 16 |
| 2.4 Steam Plant Modeling | 19 |
| 2.5 Heat Exchangers | 27 |
| 2.6 Power Plant Control | 28 |
| 2.7 General Control References | 36 |
| 2.8 Numerical Methods/Mathematical Methods | 39 |

| | | Page |
|---|---|---|
| III. | SYSTEM MODEL I | 41 |
| | 3.1 Basis for Model I | 41 |
| | 3.2 Combustion Calculations | 43 |
| | 3.3 Model I Block Diagram | 45 |
| | 3.4 Description of System Variables | 47 |
| | 3.5 Initial Conditions, Values of Constants, and System Equations | 48 |
| | 3.6 System Equation Solutions | 49 |
| | 3.6.1 MHD generator efficiency $\eta_1$ variations | 50 |
| | 3.6.2 Valve control signal $X_4$ | 50 |
| | 3.6.3 Fuel thermal input power $X_6$ | 51 |
| | 3.6.4 Combustor output power $X_{10}$ | 53 |
| | 3.6.5 Steam plant output power $X_{15}$ | 54 |
| | 3.6.6 Inverter output power $X_{17}$ | 55 |
| | 3.6.7 Net plant output power $X_{19}$ | 55 |
| | 3.7 Classical Stability Analysis | 79 |
| IV. | SYSTEM MODEL II | 85 |
| | 4.1 Basis for Model II | 85 |
| | 4.2 Combustion Calculations | 87 |
| | 4.3 Heat Exchanger Cycle Model | 92 |
| | 4.4 Description of System Variables | 97 |
| | 4.5 Initial Conditions, Values of Constants, and System Equations | 99 |
| | 4.6 System Equation Solutions | 103 |

Page

4.6.1 Fuel thermal input power $X_7$ . . . . . 107
4.6.2 Preheated air temperature (subtracting ambient) $X_{12}$ . . . . . 108
4.6.3 Inverter output power $X_{16}$ . . . . . 110
4.6.4 Net steam plant output power $X_{28}$ . . . . . 110
4.6.5 Net plant output power $X_{30}$ . . . . . 111

V. SYSTEM MODEL III . . . . . 133

5.1 Model III Features . . . . . 133

5.2 Model III Block Diagram . . . . . 135

5.3 Detailed Block Diagrams . . . . . 141

5.3.1. Generation controller . . . . . 141
5.3.2 Governor dynamics . . . . . 145
5.3.3 Boiler and turbine valve dynamics . . . . . 145
5.3.4 Turbine dynamics . . . . . 149
5.3.5 Firing rate controller . . . . . 151
5.3.6 Firing system . . . . . 154
5.3.7 Combustor/Nozzle/Channel/Diffuser model . . . 155
5.3.8 Air preheaters . . . . . 160
5.3.9 Thermal lag . . . . . 160

5.4 Description of System Variables . . . . . 160

5.5 Initial Conditions, Values of Constants, and System Equations . . . . . 166

5.6 System Equation Solutions . . . . . 179

5.6.1 Net plant output power $X_2$ . . . . . 186
5.6.2 Net steam turbine output power $X_{41}$ . . . . . 187
5.6.3 Net MHD electrical output power $X_{42}$ . . . . . 188
5.6.4 Thermal power of fuel in combustor $X_{55}$ . . . . 190
5.6.5 Preheated air temperature $X_{73}$ . . . . . 191

| | Page |
|---|---|
| VI. SUMMARY OF RESULTS | 222 |
| 6.1 Introduction | 222 |
| 6.2 System Model I | 222 |
| 6.3 System Model II | 223 |
| 6.4 System Model III | 226 |
| 6.5 Comparisons Between Model Simulations | 229 |
| 6.6 Conclusions | 232 |
| 6.7 Recommendations for Future Research | 235 |
| APPENDICES | 238 |
| A. Digital Computer Simulation Program for System Model I | 239 |
| B. Digital Computer Simulation Program for System Model II | 251 |
| C. Digital Computer Simulation Program for System Model III | 258 |
| REFERENCES | 265 |

LIST OF TABLES


| Table | | Page |
|---|---|---|
| 3.1 | Description of model I system variables | 47 |
| 3.2 | Model I initial conditions | 48 |
| 3.3 | Model I multipliers and time constants | 49 |
| 4.1 | Compressor parameters I | 91 |
| 4.2 | Compressor parameters II | 91 |
| 4.3 | Description of model II system variables | 97 |
| 4.4 | Model II initial conditions | 104 |
| 4.5 | Model II multiplier and time constants | 105 |
| 4.6 | Conditions for model II equation solutions | 106 |
| 5.1 | Description of model III system variables | 162 |
| 5.2 | Equation 5.21 results compared with design-center calculations | 171 |
| 5.3 | Model III initial conditions | 176 |
| 5.4 | Model III multipliers and time constants | 178 |
| 5.5 | System model III simulation cases | 181 |
| 6.1 | Simulation cases for turbine-following control | 230 |

LIST OF FIGURES


| Figure | | Page |
|---|---|---|
| 1.1 | Coal-fired, direct open-cycle MHD/steam combined cycle | 2 |
| 1.2 | MHD duct schematic | 3 |
| 1.3 | MHD duct coordinate system | 4 |
| 1.4 | Results of several studies on combined-cycle thermal efficiency as a function of air preheat temperature | 8 |
| 3.1 | Idealized heat balance for fossil-fueled open cycle | 41 |
| 3.2 | Variation of MHD/steam combined efficiency with MHD generator efficiency | 43 |
| 3.3 | Block diagram for model I | 46 |
| 3.4(a) | Variations in $X_6$ and $X_{10}$ for $\eta_1$ change from 0.3 to 0.2 | 57 |
| 3.4(b) | Variations in $X_{15}$, $X_{17}$, and $X_{19}$ for $\eta_1$ change from 0.3 to 0.2 | 58 |
| 3.5(a) | Variations in $X_6$ and $X_{10}$ for $\eta_1$ change from 0.3 to 0.4 | 59 |
| 3.5(b) | Variations in $X_{15}$, $X_{17}$, and $X_{19}$ for $\eta_1$ change from 0.3 to 0.4 | 60 |
| 3.6 | Time variations in $X_4$; $K_1 = 0.001$ | 61 |
| 3.7 | Time variations in $X_4$; $K_1 = 0.01$ | 62 |
| 3.8 | Time variations in $X_4$; $K_1 = 0.1$ | 63 |
| 3.9 | Time variations in $X_6$; $K_1 = 0.001$ | 64 |
| 3.10 | Time variations in $X_6$; $K_1 = 0.01$ | 65 |
| 3.11 | Time variations in $X_6$; $K_1 = 0.1$ | 66 |

| Figure | | Page |
|---|---|---|
| 3.12 | Time variations in $X_{10}$; $K_1 = 0.001$ . . . . . | 67 |
| 3.13 | Time variations in $X_{10}$; $K_1 = 0.01$ . . . . . | 68 |
| 3.14 | Time variations in $X_{10}$; $K_1 = 0.1$ . . . . . | 69 |
| 3.15 | Time variations in $X_{15}$; $K_1 = 0.001$ . . . . . | 70 |
| 3.16 | Time variations in $X_{15}$; $K_1 = 0.01$ . . . . . | 71 |
| 3.17 | Time variations in $X_{15}$; $K_1 = 0.1$ . . . . . | 72 |
| 3.18 | Time variations in $X_{17}$; $K_1 = 0.001$ . . . . . | 73 |
| 3.19 | Time variations in $X_{17}$; $K_1 = 0.01$ . . . . . | 74 |
| 3.20 | Time variations in $X_{17}$; $K_1 = 0.1$ . . . . . | 75 |
| 3.21 | Time variations in $X_{19}$; $K_1 = 0.001$ . . . . . | 76 |
| 3.22 | Time variations in $X_{19}$; $K_1 = 0.01$ . . . . . | 77 |
| 3.23 | Time variations in $X_{19}$; $K_1 = 0.1$ . . . . . | 78 |
| 4.1 | Block diagram for model II . . . . . | 86 |
| 4.2 | Regenerative heat exchanger schedule . . . . . | 93 |
| 4.3 | Variations in preheated air temperature and power to steam plant . . . . . | 96 |
| 4.4 | Time variations in $X_7$; $K_1 = 0.001$, $E_1(t) = T_1(t) = Z = 0$ . . . . . | 112 |
| 4.5 | Time variations in $X_7$; $K_1 = 0.001$, $E_1(t)$, $T_1(t)$, Z all functioning . . . . . | 113 |
| 4.6 | Time variations in $X_7$; $K_1 = 0.01$, $E_1(t) = T_1(t) = 0$, Z functioning . . . . . | 114 |

| Figure | | Page |
|---|---|---|
| 4.7 | Time variations in $X_7$; $K_1 = 0.01$, $E_1(t)$, $T_1(t)$, Z all functioning . . . . . | 115 |
| 4.8 | Time variations in $X_{12}$; $K_1 = 0.001$, $E_1(t) = T_1(t) = Z = 0$ . . . . . | 116 |
| 4.9 | Time variations in $X_{12}$; $K_1 = 0.001$, $E_1(t) = T_1(t) = 0$, Z functioning . . . . . | 117 |
| 4.10 | Time variations in $X_{12}$; $K_1 = 0.001$, $E_1(t)$, $T_1(t)$, Z all functioning . . . . . | 118 |
| 4.11 | Time variations in $X_{12}$; $K_1 = 0.01$, $E_1(t) = T_1(t) = Z = 0$ . . . . . | 119 |
| 4.12 | Time variations in $X_{12}$; $K_1 = 0.01$, $E_1(t) = T_1(t) = 0$, Z functioning . . . . . | 120 |
| 4.13 | Time variations in $X_{16}$; $K_1 = 0.001$, $E_1(t) = T_1(t) = Z = 0$ . . . . . | 121 |
| 4.14 | Time variations in $X_{16}$; $K_1 = 0.001$, $E_1(t)$, $T_1(t)$ functioning, $Z = 0$ . . . . . | 122 |
| 4.15 | Time variations in $X_{16}$; $K_1 = 0.01$, $E_1(t) = T_1(t) = 0$, Z functioning . . . . . | 123 |
| 4.16 | Time variations in $X_{16}$; $K_1 = 0.01$, $E_1(t)$, $T_1(t)$, Z all functioning . . . . . | 124 |
| 4.17 | Time variations in $X_{28}$; $K_1 = 0.001$, $E_1(t) = T_1(t) = Z = 0$ . . . . . | 125 |
| 4.18 | Time variations in $X_{28}$; $K_1 = 0.001$, $E_1(t)$, $T_1(t)$, Z all functioning . . . . . | 126 |

| Figure | | Page |
|---|---|---|
| 4.19 | Time variations in $X_{28}$; $K_1 = 0.01$, $E_1(t) = T_1(t) = 0$, Z functioning | 127 |
| 4.20 | Time variations in $X_{28}$; $K_1 = 0.01$, $E_1(t)$, $T_1(t)$, Z all functioning | 128 |
| 4.21 | Time variations in $X_{30}$; $K_1 = 0.001$, $E_1(t) = T_1(t) = Z = 0$ | 129 |
| 4.22 | Time variations in $X_{31}$; $K_1 = 0.001$, $E_1(t)$, $T_1(t)$, Z all functioning | 130 |
| 4.23 | Time variations in $X_{30}$; $K_1 = 0.01$, $E_1(t) = T_1(t) = 0$, Z functioning | 131 |
| 4.24 | Time variations in $X_{30}$; $K_1 = 0.01$, $E_1(t)$, $T_1(t)$, Z all functioning | 132 |
| 5.1 | Block diagram for model III | 134 |
| 5.2 | Boiler-following or conventional control mode | 137 |
| 5.3 | Turbine-following control mode | 138 |
| 5.4 | Integrated control | 139 |
| 5.5 | Transient response of three types of boiler control | 140 |
| 5.6 | Generation controller, valve feedforward, and grid lag | 142 |
| 5.7 | Generation controller | 144 |
| 5.8 | Governor dynamics | 146 |
| 5.9 | Boiler and turbine valve dynamics | 147 |
| 5.10 | Turbine valve and boiler storage effects | 150 |
| 5.11 | Turbine dynamics | 152 |

| Figure | | Page |
|---|---|---|
| 5.12 | Firing rate and fuel feedforward controllers . . . . . | 153 |
| 5.13 | Firing rate controller . . . . . | 154 |
| 5.14 | Firing system . . . . . | 156 |
| 5.15 | Air preheater . . . . . | 161 |
| 5.16 | Time variations in $X_2$; cases 4, 9, 14 . . . . . | 193 |
| 5.17 | Time variations in $X_2$; cases 4, 21 . . . . . | 194 |
| 5.18 | Time variations in $X_2$; cases 14, 26 . . . . . | 195 |
| 5.19 | Time variations in $X_2$; cases 21, 28 . . . . . | 196 |
| 5.20 | Time variations in $X_2$; case 4 (with $E_1(t)$, $T_1(t)$, Z all functioning) . . . . . | 197 |
| 5.21 | Time variations in $X_2$; case 14 (with $E_1(t)$, $T_1(t)$, Z all functioning) . . . . . | 198 |
| 5.22 | Time variations in $X_{41}$; cases 4, 9, 14 . . . . . | 199 |
| 5.23 | Time variations in $X_{41}$; cases 4, 21 . . . . . | 200 |
| 5.24 | Time variations in $X_{41}$; cases 14, 26 . . . . . | 201 |
| 5.25 | Time variations in $X_{41}$; cases 21, 28 . . . . . | 202 |
| 5.26 | Time variations in $X_{41}$; case 4 (with $E_1(t)$, $T_1(t)$, Z all functioning) . . . . . | 203 |
| 5.27 | Time variations in $X_{41}$; case 14 (with $E_1(t)$, $T_1(t)$, Z all functioning) . . . . . | 204 |
| 5.28 | Time variations in $X_{42}$; cases 4, 9, 14 . . . . . | 205 |
| 5.29 | Time variations in $X_{42}$; cases 4, 21 . . . . . | 206 |

| Figure | | Page |
|---|---|---|
| 5.30 | Time variations in $X_{42}$; cases 14, 26 . . . . . | 207 |
| 5.31 | Time variations in $X_{42}$; cases 21, 28 . . . . . | 208 |
| 5.32 | Time variations in $X_{42}$; case 4 (with $E_1(t)$, $T_1(t)$, Z all functioning) . . . . . | 209 |
| 5.33 | Time variations in $X_{42}$; case 14 (with $E_1(t)$, $T_1(t)$, Z all functioning) . . . . . | 210 |
| 5.34 | Time variations in $X_{55}$; cases 4, 9, 14 . . . . . | 211 |
| 5.35 | Time variations in $X_{55}$; cases 4, 21 . . . . . | 212 |
| 5.36 | Time variations in $X_{55}$; cases 14, 26 . . . . . | 213 |
| 5.37 | Time variations in $X_{55}$; cases 21, 28 . . . . . | 214 |
| 5.38 | Time variations in $X_{55}$; case 4 (with $E_1(t)$, $T_1(t)$, Z all functioning) . . . . . | 215 |
| 5.39 | Time variations in $X_{55}$; case 14 (with $E_1(t)$, $T_1(t)$, Z all functioning) . . . . . | 216 |
| 5.40 | Time variations in $X_{73}$; cases 4, 9, 14 . . . . . | 217 |
| 5.41 | Time variations in $X_{73}$; cases 4, 21 . . . . . | 218 |
| 5.42 | Time variations in $X_{73}$; cases 14, 26 . . . . . | 219 |
| 5.43 | Time variations in $X_{73}$; cases 21, 28 . . . . . | 220 |
| 5.44 | Time variations in $X_{73}$; case 14 (with $E_1(t)$, $T_1(t)$, Z all functioning) . . . . . | 221 |

ABSTRACT

Three dynamic computer models of an overall magnetohydrodynamic/steam electrical power generating plant are developed. Time domain solutions to the three sets of system equations are given. The three models are generated in an increasing order of complexity. Several control configurations are applied to the systems and their effects on system dynamic response are presented. The most detailed model, system model III, utilizes an input-output characterization of the Combustor/Nozzle/Channel/Diffuser developed from polynomial approximations of data resulting from the solution of energy balance, state, and continuity equations for the combustor, and the quasi one-dimensional MHD equations for the channel and diffuser. The boiler and turbine valve model has turbine valve area and power available to generate steam as inputs, and throttle pressure, power to the turbine, and boiler and stack losses as outputs. The effect of regenerative air preheater cycling is modeled, and the effect of an air preheat temperature controller is given.

# Chapter I

# INTRODUCTION

## 1.1 Problem Background

Magnetohydrodynamic (MHD) research and development is currently in progress on an international basis. The major objective of this work is to produce electric power reliably and economically. The MHD effort in the United States has the stated goal of a commercial demonstration power plant being operational by the late 1980's. Electric power companies have indicated that a realistic demonstration facility should have at least 500 megawatts (MW) of electrical output power.

A coal-fired, direct open-cycle MHD/steam combined cycle appears to be a likely plant configuration. The block diagram of such a plant is shown in Figure 1.1 [69]. The system of Figure 1.1 operates as follows: Coal is burned in a combustor in the presence of highly preheated air at approximately 7 atmospheres pressure. The combustion products are seeded with a relatively easily ionized material such as potassium. This substantially increases the conductivity of the combustion products. The output of the combustor, an ionized gas, is passed through an MHD generator at approximately the speed of sound. An elementary MHD generator is shown in Figure 1.2 [141]. A strong magnetic field ($\underline{B}$) is produced which is perpendicular to the velocity ($\underline{u}$) of the ionized gas. Two walls of the generator duct perpendicular to the magnetic field are non-conducting. The remaining

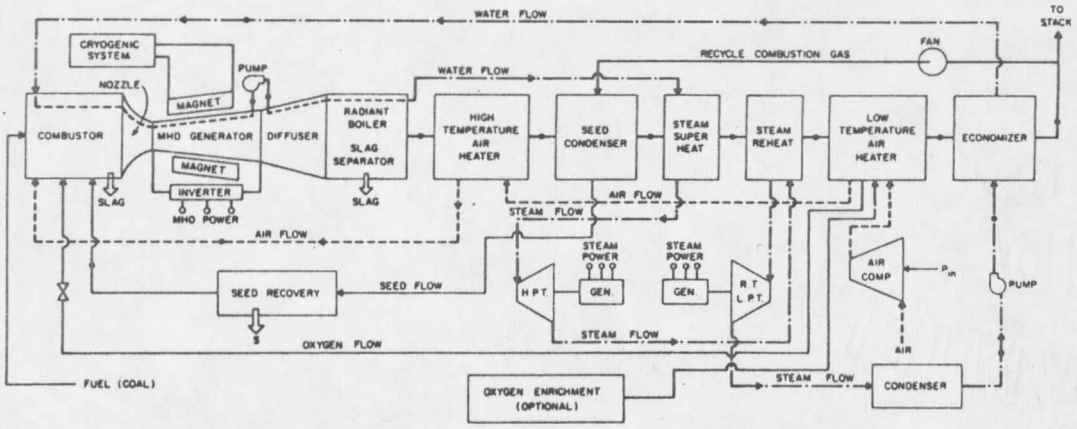



Figure 1.1. Coal-fired, direct open-cycle MHD/steam combined cycle

two walls have electrodes in them which collect the electric charges that are separated by the $q\underline{u} \times \underline{B}$ forces on the charged particles, where q is the charge of an electron. The separation of electric charge is represented by current density $\underline{J}$ (amperes/$m^2$). The resultant DC current is converted to AC by inverters to make it compatible with existing electrical power distribution systems.

The electrical power generated by the MHD duct represents enthalpy extracted from the ionized gas. Additional enthalpy is lost to the walls of the combustor, nozzle, channel, diffuser, and radiant boiler. A fraction of this is recovered in the cooling water which feeds the steam generating part of the cycle. The remaining enthalpy

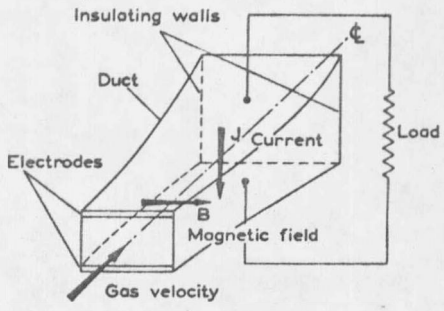



Figure 1.2. MHD duct schematic

in the combustion gas is used to preheat the combustion air and to generate steam. The enthalpy in the steam is converted to electrical power by conventional turbo-generator units. Approximately 50% of the total electrical output power of the combined cycle is supplied by the MHD generator and the remainder by the steam system. The combustion products are suitably cleaned, and the stack gas is exhausted to the atmosphere.

A closer look at the MHD generator is appropriate. Rosa [121] gives a simplified description of an ideal MHD generator that appears below.

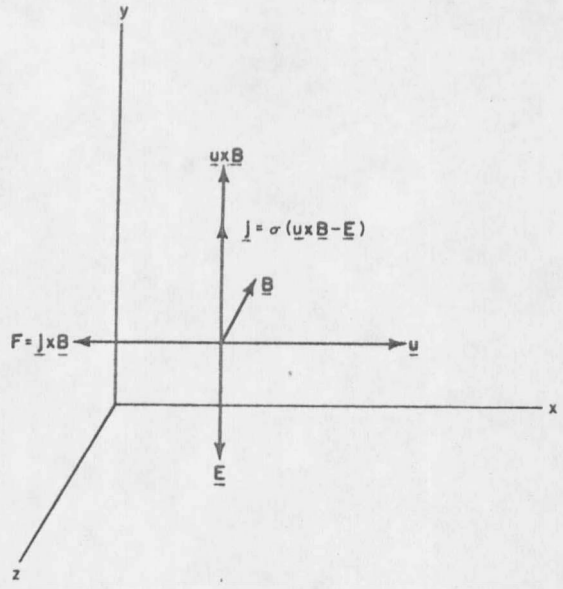



Figure 1.3. MHD duct coordinate system

$\underline{u}$ = gas velocity (meter/second)

$\sigma$ = scalar conductivity (mho/meter)

$\underline{E}$ = internal electric field due to external load (volt/meter)

$\underline{j}$ = current density (ampere/meter$^2$)

$\underline{B}$ = magnetic flux density (weber/meter$^2$)

Referring to Figure 1.3, the current per unit area induced by the motion of the gas through a magnetic field perpendicular to the motion is:

$$\underline{j} = \sigma \underline{u} \times \underline{B} - \sigma \underline{E} = \sigma(uB - E) \qquad (1.1)$$

$$K = \text{loading parameter} = E/uB \tag{1.2}$$

Therefore

$$j = (1-K)\,\sigma uB \tag{1.3}$$

The power $P_o$ delivered to an external load per unit volume of the generator is

$$P_o = jE = K(1 - K)\,\sigma u^2 B^2 \ (\text{watt/meter}^3) \tag{1.4}$$

Since $E = uB - j/\sigma$

$$P_o = juB - j^2\sigma \ (\text{watt/meter}^3) \tag{1.5}$$

The force F on a unit volume of gas that opposes the motion of the gas is given by

$$F = jB = (1 - K)\,\sigma uB^2 \ (\text{newton/meter}^3) \tag{1.6}$$

If the gas is to move through the generator against this force, a pressure difference must exist between the entrance and exit of the channel. This pressure difference is approximated by

$$\Delta p = FL = (1 - K)\,\sigma uB^2 L \tag{1.7}$$

where L = length of generator flow.

$P_p$ = rate that gas does work pushing itself through the magnetic field. It is given by

$$P_p = Fu = (1 - K)\,\sigma u^2 B^2 \ (\text{watt/meter}^3) \qquad (1.8)$$

Electrical efficiency is

$$\eta_e = \text{electrical efficiency} = P_o/P_p = K = E/uB \qquad (1.9)$$

It is evident from Equation 1.4 that gas conductivity, gas velocity, and magnetic flux density are important parameters concerning electrical generation and should be large to obtain a high power density in the MHD channel.

Current MHD power output capabilities are far below those required for commercial base load applications. The most powerful MHD generator in the world is still the Avco Corporation Mark V, built more than one decade ago. It produced 32 MW of electrical power for one minute. The Russian U-25 MHD facility has, as its best performances, a 20 MW output for 30 minutes, and a 2 MW output for 100 hours. Considering long-duration tests in the United States, the Avco Corporation Mark VI MHD generator recently completed a 100 hour unattended test run with 250 kilowatt (KW) electrical power output. Channel power density was 30 $MW/m^3$; a value greater than expected in a commercial scale plant.

Why is there interest in MHD energy conversion? A major reason is 45% to 60% thermal efficiency expected for an MHD/steam combined cycle, as seen in Figure 1.4 [69]. This compares very favorably with 40% maximum thermal efficiency for a conventional steam turbo-generator system and approximately 30% thermal efficiency for a nuclear/steam turbo-generator system. Another reason for the interest in MHD is that the combined cycle is expected to produce less wastes than conventional steam or nuclear/steam plants of comparable size. For example, cooling water requirements for an MHD/steam combined cycle are expected to be 40% of the requirements for a conventional steam cycle and 25% of the requirements for a nuclear/steam system. Removal of sulfur from the combustion products is expected to be far more efficient than existing techniques [21]. This is accomplished by formation of potassium sulfate by reaction of potassium seed with sulfur and oxygen. The potassium sulfate is then removed in a seed condenser.

Still another reason for interest in MHD is nitrogen fixation. At the high combustion temperatures required by MHD (2500°K to 2800°K), large amounts of nitrogen oxides, called $NO_x$ compounds, may be formed. These compounds are basic to nitrogen fertilizer production, and it has been speculated that MHD power plants might actually be fertilizer plants that produce electricity as a by-product. In the event that $NO_x$ fixation is not feasible, it is possible to achieve considerably lower $NO_x$ emissions with a two-stage MHD combustor than with

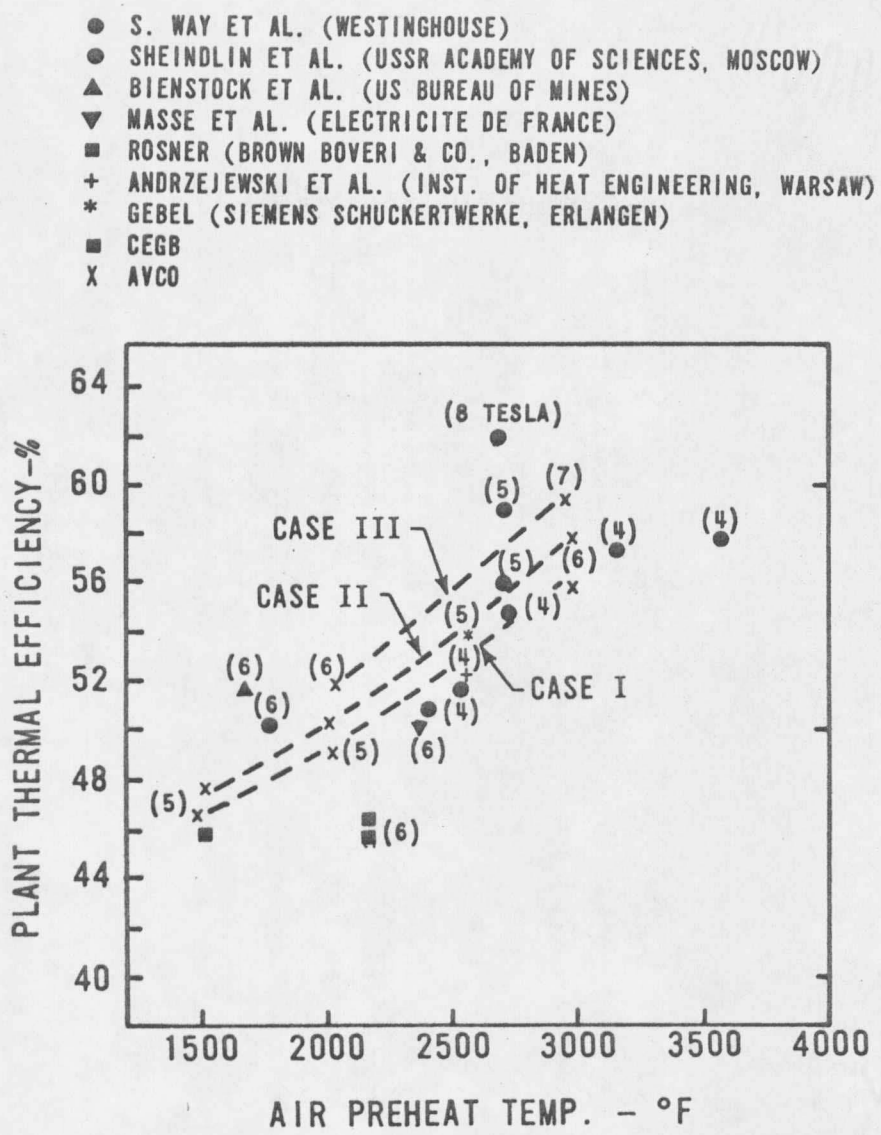



Figure 1.4. Results of several studies on combined cycle thermal efficiency as a function of air preheat temperature

conventional coal combustors. In fact, two-stage combustion has been shown to produce as little as 0.052 Kg per $10^9$ joules input or 17% of the EPA regulations on new coal-fired plants [21].

In order that a complex system such as an MHD/steam combined-cycle power plant can operate reliably and efficiently, it is essential that systems analysis be performed on the entire set of system components and that control system analysis be carried out concurrently. Systems analysis provides analytical models of the various system components which may, in turn, be used in formulating suitable control algorithms for the dynamic characteristics of the plant. Systems analysis is the most efficient means known to optimize plant design, identify technological problems, and predict system performance. Systems analysis also aids in giving direction for future technical development.

In view of the above, the research described in this report was supported by the National Science Foundation and by the Montana Energy and MHD Research and Development Institute under Task H III, Cycle Analysis and Control, of contract No. E(49-18) - 1811 with the Energy Research and Development Administration.

## 1.2 Research Objectives

The objectives of the research presented in this report are: (1) to develop dynamic computer models of a large-scale MHD/steam electrical power generating system; and (2) to utilize these models in control system development which will (a) assess the feedback

information needed to control a large combined-cycle facility in an acceptable manner, and (b) determine the type of control required [113].

To achieve the stated objectives, it was necessary to perform a digital computer simulation on a nominal 4000 MW (thermal) MHD/steam combined-cycle power plant. The simulation involved the interconnection of models of the individual system components to form a computer model of the entire plant. Many different control configurations were used, ranging from proportional-integral control of the firing system, utilizing power generation error as the input, to various combinations of proportional-integral-derivative and feedforward controllers. These controllers affect not only firing rate in the combustor, but generation rate as well, via the steam turbine valves. The effect of preheated air temperature control was also investigated.

The reason that a digital computer simulation was required in meeting the research objectives is that the alternative would have been to construct a demonstration power plant which was clearly impossible because of capital cost and time limitations. The research contract duration was 15 months, ending July 31, 1976, and money is only now becoming available for the construction of a 20 MW pilot plant in Butte, Montana. The construction and operation of a commercial scale MHD/steam combined-cycle power plant is not likely to occur until the late 1980's.

## 1.3 Scope of This Work

The scope of the work described in this paper consists of the development of three system models in Chapters III, IV, and V. Computer simulation results are presented for all three models. Many different controller parameter values are represented in the simulations.

The three system models are developed in an ever-increasing order of complexity. This is done so that the initial model may be relatively easily understood and serve as a comparison for the next model which contains more detail. Model I is evolved from an idealized heat balance including the effect of the MHD generator enthalpy extraction, regenerative air preheaters, air compressor, steam (bottoming) plant, and stack and auxiliary losses. Proportional-integral control is used. Model II retains many of the model I features and includes a more detailed air preheater model. The system response to effects of air preheater cycling is of major interest. An air preheat temperature control loop is added. Model III, described in Chapter V, has much more detailed characterization of the steam plant (including the turbines), the Combustor/Nozzle/Channel/Diffuser, and the controls than do previous models.

As mentioned in Section 1.1, modeling and simulation of systems is tremendously useful in optimizing complex plant design,

determining regions of acceptable dynamic behavior, developing appropriate controls, and identifying and predicting technological problems.

Important results to be obtained are: (1) dynamic computer models of the overall MHD/steam system; (2) computer simulations which solve the system equations to give the time domain response of system variables; and (3) an evaluation of types of control required.

# Chapter II

# LITERATURE REVIEW

## 2.1 Introduction

This chapter describes literature pertaining to MHD/steam combined-cycle systems analysis and control. The literature description is subdivided into the following 7 categories.

1. Overall MHD/steam system description and systems analysis
2. MHD generators and Combustor/Nozzle/Channel/Diffuser modeling
3. Steam plant modeling
4. Heat exchangers
5. Power plant control
6. General control references
7. Numerical methods/mathematical methods

References are presented in chronological order within each section. Additional references on MHD are to be found in a recent comprehensive bibliography [147] published by the U.S. Energy Research and Development Administration.

## 2.2 Overall MHD/Steam System Description and Systems Analysis

Several studies have been conducted on systems analysis of MHD/steam combined-cycle power plants. These studies are generally concerned with optimization of parameters such as plant thermal

efficiency and investigate the effect of variation of parameters on plant cost. Steady-state results are used, with no work reported on transient behavior of a complete system. Control simulation studies of MHD/steam combined-cycle systems are not, to the author's knowledge, available in the literature.

Tsu, Young, and Way [137] performed optimization studies of a complete MHD/steam system in 1966. The goal was to determine a design for the most efficient plant and one for the least cost. Time variations were not considered.

Rosa [121] gives a review of fundamental principles and engineering considerations of MHD energy conversion system components. Several applications for MHD energy conversion are suggested including commercial power generation and aerospace use.

Womack and Heywood [141] describe, in general terms, an MHD duct. In addition, schematics for direct and separately fired open cycles, a closed cycle, and a liquid metal cycle are given. An idealized heat balance diagram for a fossil-fired open cycle is developed, and an equation for combined plant efficiency as a function of MHD enthalpy extraction efficiency is obtained from the diagram.

Harrowell, Heywood, and Womack [58] evolve parameter values, and reasons for their selection, for optimum MHD/steam combined cycles. The study is done for a 2000 MW (thermal) plant for both directly and separately fired open cycles. The effect of variations in

low-grade heat absorption is studied. No time variations are considered.

Hals and Jackson [57] give the results of studies on how preheat air temperature and magnetic field strength affect MHD/steam combined-cycle efficiency. Hall parameter, Hall field, and steam plant heat absorption considerations are discussed. $NO_x$ and sulfur removal is briefly considered.

Oliver and Byer [105] give physical and economic models of an open-cycle, coal-fired, MHD/steam combined cycle. Components considered are the combustor, MHD generator, heat exchangers (air preheater), seed recovery and gas cleaning systems, steam generating plant, and auxiliaries. Time variations are not considered. Physical, chemical, and economic equations used in describing system components are given. A brief discussion of computer implementation of the model is included.

Bienstock, et al. [21] consider the air-pollution aspects of MHD combustor-generators. Sulfur and $NO_x$ emissions are shown to be substantially lower with MHD than with conventional systems. Potassium seed is instrumental in sulfur removal, and two-stage combustion reduces $NO_x$ output to as low as 0.052 Kg per $10^9$ joules input.

Bergman, et al. [18] present cycle analyses and cost estimates for two 300 MW (thermal), coal-fired, open-cycle MHD/steam pilot plant design configurations. Separately fired and directly fired air

preheaters are considered. Because the separately fired system requires clean fuel (low sulfur residual oil), it is considered to be the least favorable alternative, given the availability of oil in the United States.

Jackson, et al. [69] review previous open-cycle MHD/steam system analyses. A base reference design for a 2000 MW (thermal) plant is developed with parametric variations. An overall development program leading toward commercial MHD power generation is given.

Robles [120] develops a quasi one-dimensional MHD generator model, and dynamic models of a DC/AC inverter, steam plant, and air heaters. Open-loop responses of the models are presented.

Pierre and Rudberg in [113] delineate objectives of the Montana State University MHD system cycle analysis and control effort. A description of an input-output model of the Combustor/Nozzle/Channel/Diffuser part of the system is included, as is a preliminary overall system block design.

## 2.3 MHD Generators and Combustor/Nozzle/Channel/Diffuser Modeling

The three-dimensional MHD duct or generator is a very complex device to describe. A standard simplification is to use one-dimensional fluid flow equations in the direction of gas flow through the channel. The combustor, nozzle, and diffuser all affect generator

performance and must be considered if accurate modeling is to be achieved.

Sutton and Sherman [130] describe fundamentals of charged particle motion, behavior of plasmas, magnetohydrodynamic flows, and MHD applications.

Hughes and Young [64] include work on incompressible viscous magnetohydrodynamic flow. A Thevenin equivalent circuit for an MHD channel is derived assuming one-dimensional steady, viscous laminar flow. Approximations of fluid equations applicable to MHD are suggested.

Carter and Heywood [26] develop an optimization theory that predicts variations of thermodynamic properties (pressure, temperature, enthalpy), duct shape and electrical loading along an MHD generator for minimum duct length, surface area, or volume. One-dimensional fluid flow equations are used.

Baylis, et al. [15] give a very detailed exposition of MHD duct physics. Physical principles are explained with one-dimensional flow equations. Equations for gas enthalpy are given. Performance of an MHD generator is predicted with the aid of a compressor power equation.

El'kin and Yantovskii [45] find volt-ampere characteristics of an MHD generator with fixed electric field direction and single load.

Three regions of operation are considered; 1) shock-free flow, 2) shock in the channel, and 3) shock in the nozzle.

Kazachkov and Shipulin [71] investigate regulation of inverters on a segmented electrode Faraday MHD generator. Constant current, constant voltage, and constant load coefficients are considered.

Gigauri [53] determines external characteristics of a single-load, cross-connected, segmented MHD generator for subsonic flow. These characteristics are found to be nonlinear.

Oliver [106] presents a theory of time-dependent MHD channel flows. A computational approach is developed and illustrated by several generator response curves.

Takano, Homma, and Mori [132] discuss design conditions for MHD generator ducts applied to pilot plants of approximately 20 MW (electrical) output.

Pierre, et al. [114] develop an input-output model of a Combustor/Nozzle/Channel/Diffuser. Input variables are fuel thermal input power and preheated air temperature. Outputs are enthalpy extraction, thermal power in water heating, and thermal power in combustion gas leaving the diffuser. Polynomial approximations are generated for the input-output data.

## 2.4 Steam Plant Modeling

Steam plant, or boiler-turbine modeling has been approached in two distinct ways by workers in this area. One method of analysis is large-scale modeling in which the models are very detailed, often nonlinear, and are developed from physical properties such as conservation of mass, energy, and momentum, inertia effects, and heat transfer. The resulting models are high order. A second method of analysis is the black-box approach. In this case the boiler is modeled as an input-output device with first-order lags usually describing the dynamic response. Some black-box models are nonlinear. Inputs are generally turbine valve area and steam generation. Outputs are throttle pressure and steam flow to the turbines.

Profos [116] developed, in an early paper (1955), mathematical descriptions of firing systems and once-through steam generators. Experimental results were presented.

Chien, et al. [30] perform a dynamic analysis of a drum-type marine boiler. Approximations reduce nonlinear, partial differential equations to linear, ordinary time differential forms. The system of equations for the boiler is 17th order. Analog computer solutions of the system equations are generated.

Profos [117] gives transfer characteristics of superheaters and discusses various types of superheater temperature control.

Kirchmayer [74] includes a block diagram representation of a speed governing system, a turbine, and a power system. First-order lags model the three systems.

Enns [46] develops several dynamic models for single-pass heat exchangers as used in boiler superheaters. Lumped-parameter and distributed-parameter models are considered.

Nicholson [97] presents a large-scale 50th order oil-fired drum boiler model which is reduced to a 9th order linear model. Optimal and suboptimal digital controllers are developed.

Adams, et al. [1] describe an analog computer simulation of a 191 MW (electrical) once-through boiler. Mass balance, energy balance, and momentum equations are used in the modeling process. Small perturbation techniques solve the system equations. Therefore, dynamic studies are limited to small excursions about any given operating point. One percent variations are typical.

Fryling [52] includes material on modeling superheaters and controls for drum water level and combustion. Steam flow is used to develop the primary combustion control signal.

Littman and Chen [86] present a linearized mathematical model of a coal-fired, twin furnace, supercritical, once-through boiler with 900 MW (electrical) output. The model is based entirely on physical laws and design data. Transient responses are obtained, using both digital and analog techniques.

Nicholson [99] uses the same boiler model as [97] to obtain optimal control of a combined boiler-turbine-generator model. Overall control of fuel, feedwater, valve position, and alternator field excitation is developed utilizing dynamic programming. Anderson and Qualtrough [2] present a critical review of [99]. They assert that the system model used by Nicholson is too crude to use for simulating on-line digital control.

Meyer, et al. [94] present numerous properties of water and steam in the classic 1967 ASME Steam Tables. These data are invaluable if detailed, large scale boiler modeling is done.

Thompson [135] describes a dynamic model of a drum-type boiler. The model is linear and suitable for representing plant dynamics about some steady-state operating condition. Design of a multivariable controller is discussed, utilizing the boiler model.

Stagg and El-Abiad [128] show a simplified block diagram representation of a speed governor control system. The control system is described by a dead-band, limiter, and first-order lag in cascade. The steam system is represented by a first-order lag. Turbine dynamics are neglected.

Laxton and Stevens [83] give steady-state design considerations for steam plant equipment associated with an MHD/steam combined cycle. The entire feedwater train is considered, including Combustor/Nozzle/

Channel/Diffuser cooling, feed heaters, superheater and reheater, and economizers.

Kwan and Anderson [77] present a model of a 200 MW coal-fired, drum-type boiler. It is an extremely detailed analysis consisting of 109 boiler equations which are reduced to 73 simultaneous equations through linearization and substitutions. Various open-loop responses are given.

Mizutani and Kitami [96] report results of applying adaptive control techniques to a drum-type coal-fired power plant. On-line, real-time identification of suitable parameters is used to control drum water level and steam pressure.

Speedy, Bell, and Goodwin [127] give results of a dynamic modeling study of a 50 KW drum-type steam generating plant. Least-squares analysis is used in which model equation parameters are chosen to minimize mean-squared error between measured output variable derivatives and derivatives calculated from model equations. Results are given for data runs as long as 2800 seconds.

Berg and Kar [17] develop mathematical models of bus loads in power systems. The models are given in terms of characteristic coefficients which are rates of change in real and reactive power for changes in applied voltage and frequency. Loads considered are resistance elements including filament lamps, discharge lamps, arc furnaces, converters, and induction motors.

McDonald, Kwatny, and Spare [78,90] describe the development of a nonlinear mathematical model of a drum-type reheat boiler-turbine-generator system. First principles (physical laws) are used and detailed assumptions are given. The resulting model uses 14 state variables to describe the boiler.

Laubli and Fenton [81] present a linear, time-invariant model of a once-through boiler that is a black-box type. Input variables are steam generation and turbine valve area. Output variables are steam flow to the turbines (proportional to output power), and throttle pressure. The effect of generation controller variations on grid stability is discussed.

Astrom and Eklund [9] give a derivation of a nonlinear model for a drum boiler-turbine unit. The model is characterized by five parameters. Major control variables are fuel flow and steam flow valve setting. The output variables are drum pressure and output power. Experimental verification is included.

Astrom [10] published a review paper discussing power system modeling based on physical equations and on plant experiments. Parameter estimation techniques are emphasized. Applications include an electric generator, a nuclear reactor, and a drum boiler.

Caseau, Chaussard, and Godin [27] present a detailed model of a drum-type boiler. Elements of the boiler are categorized into long elements (pipes and heat exchangers), short elements (drums, tanks,

condensers), and short, complex elements (turbines, furnaces). This allows separation of cases in which propagation delay is important from cases in which mass and energy storage predominates. Appropriate equations are given.

Eklund [43] compares a 160 MW drum boiler-turbine model with experimental results and with linear models obtained by maximum likelihood identification. The original model is 9th order.

The IEEE Working Group on Power Plant Response to Load Changes [67] gives some modeling information on turbines and boiler pressure effects. Power system response to load changes is given for boiler following, turbine following, and coordinated boiler-turbine control.

Young [146] published block diagrams of excitation systems, a hydraulic turbine, and a steam boiler-turbine system. The boiler-turbine model is quite detailed but still remains in the black-box category. It is used in a large-scale stability program.

Anderson [5] presents an excellent survey of low-order boiler models and different types of boiler-turbine control. Turbine models are also discussed.

An IEEE committee report [65] gives models of speed governing systems and turbines for use in system stability studies. Hydro and steam turbines are represented. Typical parameters are given.

Laubli [82] describes large-scale boiler simulation. The approach gives detailed modeling procedures for tube elements, discusses

incompressible single-phase flow and two-phase flow, and describes open- and closed-loop response of a 425 MW once-through boiler.

Anderson and Nanakorn [7] compare three low-order boiler models in terms of dynamic response. The three models are also compared with a linear two-port network equivalent. It is observed that all three models can be described as a linear two-port network. The results of analog simulation are given.

Bailey and Pierce [12] describe coal pulverizer systems in considerable detail. They present a case for making modeling information of a transfer function nature available to practicing control engineers rather than state variable models.

Choung and Dziubakowski [32] present results of work at Bailey Meter Company in modeling a boiler at start-up. Nonlinearities of the process variables are simulated by using reference functions internal to the model. The boiler bypass system is not included in the model.

Kundur and Bayne [76] describe studies of early valve actuation effects on nuclear and fossil-fired power plant stability. A steam turbine model is given which includes an intercept valve placed in the steam piping between the reheater and the intermediate pressure turbine.

McDonald [92] gives guidelines for development of useful mathematical models of complex physical processes. Accuracy and usefulness of results are considered to be determined by parallelism between the

model and the physical process of interest. A boiler-turbine model is developed using the guidelines presented.

Nielsen and Berkowitz [102] conclude that a "model and validate" approach to describing power plant behavior is more economical and accurate than either exhaustive testing or purely analytical modeling. The results of applying this approach to a once-through boiler-turbine system is given.

Yahalom [144] presents reasons for simplifications and assumptions used in approximating two-phase steam flow.

Paynter [110] discusses process dynamics in boiler modeling. Mass, momentum, and energy balances are stressed.

Bloethe and Anderson [22] apply a low-order boiler model to a transient stability program. A boiler-following control mode is assumed, utilizing a PID controller. The study concludes that the effect of the boiler is to reduce system stability.

Herget and Park [62] describe parameter identification of a linear fourth-order boiler model with eight unknown parameters, two inputs, and two outputs. Experimental verification is given for time periods as long as 1800 seconds.

## 2.5 Heat Exchangers

The references listed in this section give information regarding transient response of heat exchangers. Transfer functions and electrical analogs are also considered.

Ford [50] derives electrical analogs for heat exchangers based on idealized equations. Two analogs are developed; one using entirely passive electrical components, and one containing amplifiers and feedback.

Paynter and Takahasi [109] develop solutions for transient response of heat exchangers using exact solutions for frequency response of the exchangers.

Masubuchi [88] obtains transfer functions for one shell pass and 2, 3, 4, $\cdots$, 2n, 2n + 1 tube pass heat exchangers as distributed parameter systems. The heat exchange process is found to be governed by third-order characteristic equations with complex coefficients.

Thal-Larsen [133] develops models of heat exchangers and gives impulse and frequency response plots for them.

Chen and Galle [28] develop differential equations for steam generating heat exchangers from distributed parameter considerations.

Thal-Larsen and Luscutoff [134] present a study of fluid temperature transients in an experimental heat exchanger system based on analog simulations.

Watts and Schlenhals [140] discuss optimization of outlet temperature control of a single fluid heat exchanger. Location of a temperature probe (the error signal source) and the value of a proportional gain constant are simultaneously optimized to produce a large improvement in system performance.

Schmidt and Clark [122] determine dynamic behavior of parallel flow heat exchangers with lumping of the time variable, rather than lumping physical parameters. An analog simulation is included.

Chojnowski, Fussey, and Chew [31] design a checker brick regenerative heat exchanger for use as an air preheater for an MHD/steam combined cycle. A complete system of 12 units, associated valves and ductwork is a part of the design. A suggested liquid slag regenerator is discussed.

Womack [142] presents an excellent introductory overview of the air heater problem as applied to MHD particularly. The feasibility of various types of air heaters is discussed, and a possible cycling mode is presented.

## 2.6 Power Plant Control

A considerable amount of work has been done on conventional plant control, ranging from classical linear proportional-integral-derivative techniques to applied modern concepts such as adaptive control, optimal regulator theory, and parameter and state estimation.

Schultz [124] gives a broad coverage of topics pertaining to nuclear reactor and nuclear power plant control.

Scutt [126] describes work done on control of once-through boiler units. Conventional, or boiler-following control is mentioned as well as a direct energy-balance approach, also called turbine-following control. These methods of control are combined to give an integrated control of both the firing system and the turbine governor.

Concordia [33] shows the effect of steam turbine reheat on frequency stability and response of an electric power system. In general, reheat tends to decrease the damping of the frequency variations of the system as a whole, and increase maximum frequency deviation produced by an abrupt load change. Analog computer simulations are given.

Nicholson [98] describes a time-varying mathematical model of an oil-fired boiler. Parameter and state estimation is used with adaptive digital control.

Concordia, et al. [34] gives general information on hydro and steam generation equipment response associated with load changes in isolated and interconnected systems. A description of coordinated boiler-turbine control is included.

Nicholson [100] uses a linearized model of a nonlinear system to form a reference for adaptive digital control. The nonlinear system is an oil-fired drum boiler with equations derived from mass and heat balance, heat transfer and momentum considerations.

An IEEE committee report [66] is the result of a survey on power plant response. System load characteristics and plant operating practices are given. Prime mover characteristics are discussed in terms of allowable response rates.

Kenny [7] describes the differences between drum-type and once-through boilers and what the differences imply in terms of plant controls. Cycle diagrams are given for once-through boilers produced by four major boiler manufacturers. Several different levels of detail are presented in descriptions of commercially available once-through boiler controls.

Nicholson [101] gives the definition of a state vector associated with a matrix differential equation containing input derivatives. Optimal control of the system defined by the matrix equation is developed.

Giras and Birnbaum [54] show the application of a digital controller to a large steam turbine-generator. A functional block diagram of the turbine-generator unit is included.

Lee, Adams, and Gaines [84] illustrate techniques for developing physical models. Characteristics of physical processes are given. Linear and multiple regression models (least-squares curve fitting) are derived.

Anderson [3] compares alternative control methods for a dynamic model of a drum boiler. The control methods considered are

conventional analog PI controllers, digital computer simulation of the analog controllers, and on-line direct digital control.

Brown, et al. [23] present results of studies of the effect of several parameters on transient stability of power systems. The parameters considered are switching time, machine inertia, transmission reactances before and after a fault, excitation system response, and early valving. Early valving is believed to aid system first-swing transient stability.

Durrant [42] reports on a number of tests conducted on once-through boilers forced to operate under simulated emergency conditions. The emergency conditions include rapid load changes over the entire load range, system frequency upsets, and total external load rejection.

Davis [38] gives block diagrams of a hybrid digital-analog power plant control system. The system controls a once-through boiler, a turbine-generator, and auxiliary equipment. Very little detail is included.

Fenton and Pigford [47] summarize the main features of a coordinated control system and give the results of power plant response tests.

Concordia and Brown [35] conclude that the trend toward larger boiler-turbine-generator units has an adverse effect on power system stability.

Workman and Vollmer [143] describe testing three once-through boiler units for response to system upsets. Normal load change rates are 2% to at most 5% per minute. Unit control of a 600 MW (electrical) once-through boiler is described in detail.

Louis [87] illustrates, in functional block form, some of the controls for a once-through boiler. Overall control is not considered.

Hastings and Louis [59] show a functional block diagram of a control system for a high-temperature gas-cooled reactor. System disturbance test results are given.

Pinnello and Van Ness [1] give the dynamic response of a large power system to the cyclic load of a 200 BEV nuclear acceleration. Included is a block diagram of a generator with its voltage regulator and governor.

Bailey [14] reports on the response to a survey of 100 public utilities concerning their control practices.

deMello, Mills, and B'Rells [40] outline methods and philosophy of modeling power system components for simulation studies. A boiler model is shown and digital control techniques are described.

Babcock and Wilcox Co. [11] give a functional block diagram description of overall controls for a once-through fossil-fired boiler and for a nuclear power plant.

Herbrick and Jamshidi [61] present the design of an optimum state regulator for a once-through boiler. Variable pressure and

constant temperature operation is desired. The optimal system is compared with actual PID control equipment.

Yoshie [145] describes variable pressure control systems for a drum boiler and a once-through boiler optimized by computer.

Quazza and Ferrari [118] discuss typical responses of hydro and steam electric power generating plants with various control modes. A block diagram of a power control loop is given.

Anderson [4] compiled an annotated bibliography on power plant control and energy source system modeling. The publication period covered by the bibliography is from 1957 through 1971.

Cushing, et al. [37] observe that power system stability problems have become worse as generator ratings have increased. Fast valving, in which the turbine intercept valves are rapidly closed after a disturbance (within 0.1 to 0.2 seconds) and reopened within approximately 11 seconds, is shown to increase critical switching time or time in which a fault must be cleared to prevent generator runaway.

Watson and Manchur [139] review stabilizing systems in generator exciters and include block diagrams of such systems.

Kwatny, et al. [79] give a design of load-following power plant control systems based on optimal linear regulators. Simulation studies are described.

Giras and Papas [55] present the features of Westinghouse power plant simulation facilities. These facilities are used to verify

control systems at the place of manufacture and to train plant operators under real-time conditions.

McDonald and Kwatny [91] describe a 14 state-variable boiler model and develop boiler-turbine-generator controls using optimal linear regulator theory.

Mika [95] reviews classical control theory, expresses the dynamics of a steam generator by a cascade of two first-order lags, and discusses modern control theory as applied to power plants. State variables, optimal solutions, and effects of noise and nonlinearities are considered.

Buntzel [24] gives scaling and calibrating procedures for analog boiler controls based on design specifications and operating data.

Giras and Berman [56] describe the Westinghouse PACE (Power At Combined Efficiency) combined-cycle power plant control system. Two gas turbine-generator units are used in conjunction with a steam bottoming plant. The control system is hybrid, with two digital computers for data acquisition and display, and real-time digital control. Actual plant operation is carried out by analog controllers.

Nikravesh and Hoft [103] present a Lyapunov stability analysis of a single-phase bridge inverter system. The system includes closed-loop control. A digital computer simulation of the system is given.

Hayes and Crawford [60] give results of start-ups with a third-generation coordinated boiler-turbine control system applied to two

600 MW once-through boilers. Two basic concepts employed are: (1) apply generation control directly to the turbine to obtain best response to load requirements and (2) normally coordinate boiler with turbine but coordinate turbine with boiler during abnormal operating conditions.

Koekebakker [75] describes favorable results of Canadian operating experience with direct digital control of nuclear power stations.

Bethune [20] reports on the application of a digital computer to gather data for dynamic analysis of a 700 MW coal-fired once-through boiler-turbine-generator. The results of many of the tests are given.

Fink [49] discusses how a successful power plant modeling program was evolved at the Philadelphia Electric Company. Modeling philosophy is given. Modeling efforts with respect to the Philadelphia Electric Company's Cromby station dynamic characteristics and controls are detailed.

McDonald [93] gives an overview of an extensive effort to evolve a dynamic simulation of a nuclear power plant during the design phase. The simulation is used as a design evaluation tool and to identify operational problems before they occur.

Berkowitz, Jones, and Markunas [19] present details of modeling a 380 MW, sub-critical once-through boiler. Eight state variables are

used in the boiler model, which has been validated for steady-state plant performance.

Kerlin [73] describes dynamic testing and model verification for nuclear reactors. System transient and frequency responses are shown.

Fenton [48] gives information about low-order boiler models using boiler load demand and turbine control valve area as inputs and high-pressure steam flow and throttle pressure as outputs. Experimental verification is included.

El-Abiad and Keyhani [44] discuss optimal dynamic generation control of fossil-fired generating plants. Variable pressure operation is utilized. Forecasting of system load demand is achieved by stochastic load modeling.

Bailey [13] presents details on the properties of coal pulverizers.

Kwatny [80] considers the application of optimal regulator techniques to power plant control system design.

## 2.7 General Control References

The books listed in this section are representative of some of the excellent references available in the subject area of automatic control.

Lindorff [85] has devoted a text to sampled-data control theory. Topics include difference equations, the z-transform method, pulse system stability tests, the pulse model applied to sampled-data systems, compensation methods, statistical design, state variables applied to sampled-data systems, Lyapunov's stability theorems, and nonlinear sampled-data system design techniques.

Schultz and Melsa [123] discuss state variable representation of systems, the state function of Lagrange, linear system time response, stability concepts including the second method of Lyapunov, optimal control concepts, and linear system synthesis.

Hsu and Meyer [63], in a book on modern control theory, introduce the state-space approach to system analysis and the state plane. System stability topics include local and equivalent linearization, Lyapunov stability, limit cycles, describing functions, analysis of relay control systems, the second method of Lyapunov, frequency domain stability criteria, the Popov criterion, and stability concepts for systems with inputs. A section on optimal control contains time optimal control, the calculus of variations, the Maximum Principle of Pontryagin, and dynamic programming.

Raven [119] presents a hardware oriented text on control systems with considerable material on classical time and frequency domain analysis techniques.

Pierre [112] has included the following topics in a book on optimization theory: introduction to optimization, classical theory of minima and maxima, classical calculus of variations, frequency domain optimization, linear programming, search techniques and nonlinear programming, dynamic programming, and a maximum principle.

Ogata [104] gives a background in mathematical tools, transient response and frequency domain analysis, compensation techniques, sampled-data systems, state-space analysis, Lyapunov stability analysis, and an introduction to optimal and adaptive control.

Takahashi, Rabins, and Auslander [131] have published a book on automatic controls and dynamic systems. The text is written to cover both modern and classical control concepts and is subdivided into four major areas. These areas are: (1) linear systems theory, including representations, response, and stability of lumped-parameter systems, (2) formulation of dynamic systems, which includes mathematical system modeling, bilaterally coupled systems, and distributed-parameter systems, (3) control of linear systems, including scalar input-output systems, frequency response, multivariable systems, and linear digital control, and (4) nonlinear, stochastic, optimal control, and logic systems.

## 2.8 Numerical Methods/Mathematical Methods

The references described in this section deal with computer methods and mathematical methods applied to systems analysis.

Davison [39] advances a method of reducing the number of equations required to describe a physical system. The system matrix is approximated by one of lower order containing the same dominant eigenvalues and eigenvectors as the original.

Carnahan, Luther, and Wilkes [25] include the following topics in a book on numerical methods: interpolation and approximation, numerical integration, solution of equations, matrices, systems of equations, approximation of the solution of ordinary and partial differential equations, and statistical methods. Numerous computer examples are included.

Chidambara [29] proposes techniques for reducing the order of system models and measuring the accuracy of the resulting approximation.

Bekey [16] presents a survey paper on system identification. Techniques discussed and compared include spectral analysis, search and gradient methods, quasi-linearization, and stochastic approximation.

Franks [51] describes modeling and simulation techniques in a book including the following topics: numerical solution of algebraic, ordinary differential, and partial differential equations, modeling, and process control.

Peterson and Schweppe [111] give details of a computer program (publicly available) called GPSIE or General Purpose System Identifier and Evaluator. The program searches for maximum-likelihood estimates of unknown model parameters and tests for consistency between the model and given data.

Crevier and Schweppe [36] show a method of simulating power system frequency transients. Differential equations used to describe a frequency transient are solved in the Laplace domain. The method may be used to determine solution sensitivity to model changes, thereby enabling model reduction.

Schweppe [125] discusses fitting nonlinear dynamic models to data. Included are state estimation and system identification concepts. System identification is applied to the simulation of a 1000 MW pressurized-water-reactor power plant.

Undrill and Laskowski [138] describe an interactive digital simulation facility which combines the rapid turnaround time advantage of an analog computer with the flexibility of a digital machine. Applications are given in the areas of automatic generation control.

Chapter III

SYSTEM MODEL I

## 3.1 Basis for Model I

System model I represents initial efforts in dynamic studies of a large-scale magnetohydrodynamic (MHD)/steam combined-cycle electrical power generating plant.

The starting point for a complete system model was chosen to be an idealized heat balance for a 4000 MW (thermal) fossil-fueled open cycle [141]. Initial thermal input power of the fuel was taken to be 3500 MW with a limit of 4040 MW imposed on the system. The normalized heat balance diagram is shown in Figure 3.1. The source of the diagram is Figure 1.9 of [141].

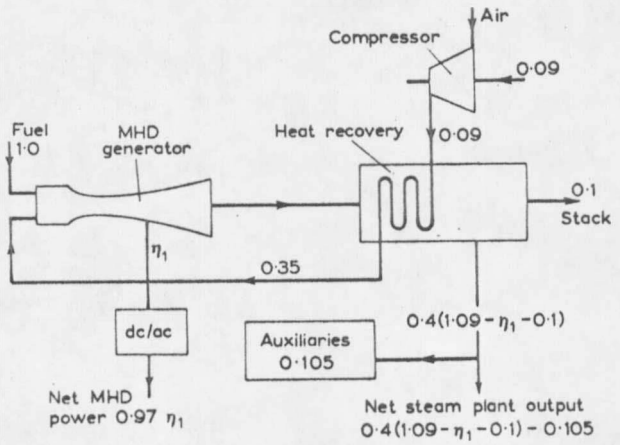



Figure 3.1. Idealized heat balance for fossil-fueled open cycle

The assumptions made in Figure 3.1 are:

1) All numbers are normalized units of power. They are normalized to 1000 MW heat input of the fuel.

2) Combustion air is preheated to 1473.15°K.

3) Heat losses from the combustor and MHD channel are recovered at a steam plant efficiency of 40%.

4) The combustion gases exhaust at 393.15°K with a stack loss of 0.1 of the fuel heat input.

5) Inverter efficiency is 97%.

6) Compressor power for 7 atmospheres is 0.09 heat input of the fuel.

7) Total auxiliary power is 0.0125 for the steam plant auxiliaries, 0.0025 for the MHD plant auxiliaries, and 0.09 for the compressor.

8) MHD generator efficiency $\eta_1$ is defined as:

$$\eta_1 = \frac{\text{MHD electrical output power}}{\text{fuel thermal input power}} \tag{3.1}$$

Note that MHD generator efficiency is referenced to fuel thermal input power and not to the actual thermal input power. Actual power entering the channel includes power supplied by the combustion air compressor and air preheaters in addition to the fuel thermal input power.

9) Overall plant combined efficiency $\eta_0$ is defined by:

$$\eta_0 = \frac{\text{net electrical output power}}{\text{fuel thermal input power}} \tag{3.2}$$

$$\eta_0 = \frac{0.97\,\eta_1 + 0.4(1.09 - \eta_1 - 0.1) - 0.105}{1.0 \text{ (fuel thermal input power)}}$$

$$= 0.57\,\eta_1 + 0.291 \qquad (3.3)$$

Combined plant efficiency, $\eta_0$, is plotted against MHD generator efficiency $\eta_1$ in Figure 3.2 [141]. MHD generator efficiency must be greater than 19.12% in order that combined plant efficiency rise above 40%. The figure of 40% is of interest because it is an upper bound on the efficiency currently attainable with steam generating plants.

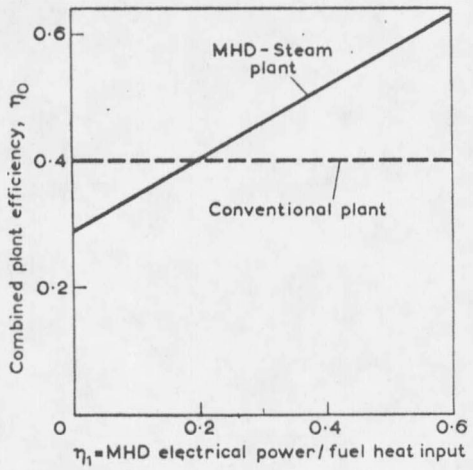



Figure 3.2. Variation of MHD/steam combined efficiency with MHD generator efficiency

## 3.2 Combustion Calculations

Thirty-five hundred MW (thermal) input power is assumed. From [11], the air (Kg) theoretically required for complete combustion of 1 Kg of fuel is:

$$\frac{\text{Wt. air}}{\text{Wt. fuel}} = 11.53C + 34.34(H_2 - O_2/8) + 4.29S \qquad (3.4)$$

where C, $H_2$, $O_2$, and S are the fractions by weight of carbon, hydrogen, oxygen, and sulfur. The factor $O_2/8$ corrects for the hydrogen already combined with oxygen in the fuel, but not as oxygen in moisture. Based on a representative analysis of Colstrip coal, 11.8 Kg of air is required per Kg of fuel used. This allows for 19.6% excess air, a representative value when pulverized coal is burned.

Assuming 9000 Btu/lb coal as fuel, the following observations may be made:

$$3.412 \text{ Btu/hr} = 1 \text{ watt}$$

$$1.194 \times 10^{10} \text{ Btu/hr} = 3500 \text{ MW}$$

For 3500 MW fuel thermal input power, $1.327 \times 10^6$ of 9000 Btu/lb coal and $1.565 \times 10^7$ lbs/hr of air are required. This corresponds to 664 tons/hr or $6.02 \times 10^5$ Kg/hr of coal and 7825 tons/hr or $7.10 \times 10^6$ Kg/hr of air.

Returning to Figure 3.1, if fuel thermal input power is 3500 MW and MHD generator efficiency $\eta_1$ is set equal to 0.3 to give 46% cycle efficiency, the following steady-state values result:

MHD electrical power output = 0.3(3500 MW) = 1050 MW

Inverter output = 0.97(1050 MW) = 1018.5 MW where 97% inverter efficiency is assumed

Power from preheated airflow = 0.35(3500 MW) = 1225 MW

Power out of combustor = 3500 MW + 1225 MW = 4725 MW

Power for air compressor = 0.09(3500 MW) = 315 MW

Power to preheat air = 0.26(3500 MW) = 910 MW

Steam plant output = 0.4(0.99 - 0.3)(3500 MW) = 966 MW

Stack losses = 350 MW

Auxiliary power losses = 367.5 MW

Net output power = 1018.5 + 966 - 367.5 = 1617.0 MW

Combined plant efficiency = $\eta_0$ = 1617/3500 = 46.2%. This value of $\eta_0$ is predicted by Equation (3.3) if $\eta_1$ = 0.3.

## 3.3 Model I Block Diagram

The block diagram of System Model I is shown in Figure 3.3. Actual plant output power is compared with desired output MW(REF). The difference is the input to the controller. Proportional-plus-integral control is used. The controller output operates the fuel supply system, characterized by a limiter in cascade with a first-order lag [81]. Fuel thermal input power is the output of the fuel supply system and has an assumed maximum value of 4040 MW. MHD channel input power is the sum of fuel thermal input power and power in the preheated combustion air. The MHD channel is described by a negligible time constant compared with the rest of the system time constants and by enthalpy extraction which accounts for electrical output power of the channel.

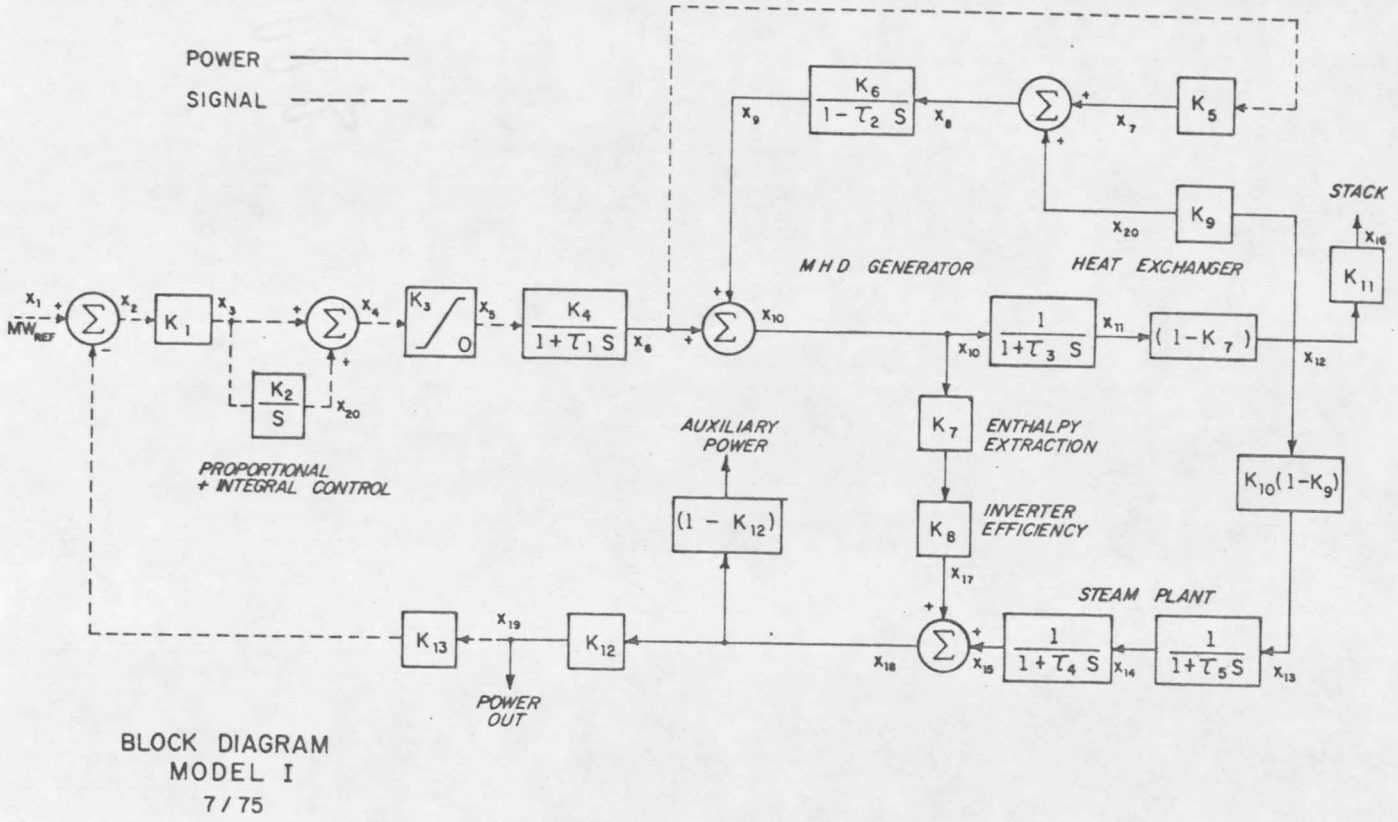



Figure 3.3. Block diagram for model I

Compressor power is assumed proportional to fuel thermal input power. The heat exchangers are assumed to be regenerative, directly fired, and cycle every 360 seconds. Power available to reheat the exchangers is proportional to the MHD diffuser output. The steam plant is characterized by a cascade of two first-order lags, one having a 62 second and the other a 67.5 second time constant [96].

## 3.4 Description of System Variables

The variables for model I are tabulated in Table 3.1.

Table 3.1. Description of model I system variables

| Variable | Units | Description |
|---|---|---|
| $X_1$ | MW | desired plant output; MW reference |
| $X_2$ | MW | generation error |
| $X_3$ | -- | proportional control signal |
| $X_4$ | -- | composite valve control signal |
| $X_5$ | -- | limited composite control signal |
| $X_6$ | MW | fuel thermal input power |
| $X_7$ | MW | compressor power |
| $X_8$ | MW | power in preheated air |
| $X_9$ | MW | power from preheated air to combustor |
| $X_{10}$ | MW | combustor output power (input to MHD generator) |
| $X_{11}$ | MW | power available to MHD generator ($\tau_3$ was considered to be negligible compared with $\tau_2$, $\tau_4$, and $\tau_5$) |
| $X_{12}$ | MW | diffuser output power (includes cooling loss) |
| $X_{13}$ | MW | steam plant input power |
| $X_{14}$ | MW | intermediate steam plant variable |
| $X_{15}$ | MW | steam plant output power |
| $X_{16}$ | MW | stack loss |
| $X_{17}$ | MW | inverter output power |
| $X_{18}$ | MW | gross plant generated power |
| $X_{19}$ | MW | net plant output power |
| $X_{20}$ | -- | integral control signal |

## 3.5 Initial Conditions, Values of Constants, and System Equations

Initial conditions for the variables and values of constants are developed from the combustion calculations. The system is assumed to be in steady-state at the start of all computer solutions. Initial conditions are listed in Table 3.2.

Table 3.2. Model I initial conditions

| | |
|---|---|
| $X_1(0) = 1620$ MW | $X_{11}(0) = 4725$ MW |
| $X_2(0) = 0$ | $X_{12}(0) = 3675$ MW |
| $X_3(0) = 0$ | $X_{13}(0) = 966$ MW |
| $X_4(0) = 0.866$ | $X_{14}(0) = 966$ MW |
| $X_5(0) = 0.866$ | $X_{15}(0) = 966$ MW |
| $X_6(0) = 3500$ MW | $X_{16}(0) = 350$ MW |
| $X_7(0) = 315$ MW | $X_{17}(0) = 1020$ MW |
| $X_8(0) = 1225$ MW | $X_{18}(0) = 1988$ MW |
| $X_9(0) = 1225$ MW | $X_{19}(0) = 1620$ MW |
| $X_{10}(0) = 4725$ MW | $X_{20}(0) = 0.866$ |

Nominal values of constant multipliers and time constants appear in Table 3.3. $K_1$ and $K_2$ are controller constants and therefore are adjustable design parameters.

System equations follow directly from the block diagram. They are listed in the computer program of Appendix A.

Table 3.3. Model I multipliers and time constants

Constant multipliers:

| | |
|---|---|
| $K_1 = 0.001$ | $K_8 = 0.97$ |
| $K_2 = 0.1$ | $K_9 = 0.248$ |
| $K_3 = 1.0$ | $K_{10} = 0.351$ |
| $K_4 = 4040$ MW | $K_{11} = 0.953$ |
| $K_5 = 0.09$ | $K_{12} = 0.815$ |
| $K_6 = 1.0$ | $K_{13} = 1.0$ |
| $K_7 = 0.2225$ | |

Time constants:

| | |
|---|---|
| $\tau_1 = 10.0$ seconds | $\tau_4 = 67.5$ seconds |
| $\tau_2 = 360.0$ seconds | $\tau_5 = 62.0$ seconds |
| $\tau_3 = 0.0$ seconds | |

## 3.6 System Equation Solutions

Figures 3.4 and 3.5 show the behavior of five system variables for changes in MHD generator efficiency $\eta_1$. The variables are:

$X_6$ (fuel thermal input power)

$X_{10}$ (combustor output power)

$X_{15}$ (steam plant output power)

$X_{17}$ (inverter output power)

$X_{19}$ (net plant output power)

Figures 3.6 through 3.23 illustrate the effect of load demand changes on six system variables for various values of controller parameters. The six variables are the above five and valve control signal, $X_4$.

### 3.6.1 MHD generator efficiency $\eta_1$ variations

Figure 3.4 shows time variations of five system variables as enthalpy extraction $K_7$ changes from 0.22225 to 0.1484 at t = 0+. This change in $K_7$ corresponds to a change in $\eta_1$ from 0.3 to 0.2. Controller constants are $K_1$ = 0.001 and $K_2$ = 0.1. At 1230 seconds, $X_6$ comes out of saturation, which accounts for the sudden changes in all curves. $X_{19}$ overshoots past MW(REF) = 1620 MW to 1669.5 MW at 1230 seconds and then settles to 1619.98 MW at t = 2000 seconds.

Figure 3.5 displays the same variables as Figure 3.4 with enthalpy extraction $K_7$ changing from 0.2225 to 0.2967 at t = 0+. This corresponds to a change in $\eta_1$ from 0.3 to 0.4. $X_{19}$ instantaneously increases to 1897 MW and drops to 1620 MW at t = 310 seconds. At t = 2000 seconds, $X_{17}$ = 1208 MW and $X_6$ = 3180 MW giving $\eta_1$ = 0.3918. As a check on results, $\eta_0$ = 1620/3180 = 0.509. Equation 3.3 predicts $\eta_0$ = 0.514 based on the above value of $\eta_1$. The two values of $\eta_0$ are within 1% of each other.

### 3.6.2 Valve control signal $X_4$

Figure 3.6 shows four plots of $X_4$ as a function of time corresponding to $K_1$ = 0.001 and $K_2$ = 0.01, 0.1, 1.0, and 10.0. MW(REF) $X_1$ changes from 1620 MW to 1570 MW at t = 0+. More well-damped behavior is exhibited with smaller values of $K_2$. The periods of the damped

oscillations that occur for larger values of $K_2$ are 24.5 seconds if $K_2$ = 1.0, and 8.0 seconds if $K_2$ = 10.0.

Figure 3.7 illustrates four plots of $X_4$ under the same conditions as Figure 3.6 except that $K_1$ = 0.01. The transients are larger, particularly for the case $K_2$ = 10.0, but steady-state is reached in approximately one-third the time required when $K_1$ = 0.001, or about 20 seconds.

Figure 3.8 displays the time response of $X_4$ with the same conditions as Figure 3.6, except that $K_1$ = 0.1. $X_4$ approaches steady-state in 1.1 seconds when $K_2$ = 0.01, in 1.15 seconds when $K_2$ = 0.1, and in 1.25 seconds when $K_2$ = 1.0. There is no overshoot when $K_2$ = 0.01 or $K_2$ = 0.1 and negligible overshoot when $K_2$ = 1.0. When integrator constant $K_2$ = 10.0, nonlinear behavior occurs with the limits on the fuel valve being greatly exceeded ($0 \leq X_5 \leq 1.0$). The maximum value of $X_4$ is 47.7, occurring at t = 4.05 seconds. Steady-state is reached in approximately 12 seconds. Data were taken for $K_1$ = 1.0 and 10.0 with all other conditions being the same as in Figure 3.8. Plots were not included because the magnitude of $X_4$ increased nearly linearly with $K_1$, making the shape of the curves the same.

### 3.6.3 Fuel thermal input power $X_6$

Figure 3.9 shows four plots of $X_6$ corresponding to the same conditions as Figure 3.6. $X_6$ is nearly critically damped with

$K_2$ = 0.01 and shows an undershoot of 138 MW when $K_2$ = 0.1. Oscillations occur with $K_2$ = 1.0 and 10.0 but are damped to zero in approximately 60 seconds. The periods of the damped oscillations are 23.5 seconds if $K_2$ = 1.0, and 7.5 seconds if $K_2$ = 10.0.

Figure 3.10 displays four plots of $X_6$ under the same conditions as Figure 3.7. In the case of $K_2$ = 0.01, an undershoot of 134 MW occurs at 8.6 seconds. When $K_2$ = 0.01, an undershoot of 163 MW is observed. The oscillations noted when $K_2$ = 1.0 and 10.0 are damped to zero in approximately 20 seconds. The period of the oscillation is 8.0 seconds if $K_2$ = 1.0 and is 4.0 seconds if $K_2$ = 10.0.

Figure 3.11 illustrates four plots of $X_6$ under the conditions $K_1$ = 0.1, and $K_2$ = 0.01, 0.1, 1.0, and 10.0. MW(REF) $X_1$ undergoes a step change of -50 MW at t = 0+. When $K_2$ = 0.01, $X_6$ approaches its steady-state value in approximately 0.9 seconds, and undershoots that value by 10 MW at t = 1.6 seconds. With $K_2$ = 0.1, the steady-state value is reached in 0.87 seconds, and a maximum undershoot of 15 MW occurs at t = 1.5 seconds. For the case $K_2$ = 1.0, the steady-state value of $X_6$ is reached in 0.83 seconds, and a maximum undershoot of 101 MW occurs at t = 1.25 seconds. A very interesting plot corresponds to the $K_2$ = 10.0 case. The effect of the limiter is clearly shown with $X_6$ either exponentially increasing toward a limit of 4040 MW or exponentially decreasing toward a limit of 0 MW with a time constant $\tau_1$ = 10.0 seconds when $X_4$ is greater than 1 or less than 0.

$X_4$ passes through the linear region of the limiter in approximately 0.03 seconds. The extremely nonlinear oscillation just described approaches zero at t = 12 seconds. Plots for the cases $K_1$ = 1.0 and 10.0 were not included because they are virtually identical to Figure 3.11. The dynamic response of $X_6$ remains essentially unchanged for larger values of $K_1$ because of the limiter action.

### 3.6.4 Combustor output power $X_{10}$

Figure 3.12 shows four plots of $X_{10}$ drawn for the same conditions as Figures 3.6 and 3.9. The dynamic response of $X_{10}$ is almost equivalent to that of $X_6$, being equal to the sum of $X_6$ and the power from the preheated combustion air $X_9$. $X_9$ is essentially constant, being the output of a first-order lag block having a 360 second time constant. The remarks pertaining to Figure 3.9 are applicable here.

Figure 3.13 displays four plots of combustor output power $X_{10}$ with the same conditions as Figure 3.7 and 3.10. The time response of $X_{10}$ is effectively the same as $X_6$ for reasons described in the previous paragraph. Therefore, the magnitudes of undershoot and periods of oscillation given for Figure 3.10 may be applied to Figure 3.13.

Figure 3.14 shows four plots of combustor output power $X_{10}$ for the same conditions as Figures 3.8 and 3.11. For reasons given in the Figure 3.12 description, the dynamic response of $X_{10}$ is essentially equivalent to the response of $X_6$, and the values of undershoot and

settling time given in the Figure 3.11 description are again applicable. There is no significant difference between Figure 3.14 results and the cases where $K_1$ = 1.0 and 10.0.

### 3.6.5 Steam plant output power $X_{15}$

Figure 3.15 illustrates four plots of $X_{15}$ for $K_1$ = 0.001 and $K_2$ = 0.01, 0.1, 1.0, and 10.0. MW(REF) $X_1$ changes by -50 MW at t = 0+. The response of the steam plant is predictably slow relative to the combustor output and is limited by the controller only when $K_2$ = 0.01 and, to a lesser extent, when $K_2$ = 0.1.

Figure 3.16 shows four plots of $X_{15}$ for the same conditions as Figure 3.15 except that $K_1$ = 0.01. Again, response is slow and limited by the controller only when $K_2$ = 0.01. The $K_1$ = 0.001, $K_2$ = 1.0 case corresponds to the $K_1$ = 0.01, $K_2$ = 0.1 case, and the $K_1$ = 0.001, $K_2$ = 10.0 case corresponds to both the $K_1$ = 0.01, $K_2$ = 1.0 and $K_1$ = 0.01, $K_2$ = 10.0 cases.

Figure 3.17 displays the first 14 seconds of dynamic response of $X_{15}$ for $K_1$ = 0.1 and $K_2$ = 0.01, 0.1, 1.0, and 10.0. The same input disturbance is used as before. As may be noted, there is essentially no difference between the four curves.

### 3.6.6 Inverter output power $X_{17}$

Figures 3.18, 3.19, and 3.20 each show four plots of $X_{17}$ corresponding to the conditions for Figures 3.12, 3.13, and 3.14, respectively. Because $X_{17}$ is directly proportional to combustor output power $X_{10}$, Figure 3.18 is a scaled version of Figure 3.12, Figure 3.19 is a scaled version of Figure 3.13, and a similar relationship exists between Figures 3.20 and 3.14. Time response is unchanged, and $X_{17} = (0.2158)(X_{10})$.

### 3.6.7 Net plant output power $X_{19}$

Figure 3.21 illustrates four plots of $X_{19}$ as a function of time. The conditions for the plots are the same as those for Figures 3.6, 3.9, 3.12, 3.15, and 3.18. $X_{19}$ is proportional to the sum of $X_{15}$ and $X_{17}$, and thus has the characteristics of both these variables. A wide range of transient response is evident. For example, if $K_1 = 0.001$ and $K_2 = 0.01$, the system has no undershoot and reaches the new steady-state value in approximately 270 seconds. If $K_2 = 0.1$, a 3.5 MW undershoot occurs at approximately 87 seconds and steady-state is reached in about 230 seconds. For the cases of $K_2 = 1.0$, and 10.0, damped oscillations of the form appearing in Figure 3.18 exist but disappear in approximately 80 seconds. The period of the oscillation is 25 seconds if $K_2 = 1.0$ and is 7.5 seconds if $K_2 = 10.0$.

Figure 3.22 shows four plots $X_{19}$ for the same conditions as Figure 3.21 except that $K_1 = 0.01$. Response to the -50 MW step input at t = 0+ is significantly faster in this case than for $K_1 = 0.001$. If $K_2 = 0.01$, the new steady-state value is reached at t = 120 seconds with no undershoot. If $K_2 = 0.1$, steady-state is reached in 8 seconds. Slight undershoot occurs, reaching a maximum value of 0.4 MW at 50 seconds. Thus, for all practical purposes, the output of the system is critically damped. For the case $K_2 = 1.0$, an oscillation having a period of 8.5 seconds is damped to zero in approximately 20 seconds. If $K_2 = 10.0$, an oscillation occurs with a period of 4.0 seconds. It decays to a negligible value in about 20 seconds.

Figure 3.23 displays four plots of $X_{19}$ for the same conditions as Figure 3.21 except that $K_1 = 0.1$. For the case $K_2 = 0.01$, no undershoot occurs, and the steady-state value is approached within 0.5 MW in 1.5 seconds. If $K_2 = 0.1$, the response is similar to the $K_2 = 0.01$ case except undershoot exists with a maximum value of 1.3 MW at t = 1.6 seconds. If $K_2 = 1.0$, undershoot again occurs. Its maximum value is 16 MW at t = 1.25 seconds. Steady-state is reached at t = 9.6 seconds, but $X_{19}$ is within 0.1 MW of steady-state at t = 5.8 seconds. For the case $K_2 = 10.0$, nonlinear oscillations exist because of the limiter action of the fuel feed system. The maximum amount of undershoot is 41 MW at t = 1.65 seconds. The oscillation decays to zero in approximately 12 seconds. Plots for $K_1 = 1.0$ and

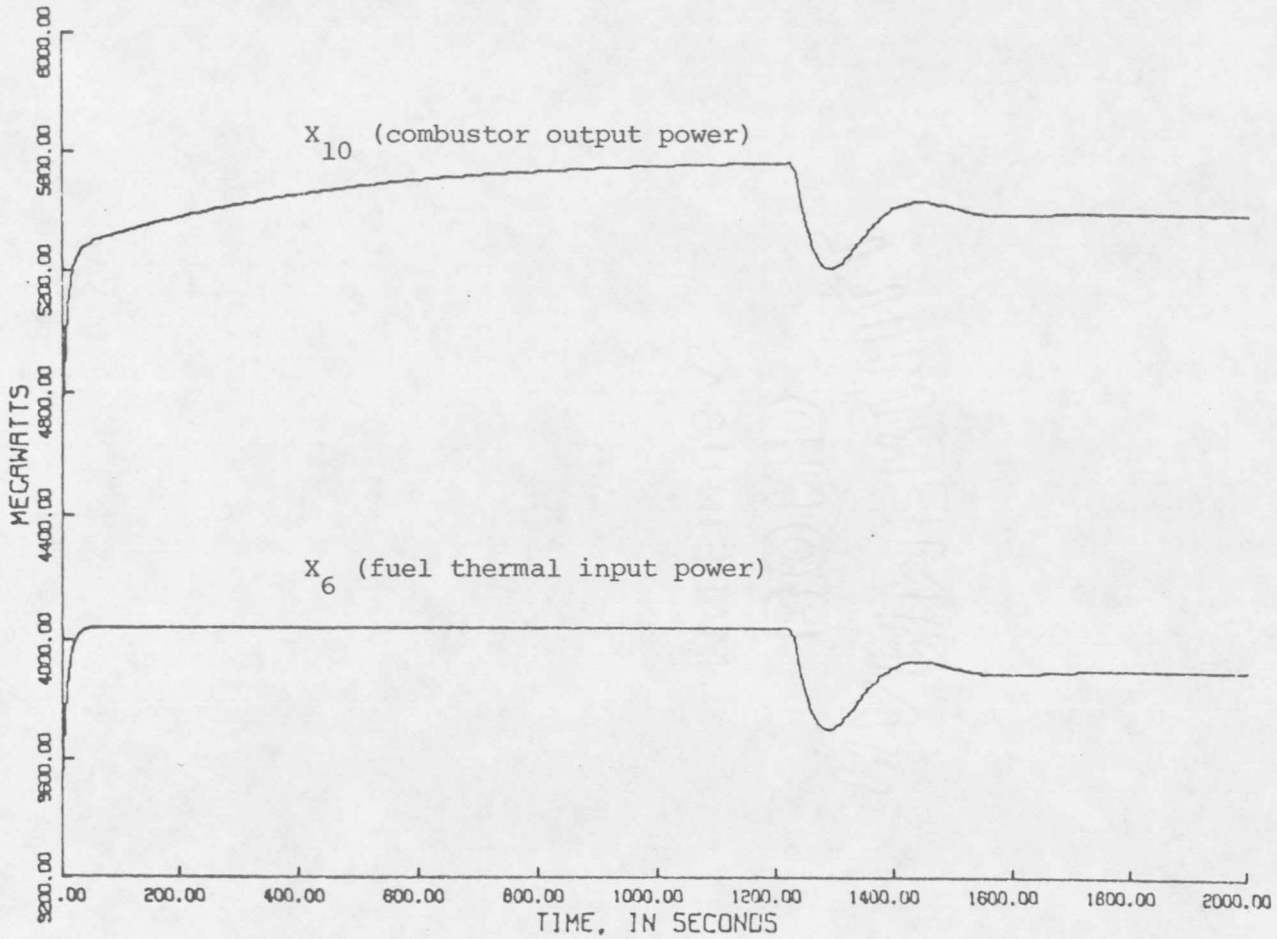



Figure 3.4(a). $\eta_1$ changes from 0.3 to 0.2 at t = 0+; $K_1$ = 0.001, $K_2$ = 0.1

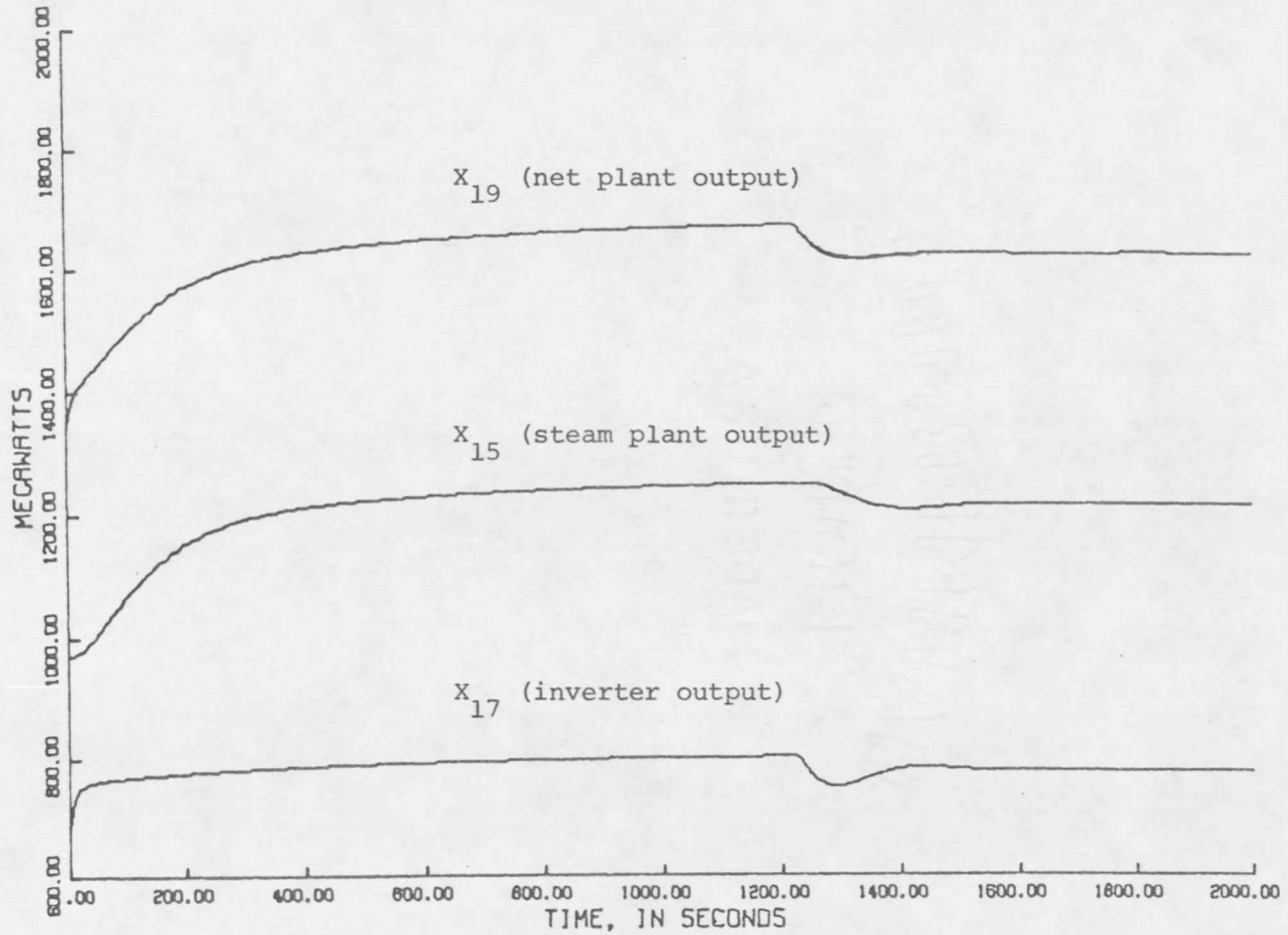



Figure 3.4(b). $\eta_1$ changes from 0.3 to 0.2 at t = 0+; $K_1$ = 0.001, $K_2$ = 0.1

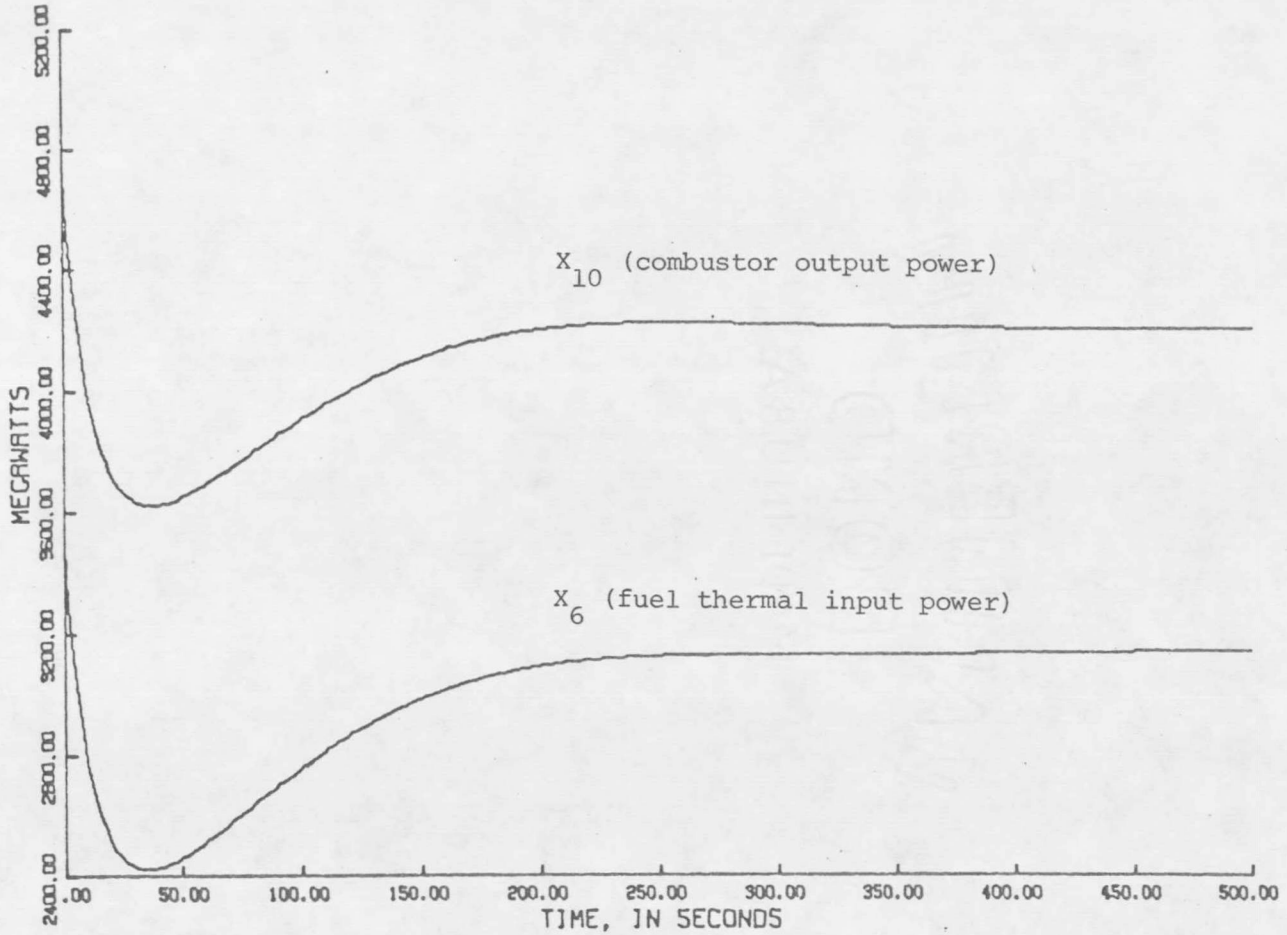



Figure 3.5(a). $\eta_1$ changes from 0.3 to 0.4 at t = 0+; $K_1$ = 0.001, $K_2$ = 0.1

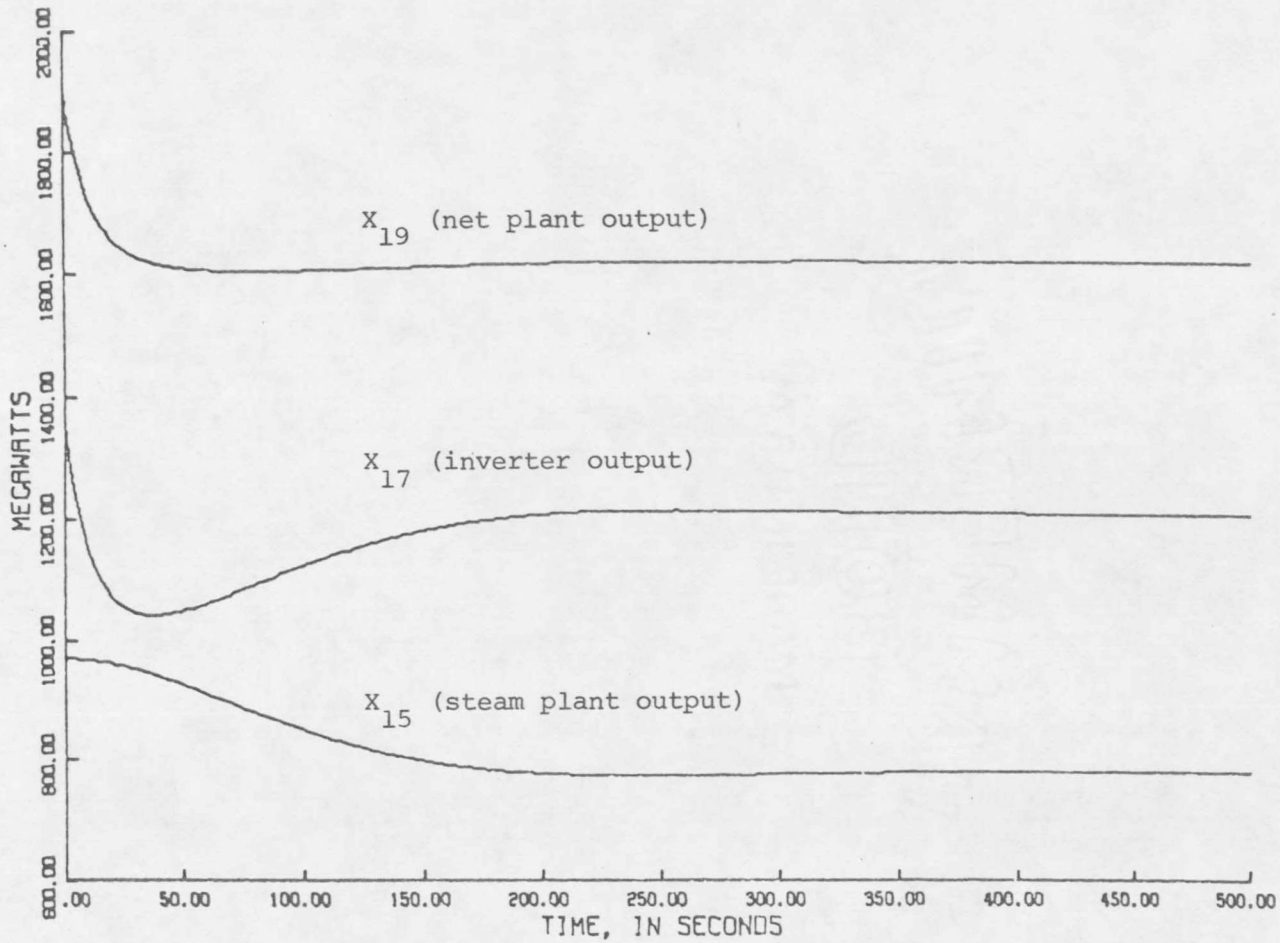



Figure 3.5(b). $\eta_1$ changes from 0.3 to 0.4 at t = 0+; $K_1 = 0.001$, $K_2 = 0.1$

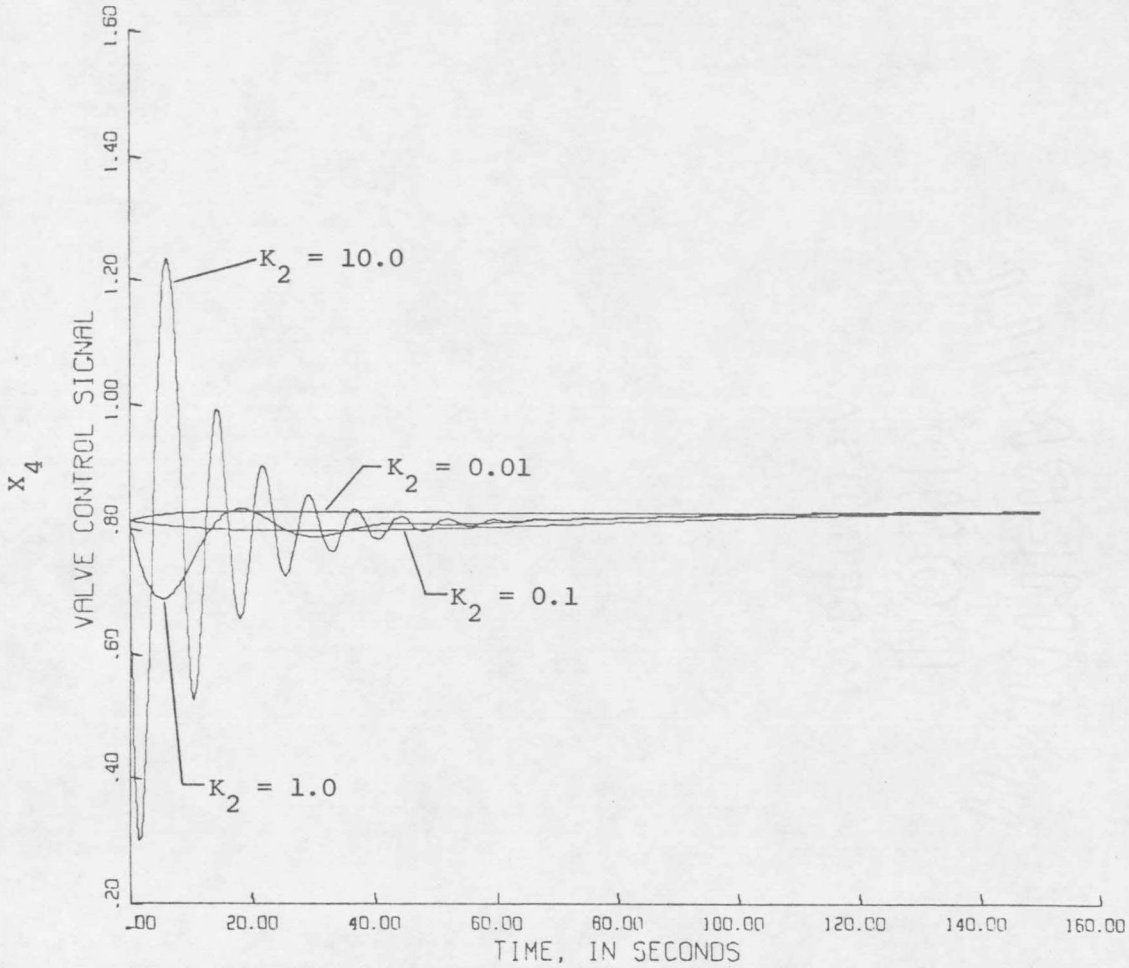



Figure 3.6. MW(REF) $X_1$ changes from 1620 MW to 1570 MW at t = 0+; $K_1$ = 0.001

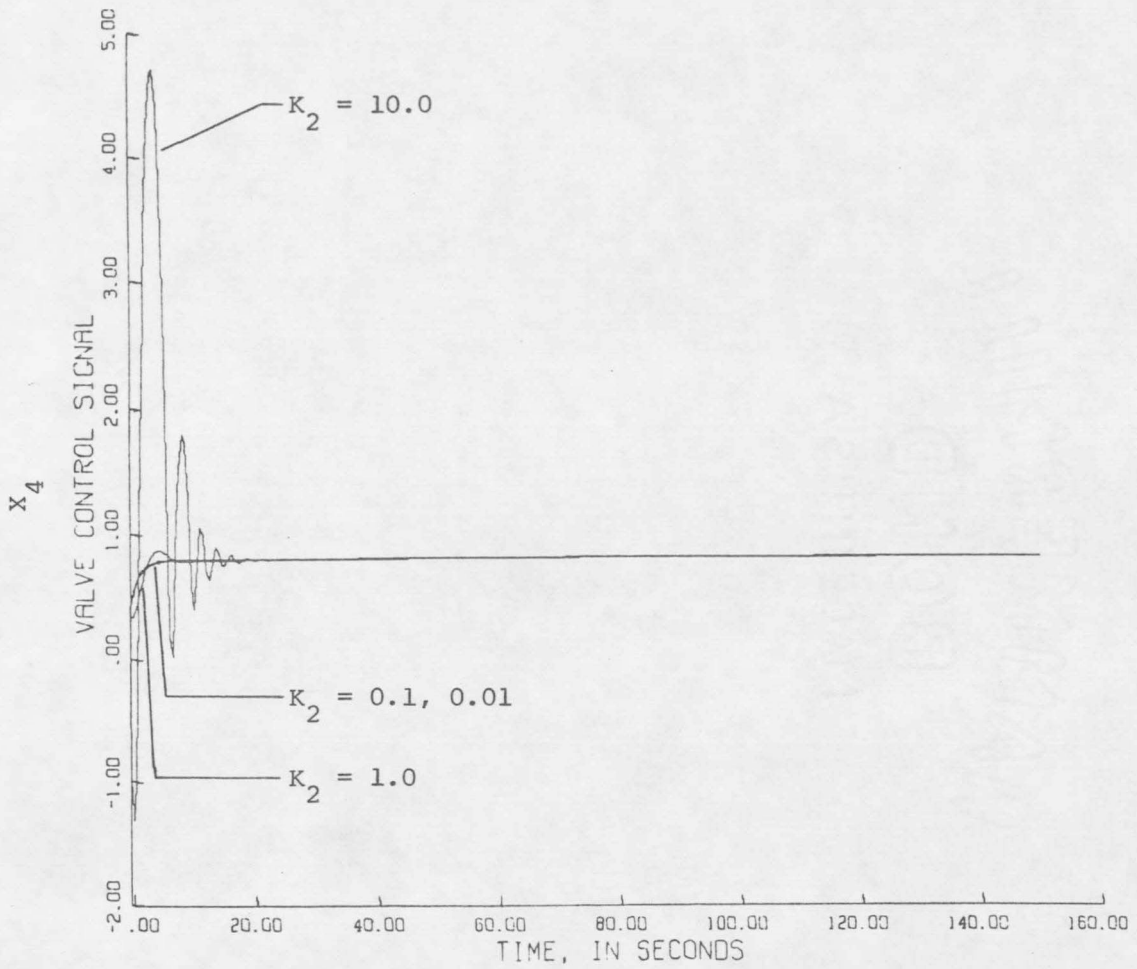



Figure 3.7. MW(REF) $X_1$ changes from 1620 MW to 1570 MW at t = 0+; $K_1$ = 0.01

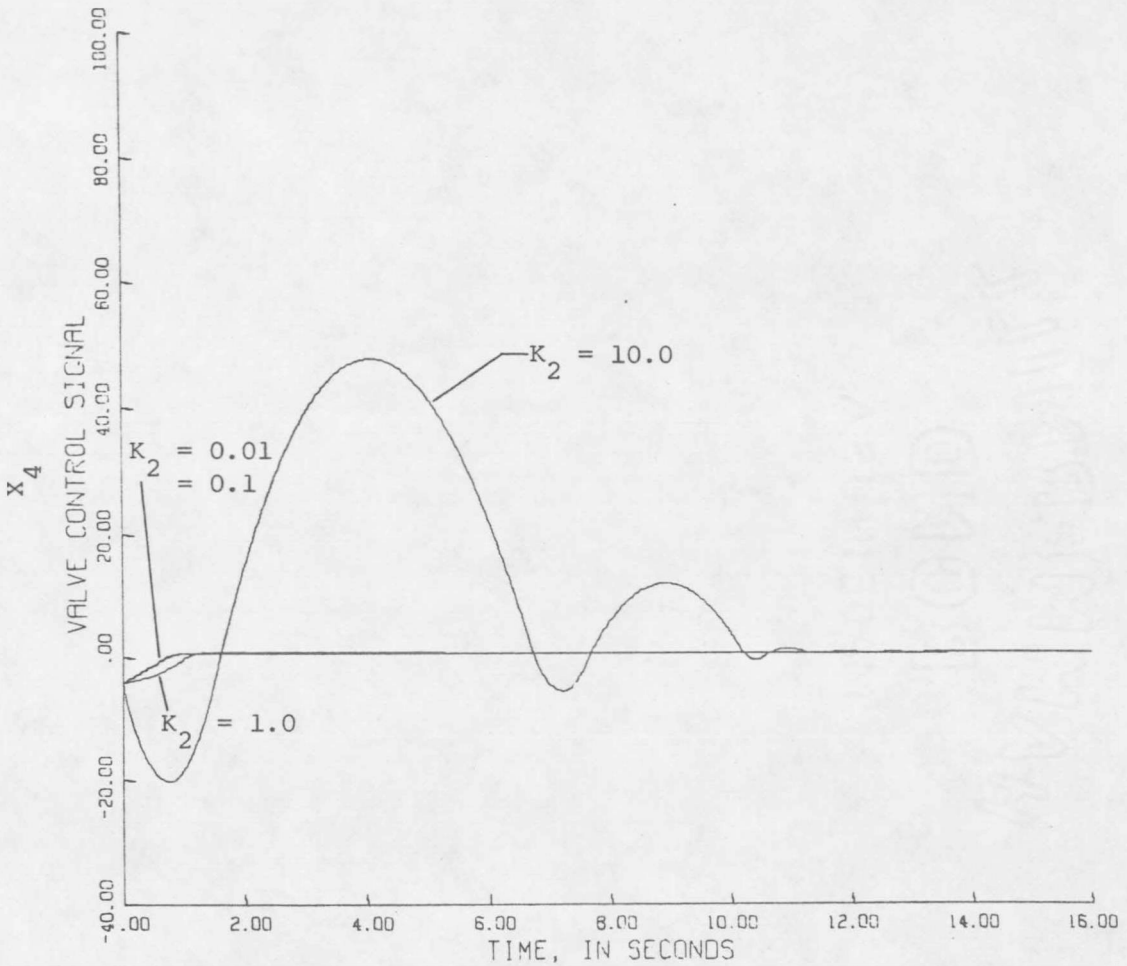



Figure 3.8. MW(REF) changes from 1620 MW to 1570 MW at t = 0+; $K_1$ = 0.1

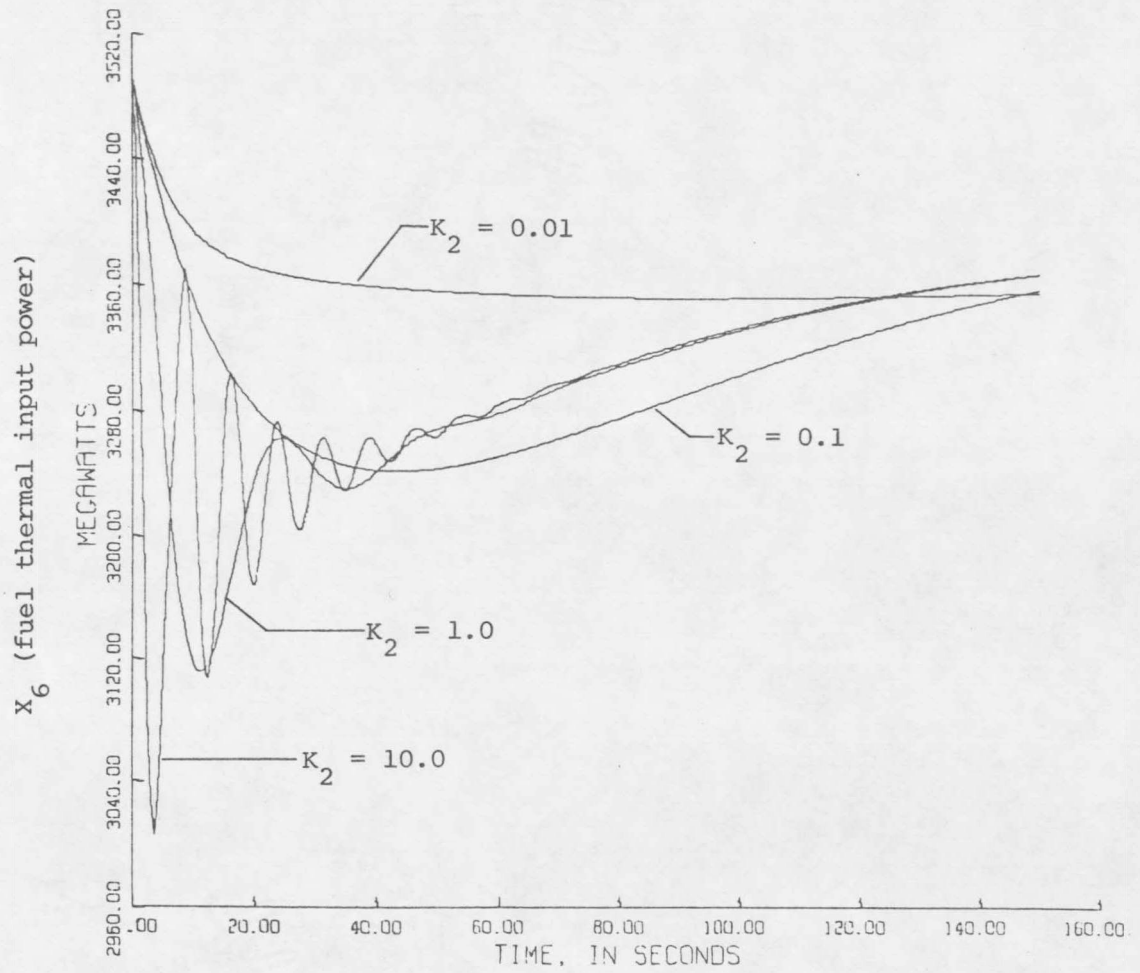



Figure 3.9. MW(REF) $X_1$ changes from 1620 MW to 1570 MW to t = 0+; $K_1$ = 0.001

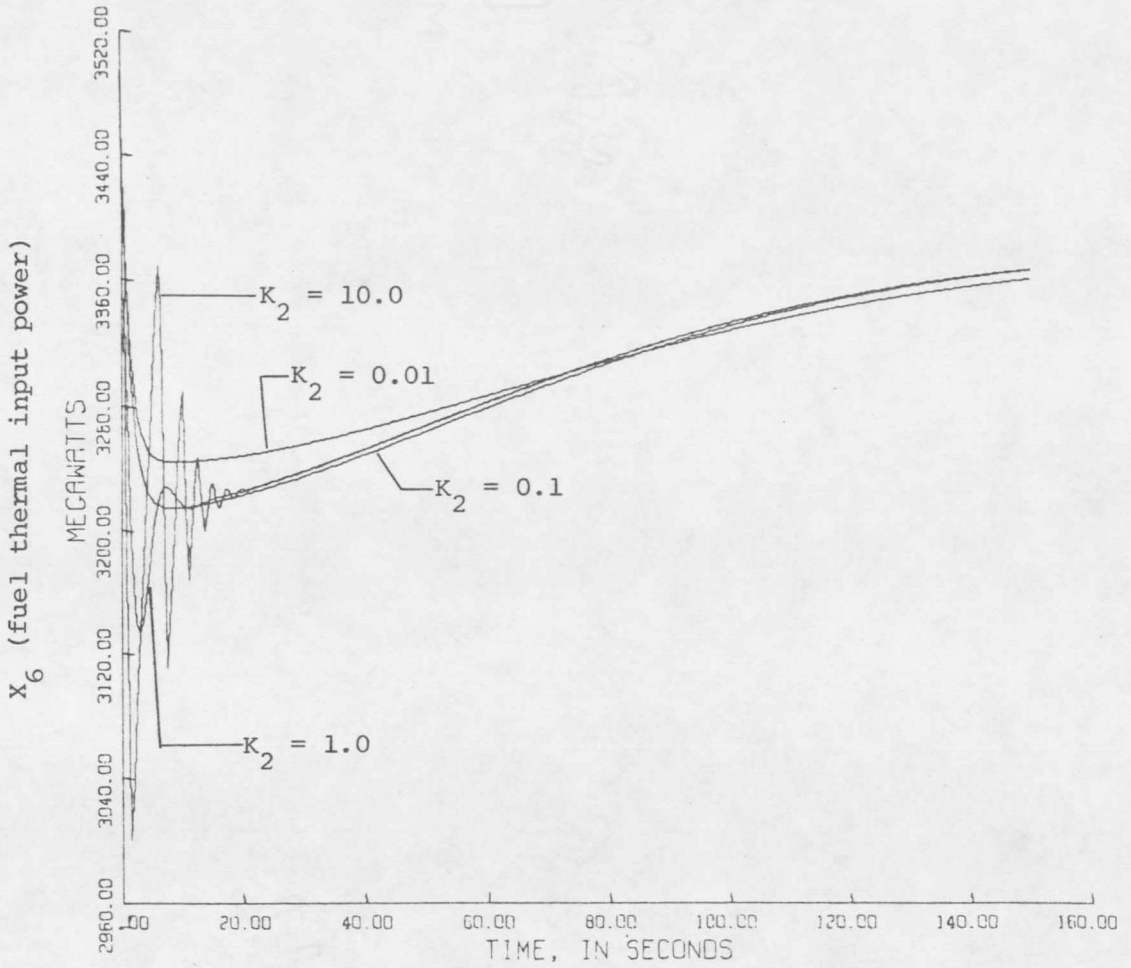



Figure 3.10. MW(REF) $X_1$ changes from 1620 MW to 1570 MW at t = 0+; $K_1$ = 0.01

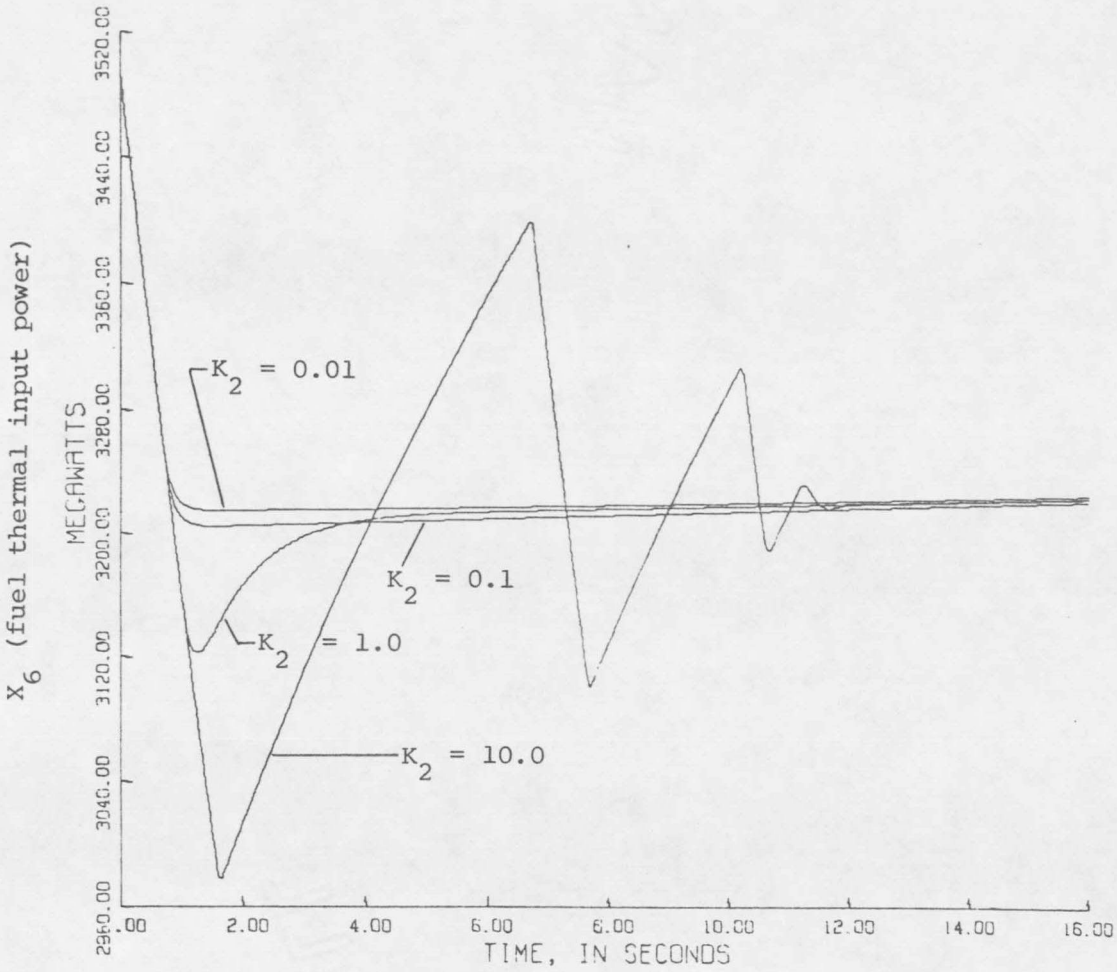



Figure 3.11. MW(REF) $X_1$ changes from 1620 MW to 1570 MW at t = 0+; $K_1$ = 0.1

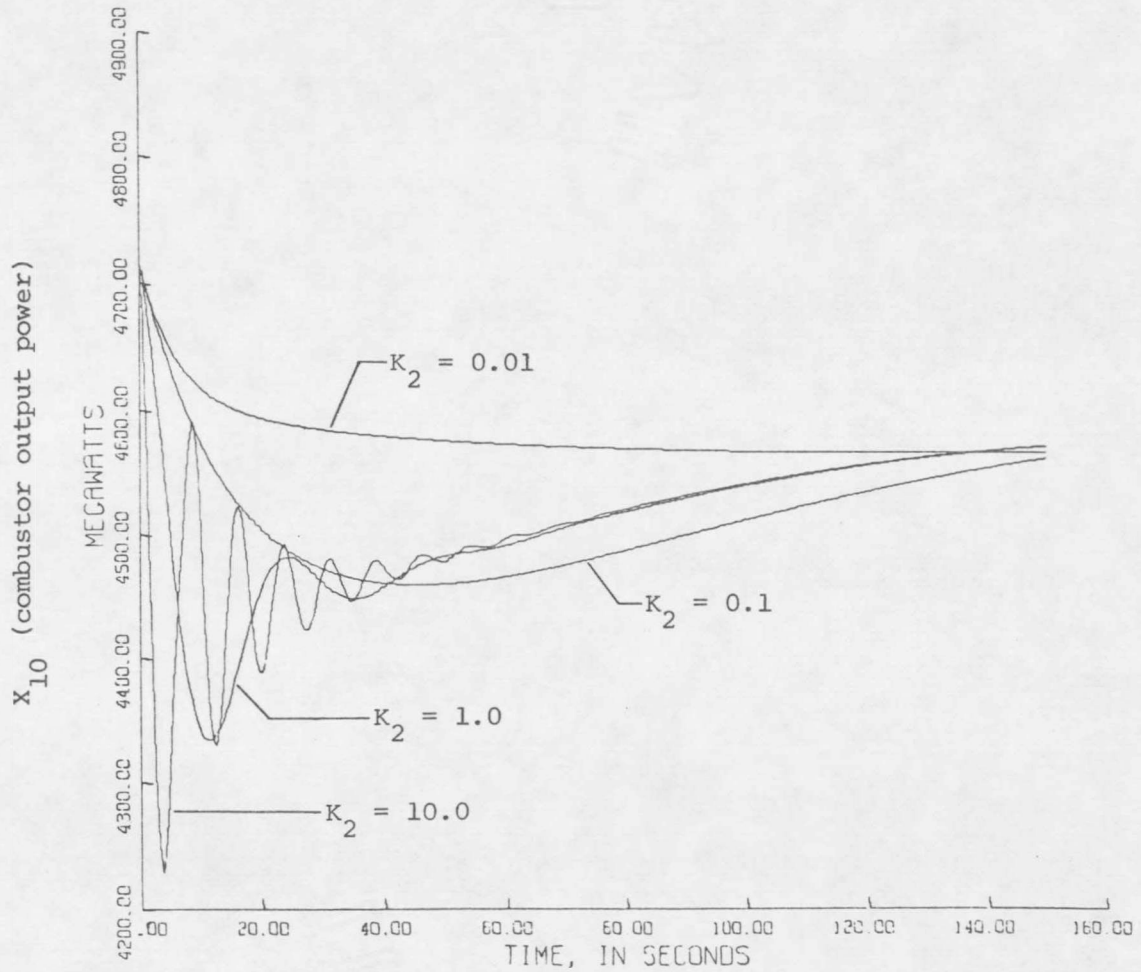



Figure 3.12. MW(REF) $X_1$ changes from 1620 MW to 1570 MW at t = 0+; $K_1$ = 0.001

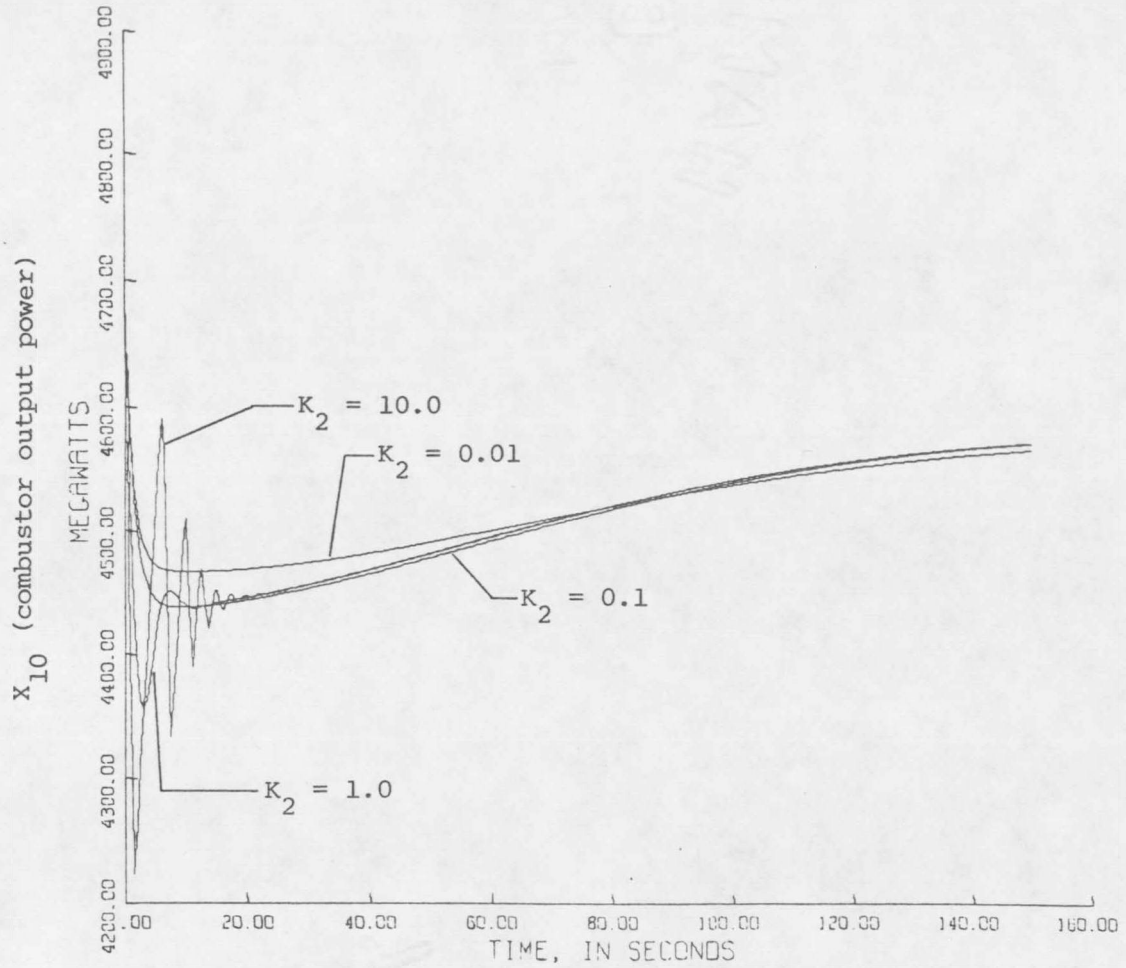



Figure 3.13. MW(REF) $X_1$ changes from 1620 MW to 1570 MW at t = 0+; $K_1$ = 0.01

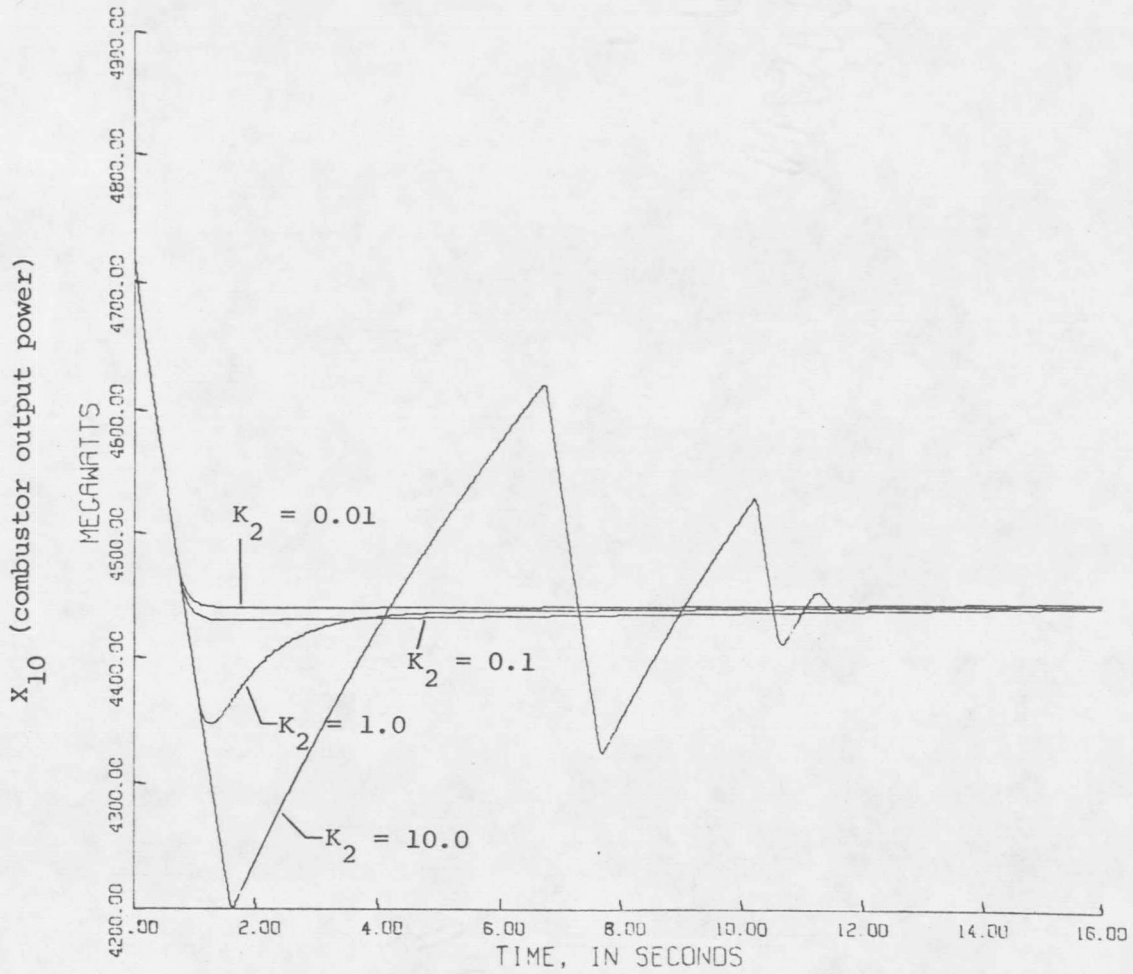



Figure 3.14. MW(REF) $X_1$ changes from 1620 MW to 1570 MW at t = 0+; $K_1$ = 0.1

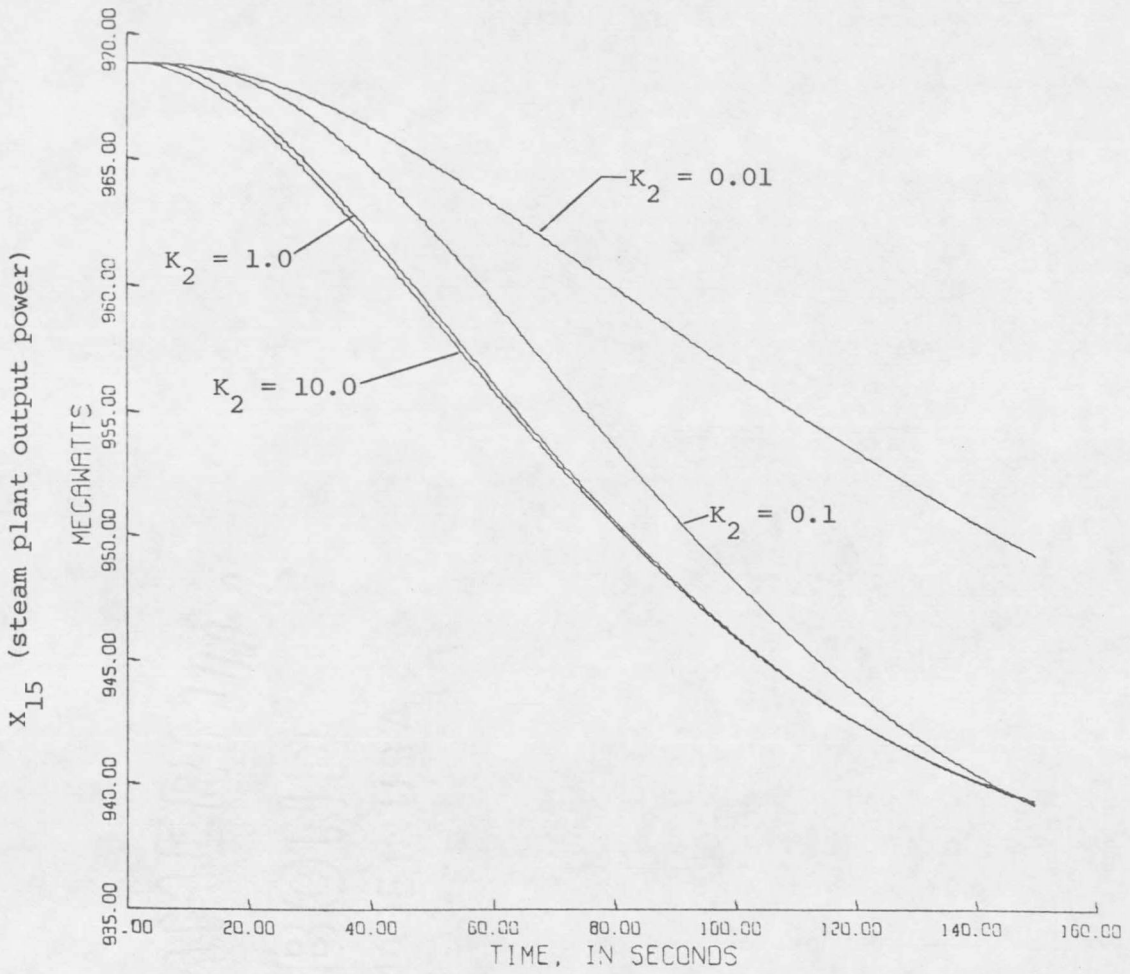



Figure 3.15. MW(REF) $X_1$ changes from 1620 MW to 1570 MW at t = 0+; $K_1$ = 0.001

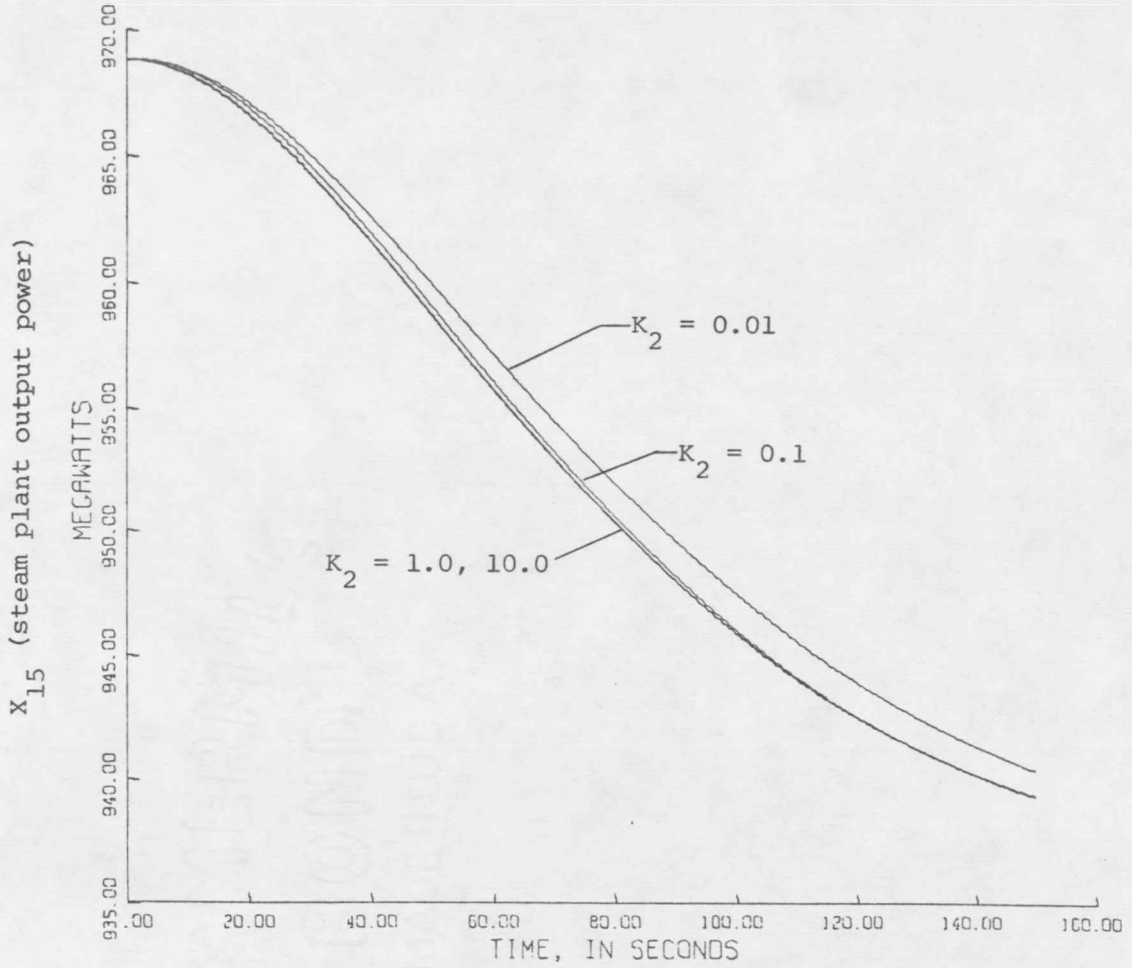



Figure 3.16. MW(REF) $X_1$ changes from 1620 MW to 1570 MW at t = 0+; $K_1$ = 0.01

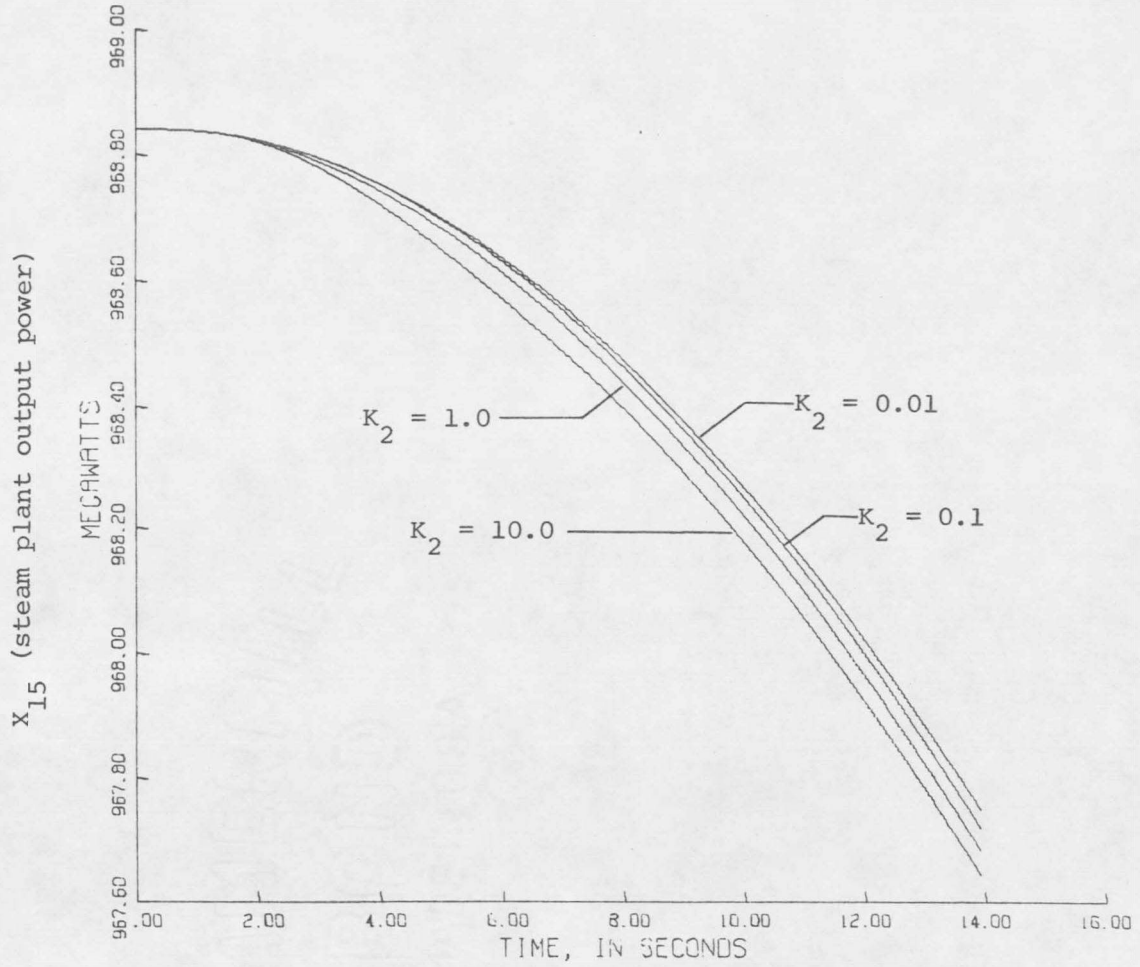



Figure 3.17. MW(REF) $X_1$ changes from 1620 MW to 1570 MW at t = 0+; $K_1$ = 0.1

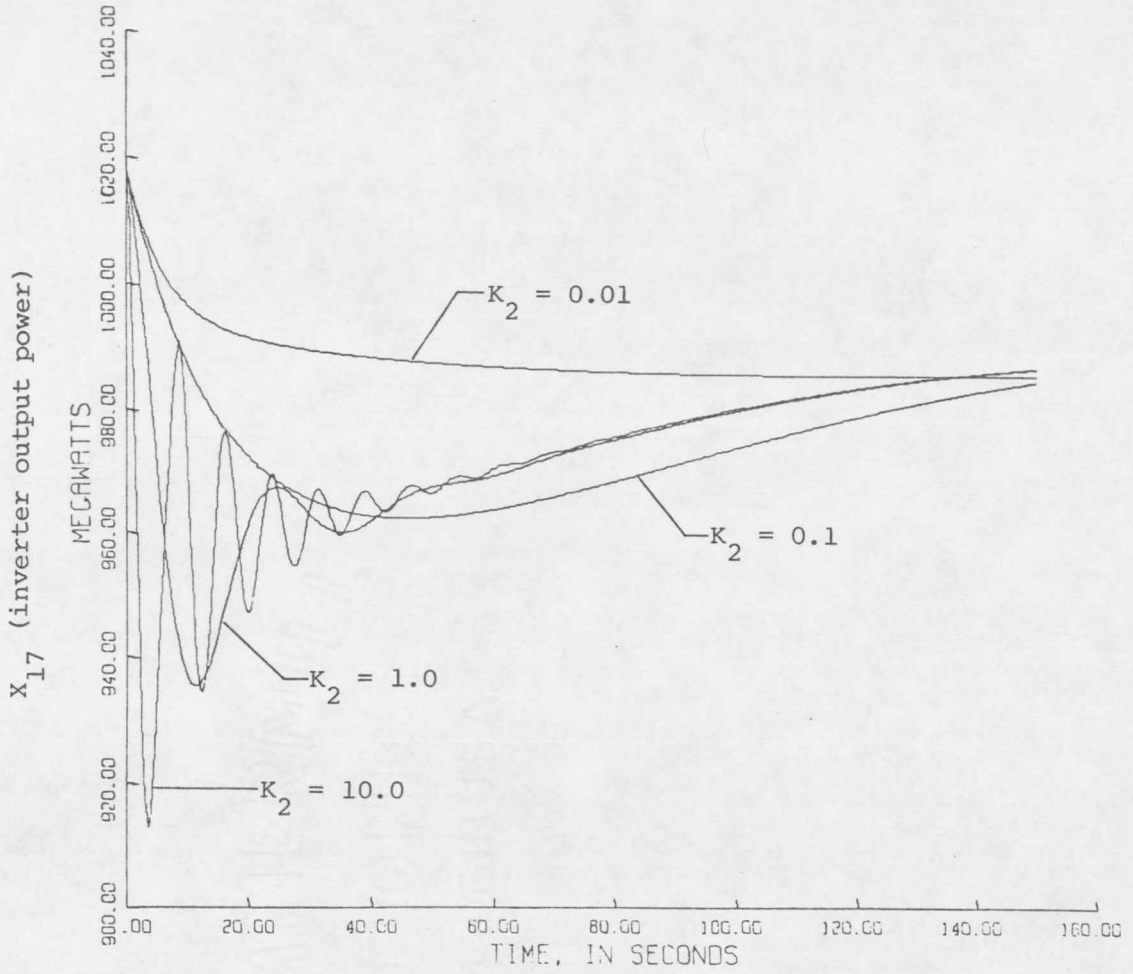



Figure 3.18. MW(REF) $X_1$ changes from 1620 MW to 1570 MW at t = 0+; $K_1$ = 0.001

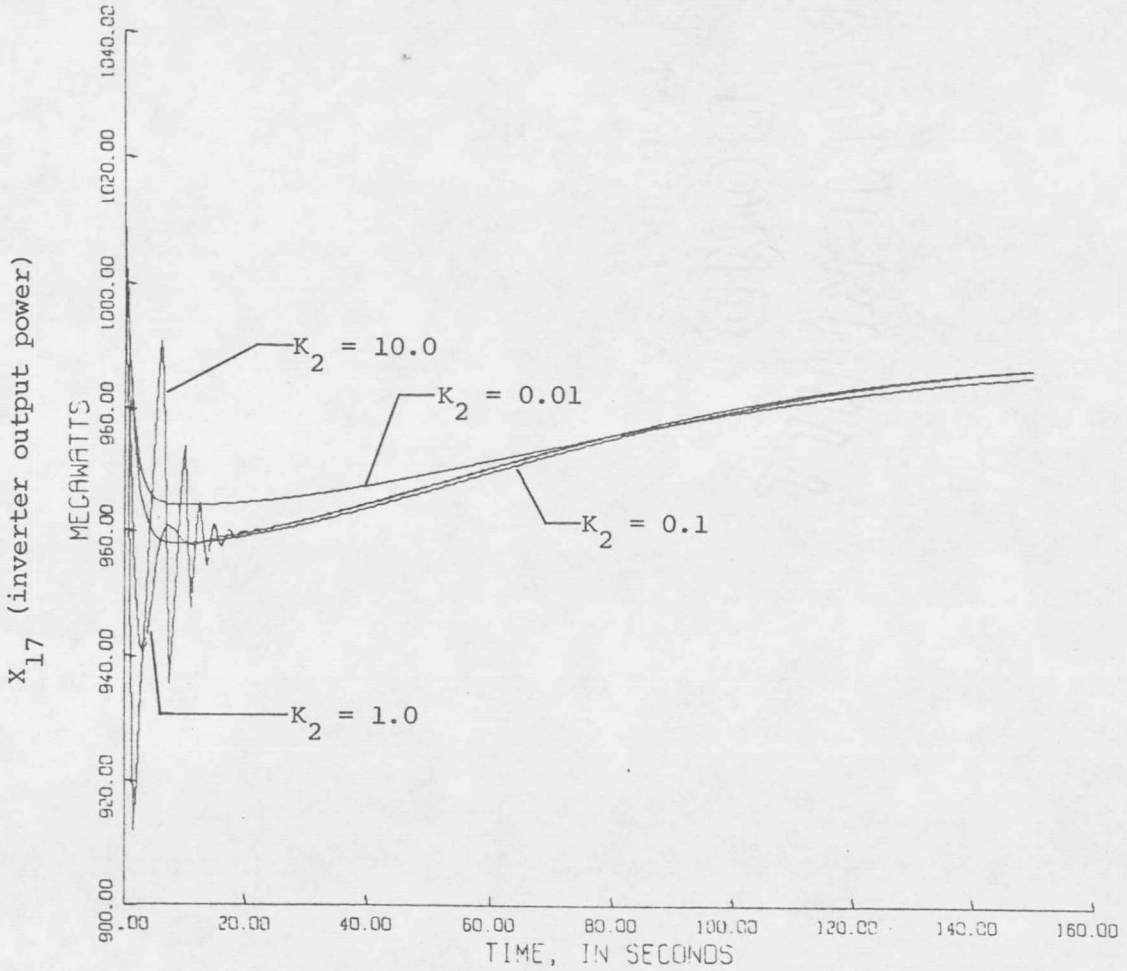



Figure 3.19. MW(REF) $X_1$ changes from 1620 MW to 1570 MW at t = 0+; $K_1$ = 0.01

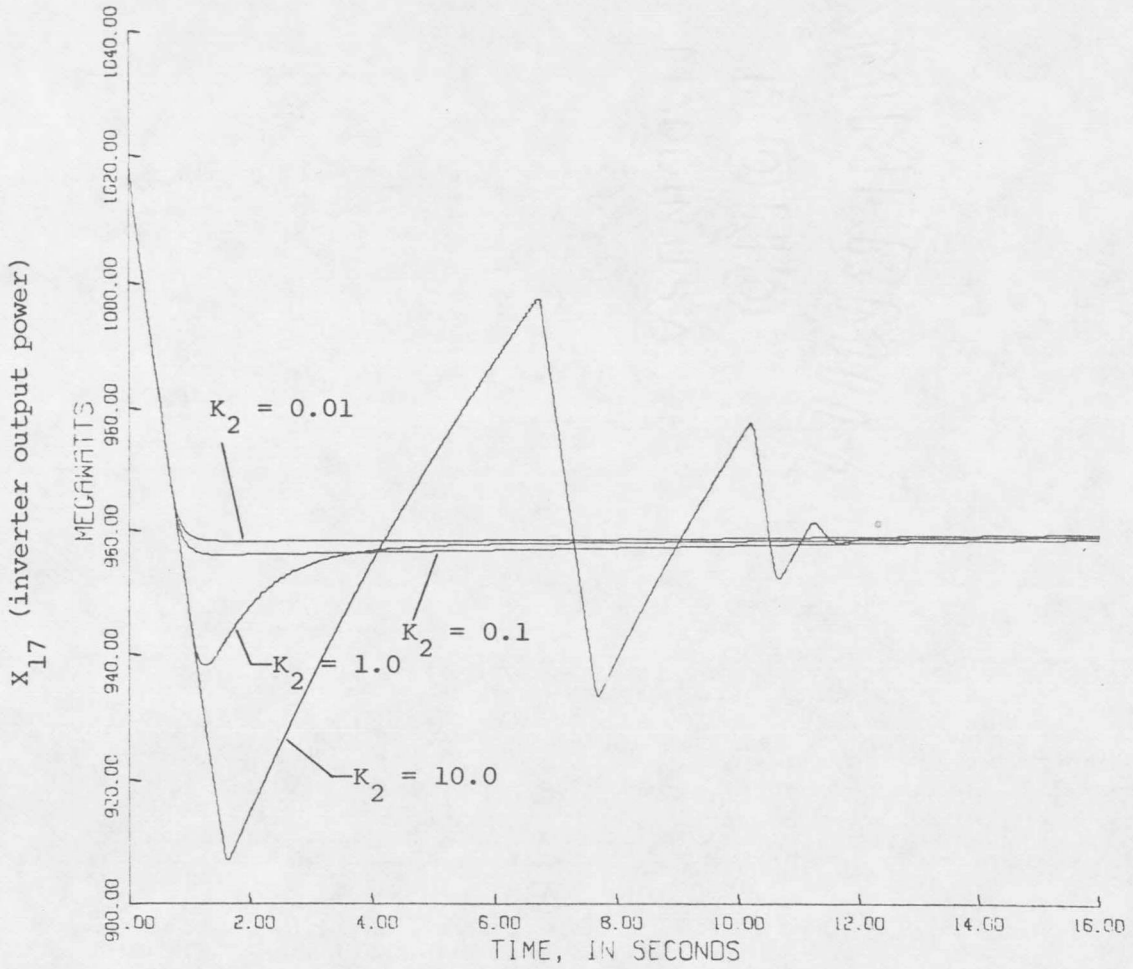



Figure 3.20. MW(REF) $X_1$ changes from 1620 MW to 1570 MW at t = 0+; $K_1$ = 0.1

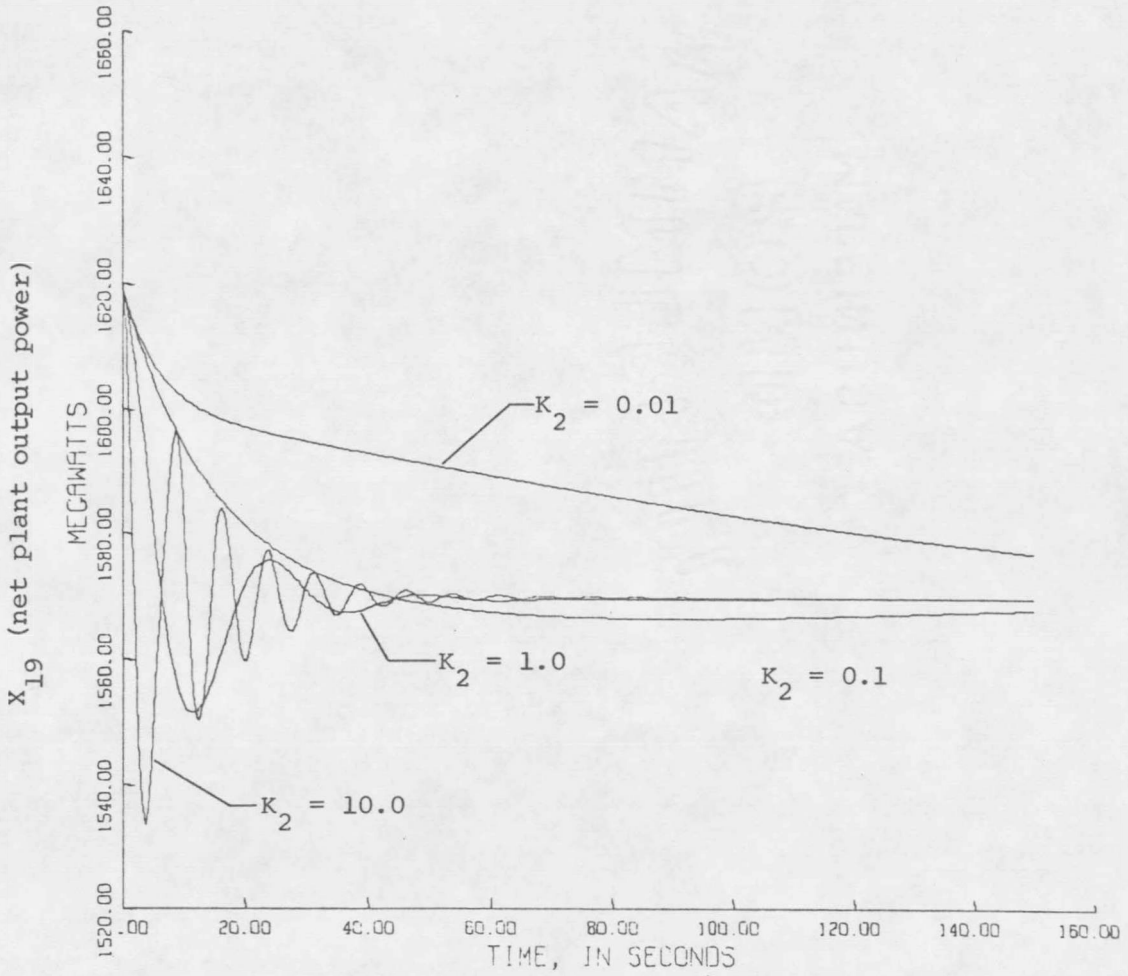



Figure 3.21. MW(REF) $X_1$ changes from 1620 MW to 1570 MW at t = 0+; $K_1$ = 0.001

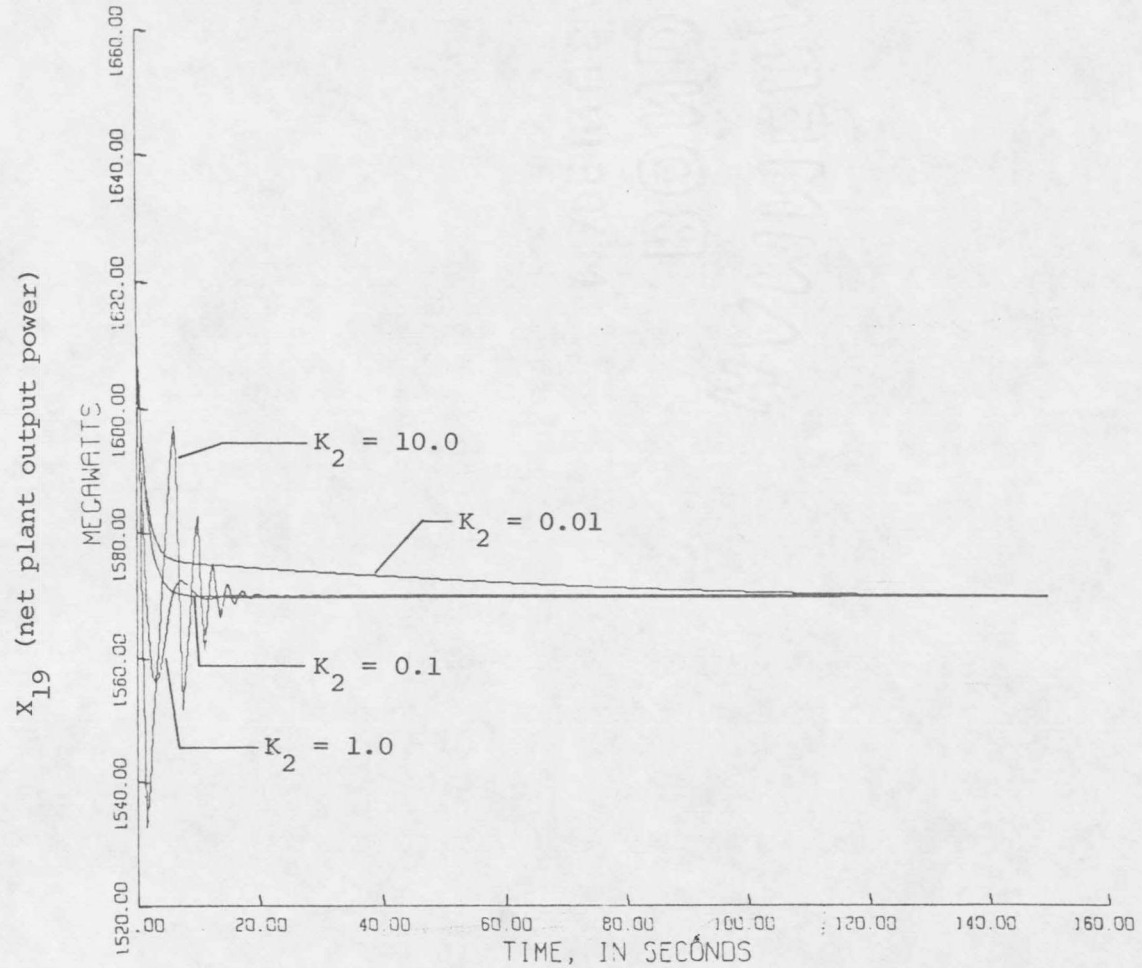



Figure 3.22. MW(REF) $X_1$ changes from 1620 MW to 1570 MW at t = 0+; $K_1$ = 0.01

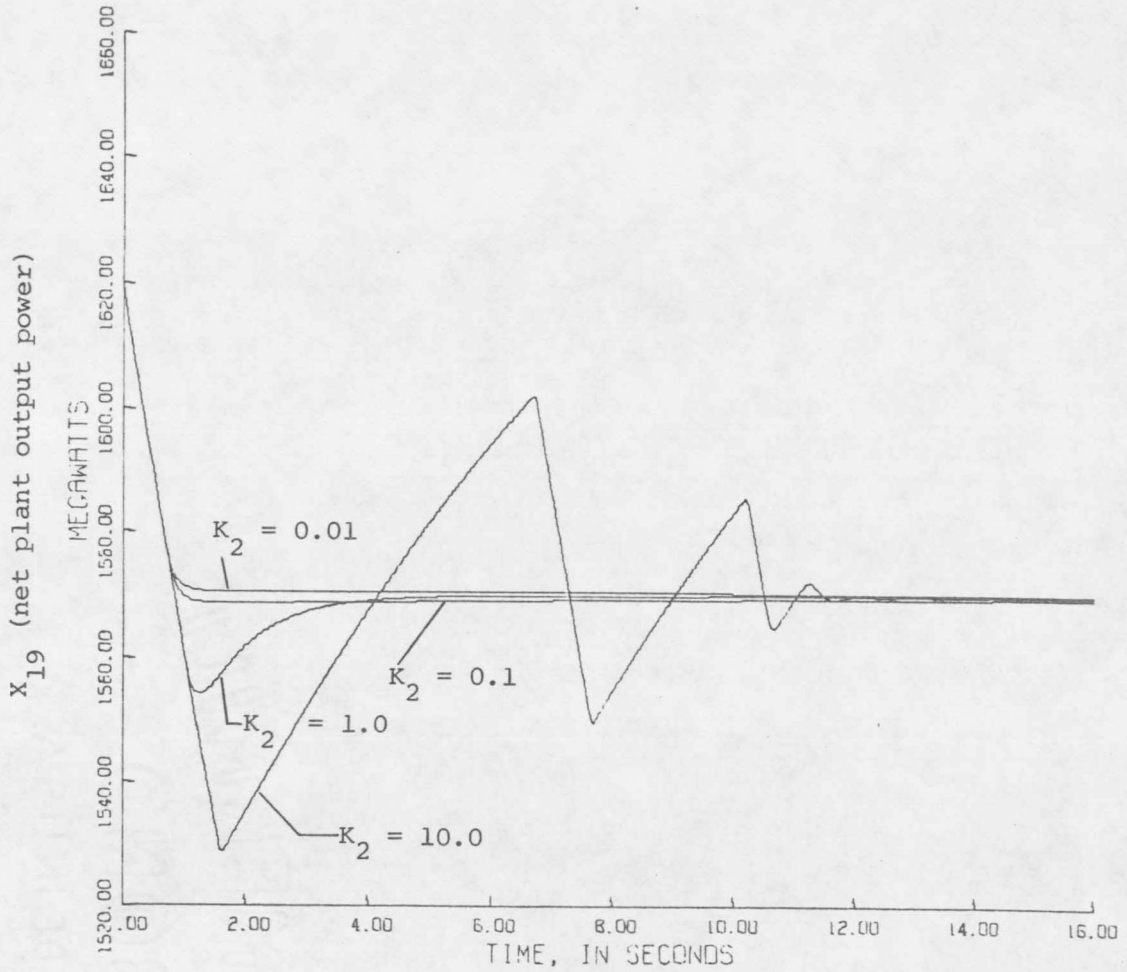



Figure 3.23. MW(REF) $X_1$ changes from 1620 MW to 1570 MW at t = 0+; $K_1$ = 0.1

$K_1$ = 10.0 were not included because they are nearly identical to Figure 3.23. In both cases limiter action is the dominant effect.

## 3.7 Classical Stability Analysis

Classical system stability analysis was performed on model I. This was done as a partial check on the computer solutions of the system equations. The model was assumed to be operating linearly, i.e., the magnitude limiter was considered to be bypassed. Mason's gain formula was utilized in finding the system characteristic equation, and the roots of the characteristic equation were examined for positive real parts for several value of controller constants $K_1$ and $K_2$.

The model I block diagram of Figure 3.3 contains four forward paths and five individual feedback loops. $X_1$ is the input variable and $X_{19}$ the output variable. Transfer functions for the forward paths are:

Forward path 1 gain:

$$M_1 = K_1\left(1 + \frac{K_2}{s}\right)\left(\frac{K_4}{1 + \tau_1 s}\right) K_7 K_8 K_{12} \tag{3.5}$$

Forward path 2 gain:

$$M_2 = K_1\left(1 + \frac{K_2}{s}\right)\left(\frac{K_4}{1 + \tau_1 s}\right)(1 - K_7)(1 - K_9)(K_{10})\left(\frac{1}{1 + \tau_4 s}\right)\left(\frac{1}{1 + \tau_5 s}\right)K_{12} \tag{3.6}$$

Forward path 3 gain

$$M_3 = K_1\left(1 + \frac{K_2}{s}\right)\left(\frac{K_4}{1 + \tau_1 s}\right)(K_5)\left(\frac{K_6}{1 + \tau_4 s}\right)K_7K_8K_{12} \tag{3.7}$$

Forward path 4 gain:

$$M_4 = K_1\left(1 + \frac{K_2}{s}\right)\left(\frac{K_4}{1 + \tau_1 s}\right)(K_5)\left(\frac{K_6}{1 + \tau_2 s}\right)(1 - K_7)(1 - K_9)(K_{10})\left(\frac{1}{1 + \tau_4 s}\right) \tag{3.8}$$

$$\cdot\left(\frac{1}{1 + \tau_5 s}\right)$$

The five individual feedback loops are:

$$P_{11} = -K_{13}M_1 \tag{3.9}$$

$$P_{21} = -K_{13}M_2 \tag{3.10}$$

$$P_{31} = -K_{13}M_3 \tag{3.11}$$

$$P_{41} = -K_{13}M_4 \tag{3.12}$$

$$P_{51} = (1 - K_7)(K_9)\left(\frac{K_6}{1 + \tau_2 s}\right) \tag{3.13}$$

By Mason's gain formula,

$$\frac{X_{19}}{X_1} = M = \sum_k \frac{M_k\Delta_k}{\Delta} = \sum_k \frac{M_k\Delta_k}{(1 - \sum_m P_{m1}} \tag{3.14}$$

Therefore,

$$\Delta = 1 + K_{13}(M_1 + M_2 + M_3 + M_4) - (1 - K_7)(K_9)\left(\frac{K_6}{1 + \tau_2 s}\right) \tag{3.15}$$

and

$$\frac{X_{19}}{X_1} = \frac{M_1 + M_2 + M_3 + M_4}{\Delta} \tag{3.16}$$

The characteristic equation of model I is obtained by setting $\Delta = 0$. The equation must not have any roots with positive real parts if the system is to be stable. The characteristic equation was found to be:

$$As^5 + Bs^4 + Cs^3 + Ds^2 + Es + F = 0 \tag{3.17}$$

where;

$$A = \tau_1\tau_2\tau_4\tau_5 \tag{3.18}$$

$$B = \tau_1\tau_2\tau_4 + \tau_1\tau_2\tau_5 + \tau_1\tau_4\tau_5 + \tau_2\tau_4\tau_5 + K_1K_4K_7K_8K_{12}\tau_2\tau_4\tau_5 + K_6K_9(K_7 - 1)\tau_1\tau_4\tau_5 \tag{3.19}$$

$$C = \tau_1\tau_2 + \tau_1\tau_4 + \tau_2\tau_4 + \tau_1\tau_5 + \tau_2\tau_5 + \tau_4\tau_5 + K_1K_4K_7K_8K_{12}(\tau_2\tau_4 + \tau_2\tau_5 + \tau_4\tau_5 + \tau_2\tau_2\tau_4\tau_5) + K_1K_4K_5K_6K_7K_8K_{12}\tau_4\tau_5 + K_6K_9(K_7 - 1)(\tau_1\tau_4 + \tau_1\tau_5 + \tau_4\tau_5) \tag{3.20}$$

$$D = \tau_1 + \tau_2 + \tau_4 + \tau_5 + K_1K_4K_7K_8K_{12}(\tau_2 + \tau_4 + \tau_5 + K_2\tau_2\tau_4 + K_2\tau_2\tau_5 + K_2\tau_4\tau_5) + K_1K_4K_5K_6K_7K_8K_{12}(\tau_4 + \tau_5 + K_2\tau_4\tau_5) + K_1K_4K_{10}K_{12}(1 - K_7)(1 - K_9)(\tau_2) + K_6K_9(K_7 - 1)(\tau_1 + \tau_4 + \tau_5) \tag{3.21}$$

$$E = 1 + K_1K_4K_7K_8K_{12}(1 + K_2\tau_2 + K_2\tau_4 + K_2\tau_5)$$
$$+ K_1K_4K_5K_6K_7K_8K_{12}(1 + K_2\tau_4 + K_2\tau_5)$$
$$+ K_1K_4K_{10}K_{12}(1 - K_7)(1 - K_9)(1 + K_2\tau_2)$$
$$+ K_1K_4K_5K_6K_{10}K_{12}(1 - K_7)(1 - K_9) + K_6K_9(K_7 - 1) \qquad (3.22)$$

$$F = K_1K_2K_4K_7K_8K_{12} + K_1K_2K_4K_5K_6K_7K_8K_{12}$$
$$+ K_1K_2K_4K_{10}K_{12}(1 - K_7)(1 - K_9)$$
$$+ K_1K_2K_4K_5K_6K_{10}K_{12}(1 - K_7)(1 - K_9) \qquad (3.23)$$

The characteristic equation roots were found for the following cases, defined in terms of controller constants $K_1$ and $K_2$.

| | | | |
|---|---|---|---|
| Case I. | (a) | $K_1 = 0.001$ | $K_2 = 0.01$ |
| | (b) | $K_1 = 0.001$ | $K_2 = 0.1$ |
| | (c) | $K_1 = 0.001$ | $K_2 = 1.0$ |
| | (d) | $K_1 = 0.001$ | $K_2 = 10.0$ |
| Case II. | (a) | $K_1 = 0.01$ | $K_2 = 0.01$ |
| | (b) | $K_1 = 0.01$ | $K_2 = 0.1$ |
| | (c) | $K_1 = 0.01$ | $K_2 = 1.0$ |
| | (d) | $K_1 = 0.01$ | $K_2 = 10.0$ |

Case III. (a) $K_1 = 0.1$ $K_2 = 0.01$

(b) $K_1 = 0.1$ $K_2 = 0.1$

(c) $K_1 = 0.1$ $K_2 = 1.0$

(d) $K_1 = 0.1$ $K_2 = 10.0$

Case IV. (a) $K_1 = 1.0$ $K_2 = 0.01$

(b) $K_1 = 1.0$ $K_2 = 0.1$

(c) $K_1 = 1.0$ $K_2 = 1.0$

(d) $K_1 = 1.0$ $K_2 = 10.0$

Case V. (a) $K_1 = 10.0$ $K_2 = 0.01$

(b) $K_1 = 10.0$ $K_2 = 0.1$

(c) $K_1 = 10.0$ $K_2 = 1.0$

(d) $K_1 = 10.0$ $K_2 = 10.0$

In all cases the following constant values were used:

$K_3 = 1.00$ $K_8 = 0.97$

$K_4 = 4040.00$ $K_9 = 0.248$

$K_5 = 0.09$ $K_{10} = 0.351$

$K_6 = 1.00$ $K_{11} = 0.0953$

$K_7 = 0.2225$ $K_{12} = 0.815$

$\tau_1 = 10.0$ $\tau_4 = 67.5$

$\tau_2 = 360.0$ $\tau_5 = 62.0$

$\tau_3 = 0.0$

None of the roots of the characteristic equation cases investigated have positive real parts. These results agree with the computer solutions described earlier in this chapter as all are stable.

# Chapter IV

# SYSTEM MODEL II

## 4.1 Basis for Model II

System model II represents a logical extension of the model I order of complexity. A block diagram of model II is shown in Figure 4.1, and a comparison between Figure 4.1 and the block diagram of model I in Figure 3.3 is appropriate. The idealized heat balance of Figure 3.1 is retained, which means that power flow in model II is similar to model I. The form of the proportional-integral controller and the fuel supply system is unchanged, except for a pure time delay $\tau_1$. Generated power is still the controlled variable, being compared with desired generation, MW(REF), to form the basis of control. The MHD channel enthalpy extraction representation remains the same as does the steam plant model.

Model II extends model I in the following ways:

1) Transport delays are included between the fuel valve and the MHD channel ($\tau_1$), between the radiant boiler and steam plant ($\tau_4$), and between the MHD channel and heat exchangers ($\tau_5$).

2) $T_1(t)$ and $E_1(t)$ describe time variations in preheated air temperature and variations in input power to the steam bottoming plant due to cycling of the heat exchangers.

3) A feedback path denoted by the variable Z has been introduced to reduce variations in combustion air preheat temperature.

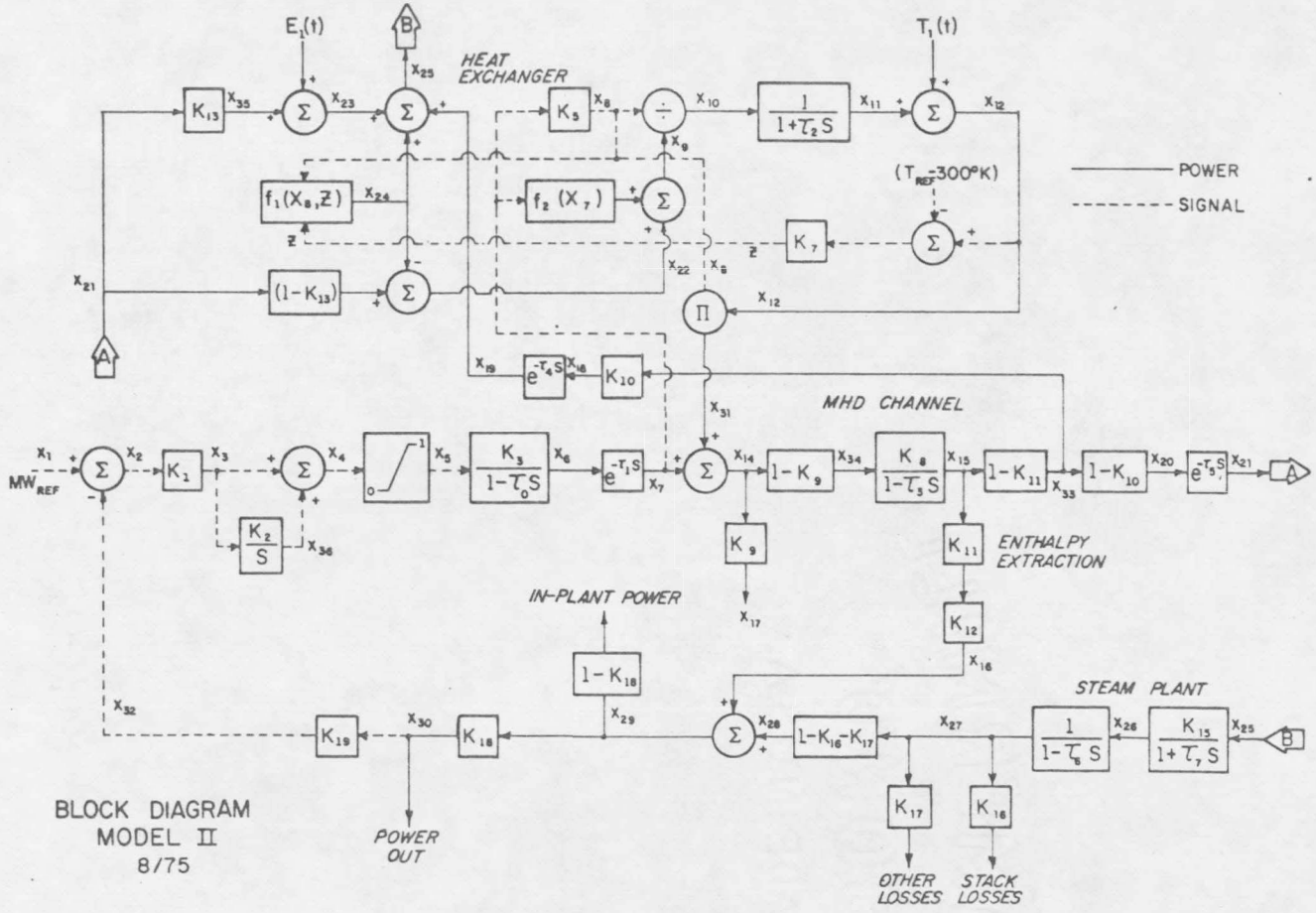



Figure 4.1. Block diagram for model II

4) A radiant boiler in the diffuser has been added.

5) A nonlinear block ($f_1$) is used to implement the combustion air preheat temperature control, where $f_1 = Z\ X_8$.

6) A nonlinear block ($f_2$) describes compressor power, where $f_2$ is given in Equation 4.12 on page 99.

## 4.2 Combustion Calculations

The assumption leading to the air/fuel mass ratio and calorific value of the fuel are the same for model II and model III, discussed in Chapter V. They give:

$$\frac{\text{mass of air}}{\text{mass of fuel}} = 9.27$$

Calorific value of fuel = $0.29257 \times 10^8$ J/Kg

Thus, if fuel thermal input power PT is known, the mass flow rate of combustion air, $\dot{m}$, may be determined.

$$\dot{m} = \frac{PT\ (J/sec)}{0.29257 \times 10^8\ (J/Kg)}$$

$$= (3.1685 \times 10^{-7})(PT)\ \ Kg/sec \qquad (4.1)$$

where the dimensions of PT are joules/second or watts.

In model II, it is necessary to convert between fuel thermal input power PT in megawatts ($MW_T$) and air temperature in degrees Kelvin (°K). A mean specific heat of air at constant pressure,

$C_p$ = 1122 J/Kg °K, is used, and ambient air temperature is taken to be 300°K. Preheated air temperature can then be predicted, knowing the air mass flow rate and power PA required to increase air temperature. At any fuel thermal input power PT, the power required to raise combustion air 1°K is:

$$\frac{PA}{°K} = (3.1685 \times 10^{-7} \frac{Kg}{J})(PT \frac{J}{sec})(1122 \frac{J}{Kg\ °K})$$

$$= (3.555 \times 10^{-4})(PT) \quad \frac{watts}{°K} \tag{4.2}$$

Equation 4.2 may be written as

$$\frac{PA}{°K} = (PT)(3.555 \times 10^{-4} \frac{MW}{MW_T\ °K}) \quad \frac{MW}{°K} \tag{4.3}$$

where PT is dimensioned in megawatts ($MW_T$). Since 1200°C (1473.15°K) air is desired out of the air preheaters and ambient air is 300°K, $\Delta$°K = 1173.15°K. Required power to achieve this temperature increase at PT = 3500 $MW_T$ is

$$PA = (1173.15°K)(3500\ MW_T)(3.555 \times 10^{-4} \frac{MW}{MW_T\ °K})$$

$$= 1459.69\ MW \tag{4.4}$$

and

$$\frac{PA}{°K} = 1.244\ MW/°K$$

Mean specific heat of air at constant pressure was found by approximating the partial derivatives of air enthalpy, HA, with respect to temperature T. Equation 4.5 [105] was solved for values of T between 250°K and 1950°K in 100°K steps. $C_p = \frac{\partial HA}{\partial T}$ was approximated $\frac{\Delta HA}{\Delta T}$.

$$HA(T) = \frac{2.93\times10^4(1+PSIA)T + 8.37\times10^3\left[\frac{2230}{e^{(2230/T)-1}} + \frac{(3340)(PSIA)}{e^{(3340/T)-1}}\right]}{32 + (28)(PSIA)} \qquad (4.5)$$

PSIA = nitrogen/oxygen ratio of air and was taken to be 3.76. The function $\Delta HA/\Delta T$ vs. T was approximated by a straight line, and $C_p$ was averaged between T = 1473.15°K and T = 300°K.

A check on the value of $C_p$ was made by the following equation.

$$PA = [HA(1473.15°K) - HA(300°K)]\,\dot{m} \qquad (4.6)$$

where $\dot{m}$ = 1108.9 Kg/sec at PT = 3500 $MW_T$, and HA(T) is given in Equation 4.5. PA = 1461.5 MW if determined by Equation 4.6, and equals 1459.7 MW if found by using mean specific heat $C_p$ and Equation 4.4. This represents an error in PA of 0.12%, which was considered acceptable.

The compressor power function, $f_2$, was determined by the compressor Equations 4.7 and 4.8 [15], and by combustor pressure data given by the Combustor/Nozzle/Channel/Diffuser simulation described in Chapter V [114].

$$PCOMP = (\dot{m})(C_p)(T_a)(P_c^{0.286} - 1)/\eta_c \quad (4.7)$$

$$T(OUT) = \frac{PCOMP}{(\dot{m})(C_p)} + T_a = T_a[(P_c^{0.286} - 1)/(\eta_c) + 1] \quad (4.8)$$

where

PCOMP = compressor power (MW)

$\dot{m}$ = mass flow rate of air (Kg/sec)

$C_p$ = mean specific heat of air at constant pressure (M Joules/Kg °K)

$T_a$ = ambient air temperature (°K)

$P_c$ = ratio of stagnation pressure at compressor exit to inlet pressure

$\eta_c$ = compressor efficiency (taken to be 0.87)

T(OUT) = air temperature at compressor exit (°K)

Table 4.1 illustrates the dependence of $P_c$ and T(OUT) on PT. The $P_c$ values were obtained from Combustor/Nozzle/Channel/Diffuser data [114] and T(OUT) values were found solving Equation 4.8. $T_a$ = 300°K and preheat air temperatures at the heat exchanger exit, TPHAO, was assumed to be 1800°K. The variation of T(OUT) with PT is nearly linear and was approximated by

$$\frac{\Delta T(OUT)}{\Delta PT} = 0.029 \text{ °K/MW} \quad (4.9)$$

Table 4.1. Compressor parameters I

| PT(MW) | TPHAO(°K) | $p_c$(atmospheres) | T(OUT)(°K) |
|---|---|---|---|
| 3000 | 1800 | 6.95 | 555.53 |
| 3250 | 1800 | 7.265 | 563.19 |
| 3500 | 1800 | 7.576 | 570.52 |
| 3750 | 1800 | 7.885 | 577.60 |
| 4000 | 1800 | 8.193 | 584.46 |
| 4250 | 1800 | 8.502 | 591.16 |

Table 4.2 shows the dependence of $p_c$ and T(OUT) on TPHAO. PT is constant.

Table 4.2. Compressor parameters II

| PT(MW) | TPHAO (°K) | $p_c$(atmospheres) | T(OUT)(°K) |
|---|---|---|---|
| 3500 | 1700 | 7.255 | 563.0 |
| 3500 | 1800 | 7.576 | 570.5 |
| 3500 | 1900 | 7.90 | 581.2 |

The three data points of Table 4.2 were linearly extrapolated to give T(OUT) = 539°K at TPHAO = 1473.15°K.

Assuming that TPHAO variations are not significant for the cases of interest, T(OUT) can be considered a function of PT only. From Equation 4.9,

$$T(OUT) = [539 + (0.029)(PT - 3500)]\ °K \qquad (4.10)$$

where PT is in megawatts ($MW_T$). Solving Equation 4.8 for PCOMP gives,

$$PCOMP = (T(OUT) - T_a)(\dot{m})(C_p)$$

$$= (239 + (0.029)(PT - 3500)(3.55x10^{-4})(PT) \quad MW \qquad (4.11)$$

If PT = 3500 $MW_T$ and TPHAO = 1473.15°K, PCOMP = 297.4 MW. Using Equation 4.4, the power supplied to the air by the heat exchangers is (1459.69 - 297.4)MW or 1162.29 MW.

## 4.3 Heat Exchanger Cycle Model

A model of heat exchanger cycling is a feature of system model II. The effect of cycling individual heat exchangers between reheat and blowdown is to introduce a periodic fluctuation in both preheated combustion air temperature and power available at the exit of the heat exchangers for steam generation. The fluctuations appear in Figure 4.3 as $T_1(t)$ and $E_1(t)$. These time functions are a consequence of a non-unique regenerative heat exchanger cycling schedule. Reheat is the part of the exchanger cycle in which the ceramic core of the heat exchanger is heated by combustion gas passing through the core from the diffuser to the steam plant. Blowdown occurs when air is heated by being moved through the heat exchanger from the compressor to the combustor.

One possible heat exchanger cycling schedule is shown in Figure 4.2. It is based on the tentative design of a heat exchanger system

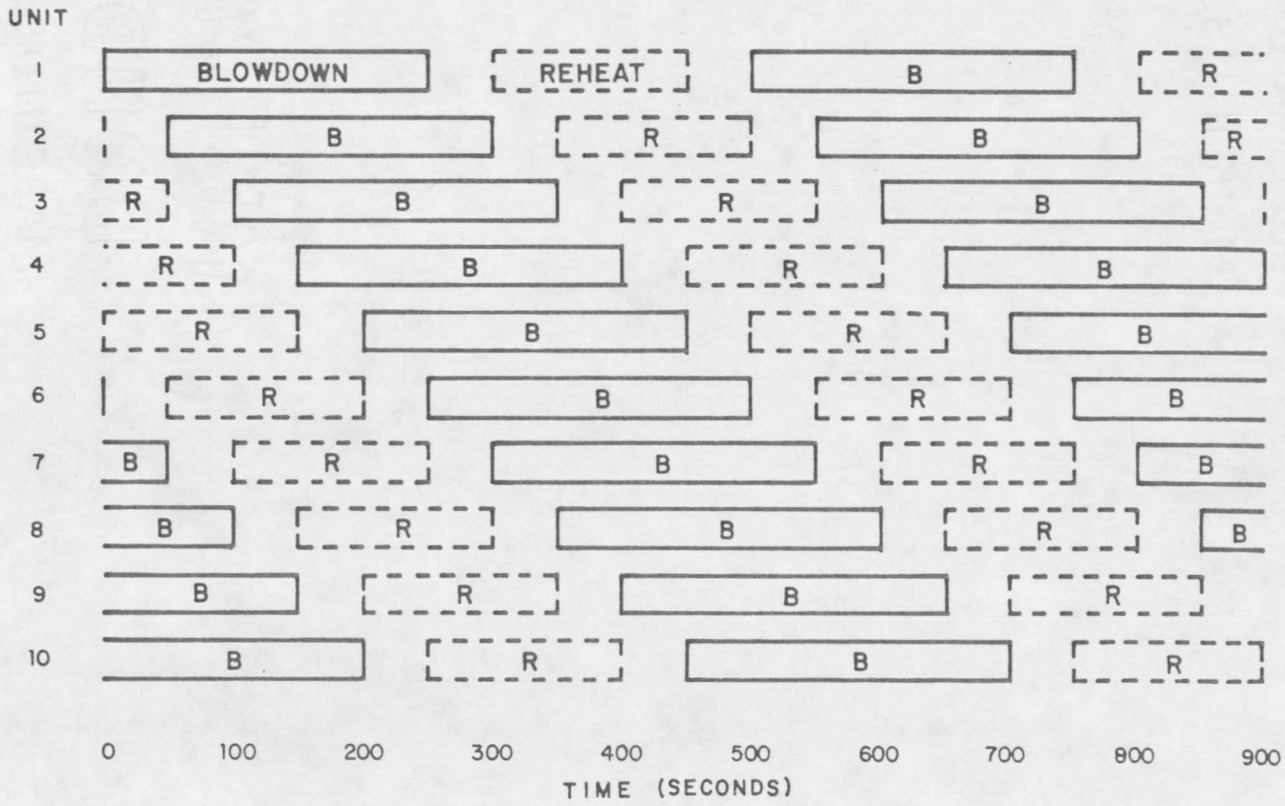



Figure 4.2. Regenerative heat exchanger schedule

for ECAS Base Case 1, an 1877 MW (electrical) MHD/steam combined cycle [136]. Ten individual heat exchanger units are used. There are always three units on reheat, five on blowdown, and two on hold. For any given unit, reheat time is 150 seconds, blowdown time is 250 seconds, and hold time is 50 seconds between each reheat and blowdown. Cycle time for a given unit is 500 seconds.

The switching procedure must allow constant mass flow of air and combustion gas. This implies that as a valve in one heat exchanger opens or closes, a valve in another heat exchanger must be acting in the opposite manner at exactly the same time. This action must apply to both valving combustion gas at the beginning or end of reheat and valving air at the beginning or end of blowdown. Valves are assumed to open or close instantaneously at the beginning or end of blowdown and reheat. For example, if a unit were switching between blowdown and reheat, the air flow is shut off immediately at the end of blowdown with no throttling action of the valve. No flow of either air or combustion gas occurs for the 50 second hold period. At the end of the hold period (beginning of reheat), combustion gas immediately flows at full mass flow rate and continues to do so until the end of reheat.

Several interesting observations may be made with the aid of Figure 4.2 [136].

1) Blowdown time, reheat time, and total cycle period are all integral multiples of hold time.

2) The number of heat exchangers required in the system equals total cycle period divided by hold time.

3) The number of heat exchangers in blowdown equals blowdown time divided by hold time and must be an integer. A similar relationship holds for the number of heat exchangers in reheat.

Using the heat exchanger schedule of Figure 4.2, it has been found by the authors of [136] that preheated air temperature (blowdown outlet temperature) drops linearly throughout blowdown for a given heat exchanger. The temperature variation is approximately 100°K for the 250 second blowdown period. Since a heated exchanger is valved into blowdown every 50 seconds while a cooled exchange is valved into reheat simultaneously (and instantaneously), time functions for $T_1(t)$ and $E_1(t)$ follow directly. These time functions have a period of 50 seconds and are sawtooth waveforms. Peak-to-peak amplitude of $T_1(t)$ is (100°K)/5 or 20°K. Peak-to-peak amplitude of $E_1(t)$ is found from Equation 4.4 and is (1.244 MW/°K)(20°K) = 24.88 MW at PT = 3500 $MW_T$.

The relative phase of $T_1(t)$ and $E_1(t)$ may be determined by the following argument. Air preheat temperature is a maximum just after a

reheated exchanger is valved into blowdown. At the same time, a cooled exchanger is valved into reheat so that maximum heat is absorbed by the cooled ceramic and minimum heat or thermal power is available to the steam plant. As the exchanger progresses through the reheat part of the cycle, the ceramic temperature increases and therefore absorbs less heat from the combustion gas, leaving more for the steam cycle. During the same time interval, the heat exchanger on blowdown continually cools, causing air preheat temperature to decrease. Thus, $T_1(t)$ and $E_1(t)$ are 180° out of phase from each other. Plots of $T_1(t)$ and $E_1(t)$ appear in Figure 4.3.

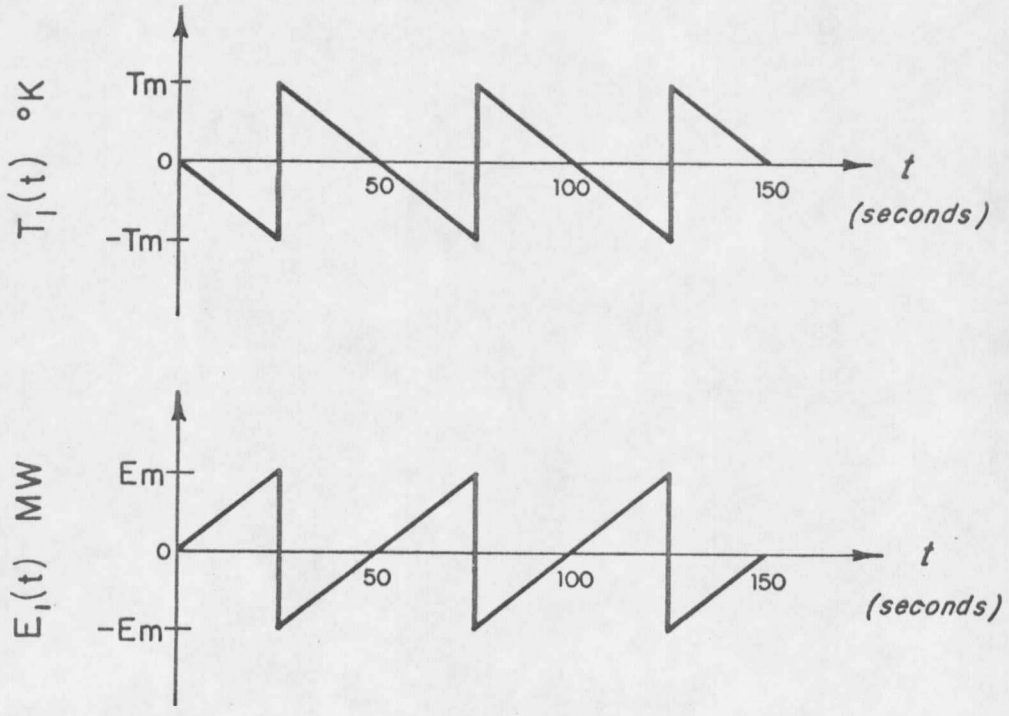



Figure 4.3. Variations in preheated air temperature and power to steam plant

## 4.4 Description of System Variables

The variables for model II are tabulated in Table 4.1. Refer to the block diagram of Figure 4.3.

Table 4.3. Description of model II system variables

| Variable | Units | Description |
|---|---|---|
| $X_1$ | MW | desired plant output; MW reference |
| $X_2$ | MW | generation error |
| $X_3$ | -- | proportional control signal |
| $X_4$ | -- | composite valve control signal |
| $X_5$ | -- | limited composite control signal |
| $X_6$ | MW | intermediate firing system variable |
| $X_7$ | $MW_T$ | fuel thermal input power |
| $X_8$ | MW/°K | conversion between power in air, PA, and air temperature |
| $X_9$ | MW | total power to preheat air |
| $X_{10}$ | °K | increase in air temperature above ambient |
| $X_{11}$ | °K | increase in air temperature above ambient accounting for lag due to heat exchanger cycling |
| $X_{12}$ | °K | actual preheated air temperature neglecting ambient |
| $X_{13}$ | -- | not used |
| $X_{14}$ | MW | combustor output power (input to MHD generator) |
| $X_{15}$ | MW | MHD generator input power, accounting for losses to ambient and time lag for combustor residence time |
| $X_{16}$ | MW | inverter output power |
| $X_{17}$ | MW | Combustor/Nozzle/Channel/Diffuser ambient losses |
| $X_{18}$ | MW | fraction of thermal power at diffuser absorbed by radiant boiler |

Table 4.3 (contin.)

| Variable | Units | Description |
|---|---|---|
| $X_{19}$ | MW | radiant boiler output available to steam plant |
| $X_{20}$ | MW | thermal power in combustion gases leaving diffuser |
| $X_{21}$ | MW | thermal power in combustion gases available to preheat air or generate steam |
| $X_{22}$ | MW | power from combustion gases used to preheat air assuming no preheated air temperature error |
| $X_{23}$ | MW | power from combustion gases used to generate steam, including $E_1(t)$ effect |
| $X_{24}$ | MW | power shifted from air preheating to steam generation or vice versa, depending on preheated air temperature error |
| $X_{25}$ | MW | steam plant input power |
| $X_{26}$ | MW | intermediate steam plant variable |
| $X_{27}$ | MW | gross steam plant output power |
| $X_{28}$ | MW | net steam plant output power |
| $X_{29}$ | MW | gross plant generated power |
| $X_{30}$ | MW | net plant output power |
| $X_{31}$ | MW | power from preheated air to combustor |
| $X_{32}$ | -- | actual generation control signal |
| $X_{33}$ | MW | thermal power in combustion gas after ambient losses and enthalpy extraction by the channel are subtracted |
| $X_{34}$ | MW | thermal power in combustion gas after subtracting ambient losses in Combustor/Nozzle/Channel/Diffuser |
| $X_{35}$ | MW | thermal power in combustion gases available to generate steam, assuming no preheated air temperature error |
| $X_{36}$ | -- | integral control signal |

## 4.5 Initial Conditions, Values of Constants, and System Equations

Initial conditions for the variables of model II and nominal values of constants were developed from the idealized heat balance of Figure 3.1 and the combustion calculations of this chapter. The variables and constants may be identified with the aid of Figure 4.1.

From Equation 4.2, $K_5 = 3.555 \times 10^{-4}$ MW/MW$_T$ °K. $f_2(X_7)$ is equal to PCOMP, defined by Equation 4.11.

$$PCOMP = f_2(X_7) = (239 + (0.029)(X_7 - 3500))(3.555 \times 10^{-4})(X_7) \quad MW \tag{4.12}$$

$$f_2(X_7(0)) = 297.38 \text{ MW} \tag{4.13}$$

$$X_8(0) = K_5 X_7(0) = 1.244 \text{ MW/°K} \tag{4.14}$$

From Equation 4.4, $X_9(0) = 1459.69$ MW.

$$X_{22}(0) = X_9(0) - f_2(X_7(0)) = 1162.32 \text{ MW} \tag{4.15}$$

$$X_{11}(0) = X_{12}(0) = 1173.15°K \tag{4.16}$$

$$X_{31}(0) = X_9(0) = 1459.69 \text{ MW} \tag{4.17}$$

$$X_{14}(0) = X_9(0) + X_{31}(0) = 4959.69 \text{ MW} \tag{4.18}$$

$$X_{17}(0) = 3.0 \text{ MW} \tag{4.19}$$

$X_{17}$ is taken to be 0.5% of the power absorbed by the Combustor/Nozzle/Channel/Diffuser cooling water.

$$X_{34}(0) = X_{14}(0) - X_{17}(0) = 4956.69 \text{ MW} \tag{4.20}$$

$$K_9 = X_{17}(0)/X_{14}(0) = 6.049\text{x}10^{-4} \tag{4.21}$$

$$X_{15}(0) = X_{34}(0) = 4956.69 \text{ MW} \tag{4.22}$$

The $K_{11}$ block output is assumed to initially be $(\eta_1)(3500 \text{ MW}) =$ 1050 MW if $\eta_1$, defined by Equation 3.1, is set equal to 0.3. Inverter efficiency $K_{12}$ is taken to be 0.98.

$$K_{11} = 1050.00/5946.69 = 0.2118 \tag{4.23}$$

$$X_{16}(0) = 1029.00 \text{ MW} \tag{4.24}$$

$$X_{33}(0) = X_{15}(0) - 1050.00 = 3906.69 \text{ MW} \tag{4.25}$$

From [83], the radiant boiler output is initially 595.00 MW.

$$X_{18}(0) = X_{19}(0) = 595.00 \text{ MW} \tag{4.26}$$

$$X_{20}(0) = X_{21}(0) = X_{33}(0) - X_{18}(0) = 3311.69 \text{ MW} \tag{4.27}$$

$$X_{35}(0) = X_{21}(0) - X_{22}(0) = 2149.38 \text{ MW} \tag{4.28}$$

$$K_{13} = X_{35}(0)/X_{21}(0) = 0.6490 \tag{4.29}$$

$$X_{23}(0) = X_{35}(0) = 2149.38 \text{ MW} \tag{4.30}$$

$$Z(0) = K_7(X_{12}(0) - 1173.15°K) = 0.0°K \tag{4.31}$$

where $K_7 = 1.0$

$$X_{24}(0) = f_1(X_8(0), Z(0)) = X_8(0)\ Z(0)$$
$$= 0.0 \text{ MW} \tag{4.32}$$

$$X_{25}(0) = X_{23}(0) + X_{24}(0) + X_{19}(0)$$
$$= 2744.38 \text{ MW} \tag{4.33}$$

$$X_{26}(0) = X_{25}(0) = X_{27}(0) \tag{4.34}$$

Stack losses are assumed to be (0.1)(3500 $MW_T$) or 350.00 MW based on Figure 3.1. Initial steam plant output $X_{28}$ is 966.00 MW as in model I. Thus "other losses" of the steam plant equal (2744.38 - 966.00 - 350.00) MW or 1428.38 MW.

$$K_{16} = 350.00/2744.38 = 0.1275 \tag{4.35}$$

$$K_{17} = 1428.38/2744.38 = 0.5205 \tag{4.36}$$

$$X_{29}(0) = X_{16}(0) + X_{28}(0) = 1995.00 \text{ MW} \tag{4.37}$$

In-plant power is taken to be (0.105)(3500 MW) initially, or 367.5 MW. This includes 297.38 MW compressor power requirement.

$$X_{30}(0) = 1995.00 - 367.5 = 1627.50 \text{ MW} \tag{4.38}$$

$$K_{18} = 1627.5/1995.00 = 0.8158 \tag{4.39}$$

$$K_{19} = 1.0 \tag{4.40}$$

$$X_{32}(0) = X_{30}(0) = 1627.50 \text{ MW} \tag{4.41}$$

$K_1$ and $K_2$ are controller constants and are design parameters. $K_3$ = 4400 MW which corresponds to maximum fuel thermal input power. Then, if $X_6(0) = X_7(0) = 3500\ MW_T$,

$$X_5(0) = 3500.00/4400.00 = 0.79545 \tag{4.42}$$

$$= X_4(0) = X_{36}(0)$$

$$X_2(0) = 0 = X_3(0) \tag{4.43}$$

Eight time constants are used in model II. Five are associated with first-order lag functions and three are pure time delays. $\tau_0$ is associated with the fuel feed system first-order lag and is assumed to be 10 seconds. $\tau_1$ is a one second pure time delay in the fuel feed system. These values were chosen to be slower than gas/oil systems but faster than many existing coal firing systems in the expectation that advanced coal burning technology will be required in a combustor operating at seven to eight atmospheres pressure [81,116,146]. $\tau_4$ accounts for radiant boiler delay in transferring thermal power from the combustion gases leaving the MHD channel to the steam cycle. $\tau_5$ is to

account for transport delay of combustion gases passing from the diffuser to the steam plant. A magnitude of one second was assumed for both $\tau_4$ and $\tau_5$. These values are not critical because the $\tau_4$ delay is in cascade with two large first-order lags associated with the steam plant ($\tau_6$ = 67 seconds and $\tau_7$ = 32 seconds), while the $\tau_5$ delay is in cascade with the steam plant and/or the heat exchanger lag $\tau_2$ = 500 seconds. The value of $\tau_2$ is determined by the heat exchanger cycling period, and the steam plant characterization is as in model I [95]. $\tau_3$, the time constant associated with MHD channel enthalpy extraction, is assumed negligible compared with the other system time constants.

In summary, model II initial conditions are listed in Table 4.4. Multiplier and time constant values are tabulated in Table 4.5.

## 4.6 System Equation Solutions

Model II system equation solutions were computed for the cases shown in Table 4.6. The effects of $E_1(t)$ and $T_1(t)$ on the system are of primary interest as is the effectiveness of feedback variable Z in reducing temperature and power fluctuations. All solutions begin at steady-state as defined in Table 4.4. Constants other than $K_1$ and $K_2$ take the values given in Table 4.5. The functions $E_1(t)$, $T_1(t)$, and Z are either set equal to zero or are as defined in Figure 4.3 or the system equations given in Appendix B.

Table 4.4. Model II initial conditions

| | |
|---|---|
| $X_1(0)$ = 1627.50 MW | $X_{19}(0)$ = 595.00 MW |
| $X_2(0)$ = 0.00 MW | $X_{20}(0)$ = 3311.69 MW |
| $X_3(0)$ = 0.00 | $X_{21}(0)$ = 3311.69 MW |
| $X_4(0)$ = 0.79545 | $X_{22}(0)$ = 1162.32 MW |
| $X_5(0)$ = 0.79545 | $X_{23}(0)$ = 2149.38 MW |
| $X_6(0)$ = 3500.00 MW | $X_{24}(0)$ = 0.00 MW |
| $X_7(0)$ = 3500.00 MW | $X_{25}(0)$ = 2744.38 MW |
| $X_8(0)$ = 1.244 MW/°K | $X_{26}(0)$ = 2744.38 MW |
| $X_9(0)$ = 1459.69 MW | $X_{27}(0)$ = 2744.38 MW |
| $X_{10}(0)$ = 1173.15°K | $X_{28}(0)$ = 966.00 MW |
| $X_{11}(0)$ = 1173.15°K | $X_{29}(0)$ = 1995.00 MW |
| $X_{12}(0)$ = 1173.15°K | $X_{30}(0)$ = 1627.50 MW |
| $X_{13}(0)$ = not used | $X_{31}(0)$ = 1459.69 MW |
| $X_{14}(0)$ = 4959.69 MW | $X_{32}(0)$ = 1627.50 MW |
| $X_{15}(0)$ = 4956.69 MW | $X_{33}(0)$ = 3906.69 MW |
| $X_{16}(0)$ = 1029.00 MW | $X_{34}(0)$ = 4956.69 MW |
| $X_{17}(0)$ = 3.00 MW | $X_{35}(0)$ = 2149.38 MW |
| $X_{18}(0)$ = 595.00 MW | $X_{36}(0)$ = 0.79545 |

Table 4.5. Model II multiplier and time constants

Constant multipliers:

| | |
|---|---|
| $K_1$ = 0.001 | $K_{11}$ = 0.2118 |
| $K_2$ = 0.10 | $K_{12}$ = 0.98 |
| $K_3$ = 4400.00 MW | $K_{13}$ = 0.649 |
| $K_4$ = not used | $K_{14}$ = not used |
| $K_5$ = $3.555 \times 10^{-4}$ $MW/MW_T$ °K | $K_{15}$ = 1.00 |
| $K_6$ = not used | $K_{16}$ = 0.1275 |
| $K_7$ = 1.00 | $K_{17}$ = 0.520 |
| $K_8$ = 1.00 | $K_{18}$ = 0.816 |
| $K_9$ = $6.049 \times 10^{-4}$ | $K_{19}$ = 1.00 |
| $K_{10}$ = 0.152 | |

Time constants (seconds):

| | |
|---|---|
| $\tau_0$ = 10.0 | $\tau_4$ = 1.0 |
| $\tau_1$ = 1.0 | $\tau_5$ = 1.0 |
| $\tau_2$ = 500.0 | $\tau_6$ = 67.0 |
| $\tau_3$ = 0.0 | $\tau_7$ = 62.0 |

System equations follow directly from the block diagram of Figure 4.1. They are listed in the computer program of Appendix B.

Table 4.6. Conditions for model II equation solutions

| Case | $K_1$ | $K_2$ | $E_1(t)$ | $T_1(t)$ | Z |
|---|---|---|---|---|---|
| 1 | 0.001 | 0.01 | 0 | 0 | 0 |
| 2 | 0.001 | 0.1 | 0 | 0 | 0 |
| 3 | 0.001 | 1.0 | 0 | 0 | 0 |
| 4 | 0.01 | 0.01 | 0 | 0 | 0 |
| 5 | 0.01 | 0.1 | 0 | 0 | 0 |
| 6 | 0.001 | 0.01 | 0 | 0 | Z |
| 7 | 0.001 | 0.1 | 0 | 0 | Z |
| 8 | 0.001 | 1.0 | 0 | 0 | Z |
| 9 | 0.01 | 0.01 | 0 | 0 | Z |
| 10 | 0.01 | 0.1 | 0 | 0 | Z |
| 11 | 0.001 | 0.01 | $E_1(t)$ | $T_1(t)$ | 0 |
| 12 | 0.001 | 0.1 | $E_1(t)$ | $T_1(t)$ | 0 |
| 13 | 0.001 | 1.0 | $E_1(t)$ | $T_1(t)$ | 0 |
| 14 | 0.01 | 0.01 | $E_1(t)$ | $E_1(t)$ | 0 |
| 15 | 0.01 | 0.1 | $E_1(t)$ | $T_1(t)$ | 0 |
| 16 | 0.001 | 0.01 | $E_1(t)$ | $T_1(t)$ | Z |
| 17 | 0.001 | 0.1 | $E_1(t)$ | $T_1(t)$ | Z |
| 18 | 0.001 | 1.0 | $E_1(t)$ | $T_1(t)$ | Z |
| 19 | 0.01 | 0.01 | $E_1(t)$ | $T_1(t)$ | Z |
| 20 | 0.01 | 0.1 | $E_1(t)$ | $T_1(t)$ | Z |

Several important observations may be made by inspecting model II data. First, the air preheat temperature controller $f_1(X_8, Z)$ only affects long-term variations in air temperature $X_{12}$. It has no effect on transients occurring at the beginning of the computer runs. The temperature controller also has no effect on the magnitude jumps observed in many variables which occur as a consequence of air heater cycling. The effect of the air temperature controller on variables $X_4$, $X_7$, $X_{16}$, $X_{28}$, and $X_{30}$ is negligible. For example, if $K_1 = 0.01$, $K_2 = 0.01$ or 0.1, $E_1(t) = 0$, and $T_1(t) = 0$, the most notable difference between the $Z = 0$ and $Z \neq 0$ cases is that $X_{16}$ increases in value by 0.35 MW at the end of 400 seconds for the $Z \neq 0$ case and $X_{28}$ decreases by the same amount.

Plots of five model II variables are given as functions of time in Figures 4.4 through 4.24. The variables are:

$X_7$ (fuel thermal input power)

$X_{12}$ (preheated air temperature subtracting ambient)

$X_{16}$ (inverter output power)

$X_{28}$ (net steam plant output power)

$X_{30}$ (net plant output power)

### 4.6.1 Fuel thermal input power $X_7$

Figure 4.4 displays a family of curves of $X_7$ as a function of time. The conditions are: $K_1 = 0.001$, $K_2 = 0.01$, 0.1, and 1.0,

$E_1(t) = 0$, $T_1(t) = 0$, and $Z = 0$. $K_1$ and $K_2$ are controller constants, and $E_1(t)$ and $T_1(t)$ are defined in Figure 4.3. Setting $Z = 0$ disables the temperature controller. Figure 4.4 serves as a comparison for Figure 4.5.

$X_7$ is plotted in Figure 4.5 under the same conditions for $X_1$ and $X_2$ as in Figure 4.4. In this case, $E_1(t)$, $T_1(t)$ and Z are functioning. Representative values of magnitude jumps at t = 225 seconds are $\Delta X_7 = -5.81$ MW for $K_2 = 0.01$, $\Delta X_7 = -9.70$ MW for $K_2 = 0.1$, and $\Delta X_7 = -23.50$ MW for $K_2 = 1.0$.

Figure 4.6 illustrates $X_7$ as a function of time for $K_1 = 0.01$, $K_2 = 0.01$ and 0.1, $E_1(t) = 0$, $T_1(t) = 0$, and Z is functioning.

Figure 4.7 shows $X_7$ for the same conditions as Figure 4.6 except that $E_1(t)$, $T_1(t)$, and Z are all functioning. Magnitude jumps at t = 225 seconds are $\Delta X_7 = 23.56$ MW for $K_2 = 0.01$, and $\Delta X_7 = 25.96$ MW for $K_2 = 0.1$.

### 4.6.2 Preheated air temperature (subtracting ambient) $X_{12}$

$X_{12}$ is shown in Figure 4.8 for the following conditions: $K_1 = 0.001$, $K_2 = 0.01$, 0.1, and 1.0, $E_1(t) = 0$, $T_1(t) = 0$, and $Z = 0$. $X_{12}$ varies by 2.13°K over 400 seconds for $K_2 = 0.01$. Corresponding values of $\Delta X_{12}$ for cases in which $K_2 = 0.1$ and 1.0 are 2.40°K and 3.55°K, respectively.

$X_{12}$ is plotted in Figure 4.9 for the same conditions as Figure 4.8 except that $Z \neq 0$, allowing the temperature controller to operate. In this case, the variations in $X_{12}$ over the 400 second period are as follows: If $K_2 = 0.01$, $\Delta X_{12} = 1.59°K$. If $K_2 = 0.1$, $\Delta X_{12} = 1.68°K$. If $K_2 = 1.0$, $\Delta X_{12} = 1.62°K$. Thus, when the temperature controller operates, a reduction in $\Delta X_{12}$ is observed in all cases with a maximum reduction of 54% if $K_2 = 1.0$.

Figure 4.10 indicates the effect of $T_1(t)$ on $X_{12}$. $K_1 = 0.001$, $K_2 = 0.01$, 0.1, and 1.0, and $E_1(t)$, $T_1(t)$ and Z are all functioning. The peak to peak amplitude of $X_{12}$ is approximately 19.6°K in all cases. The same waveform is observed for $X_{12}$ if $K_1 = 0.01$ and $K_2 = 0.01$ or 0.1.

Figure 4.11 illustrates $X_{12}$ as a function of time for $K_1 = 0.01$, $K_2 = 0.01$ and 0.1, $E_1(t) = 0$, $T_1(t) = 0$, and $Z = 0$. $X_{12}$ varies by 3.55°K in each case over the 400 second time interval.

Figure 4.12 shows the effect of using the temperature controller in the cases of Figure 4.11. Z is functioning. Otherwise, the conditions for Figures 4.10 and 4.11 are the same. In Figure 4.12, the variation in $X_{12}$ is 1.61°K, compared with 3.55°K if $Z = 0$.

### 4.6.3 Inverter output power $X_{16}$

$X_{16}$ is plotted as a function of time in Figure 4.13 for the conditions of $K_1 = 0.001$, $K_2 = 0.01$, 0.1, and 1.0, $E_1(t) = 0$, $T_1(t) = 0$, and $Z = 0$.

Figure 4.14 gives the effect of $E_1(t)$ and $T_1(t)$ on $X_{16}$. The remaining conditions are the same as in Figure 4.13 except that $Z = 0$, which has negligible effect on the transient behavior of $X_{16}$. In all cases the magnitude variation in $X_{16}$ due to $E_1(t)$ and $T_1(t)$ is approximately 5 MW.

Figure 4.15 repeats Figure 4.13 for the conditions $K_1 = 0.01$, $K_2 = 0.01$ and 0.1, $E_1(t) = 0$, $T_1(t) = 0$, and Z is functioning.

Figure 4.16, to be compared with 4.15, shows the effect of $T_1(t)$ and $E_1(t)$ on $X_{16}$ otherwise operating as in Figure 4.15. The magnitude jump due to $E_1(t)$ and $T_1(t)$ is approximately 5 MW in both cases.

### 4.6.4 Net steam plant output power $X_{28}$

$X_{28}$ is given as a function of time in Figure 4.17. $K_1 = 0.001$, $K_2 = 0.01$, 0.1, and 1.0, $E_1(t) = 0$, $T_1(t) = 0$, and $Z = 0$.

Figure 4.18 illustrates the effect of $E_1(t)$ and $T_1(t)$ on $X_{28}$ for the conditions of Figure 4.17. $X_{28}$ is unaffected by $E_1(t)$ and $T_1(t)$.

Figure 4.19 shows $X_{28}$ if $K_1 = 0.01$, $K_2 = 0.01$, and 0.1, $E_1(t) = 0$, $T_1(t) = 0$, and $Z \neq 0$. Figure 4.20 gives $X_{28}$ as a function of time for the same conditions as Figure 4.19 except $E_1(t)$, $T_1(t)$, and Z are all functioning. Again, as in Figure 4.18, $X_{28}$ is not affected by $E_1(t)$ and $T_1(t)$.

### 4.6.5 Net plant output power $X_{30}$

The last variable to be considered is $X_{30}$. Figure 4.21 shows $X_{30}$ plotted for the conditions $K_1 = 0.001$, $K_2 = 0.001$, 0.1, and 1.0, $E_1(t) = 0$, $T_1(t) = 0$, and $Z = 0$.

Figure 4.22 repeats the conditions of Figure 4.21 except that $E_1(t)$, $T_1(t)$, and Z are all functioning. The magnitude jumps in $X_{30}$ due to $E_1(t)$ and $T_1(t)$ are approximately 4 MW in all cases.

Figure 4.23 illustrates $X_{30}$ for the cases $K_1 = 0.01$, $K_2 = 0.01$ and 0.1, $E_1(t) = 0$, $T_1(t) = 0$, and $Z \neq 0$.

Figure 4.24 shows the effects of $E_1(t)$ and $T_1(t)$ on $X_{30}$ for the same $K_1$ and $K_2$ conditions as in Figure 4.23. As in Figure 4.22, the magnitude jumps in $X_{30}$ due to $E_1(t)$ and $T_1(t)$ are about 4 MW in both cases.

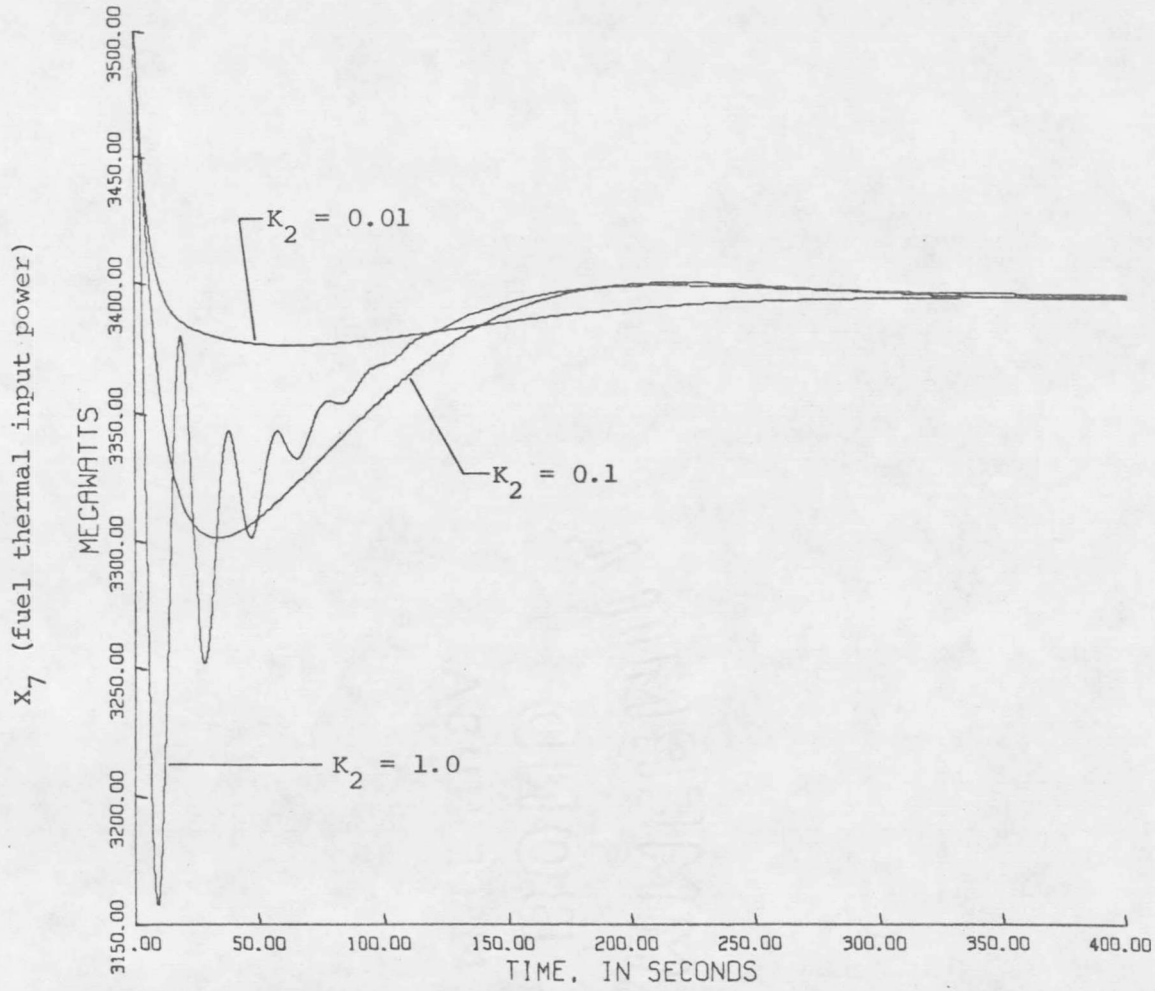



Figure 4.4. MW(REF) $X_1$ changes from 1627.5 MW to 1577.5 MW at t = 0+; $K_1 = 0.001$, $E_1(t) = T_1(t) = Z = 0$

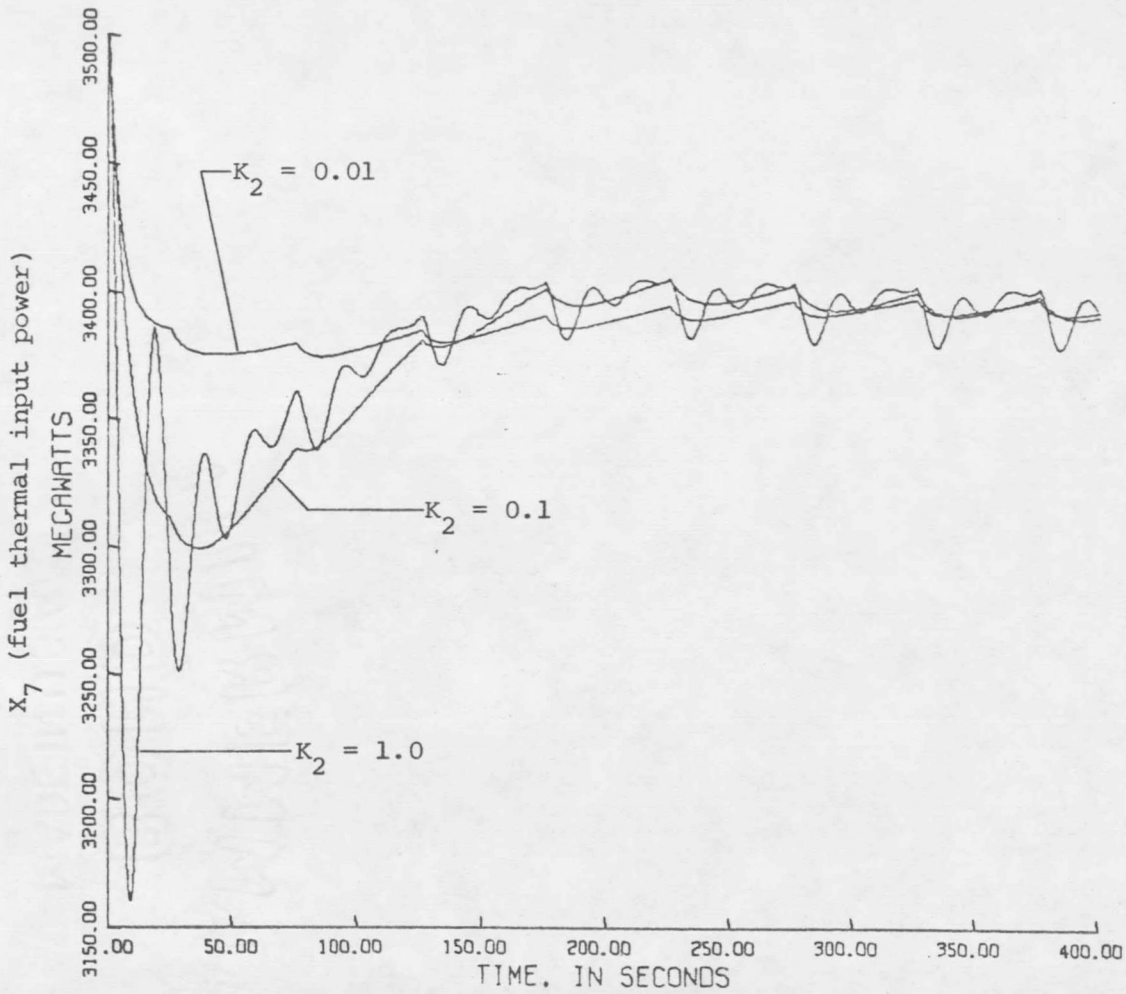



Figure 4.5. MW(REF) $X_1$ changes from 1627.5 MW to 1577.5 MW at t = 0+; $K_1$ = 0.001, $E_1(t)$, $T_1(t)$, Z all functioning

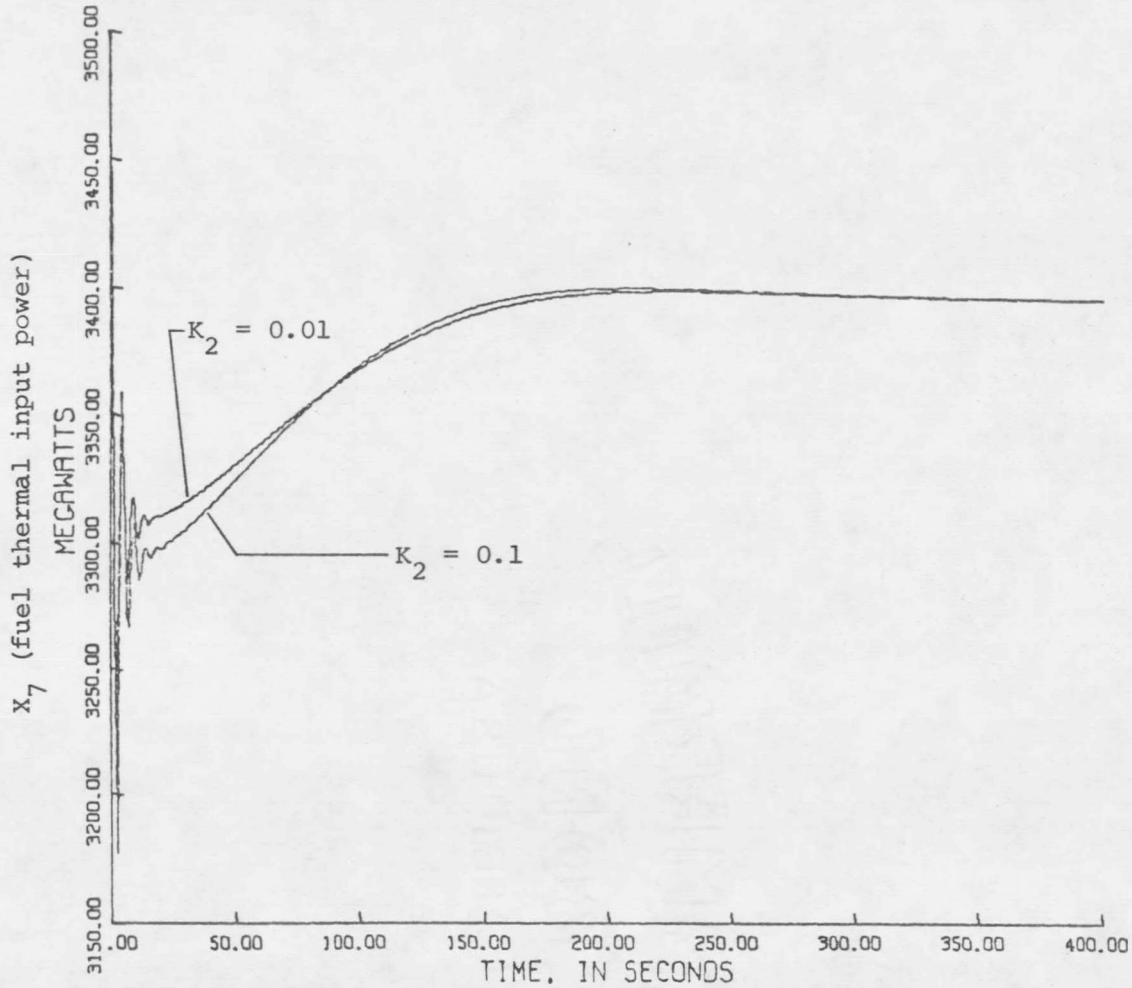



Figure 4.6. MW(REF) $X_1$ changes from 1627.5 MW to 1577.5 MW at t = 0+; $K_1 = 0.01$, $E_1(t) = T_1(t) = 0$, $Z \neq 0$

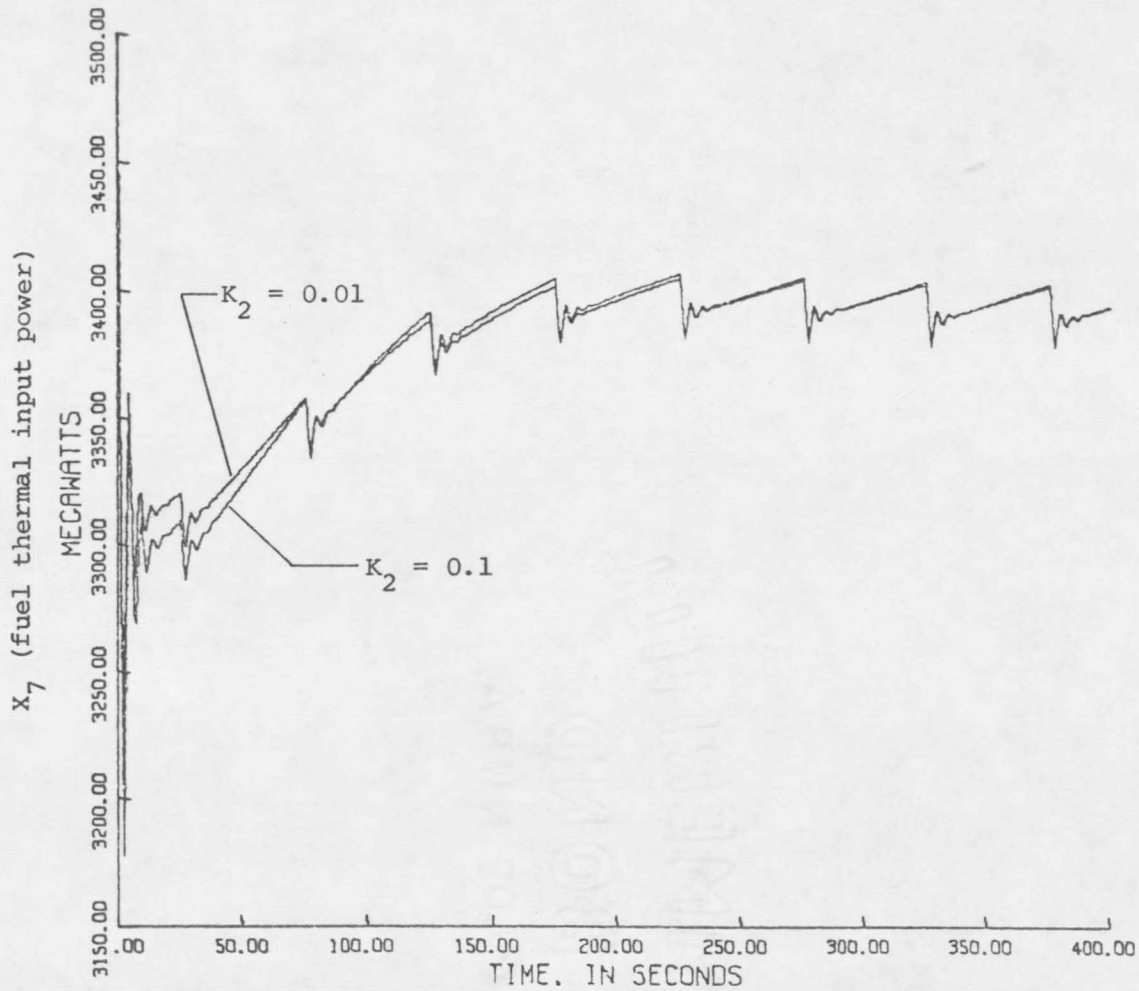



Figure 4.7. MW(REF) $X_1$ changes from 1627.5 MW to 1577.5 MW at t = 0+; $K_1$ = 0.01, $E_1(t)$, $T_1(t)$, Z all functioning

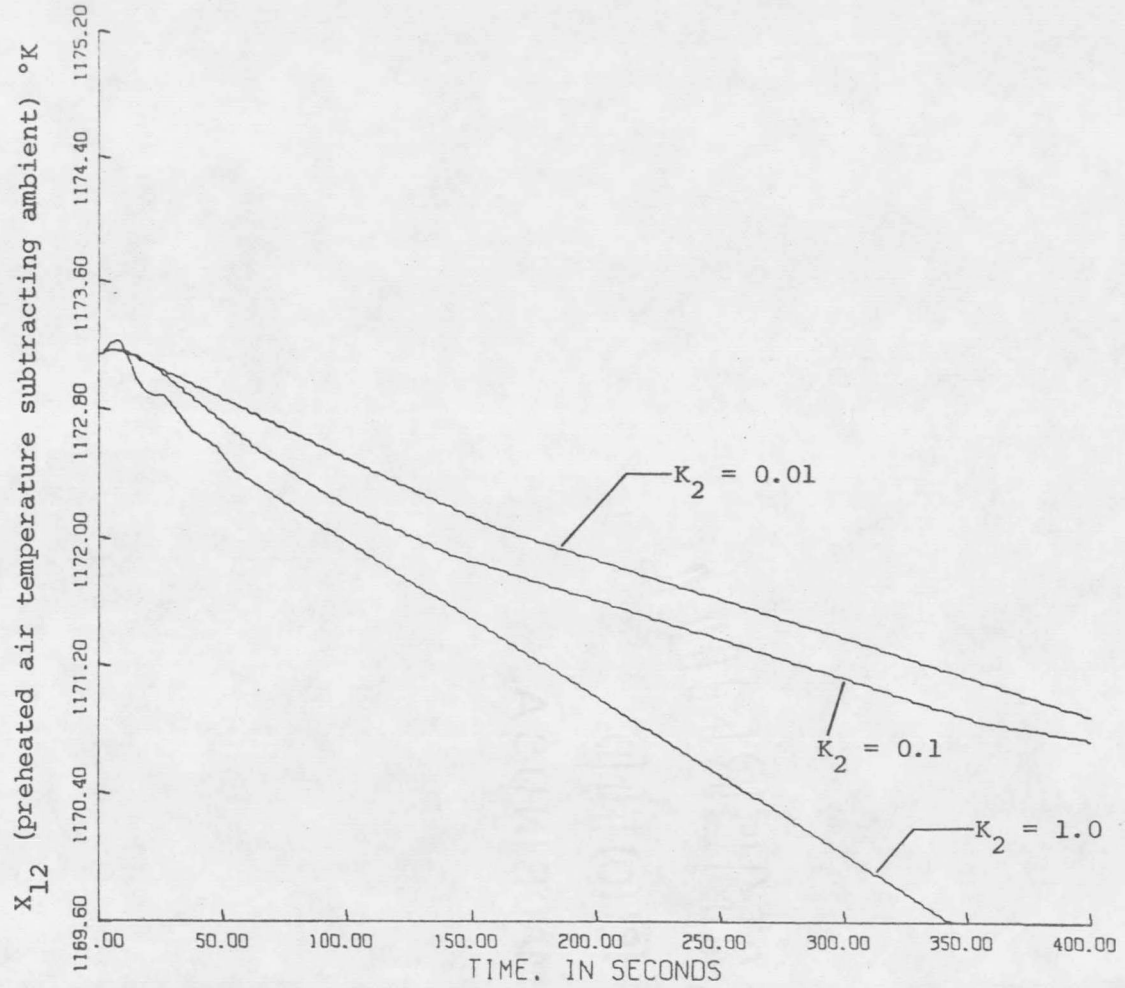



Figure 4.8. MW(REF) $X_1$ changes from 1627.5 MW to 1577.5 MW at t = 0+; $K_1 = 0.001$, $E_1(t) = T_1(t) = Z = 0$

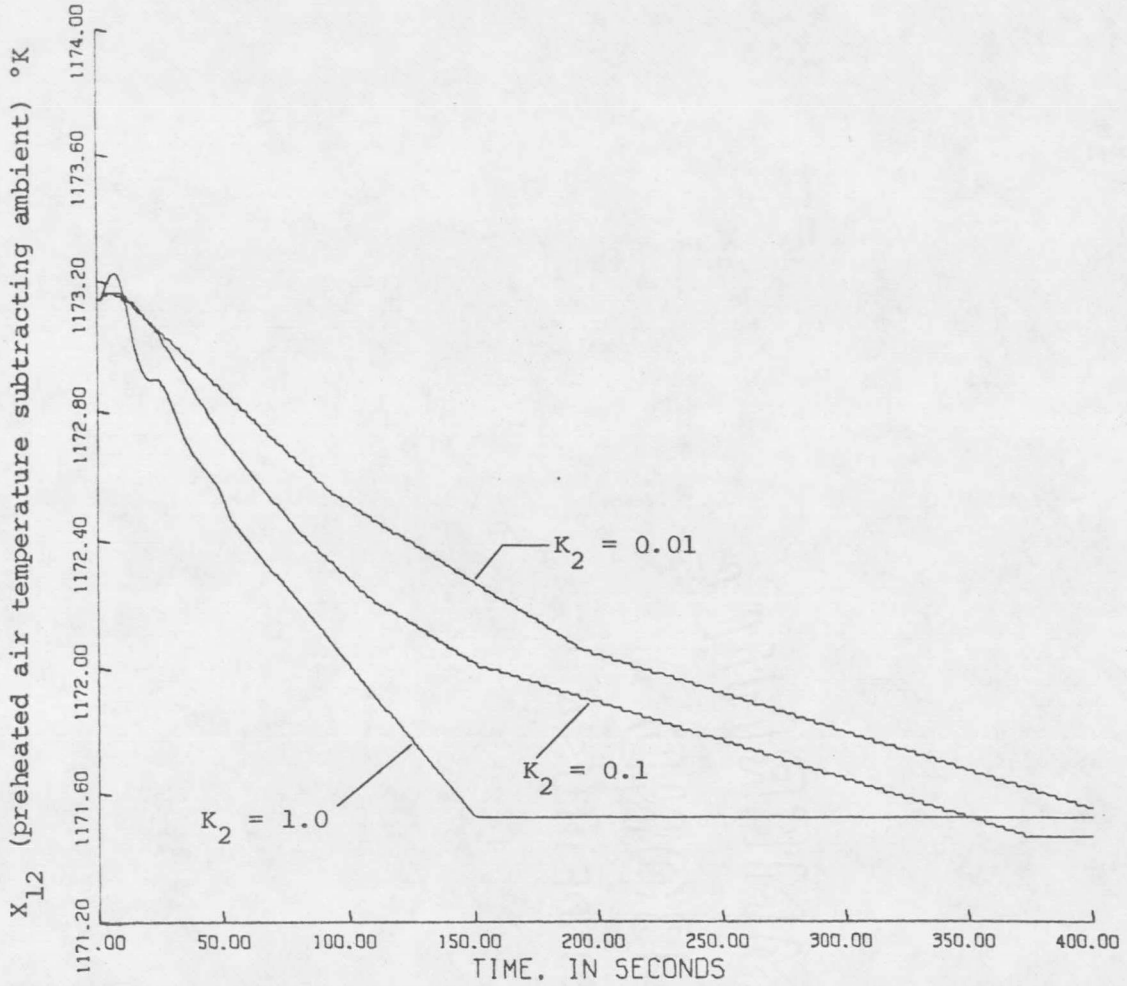



Figure 4.9. MW(REF) $X_1$ changes from 1627.5 MW to 1577.5 MW at t = 0+; $K_1 = 0.001$, $E_1(t) = T_1(t) = 0$, $Z \neq 0$

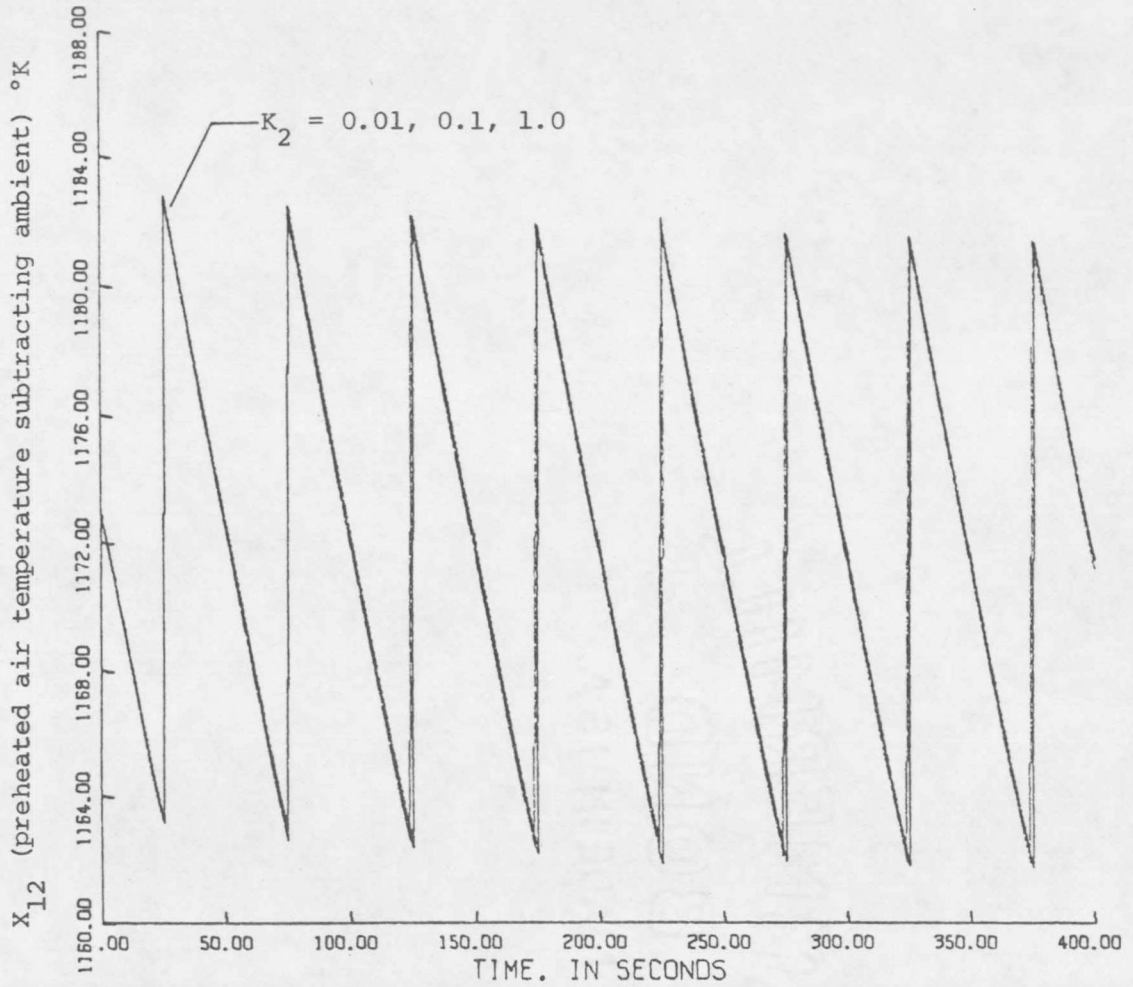



Figure 4.10. MW(REF) $X_1$ changes from 1627.5 MW to 1577.5 MW at t = 0+; $K_1$ = 0.001, $E_1(t)$, $T_1(t)$, Z all functioning

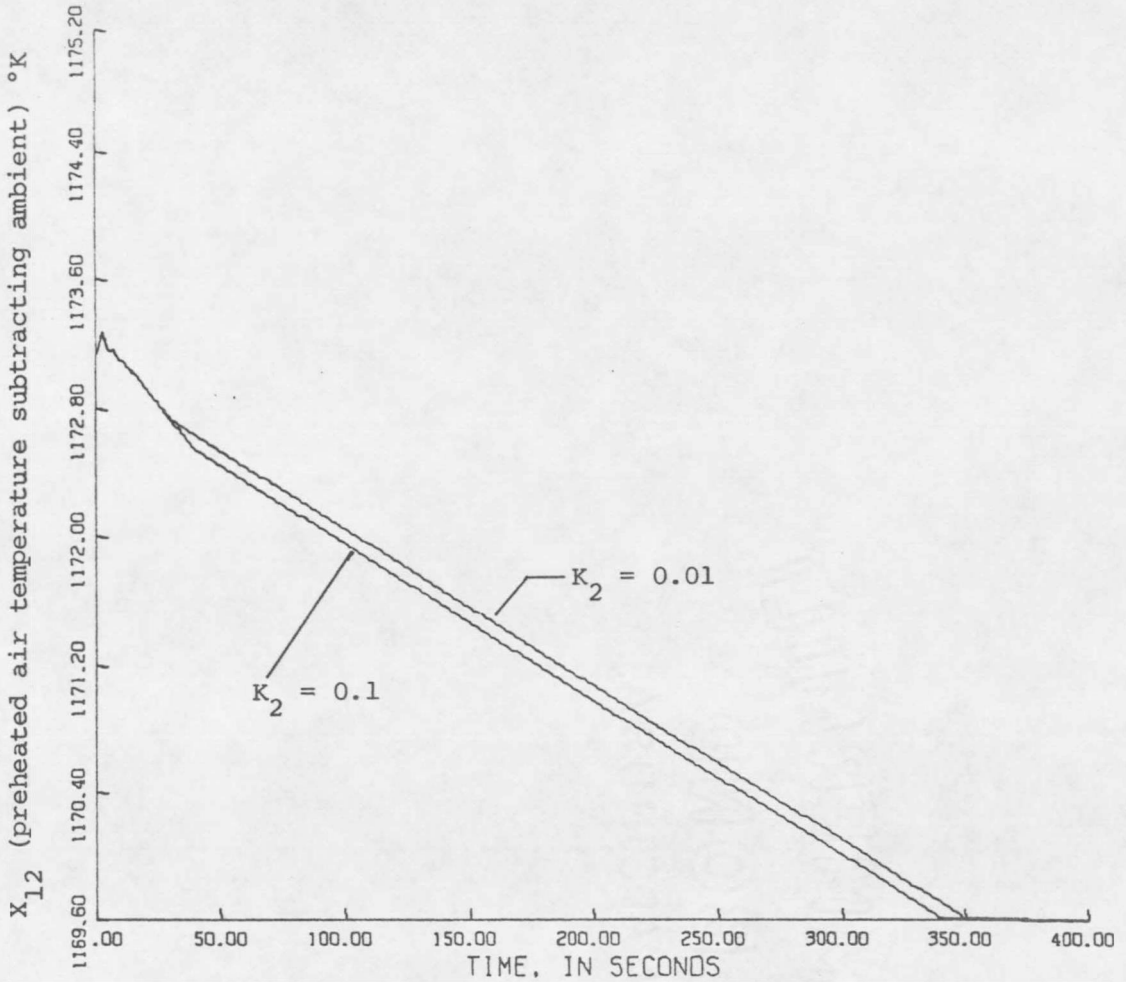



Figure 4.11. MW(REF) $X_1$ changes from 1627.5 MW to 1577.5 MW at t = 0+; $K_1 = 0.01$, $E_1(t) = T_1(t) = Z = 0$

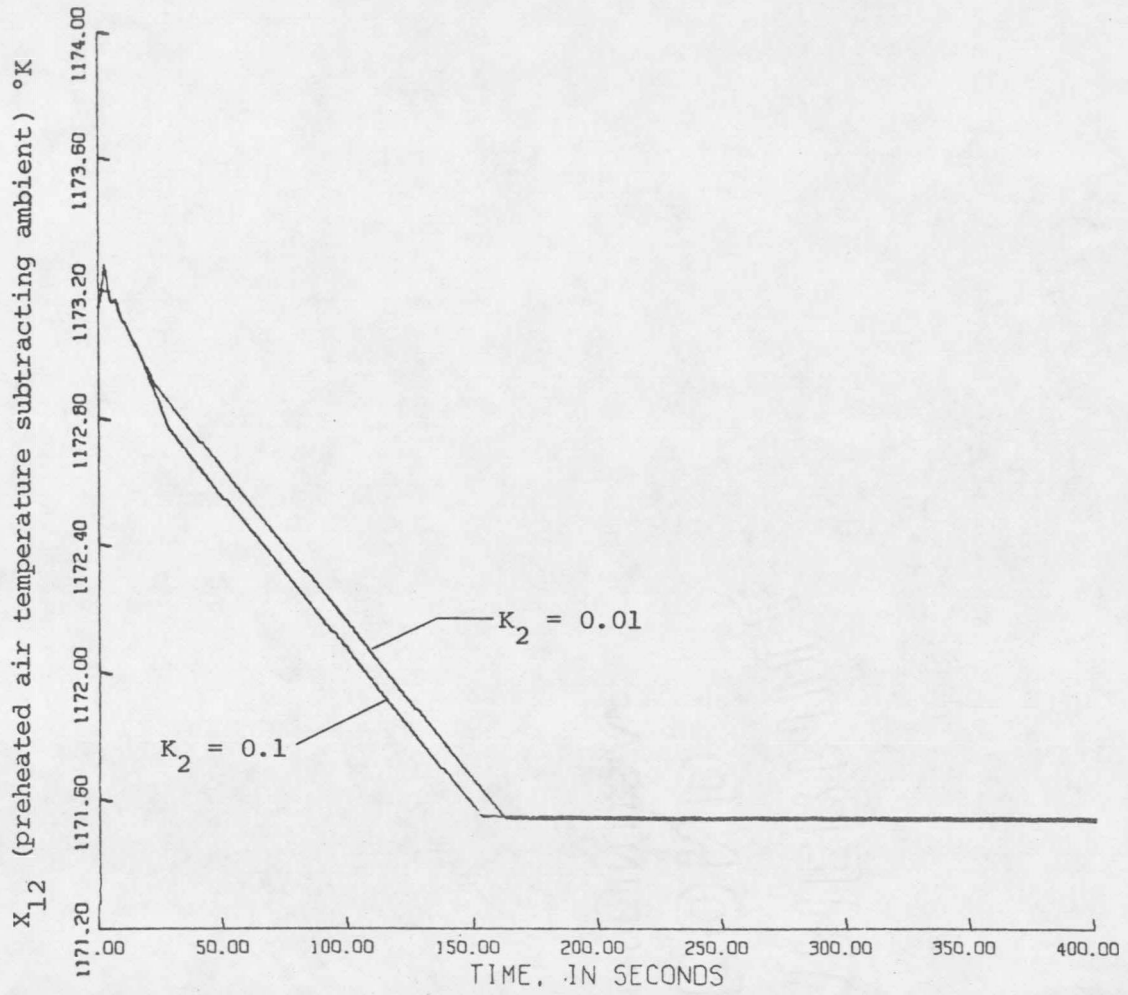



Figure 4.12. MW(REF) $X_1$ changes from 1627.5 MW to 1577.5 MW at t = 0+; $K_1 = 0.01$, $E_1(t) = T_1(t) = 0$, $Z \neq 0$

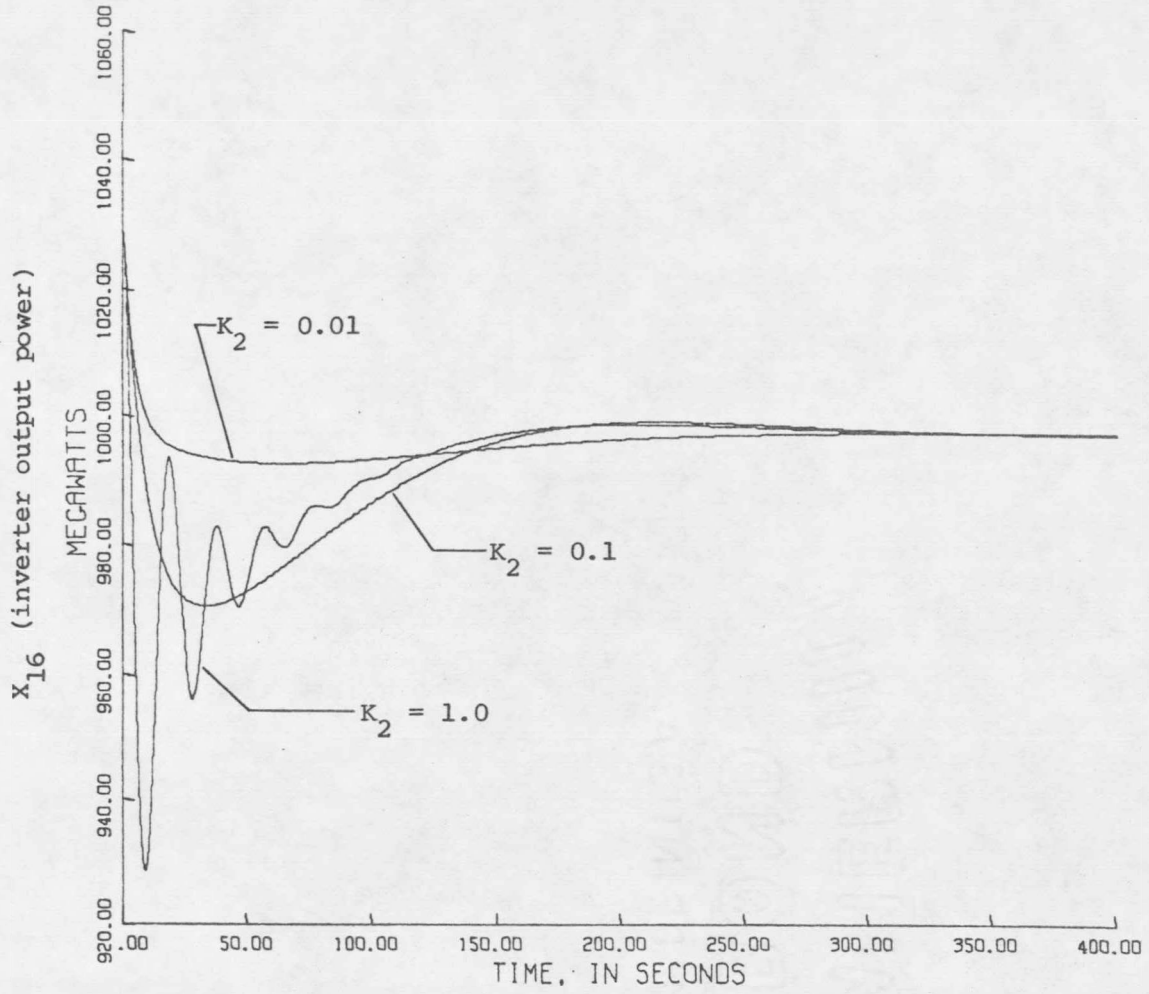



Figure 4.13. MW(REF) $X_1$ changes from 1627.5 MW to 1577.5 MW at t = 0+; $K_1 = 0.001$, $E_1(t) = T_1(t) = Z = 0$

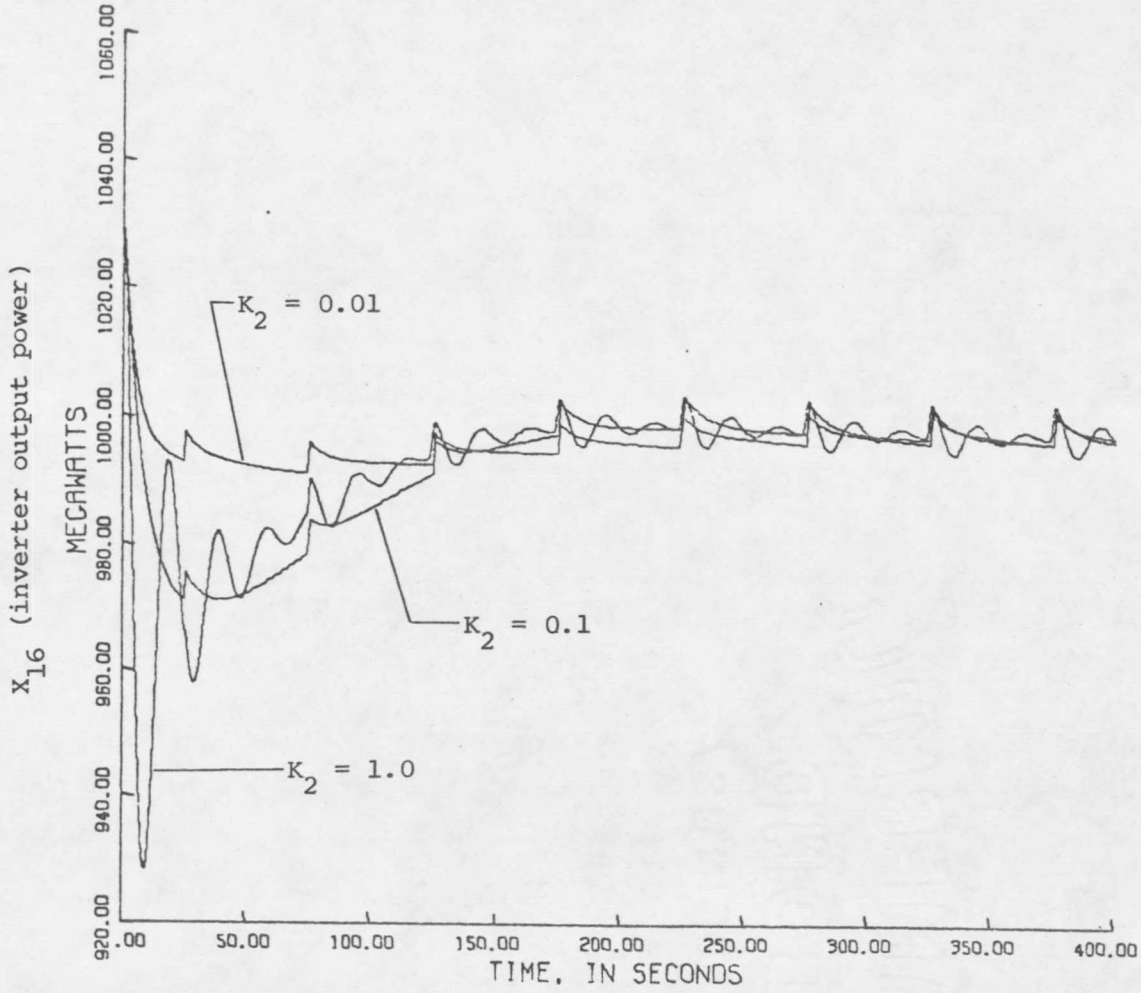



Figure 4.14. MW(REF) $X_1$ changes from 1627.5 MW to 1577.5 MW at t = 0+; $K_1$ = 0.001, $E_1(t)$ and $T_1(t)$ functioning, Z = 0

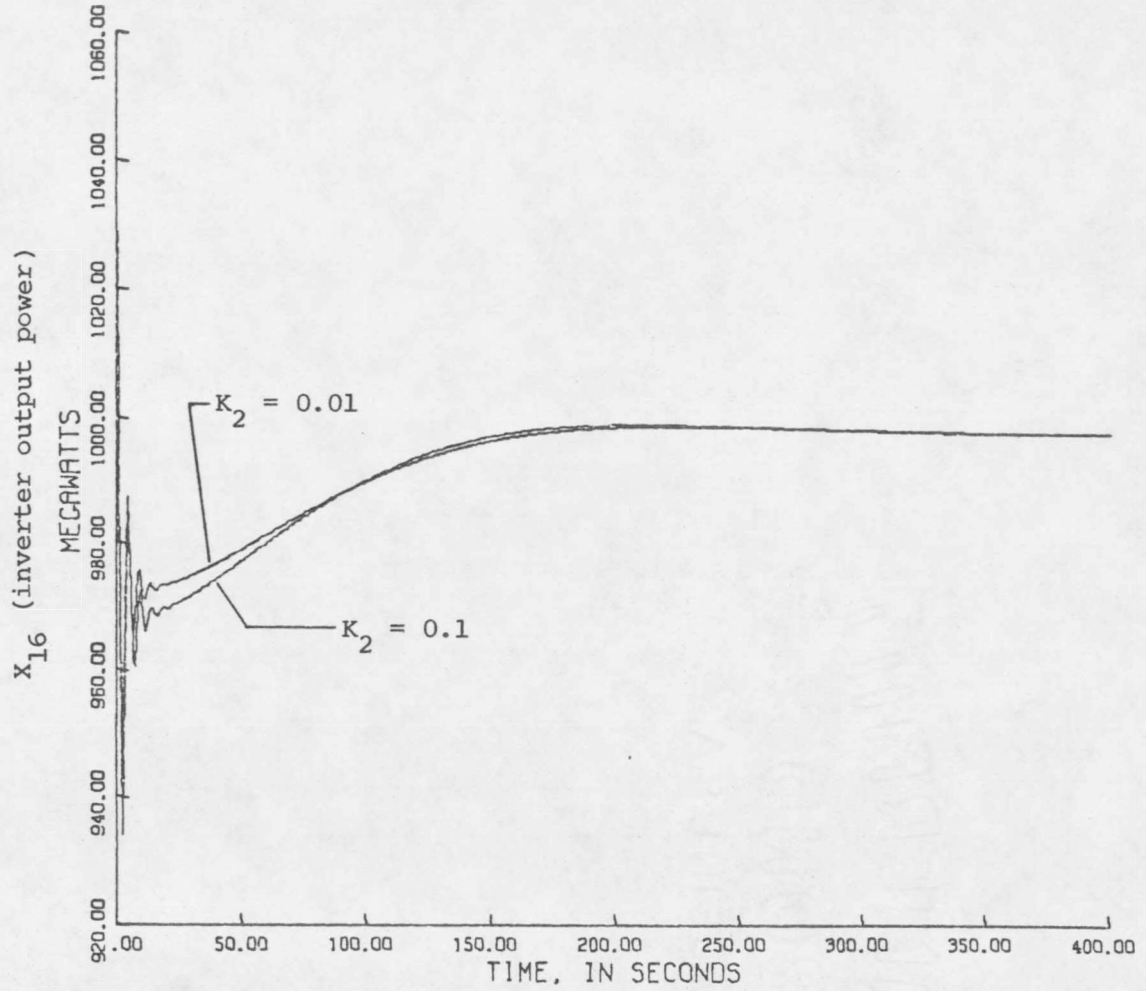



Figure 4.15. MW(REF) $X_1$ changes from 1627.5 MW to 1577.5 MW at t = 0+; $K_1 = 0.01$, $E_1(t) = T_1(t) = 0$, $Z \neq 0$

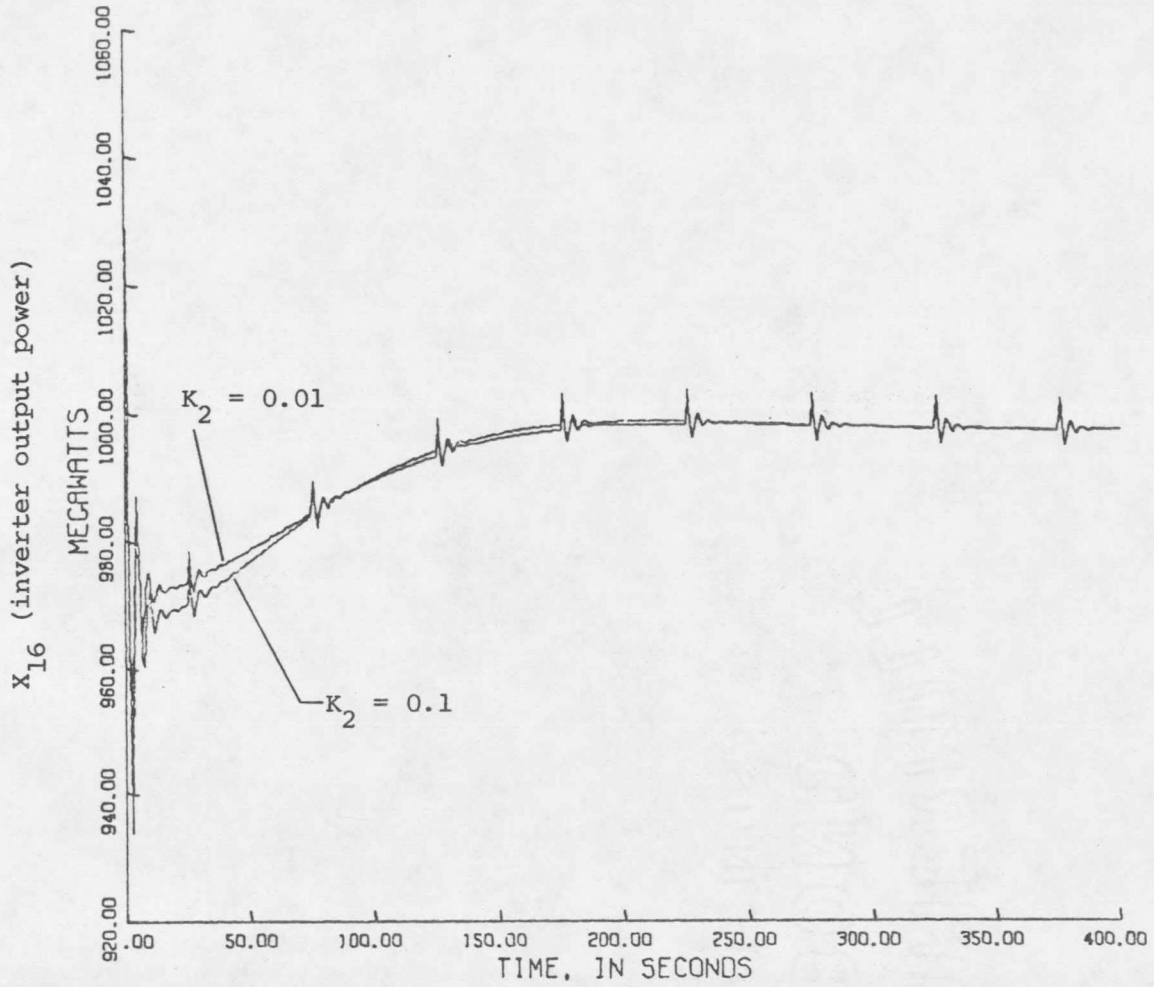



Figure 4.16. MW(REF) $X_1$ changes from 1627.5 MW to 1577.5 MW at t = 0+; $K_1$ = 0.01, $E_1(t)$, $T_1(t)$, Z all functioning

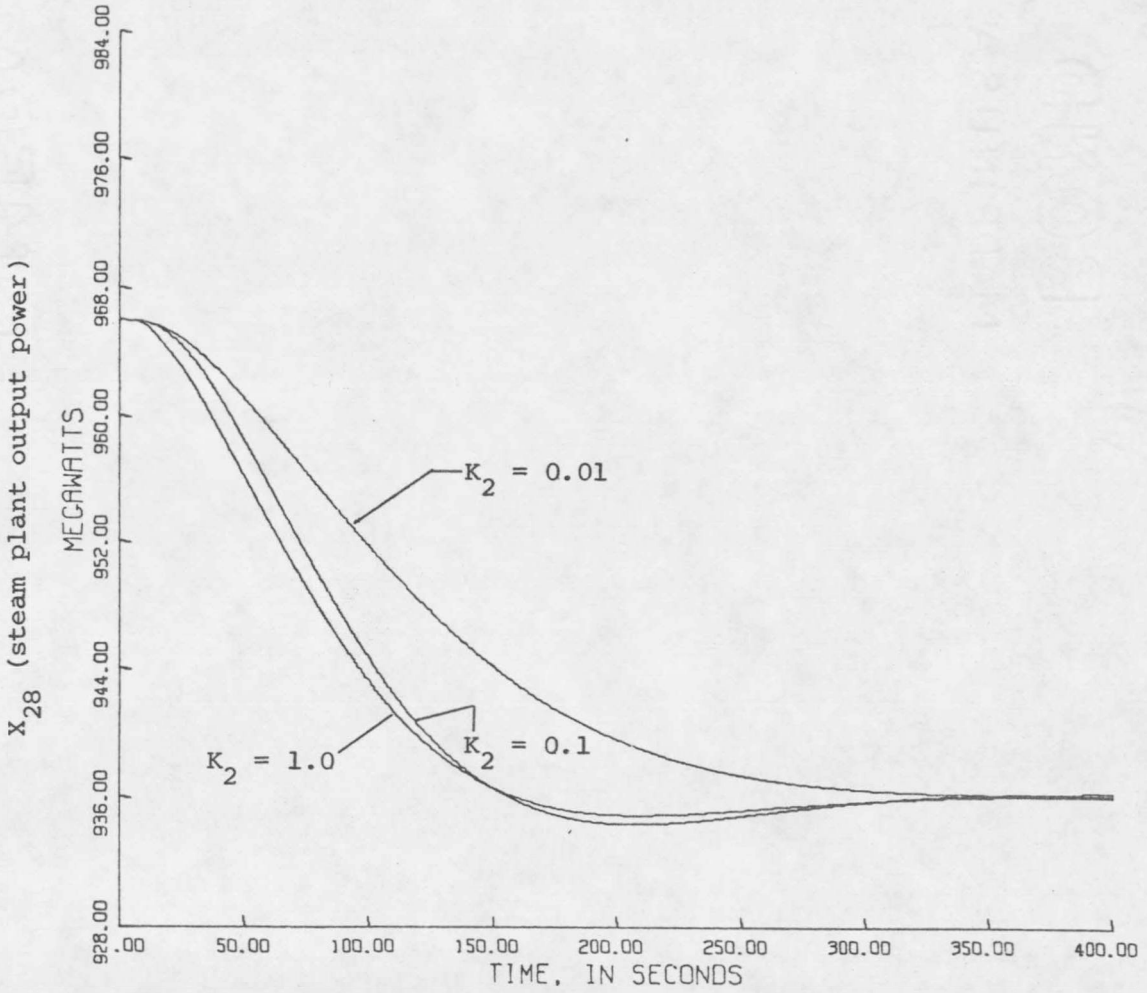



Figure 4.17. MW(REF) $X_1$ changes from 1627.5 MW to 1577.5 MW at t = 0+; $K_1 = 0.001$, $E_1(t) = T_1(t) = Z = 0$

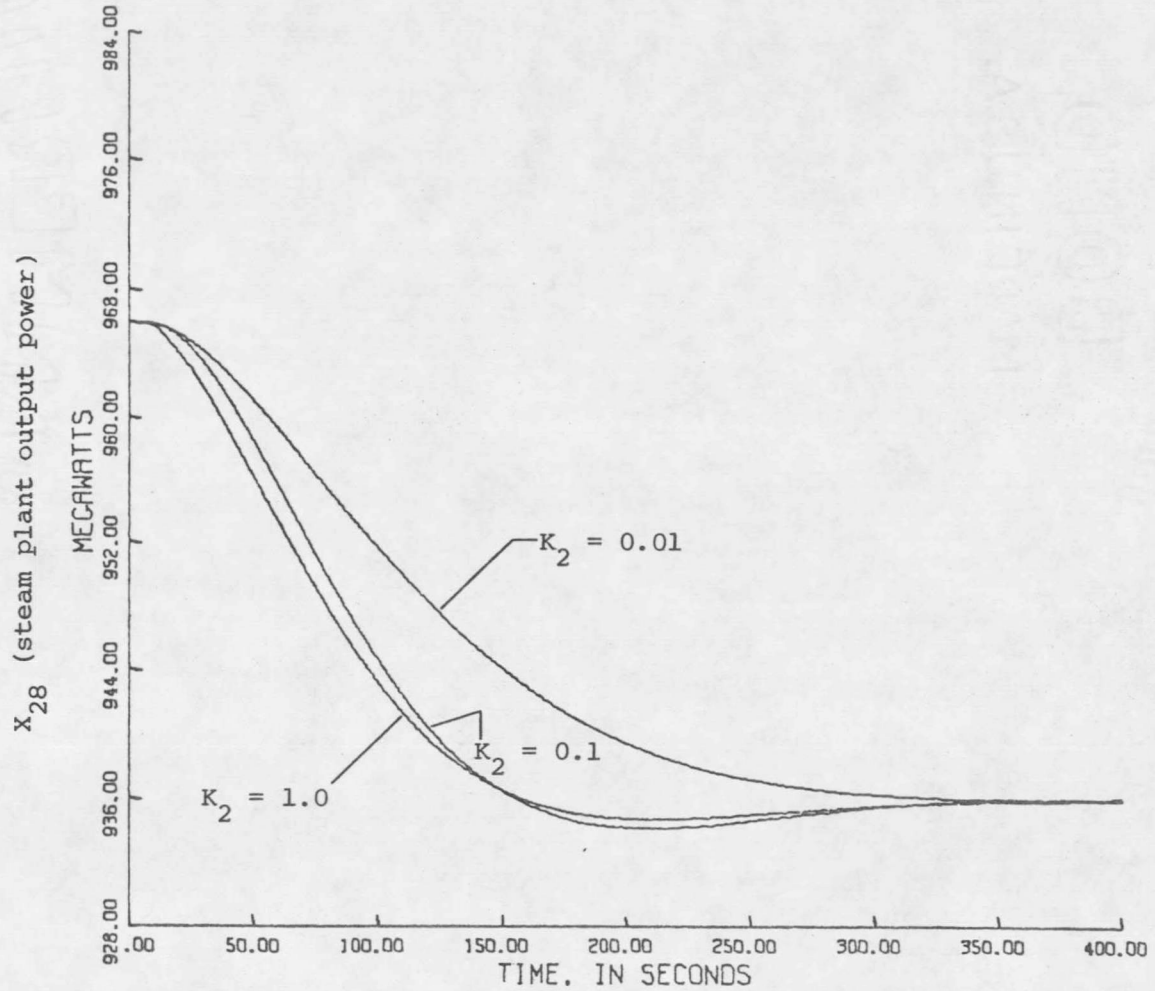



Figure 4.18. MW(REF) $X_1$ changes from 1627.5 MW to 1577.5 MW at t = 0+; $K_1$ = 0.001, $E_1(t)$, $T_1(t)$, Z all functioning

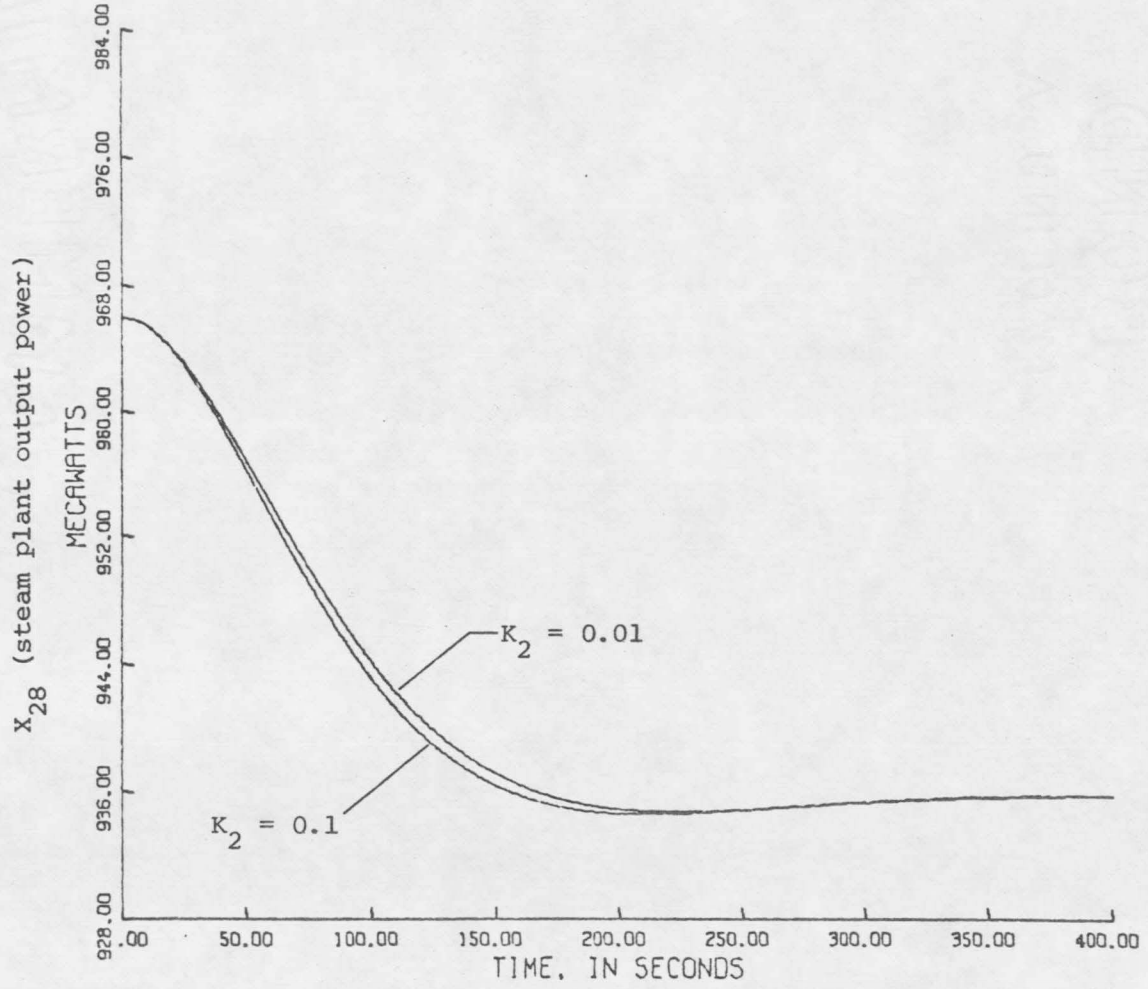



Figure 4.19. MW(REF) $X_1$ changes from 1627.5 MW to 1577.5 MW at t = 0+; $K_1 = 0.01$, $E_1(t) = T_1(t) = 0$, $Z \neq 0$

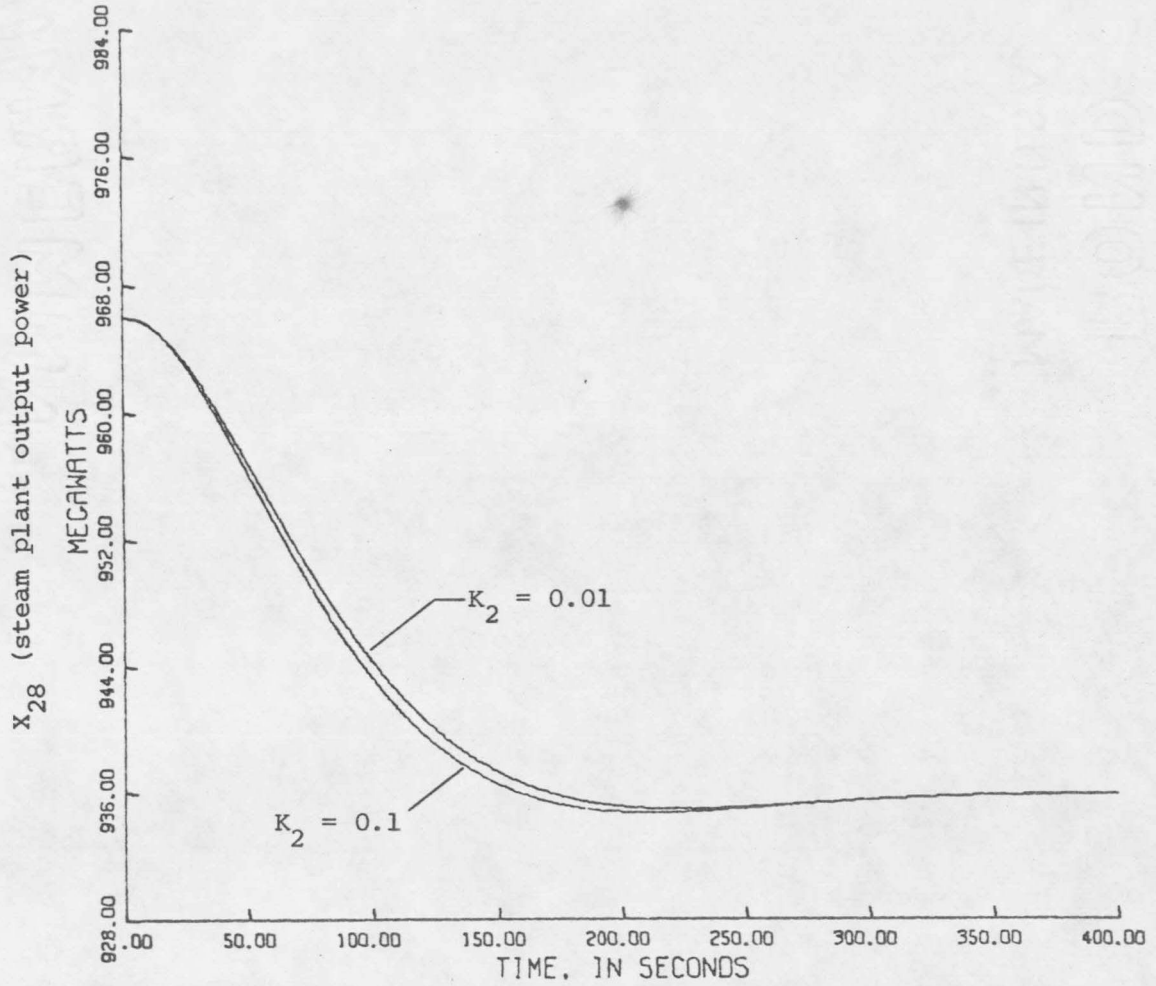



Figure 4.20. MW(REF) $X_1$ changes from 1627.5 MW to 1577.5 MW at t = 0+; $K_1$ = 0.01, $E_1(t)$, $T_1(t)$, Z all functioning

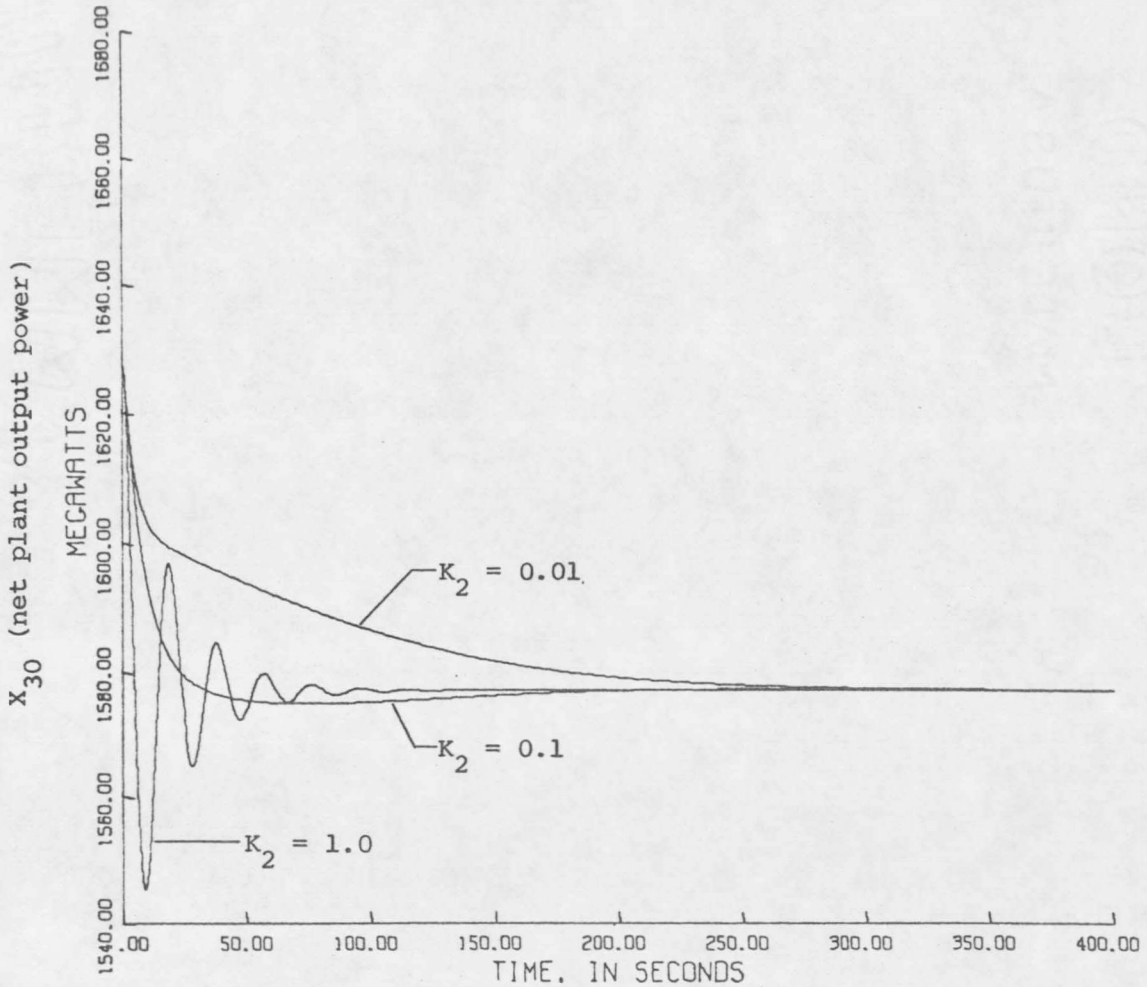



Figure 4.21. MW(REF) $X_1$ changes from 1627.5 MW to 1577.5 MW at t = 0+; $K_1 = 0.001$, $E_1(t) = T_1(t) = Z = 0$

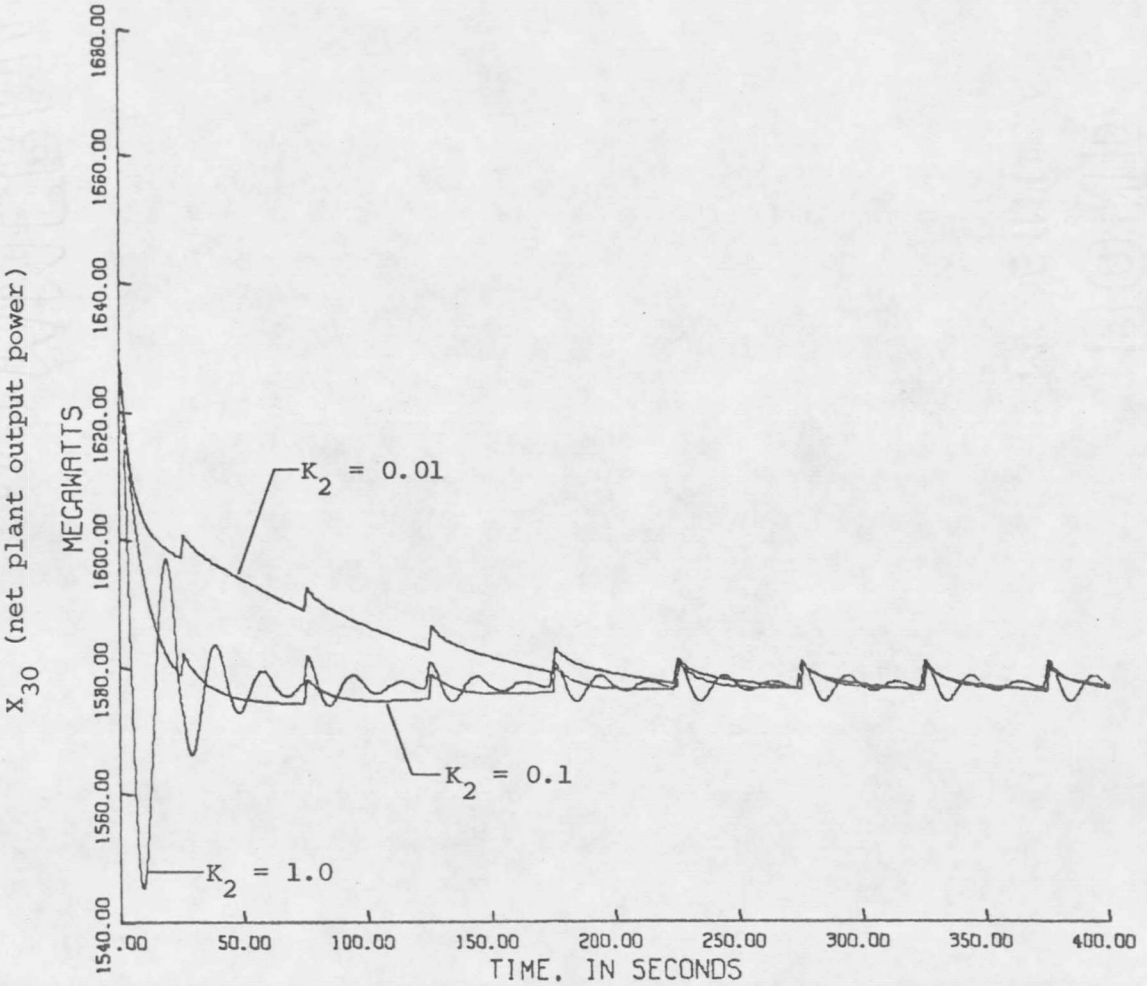



Figure 4.22. MW(REF) $X_1$ changes from 1627.5 MW to 1577.5 MW at t = 0+; $K_1$ = 0.001, $E_1(t)$, $T_1(t)$, Z all functioning

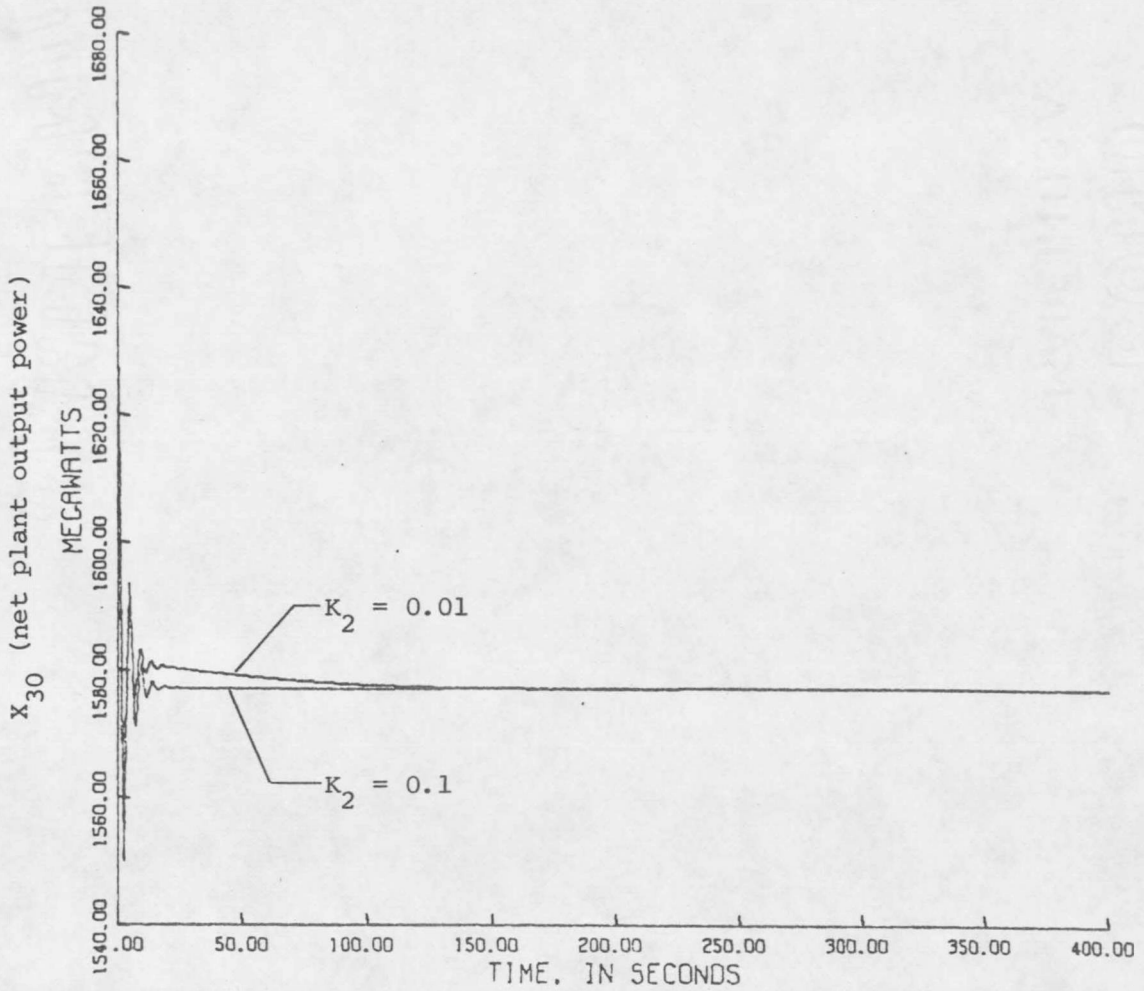



Figure 4.23. MW(REF) $X_1$ changes from 1627.5 MW to 1577.5 MW at t = 0+; $K_1 = 0.01$, $E_1(t) = T_1(t) = 0$, $Z \neq 0$

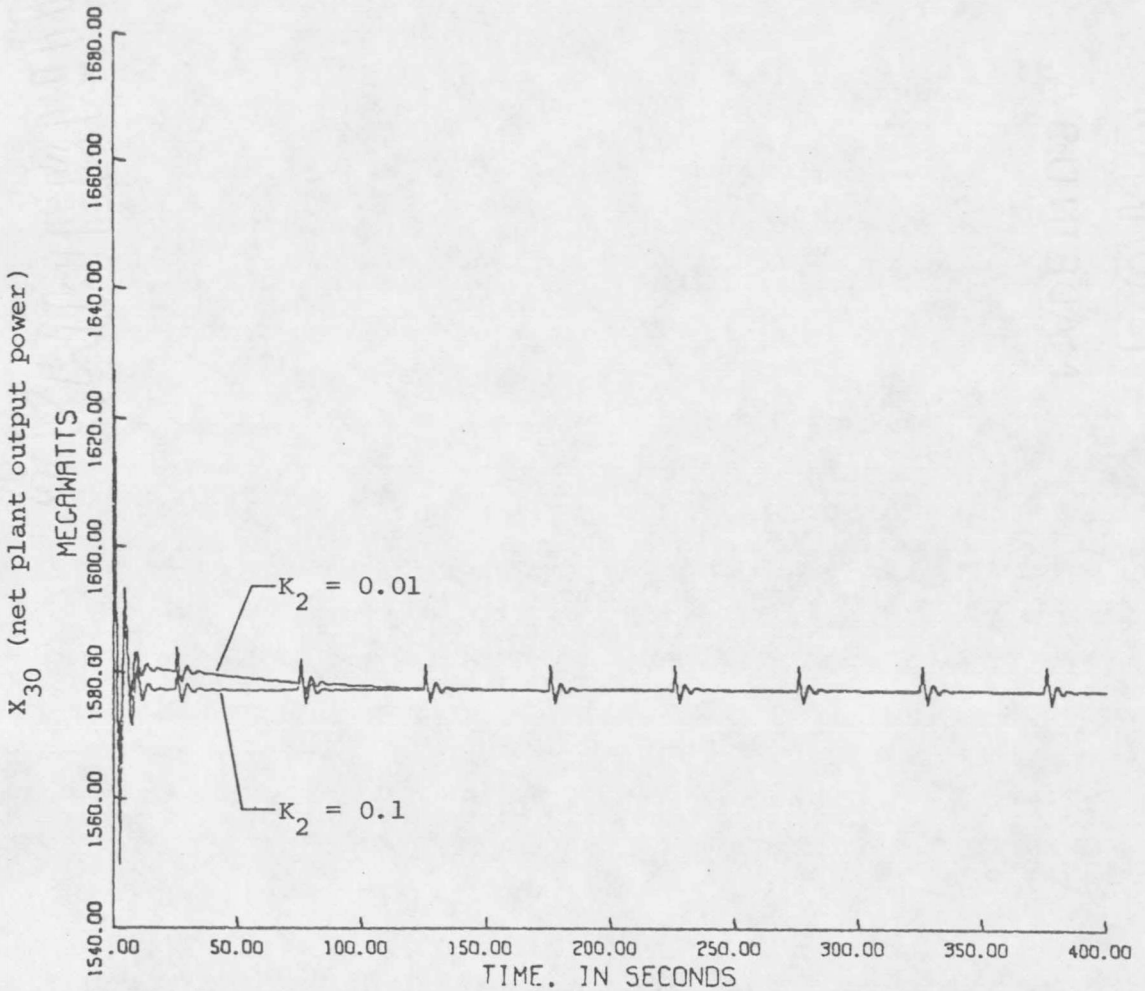



Figure 4.24. MW(REF) $X_1$ changes from 1627.5 MW to 1577.5 MW at t = 0+; $K_1$ = 0.01; $E_1(t)$, $T_1(t)$, Z all functioning

# Chapter V

# SYSTEM MODEL III

## 5.1 Model III Features

System model III is considerably more detailed than previously discussed models. The added complexity is evident in the overall model III block diagram shown in Figure 5.1. For example, the boiler and turbine valve model has two inputs and three outputs. Inputs are turbine valve area and power available to generate steam. Outputs are throttle pressure, power to the turbines, and boiler and stack loss [81]. The steam turbines are modeled on the assumption that high pressure, reheat, and low pressure turbines are used [65,69]. The Combustor/Nozzle/Channel/Diffuser (CNCD) section is much more sophisticated than in previous models, being represented by polynomial approximations of data resulting from the solution of energy balance, state, and continuity equations for the combustor, and the quasi one-dimensional MHD equations for the channel and diffuser [114]. Inputs to the CNCD are fuel thermal input power and preheated air temperature. Outputs of the CNCD are thermal power loss, power absorbed by the cooling water, thermal power in the combustion gases leaving the diffuser, and inverter electrical output power.

The additional detail in model III is not limited to component modeling but appears in the control system as well. A wide variety of controller variations are possible with two

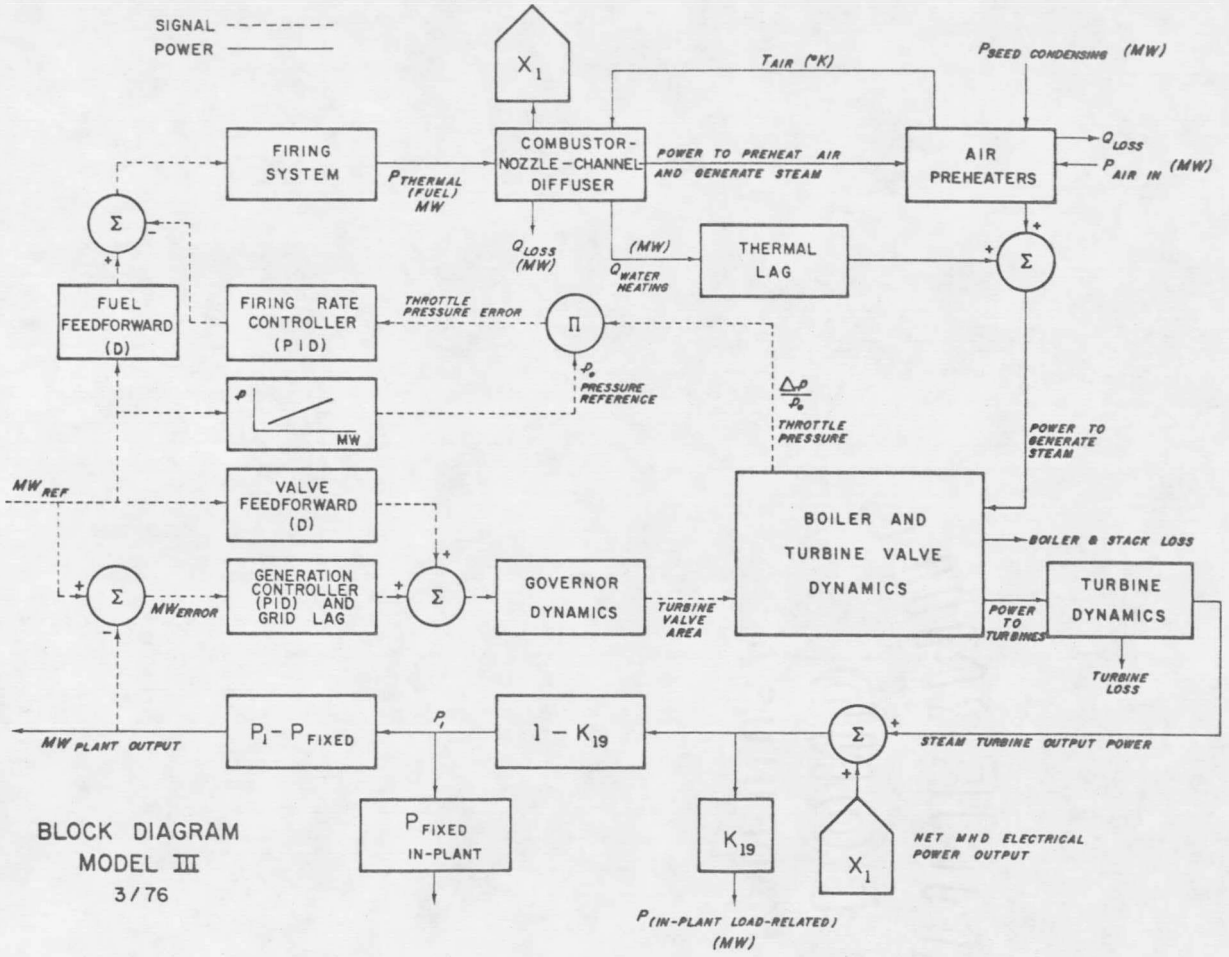



Figure 5.1. Block diagram for model III

proportional-integral-derivative (PID) controllers available; one for controlling turbine valves via a governor, and the other for adjusting the combustor firing rate. In addition, two feedforward controllers are included to allow even greater flexibility of control.

A more detailed discussion of the overall model III block diagram is given in the following section.

## 5.2 Model III Block Diagram

In Figure 5.1, desired unit generation, $MW_{REF}$, is compared with actual unit generation, $MW_{plant\ output}$, and the generation error, $MW_{error}$, serves as the input to the generation controller. The derivative of $MW_{REF}$ is available as a feedforward signal to both the turbine governor and the combustor firing system.

Control of the governor is accomplished by summing the generation controller and valve feedforward outputs. The governor, in turn, controls the turbine valve area. Power to the turbines, which is proportional to the mass flow rate of steam, is a function of both the turbine valve area and power available to generate steam. Throttle pressure is also a function of valve area and available power.

The throttle pressure error signal is the input to the PID firing rate controller. The control signal for the firing system is the sum of the firing rate controller and fuel feedforward outputs.

Regenerative air preheaters accept the combustion gases from the diffuser to heat combustion air which is supplied by an air compressor. Power recovered from condensing seed is also accounted for, as is power lost to ambient. Air preheater outputs are air preheat temperature and high-grade thermal power to the steam plant. Power to generate steam is considered to be the sum of thermal power in the CNCD coolant and the high-grade thermal power from the air preheaters.

In-plant, load-related power is taken to be air compressor power and turbogenerator auxiliary power for pumps and other internal requirements. Fixed in-plant power is the requirement for the magnet and other fixed loads such as lighting. Actual or net plant output power is the sum of steam turbine and MHD electrical output power less in-plant load requirements.

The control scheme for System Model III is essentially a boiler-following or conventional mode from the boiler-turbine point of view if the feedforward controllers are not used. Boiler following is a standard control mode for fossil-fired steam generating units and is shown in Figure 5.2 [72]. Essentially, boiler-following control uses generation error, or $MW_{error}$, as an input to a controller that operates the turbine governor. Throttle pressure error, in turn, alters firing rate through an appropriate controller. Thus, boiler-following control allows the steam turbines to quickly respond to changes in load demand while the boiler firing system follows the turbine action

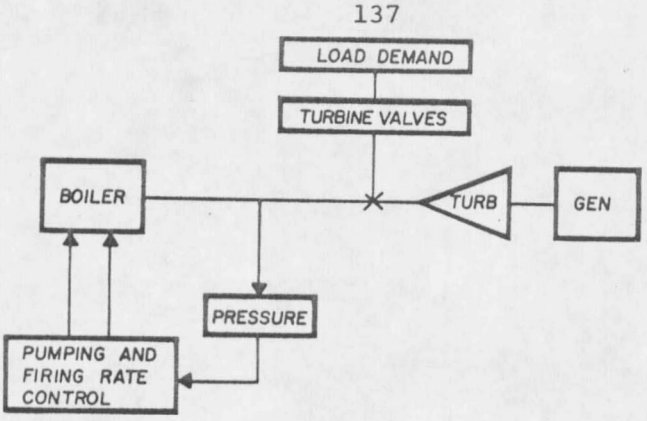



Figure 5.2. Boiler-following or conventional control mode

by acting to maintain constant throttle pressure. This method of control makes good use of stored energy in the boiler and provides the most rapid output response possible from the steam bottoming plant.

The overall MHD/steam combined cycle is, of course, different from a conventional steam plant in that a fraction of fuel thermal input power is almost immediately available as MHD electrical output power. This rapidly responding characteristic of the MHD channel is utilized by providing a feedforward control path to the firing system, making available a control signal related to the rate of change of desired unit generation, $MW_{REF}$.

For general interest, it is worthwhile to briefly describe two other types of boiler control and compare them with the conventional control mode. One type, called turbine-following control, is illustrated in Figure 5.3 [72]. In this case, generation error is used as the input to the firing system. The throttle pressure controls the

turbine governor. Thus, if a change in load is desired, the boiler steam generation characteristics must first be altered before plant output can change. This type of control is very slow but very stable. Because of the slow response, turbine-following control is not used except for emergency conditions.

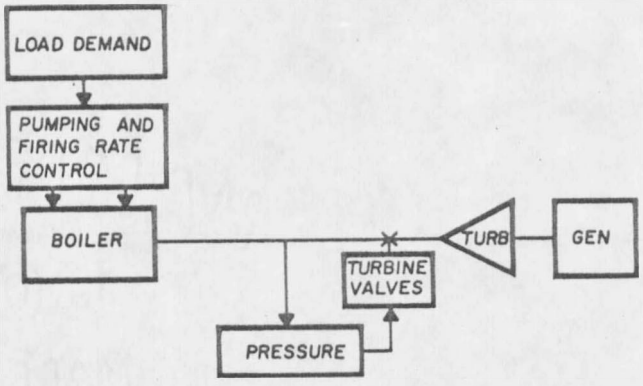



Figure 5.3. Turbine following control mode

The other type of boiler control to be described is shown in Figure 5.4 [72]. It is a combination of boiler-following and turbine-following control, and is called controlled load or integrated control. Some form of integrated control is used on most modern once-through boiler units. As indicated in Figure 5.4, a firing rate control signal is derived from both generation error and throttle pressure information. These two variables are also used to determine turbine governor setting and hence plant output power.

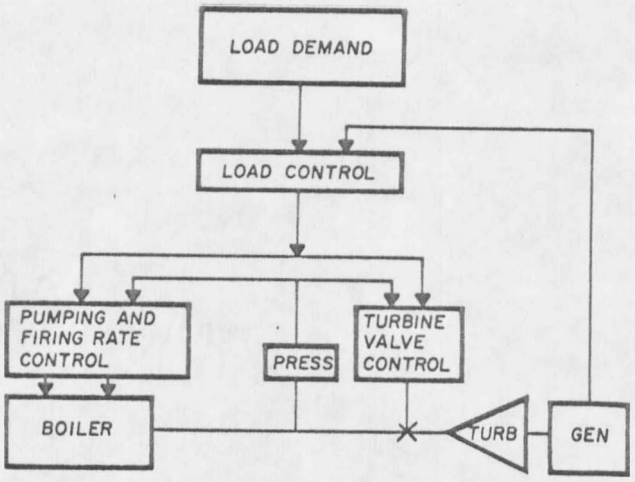



Figure 5.4. Integrated control

Comparison of boiler-following, turbine-following, and integrated types of control is most readily accomplished by considering Figure 5.5 [72]. Briefly, boiler-following or conventional control provides the most rapid response to load changes of the three configurations. This response is somewhat underdamped. Turbine-following control is the slowest type of control and exhibits overdamped response. Integrated control response rate is slower than that of boiler-following but faster than that of turbine-following control. It exhibits no overshoot.

Boiler following, or conventional control is chosen as the initial control configuration for system model III for the following reasons: (1) it takes full advantage of the energy storage characteristics of the boiler, (2) it provides the most rapid steam plant response to load variations, and (3) because of the rapid response

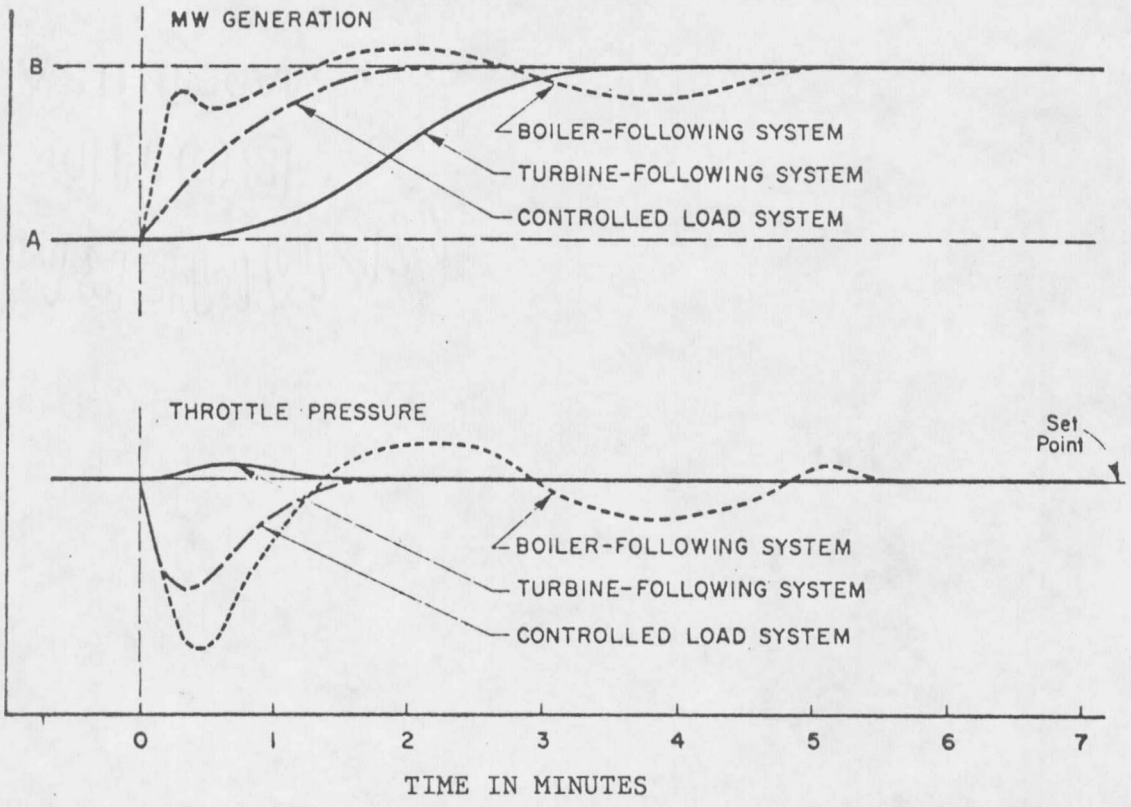



Figure 5.5. Transient response of three types of boiler control

characteristics of the turbine output with this type of control, the steam plant is expected to aid the MHD channel in load control to the maximum degree possible, in the event that load variations exceed the long-term MHD channel capability.

The system model is, of course, independent of the control configuration and future work is expected to include simulations of other types of control systems.

## 5.3 Detailed Block Diagrams

Detailed block diagrams for model III are described in this section. These diagrams define the contents of major blocks in the overall model III diagram of Figure 5.1. A complete set of system equations for model III is given in the simulation program listed in Appendix C. The equations follow directly from the detailed block diagrams.

### 5.3.1 Generation Controller

The generation controller block diagram, shown in Figure 5.6, also includes valve feedforward and power grid lag block diagrams. Power generation error $X_3$ is multiplied by a first-order lag to account for the effect of a power grid the plant may be supplying. The grid-lag time constant $\tau_1$ has been assumed to be 10 seconds in the simulations described later in this chapter. This value is considered representative for power grids in the United States [41]. The generation controller is proportional-integral-derivative (PID) and has the lag output $X_4$ as an input. The controller output $X_5$, summed with the feedforward output $X_6$, constitutes the control signal to the turbine governor.

The generation controller constants allow great flexibility in choosing the actual type of control used in a particular simulation. For example, if a PI controller were desired, $K_4$ would be set to zero.

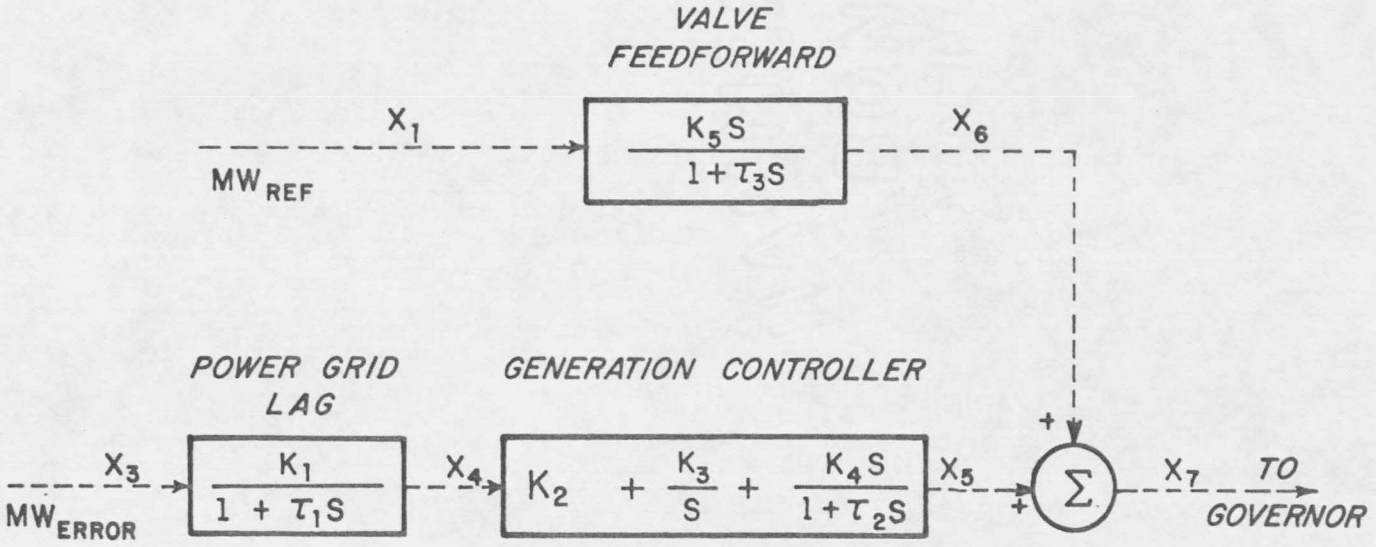



Figure 5.6. Generation controller, valve feedforward, and grid lag

The derivative portion of the controller is modified by a $1/(1 + \tau s)$ multiplier, where $\tau = 0$ gives true derivative action. The same is true for the valve feedforward derivative (D) controller. The desirability of the $1/(1 + \tau s)$ multiplier is evident if a step change in desired unit generation, $X_1$, is applied. The derivative of a step function, i.e., an impulse function, would not be a realistic control signal for either the governor or the firing system, where a similar situation occurs. If $X_1(t) = A\ u(t)$, where $u(t)$ = unit step function, then

$$X_6(s) = \frac{K_5 s}{1 + \tau_3 s} X_1(s) = \frac{AK_5}{1 + \tau_3 s} \tag{5.1}$$

and

$$X_6(t) = \frac{AK_5}{\tau_3} e^{-t/\tau_3}\ u(t) \tag{5.2}$$

$K_5$ and $\tau_3$ may be adjusted to give $X_6(t)$ a wide variety of initial values and decay rates.

The actual set of equations used to describe the generation controller appear in the Model III simulation program listing of Appendix C. The equations are based on the block diagram of Figure 5.7, and follow directly.

$$X_{76} = K_2 X_4 \tag{5.3}$$

$$X_{77} = \frac{K_3}{s} X_4 \tag{5.4}$$

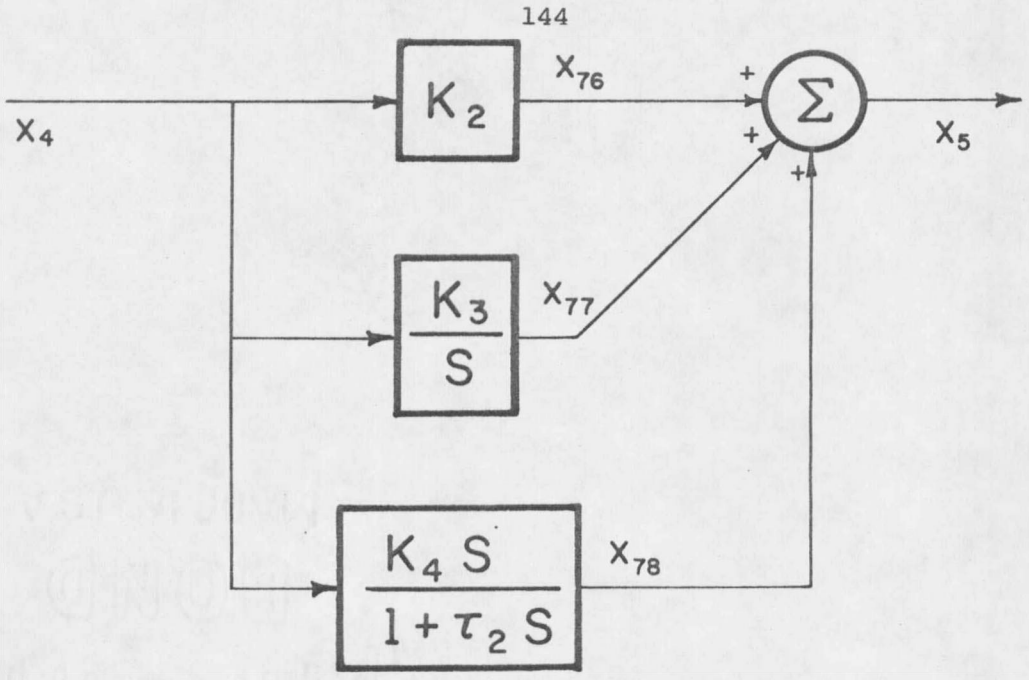



Figure 5.7. Generation controller

$$X_{78} = \frac{K_4 s}{1 + \tau_2 s} X_4 \tag{5.5}$$

$$X_5 = X_{76} + X_{77} + X_{78} \tag{5.6}$$

$$DX_{77} = K_3 X_4 \quad \text{where } D \equiv \frac{d}{dt} \tag{5.7}$$

$$DX_{78} = (K_4 DX_4 - X_{78})/\tau_2 \tag{5.8}$$

In the block diagram of Figure 5.6, $K_2$, $K_3$, $K_4$, $K_5$, $\tau_2$, and $\tau_3$ are all design parameters and may be chosen to simulate any desired response of which the system is capable.

5.3.2 Governor dynamics

The governor block diagram of Figure 5.8 processes the control signal, $X_7$, and converts it into fractional change in turbine valve area with respect to an initial valve opening, $X_{14}$. $\tau_4$ and $\tau_5$ are time constants of first-order lags which describe the governor servomotors. $X_{11}$ is turbine valve area. The valve area is magnitude limited so that it cannot be negative or greater than maximum area. The rate of valve opening and/or closing is constrained by a rate limiter. Typical values for the constants are used [65], and are tabulated in Table 5.4, page 175. $X_{13}$ is the initial value of $X_{11}$. $X_{11}$ is converted into fractional form to be compatible with the boiler model.

5.3.3 Boiler and turbine valve dynamics

The steam boiler and turbine valves are modeled as shown in Figure 5.9 [81]. Inputs are thermal power from the air preheaters and water heating, $X_{21}$, and fractional change in turbine valve area, $X_{14}$. Outputs are stack and boiler losses, $X_{22}$, fractional change in throttle pressure, $X_{31}$, and power to the turbines, $X_{20}$.

$X_{23}$ is the actual power available to the steam turbines at steady state. $X_{25}$ is the initial value of $X_{23}$. $X_{26}$ is the fractional change in $X_{23}$ relative to its initial value. A certain amount of time is required for the boiler to change steam generation after the steam

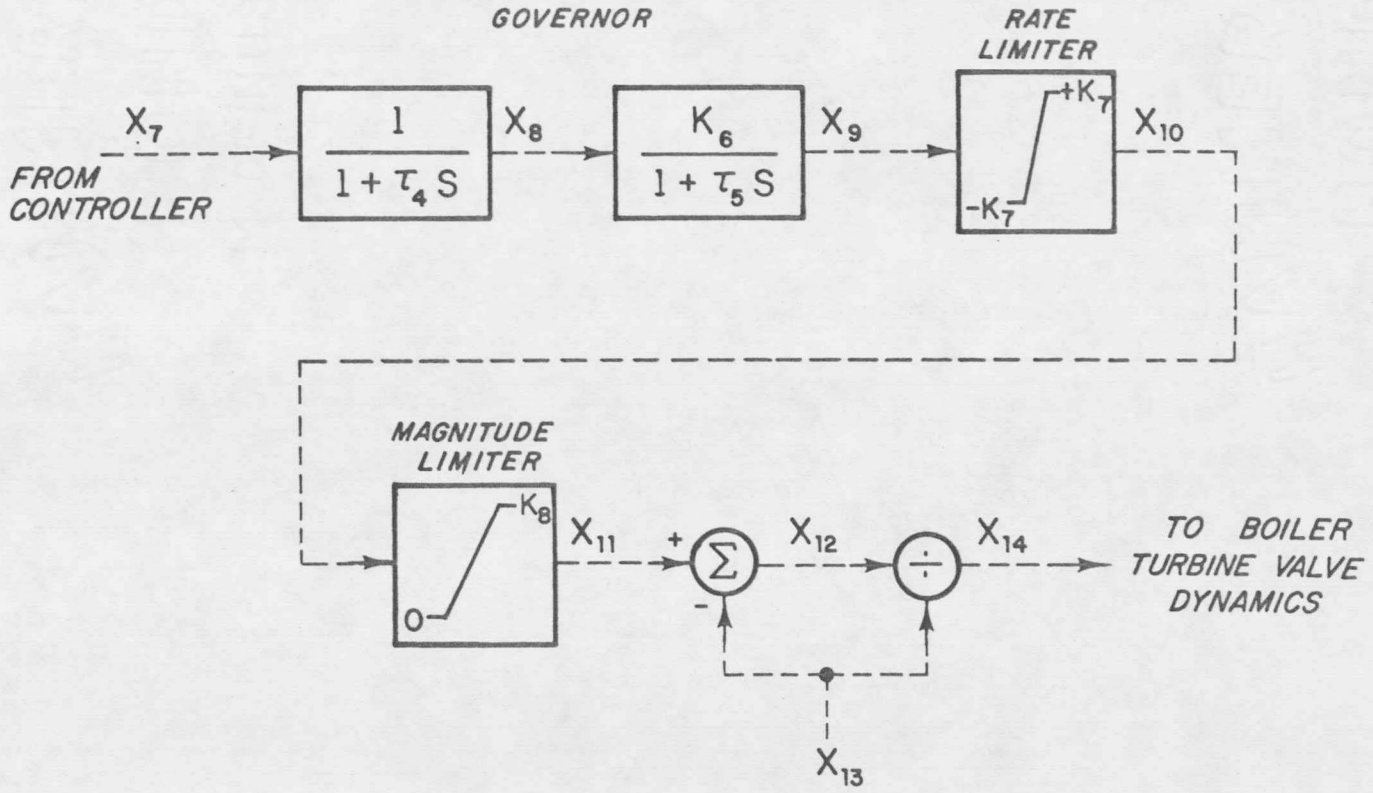



Figure 5.8. Governor dynamics

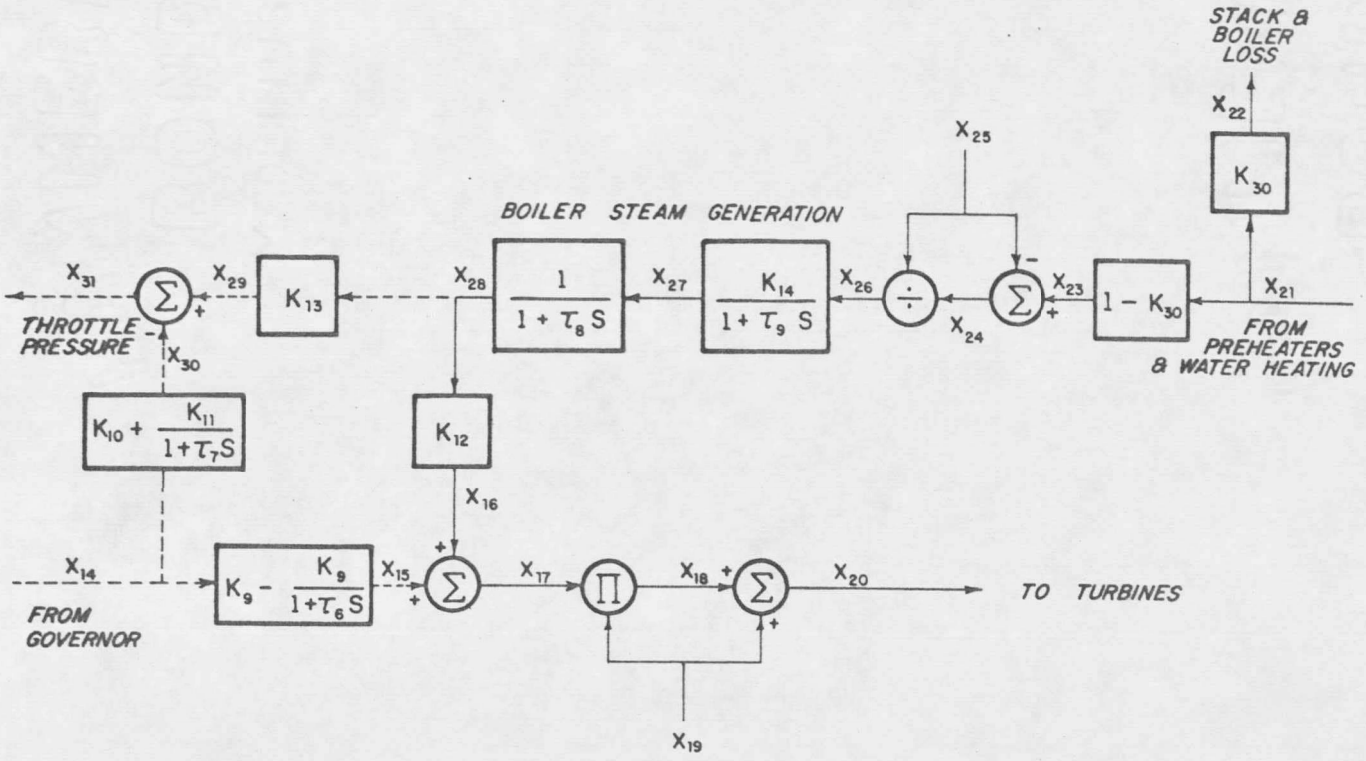



Figure 5.9. Boiler and turbine valve dynamics

plant input thermal power, $X_{21}$, is altered. This effect is modeled by a cascade of two first-order lags with time constants $\tau_8$ and $\tau_9$.

The boiler and turbine valve model should reflect the following characteristics: (1) If thermal input power to the boiler increases and turbine valve area remains unchanged, power available to the turbines increases and throttle pressure increases. (2) If thermal input power is fixed and the turbine valve opening increases, power output increases initially and throttle pressure decreases. (3) Boiler storage effects exist and affect boiler dynamic characteristics.

Condition (1) of the previous paragraph may be applied to the model by setting fractional change in turbine valve area, $X_{14}$, equal zero, and increasing thermal input power $X_{21}$. This increase in $X_{21}$ propagates through the first-order lags and the $K_{12}$ and $K_{13}$ blocks, increasing $X_{20}$ and $X_{31}$.

The effect of holding thermal power input, $X_{21}$, constant and increasing turbine valve area may be achieved by setting $X_{26}$ equal to zero and increasing $X_{14}$. If $X_{26} = 0$, $X_{16}$ and $X_{29}$ will equal zero also. As $X_{14}$ increases, multipliers $K_9$ and $K_{10}$ immediately transmit a fraction of this change to $X_{15}$ and $X_{30}$, respectively. $X_{31} = -X_{30}$ and $X_{17} = X_{15}$ because of the constraint imposed on $X_{26}$. Thus, the immediate response to increasing turbine valve area is power to the turbines, $X_{20}$, increasing, and throttle pressure, $X_{30}$, decreasing. If

the turbine valve remains at its new position and thermal input power does not change, boiler storage effects become noticeable and are modeled by first-order lags determined by time constants $\tau_6$ and $\tau_7$. Power to the turbines drops exponentially with time constant $\tau_6$ toward its original value. Simultaneously, throttle pressure $X_{31}$ drops to a lower value in an exponential manner with time constant $\tau_7$ so that in the limit $X_{31} = -X_{14}$.

The blocks defining the relationships between $X_{14}$ and $X_{15}$ and between $X_{14}$ and $X_{30}$ are expanded in Figure 5.10 to show the basis for the equations in Appendix C defining $X_{79}$, $X_{80}$, $X_{81}$, and $X_{82}$.

The boiler-turbine valve model of Figure 5.9 was chosen because; (1) it was developed to describe supercritical once-through boiler units; (2) it clearly shows the effect of turbine valve variations on steam flow (output power) and on throttle pressure; (3) representative values for the model constants are available as non-proprietary information in the published literature [81]; and (4) experimental verification of this and other similar low-order models has been published [48,62].

### 5.3.4 Turbine dynamics

The model for the steam turbines is shown in Figure 5.11. It is a standard representation of the dominant features of a reheat system

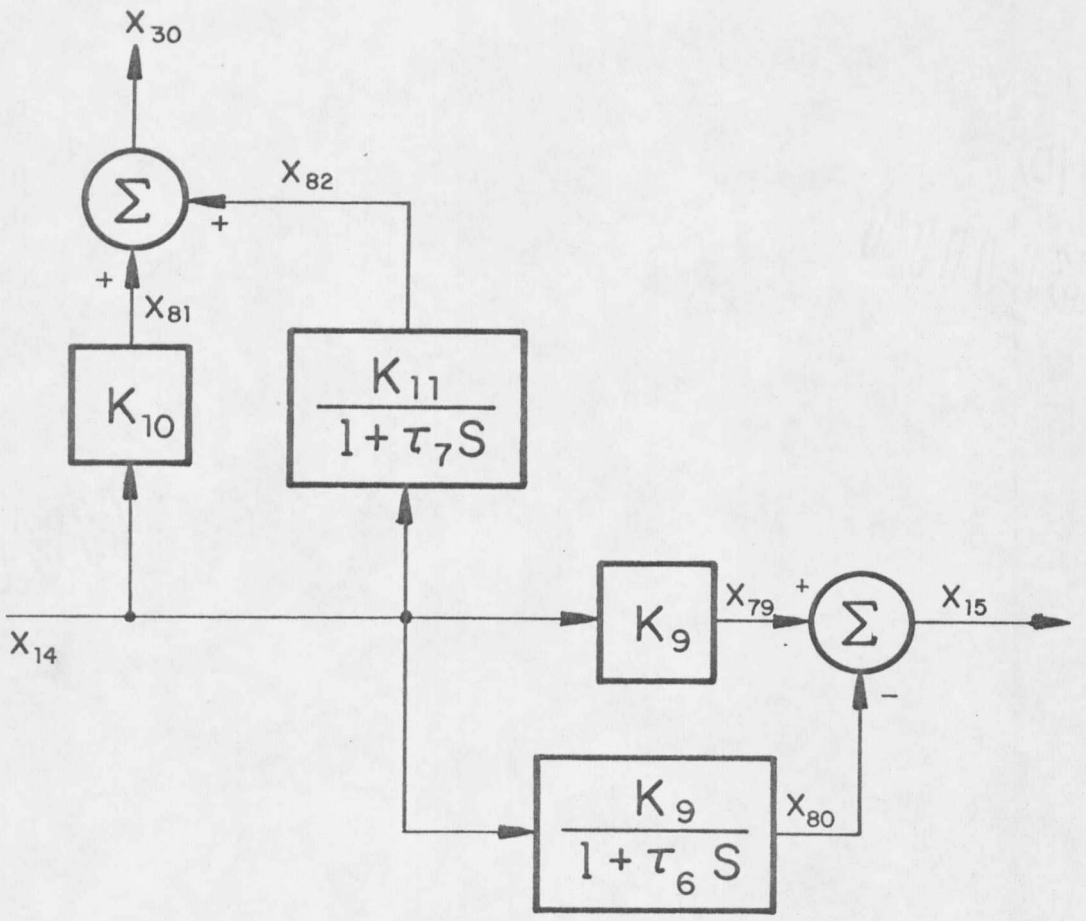



Figure 5.10. Turbine valve and boiler storage effects

[65,69]. In fact, the model is more detailed than that commonly used by a major boiler manufacturer [48].

The input to the turbines is power output from the boiler. The outputs are turbine loss and net steam turbine output power. First-order lags are associated with the steam bowl or chest, the reheat piping, and the crossover piping. The dominant time constant is

associated with reheat. Constants $K_{15}$, $K_{16}$, and $K_{17}$ are power fractions associated with the high-pressure turbine, the reheat turbine, and the low-pressure turbine, respectively. The combined turbogenerators are assumed to be 87% efficient [69]. Typical values of multiplier and time constants are suggested in [65] and are given in Table 5.4.

### 5.3.5 Firing rate controller

The firing rate controller and fuel feedforward controller are illustrated in Figure 5.12. Inputs are throttle pressure, $X_{31}$, in fractional form, and desired unit generation $X_1$. The output, $X_{51}$, is the control signal to the firing system and consists of the difference between the fuel feedforward block output and the firing rate controller output. The negative sign in the summing block which forms the algebraic sum $X_{51} = X_{50} - X_{49}$ is necessary because a positive pressure error requires a reduction in the fuel firing rate, and because constants $K_{21}$, $K_{22}$, and $K_{23}$ are positive.

Pressure reference $X_{47}$ is fixed at 3500 psig ($2.46 \times 10^7$ n/m$^2$) throttle steam pressure. This conforms to practice at the Four Corners power plant, Fruitland, NM, in controlling 755 MW (electrical) Babcock and Wilcox supercritical once-through boilers at loads greater than 25%.

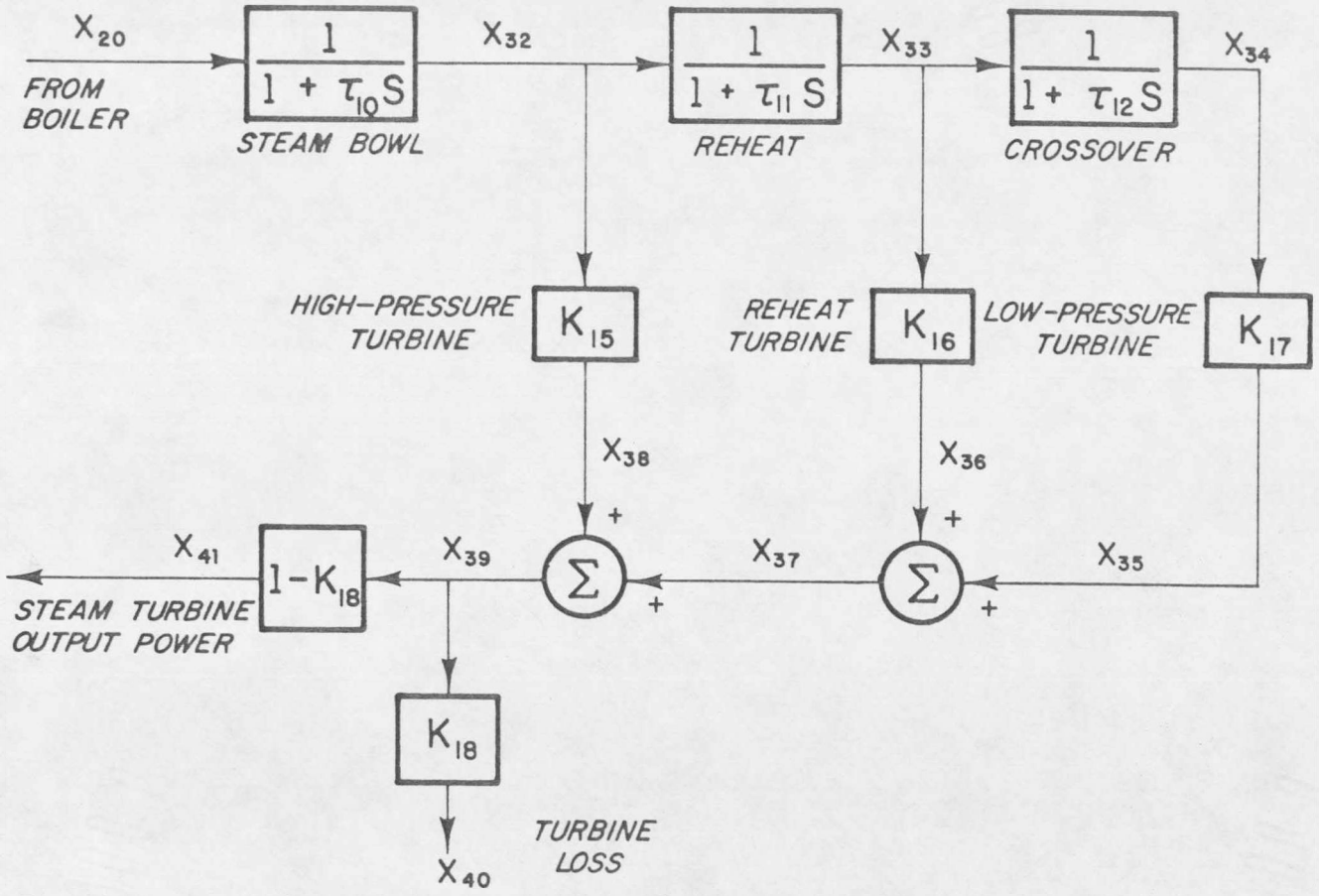



Figure 5.11. Turbine dynamics

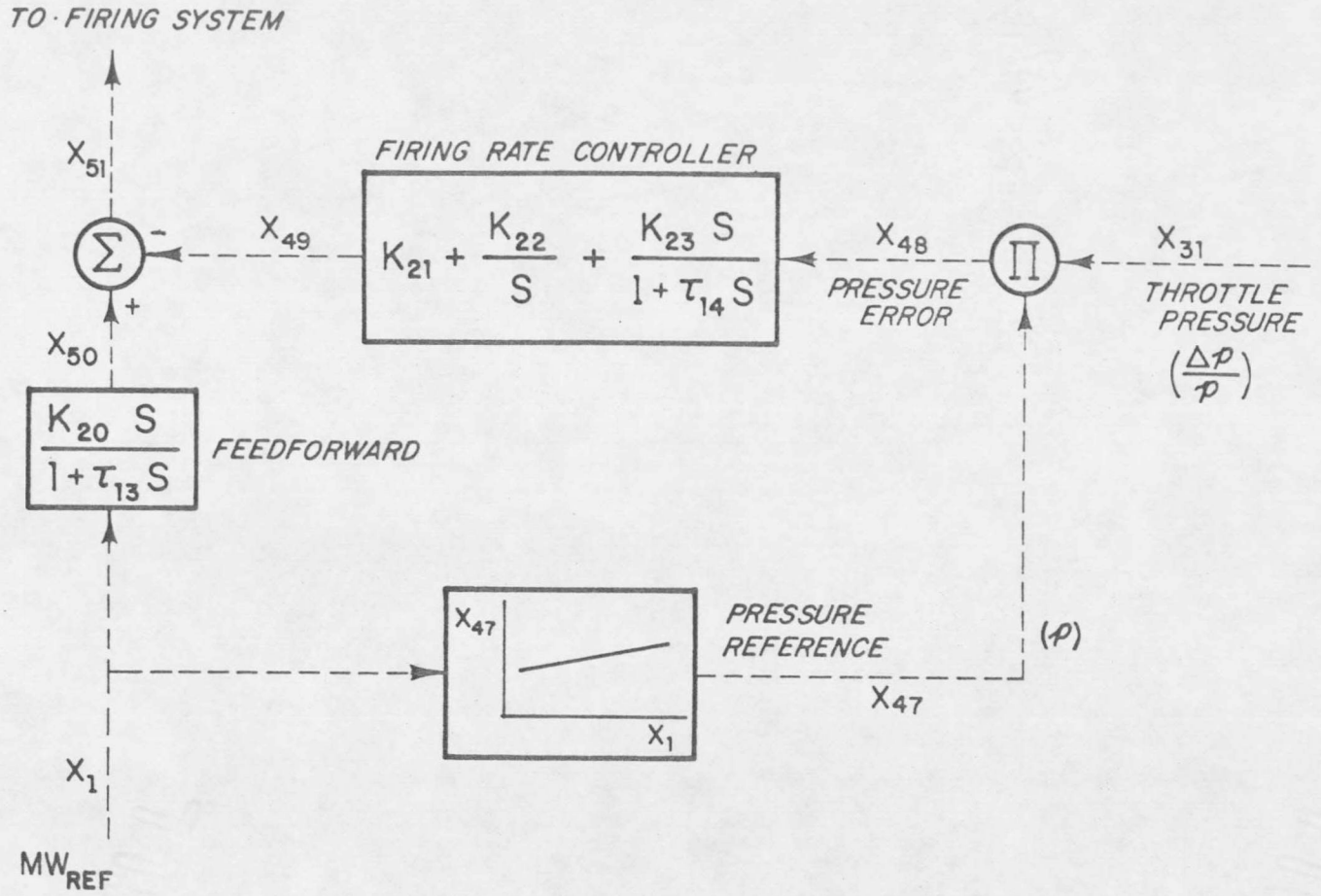



Figure 5.12. Firing rate and fuel feedforward controllers

The set of equations used to describe the firing rate controller are based on the block diagram of Figure 5.13 and are given in Appendix C. Constants $K_{20}$, $K_{21}$, $K_{22}$, $K_{23}$, $\tau_{13}$, and $\tau_{14}$ shown in Figure 5.12 are all design parameters.

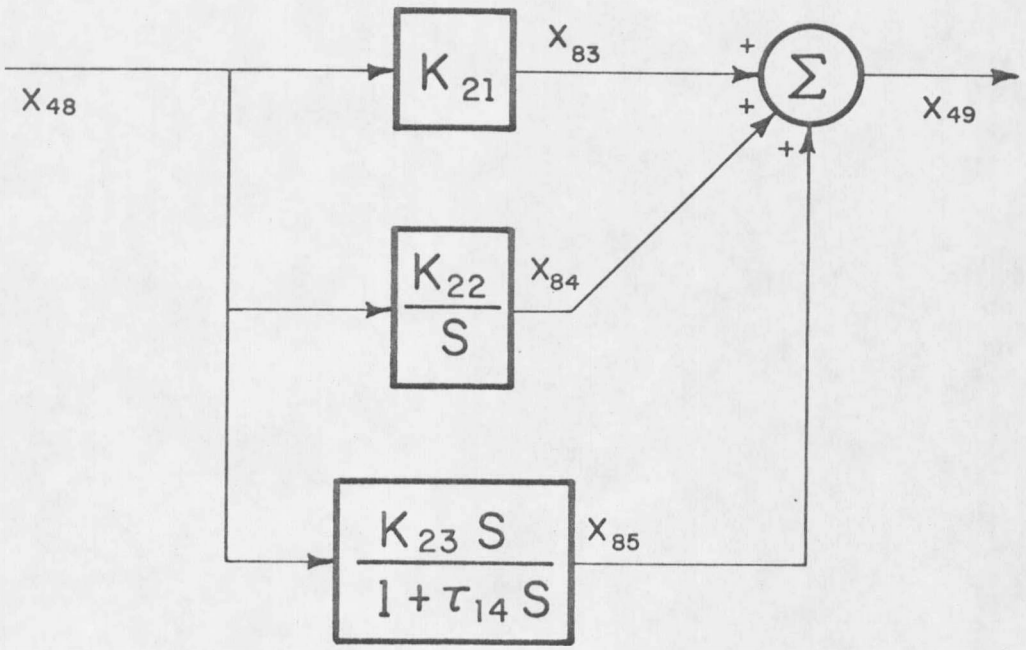



Figure 5.13. Firing rate controller

5.3.6 Firing system

The firing system for model III is shown in Figure 5.14. The firing rate controller output is magnitude limited to ensure that the fuel valve position is always between fully open and fully closed, and rate limited to $K_{24}$ (dynamic range/second). The actual firing system

dynamics are represented as in model II, with a first-order lag in cascade with a pure time delay. In all simulations, n = 1 in Figure 5.14 to give a model somewhat slower than typical gas/oil-fired systems but faster than existing coal-fired systems as in model II. The form of the denominator of the firing system function is used to allow multiple first-order lag terms if required by a particular firing system. Values of constants are given in Table 5.4.

### 5.3.7 Combustor/Nozzle/Channel/Diffuser Model

The Combustor/Nozzle/Channel/Diffuser (CNCD) representation for system model III is the result of work by Pierre, et al. [114] which is based on equations by Baylis, et al. [15] and Oliver and Byer [105]. The following discussion is abstracted from [114].

The desired form of the CNCD is an input-output model formulated from a polynomial approximation of steady-state data. The implicit assumption is that time constants and delays in the CNCD are negligible compared with the rest of the system. Input variables are chosen to be fuel thermal input power, $X_{55}$, and preheated air temperature $X_{73}$. Output variables are net MHD electrical power output, $X_{42}$, thermal power loss, $X_{56}$, power absorbed by the cooling water, $X_{57}$, and thermal power in the combustion gases leaving the diffuser, $X_{58}$.

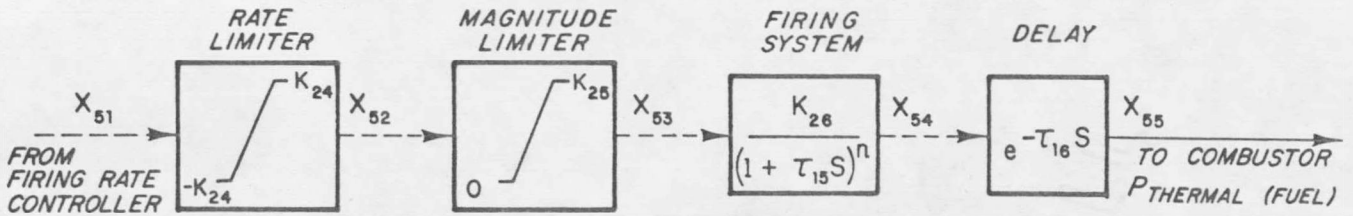



Figure 5.14. Firing system

Computational steps leading to the desired polynomial approximation are listed below. These steps are applied to a CNCD that has been designed under design-center conditions.

Step 1. CNCD inputs are specified. These include combustor inputs and appropriate inverter characteristics which affect the channel.

Step 2. A combustor pressure is assumed.

Step 3. The combustor energy balance equation is used to find combustor temperature.

Step 4. Combustion gas density is determined, using the combustion equation of state. Combustion gas velocity is found from the continuity equation.

Step 5. Quasi one-dimensional MHD equations are solved through the nozzle with magnetic field density $\underline{B}$ and current density $\underline{J}$ both zero, through the channel with the $\underline{J} \times \underline{B}$ and $\underline{J} \cdot \underline{E}$ evaluated by the gas conditions, electrode connections, and inverter characteristics, and through the diffuser with $\underline{B}$ and $\underline{J}$ again zero.

Step 6. Output pressure, $P_{out}$, is checked: If $P_{out}$ is in the range $1.19 \leq P_{out} \leq 1.2$ atmospheres, go to Step 7; if $P_{out} < 1.19$ atmospheres, increase assumed combustor pressure with a rational extrapolation algorithm and

return to Step 3; and if $P_{out}$ > 1.2 atmospheres, decrease assumed combustor pressure and return to Step 3.

Step 7. Record output gas properties and electrical output as a function of CNCD inputs.

Step 8. Select another set of CNCD inputs and repeat Steps 2 through 7, or if all input data have been processed, go to Step 9.

Step 9. Generate a polynomial approximation for the input-output data recorded in Step 7.

Equations used in the computational steps are as follows.

Equation of state: $$R = \frac{1}{Q(P,T)} \tag{5.9}$$

where $R$ = density ($Kg/m^3$)

$P$ = pressure ($N/m^2$)

$T$ = temperature (°K)

Continuity equation: $$RVA = W \tag{5.10}$$

where $V$ = velocity (m/sec)

$A$ = area ($m^2$)

$W$ = mass flow rate (Kg/sec)

Momentum equation:

$$\frac{W}{A}\frac{dV}{dx} + \frac{dP}{dx} = J \times B - F(V) \tag{5.11}$$

Energy equation:

$$\frac{W}{A}\frac{dH(P,T)}{dx} + \frac{W}{A} V \frac{dV}{dx} = J \cdot E - G(T,V) \qquad (5.12)$$

where F is the friction force per unit volume and G is the heat transfer per unit volume. Explicit forms for H(P,T), Q(P,T), F(V), and G(T,V) are given in [114].

Equations 5.11 and 5.12 are manipulated into the following matrix form to utilize P and T as state variables.

$$\begin{bmatrix} 1 + \alpha Q_P & \alpha Q_T \\ H_P + \alpha Q Q_P & H_T + \alpha Q Q_T \end{bmatrix} \begin{bmatrix} \frac{dP}{dx} \\ \frac{dT}{dx} \end{bmatrix} = \begin{bmatrix} J \times B - F + \alpha \frac{Q}{A}\frac{dA}{dx} \\ \frac{A}{W}(J \cdot E - G) + \frac{\alpha Q^2}{A}\frac{dA}{dx} \end{bmatrix} \qquad (5.13)$$

where $\alpha \triangleq (\frac{W}{A})^2$, $Q_P = \frac{\partial Q}{\partial P}$, $H_T = \frac{\partial H}{\partial T}$, etc.

Input-output data for the CNCD was developed for the following magnitude ranges of the input variables $X_{55}$ and $X_{73}$:

$$3000 \text{ MW} \leq X_{55} \leq 4200 \text{ MW}$$

$$1700°K \leq X_{73} \leq 1900°K$$

If $X_{55}$ is greater than 4200 MW, shock occurs which is to be avoided.

5.3.8 Air preheaters

The air preheaters are modeled as shown in Figure 5.15. The model is essentially the same as that used for system model II (Figure 4.1). Differences are: 1) thermal power from condensing seed is explicitly shown as an input in Figure 5.15; 2) thermal power loss to ambient is an output; and 3) air preheat temperature output, $X_{73}$, accounts for 300°K ambient air temperature. The $E_1(t)$ and $T_1(t)$ functions are unchanged from Figure 4.3 except that the maximum value of $E_1(t)$, $E_m$, is slightly different for model III than for model II.

5.3.9 Thermal Lag

The block titled "thermal lag" in Figure 5.1 consists of a simple first-order lag to account for thermal lag in the CNCD cooling system. The input to the block is $X_{57}$, power available to the steam cycle from water cooling the CNCD. The output variable is designated $X_{74}$.

5.4 Description of System Variables

The variables for model III are tabulated in Table 5.1. Refer to the detailed block diagrams of Figures 5.6 through 5.15.

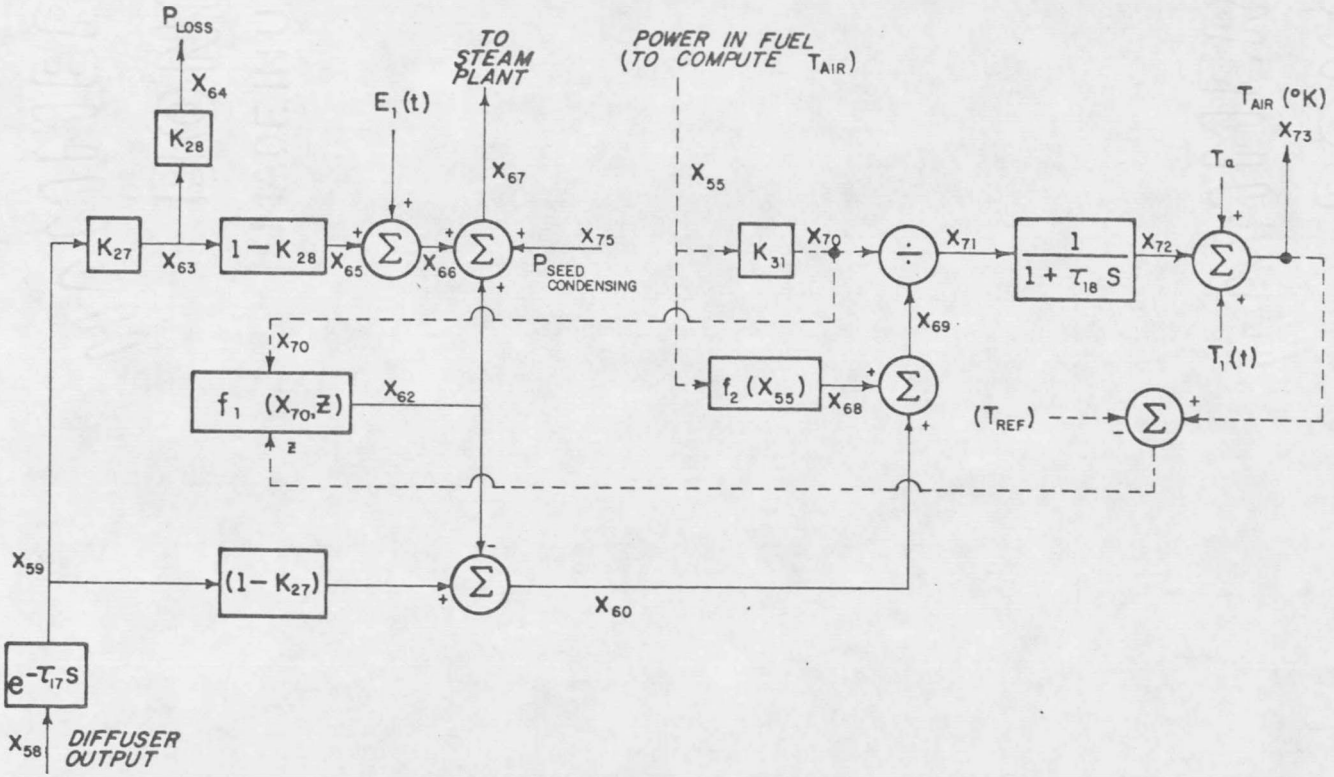



Figure 5.15. Air preheaters

Table 5.1. Description of Model III system variables

| Variable | Units | Description |
|---|---|---|
| $X_1$ | MW | desired plant output; MW reference |
| $X_2$ | MW | net plant output power |
| $X_3$ | MW | error between required and actual output (generation error) |
| $X_4$ | MW | generation error after power grid lag |
| $X_5$ | -- | generation controller output |
| $X_6$ | -- | valve feedforward controller output |
| $X_7$ | -- | composite controller signal to governor |
| $X_8$ | -- | intermediate variable in governor between two first-order lag blocks |
| $X_9$ | $m^2$ | turbine valve area (governor output not rate or magnitude limited) |
| $X_{10}$ | $m^2$ | turbine valve area (rate limited) |
| $X_{11}$ | $m^2$ | turbine valve area (rate and magnitude limited) |
| $X_{12}$ | $m^2$ | $\Delta$Area = actual valve area - initial or nominal valve area |
| $X_{13}$ | $m^2$ | initial or nominal valve area |
| $X_{14}$ | -- | ($\Delta$Area)/(initial area) = fractional change in turbine valve area with respect to initial area |
| $X_{15}$ | -- | change in fractional power from boiler to turbines due to fractional change in turbine valve area |
| $X_{16}$ | -- | change in fractional power from boiler to turbines due to fractional change in net input thermal power to steam plant |
| $X_{17}$ | -- | fractional output steam flow or fractional power from boiler to turbines ($X_{18}/X_{19}$) |
| $X_{18}$ | MW | $\Delta$Power from boiler = actual power - initial power ($X_{20} - X_{19}$) |

Table 5.1 (cont.)

| Variable | Units | Description |
|---|---|---|
| $X_{19}$ | MW | initial (reference) power from boiler |
| $X_{20}$ | MW | actual power output from boiler to turbines |
| $X_{21}$ | MW | thermal power available to steam plant from combustion gases leaving preheaters plus power available due to water heating from Combustor/Nozzle/Channel/Diffuser cooling |
| $X_{22}$ | MW | stack and boiler losses ($K_{30}$ $X_{21}$) |
| $X_{23}$ | MW | actual power available to generate steam after subtracting stack and boiler losses |
| $X_{24}$ | MW | $\Delta$ power available to generate steam = actual power - reference power |
| $X_{25}$ | MW | initial (reference) power available to generate steam |
| $X_{26}$ | -- | $\Delta$Power/reference power = fractional change in power available to generate steam with respect to reference power ($X_{24}/X_{25}$) |
| $X_{27}$ | -- | intermediate variable in steam generation between two first-order lag blocks |
| $X_{28}$ | -- | fractional change in "virtual" steam flow (steam flow related to firing rate only and not to turbine valve area) |
| $X_{29}$ | -- | effect of fractional virtual steam flow on fractional throttle pressure |
| $X_{30}$ | -- | effect of fractional turbine valve area and boiler storage on fractional throttle pressure |
| $X_{31}$ | -- | fractional throttle pressure = $\Delta$pressure/ initial pressure |
| $X_{32}$ | MW | power available at high-pressure turbine input |
| $X_{33}$ | MW | power available at reheat turbine (intermediate pressure) input |
| $X_{34}$ | MW | power available at low-pressure turbine input |
| $X_{35}$ | MW | output power of low-pressure turbine (neglecting turbine losses) |

Table 5.1 (cont.)

| Variable | Units | Description |
|---|---|---|
| $X_{36}$ | MW | output power of reheat turbine (neglecting turbine losses) |
| $X_{37}$ | MW | sum of reheat and low-pressure turbine outputs (neglecting losses) |
| $X_{38}$ | MW | output power of high-pressure turbine (neglecting turbine losses) |
| $X_{39}$ | MW | total steam turbine output power (neglecting losses) |
| $X_{40}$ | MW | turbine losses |
| $X_{41}$ | MW | net steam turbine output power |
| $X_{42}$ | MW | net MHD electrical output power |
| $X_{43}$ | MW | sum of net steam turbine output power and net MHD electrical output power |
| $X_{44}$ | MW | in-plant load-related power requirements (for example, air compressor) |
| $X_{45}$ | MW | overall plant output power including fixed in-plant power requirements |
| $X_{46}$ | MW | fixed in-plant power requirements |
| $X_{47}$ | $n/m^2$ | throttle pressure reference (PSI in program) |
| $X_{48}$ | $n/m^2$ | throttle pressure error (PSI in program) |
| $X_{49}$ | -- | output of firing rate controller |
| $X_{50}$ | -- | output of feedforward firing rate controller |
| $X_{51}$ | -- | composite controller signal to firing system |
| $X_{52}$ | -- | $X_{51}$ rate limited |
| $X_{53}$ | -- | $X_{51}$ rate and magnitude limited |
| $X_{54}$ | MW | thermal power of fuel out of firing system |
| $X_{55}$ | MW | thermal power of fuel in combustor (PT) |
| $X_{56}$ | MW | power loss from Combustor/Nozzle/Channel/Diffuser (CNCD) |

Table 5.1 (cont.)

| Variable | Units | Description |
|---|---|---|
| $X_{57}$ | MW | power available to steam cycle from water cooling the CNCD |
| $X_{58}$ | MW | power in combustion gas available for air preheaters and steam cycle |
| $X_{59}$ | MW | $X_{58}$ delayed by transit time of combustion gases from diffuser to steam plant |
| $X_{60}$ | MW | fraction of combustion gas thermal power used to preheat combustion air |
| $X_{61}$ | -- | not used |
| $X_{62}$ | MW | power out of preheat temperature control |
| $X_{63}$ | MW | diffuser output power remaining after preheater and temperature control requirements have been satisfied |
| $X_{64}$ | MW | preheater power loss |
| $X_{65}$ | MW | $X_{63}$ less preheater power loss |
| $X_{66}$ | MW | sum of $X_{65}$ and time varying power function $E_1(t)$ simulating the effect of cycling heat exchangers |
| $X_{67}$ | MW | power available to steam plant from heat exchangers |
| $X_{68}$ | MW | power in preheated air due to compressor (PCOMP) |
| $X_{69}$ | MW | power in preheated air due to compressor and air preheaters (PA) |
| $X_{70}$ | MW/°K | power required to increase air preheat temperature 1°K |
| $X_{71}$ | °K | preheated air temperature not accounting for preheater lag or effect of cycling heat exchangers |
| $X_{72}$ | °K | preheated air temperature not including effect of cycling heat exchangers |

Table 5.1 (cont.)

| Variable | Units | Description |
|---|---|---|
| $X_{73}$ | °K | temperature of preheated air leaving pre-heaters and entering combustor (T(OUT) |
| $X_{74}$ | MW | power in heated water/steam available at steam plant due to CNCD cooling |
| $X_{75}$ | MW | power recovered from condensing seed |
| $X_{76}$ | -- | generation controller proportional output |
| $X_{77}$ | -- | generation controller integrator output |
| $X_{78}$ | -- | generation controller differentiator output |
| $X_{79}$ | -- | component of $X_{15}$ proportional to $X_{14}$ (Figure 5.10) |
| $X_{80}$ | -- | component of $X_{15}$ due to boiler storage effects |
| $X_{81}$ | -- | component of $X_{30}$ proportional to $X_{14}$ |
| $X_{82}$ | -- | component of $X_{30}$ due to boiler storage effects |
| $X_{83}$ | -- | firing rate controller proportional output |
| $X_{84}$ | -- | firing rate controller integrator output |
| $X_{85}$ | -- | firing rate controller differentiator output |

## 5.5 Initial Conditions, Values of Constants, and System Equations

The initial conditions and values of constant multipliers for model III are calculated using design-center data for the CNCD [114], and steam plant assumptions from [58].

Design-center conditions for the Combustor/Nozzle/Channel/Diffuser include:

$X_{55}$ (fuel thermal input power) = 3500.00 MW

fuel calorific value = $29.257 \times 10^6$ J/Kg

$X_{73}$ (preheated air temperature) = 1800°K

combustion gas mass flow rate = 1228.6 Kg/sec

fuel mass flow rate = 119.63 Kg/sec

air mass flow rate = 1108.9 Kg/sec

potassium mass flow rate = 9.86 Kg/sec

combustor pressure = $0.666 \times 10^6$ $N/m^2$

useful electrical output from inverters = 920.63 MW

thermal power absorbed by cooling water by component:

| | |
|---|---|
| combustor | : 233 MW |
| nozzle | : 66.5 MW |
| channel | : 213.7 MW |
| diffuser | : 87.8 MW |
| electrode drop loss | : 64.35 MW |
| total | : 665.35 MW |

enthalpy before combustion = $3.956 \times 10^6$ J/Kg

enthalpy at diffuser outlet = $2.6518 \times 10^6$ J/Kg (from [114])

The following section describes how initial conditions and values of constants for model III are developed. Assumptions are stated where appropriate.

Compressor power, PCOMP, compressor outlet temperature, T(OUT), and thermal power in the preheated air, PA, are determined as in Chapter IV from equations 4.2, 4.3, 4.7, and 4.8. Mean specific heat of air, $C_p$, is found by averaging over a temperature range of 300°K

to 1800°K using the same technique as in Chapter IV, resulting in $C_p$ = 1147.5 J/Kg°K. Using this value of $C_p$ gives

$$\frac{PA}{°K} = (3.6359 \times 10^{-4} \frac{MW}{MW_T °K})(PT) \frac{MW}{°K}$$

where PT is fuel thermal input power ($MW_T$). Air temperature at the compressor outlet is 570.5°K from Table 4.2. From Equation 4.10,

$$T(OUT) = [570.5 + (0.029)(PT - 3500)] °K \quad (5.14)$$

and, following Equation 4.11,

$$PCOMP = f_2(X_{55}) = X_{68}$$

$$= [270.5 + (0.029)(X_{55} - 3500)][3.6359 \times 10^{-4} \frac{MW}{MW_T °K}][X_{55}] \ MW \quad (5.15)$$

where $X_{55}$ = PT ($MW_T$) = 3500 MW at design center. If $X_{55}(0)$ = 3500 MW, $X_{68}(0)$ = 344.23 MW.

$$X_{70} = K_{31} X_{55} = (3.6359 \times 10^{-4} \frac{MW}{MW_T °K}) X_{55} \quad (5.16)$$

$$X_{70}(0) = 1.2726 \ MW/°K$$

$$X_{71} = X_{69}/X_{70} = PA/X_{70} \quad (5.17)$$

$X_{71}(0)$ = 1500°K = rise in air preheat temperature above ambient at design center. Therefore

$$X_{69}(0) = X_{70}(0) \ X_{71}(0) = 1908.85 \ MW \quad (5.18)$$

If $X_{69}(0)$ is checked by Equation 4.5,

$$[HA(1800°K) - HA(300°K)][\text{mass flow rate of air}]$$
$$= (1.721 \times 10^6 \text{ J/Kg})(1108.9 \text{ Kg/sec}) = 1908.4 \text{ MW} \quad (5.19)$$

which is within 0.025% of the value resulting from Equation 5.18.

$$X_{60}(0) = X_{69}(0) - X_{68}(0) = 1564.62 \text{ MW} \quad (5.20)$$

Other initial values are $X_{72}(0) = 1500°K$, $X_{73}(0) = 1800°K$, TREF = 1800°K, and Z(0) = 0.

An equation for enthalpy before combustion of fuel, air, seed and water is used to determine input power in the CNCD [15,105,114] and is given as Equation 5.21.

$$HBC(T) = \left(\frac{WA}{W}\right)HA(TPHAO) + \left(\frac{WF}{W}\right)(FUEL) - \frac{WS}{W}(ED) - \frac{WV}{W}(WATER) \quad (5.21)$$

where

HBC(T) = enthalpy before combustion of fuel, air, oxygen (not used), and seed

W = total mass flow rate

WA = air mass flow rate

HA = enthalpy of air

TPHAO = preheated air temperature

WF = fuel mass flow rate

FUEL = calorific value of fuel

WS = seed mass flow rate

ED = dissociation energy of seed

WV = moisture mass flow rate

WATER = enthalpy change of water upon evaporation

Equation 5.21 does not give consistent results with design-center calculations determined from mass flow rates, air enthalpy, seed dissociation energy, and assumed calorific value of fuel. This inconsistency occurs because the last three terms of Equation 5.21 were developed for hydrocarbon liquid fuels; the sulfur and ash components in coal were not accounted for, and the water loss term (WATER) is excessive [15]. Table 5.2 provides an illustration. The assumptions include: 1) The water evaporation term in HBC(T) is not to be altered; and 2) 5% $H_2O$ exists in the fuel, accounting for the -13.50 MW entry in the right column. The ratio (total design-center power/total power predicted from HBC(T)) is 1.074. To make CNCD input power equal to output power, polynomial approximations from [114] of CNCD output $X_{42}$ (electrical output from inverters), $X_{56}$ (thermal loss) and $X_{57}$ (thermal power absorbed by cooling water) are multiplied by the above ratio and subtracted from input power to determine $X_{58}$ (thermal power out of diffuser). This requires power input to equal power output and increases output power so that it is consistent with design-center input quantities. The

Table 5.2. Equation 5.21 results compared with design-center calculations (power in MW)

| Quantity | Power from HBC(T) | Power from design-center quantities |
|---|---|---|
| PT | 2763.2 | 3500 |
| PA | 2246.63 | 1908.85 (less $P_{ambient}$) |
| $P_{SEED}$ | -97.28 | -123.28 |
| $P_{water\ evaporation}$ | -51.56 | -51.56 |
| $P_{water\ in\ fuel}$ | 0 | -13.50 |
| total | 4860.99 | 5220.51 |

resulting approximations for $X_{42}$, $X_{56}$, and $X_{57}$ are contained in Appendix C.

The above considerations only affect cycle efficiency and do not change dynamic system behavior.

Using polynomial approximation values for $X_{42}$ and $X_{57}$, and taking $X_{56}$ to be 0.5% of $X_{57}$, gives

$$X_{42}(0) = 988.83 \text{ MW} \tag{5.22}$$

$$X_{56}(0) + X_{57}(0) = 718.44 \text{ MW} \tag{5.23}$$

$$X_{58}(0) = 3503.37 \text{ MW} = X_{59}(0) \tag{5.24}$$

Power recovered from condensing seed, $X_{75}$, is assumed to be 85% of the original dissociation energy of the seed. At 3500 MW fuel thermal input,

$$X_{75}(0) = 104.79 \text{ MW} \tag{5.25}$$

$$X_{63}(0) = X_{59}(0) - X_{60}(0) = 1938.75 \text{ MW} \tag{5.26}$$

$$K_{27} = \frac{X_{63}}{X_{59}} = 0.5534 \tag{5.27}$$

Thermal power loss from the air preheaters, $X_{64}$, is assumed to be 2% of the power absorbed by the combustion air, $X_{60}$.

$$X_{64}(0) = (0.02)X_{60}(0) = 31.29 \text{ MW} \tag{5.28}$$

$$K_{28} = \frac{X_{64}}{X_{63}} = 0.016 \tag{5.29}$$

$$X_{65}(0) = X_{63}(0) - X_{64}(0) = 1907.46 \text{ MW} \tag{5.30}$$

$$X_{66}(0) = X_{65}(0) \tag{5.31}$$

$$X_{67}(0) = X_{66}(0) + X_{75}(0) = 2012.25 \text{ MW} \tag{5.32}$$

$$X_{74}(0) = X_{57}(0) = 714.87 \text{ MW} \tag{5.33}$$

$$X_{21}(0) = X_{67}(0) + X_{74}(0) = 2727.12 \text{ MW} \tag{5.34}$$

The following assumptions are used to determine boiler efficiency: First, 14% of the net thermal input to the steam plant can be

used for feedwater heating. If additional low-grade heat is available, it cannot be absorbed by the steam plant. Turbine efficiency drops as more low-grade heat is absorbed because steam bled from the turbines is no longer used to heat feedwater [58]. Second, low-grade heat is defined as power lost to the cooling water in the combustor, nozzle, and channel only. Thermal loss to the diffuser coolant is considered to be high-grade heat. Thus, at design center,

$$P_{combustor} + P_{nozzle} + P_{channel} = (1.074)(233 + 66.5 + 213.7)$$
$$= 551.16 \quad MW \qquad (5.35)$$

The maximum amount of low-grade heat the steam plant can absorb, $Q_{MAX}$ equals

$$Q_{MAX} = 0.14[X_{21} - X_{22}] \qquad (5.36)$$

where $X_{21}$ = total thermal input power to steam plant

$X_{22}$ = stack loss

$$Q_{MAX}(0) = 0.14[X_{21}(0) - X_{22}(0)] = 360.81 \quad MW$$

and rejected low grade heat $Q_E$ is

$$Q_E(0) = 551.16 - 360.81 = 190.35 \quad MW \qquad (5.37)$$

Steam plant efficiency is assumed to be 42.5% with reduced feedwater heating from the turbines. Net steam plant input power is $X_{21} - Q_E - X_{22}$.

$$X_{21}(0) - Q_E(0) - X_{22}(0) = 2386.87 \text{ MW} \quad (5.38)$$

Net steam plant output power, $X_{41}$, is

$$X_{41}(0) = (0.425)(2386.87) = 1014.42 \text{ MW} \quad (5.39)$$

The steam turbine efficiency is assumed to be 87%. Therefore, turbine input, $X_{20}$, may be found from Equation 5.40.

$$X_{20}(0) = \frac{1014.42}{0.87} = 1166.00 \text{ MW} \quad (5.40)$$

$$X_{20}(0) = X_{19} = X_{23}(0) = X_{25} \quad (5.41)$$

Turbogenerator auxiliary power is assumed to be 4% of $X_{41}(0)$. $X_{68}(0)$ gives compressor power. In-plant, load related power, $X_{44}$, is

$$X_{44}(0) = (0.04)\, X_{41}(0) + X_{68}(0) = 384.81 \text{ MW} \quad (5.42)$$

$$K_{19} = \frac{X_{44}}{X_{43}} = \frac{X_{44}}{X_{41} + X_{42}} = 0.192 \quad (5.43)$$

Fixed, in-plant power is assumed to be 8.0 MW for the magnet, lights, and other fixed loads.

Thus,

$$\begin{aligned} X_2(0) &= X_{45}(0) - 8.0 \text{ MW} \\ &= X_{43}(0) - X_{44}(0) - 8.0 \\ &= 1610.44 \text{ MW} \end{aligned} \quad (5.44)$$

Overall combined cycle efficiency $\eta_0$ is

$$\eta_0 = \frac{1610.44}{3500} = 46.01\% \qquad (5.45)$$

If all the low-grade heat is absorbed so that $Q_E = 0$, a higher cycle efficiency $\eta_0' = 48.23\%$ results.

Model III includes 19 time constants. Grid-lag time constant, $\tau_1$, is assumed zero. $\tau_2$, $\tau_3$, $\tau_{13}$, and $\tau_{14}$ are controller time constants and are design parameters. $\tau_4$ and $\tau_5$ are servomotor time constants [65]. $\tau_6$, $\tau_7$, $\tau_8$, and $\tau_9$ are representative time constants for once-through boilers [81]. $\tau_{10}$, $\tau_{11}$, and $\tau_{12}$ are associated with the turbines [65]. $\tau_{15}$ and $\tau_{16}$ define a first-order lag and a pure time delay in the firing system and have been discussed in Chapter IV. $\tau_{17}$ is the transit time for combustion gases moving between the CNCD and the steam plant, and is assumed to be 1 second. $\tau_{18}$ is the air preheater cycle time, and $\tau_{19}$ is a thermal lag associated with the CNCD cooling system, assumed to be 15 to 20% of the main boiler time constants.

To summarize, model III initial conditions are given in Table 5.3. Multiplier and time-constant values are listed in Table 5.4.

System equations for model III follow directly from the block diagrams of Figures 5.6 through 5.15. They are listed in the computer program of Appendix C.

Table 5.3. Model III initial conditions

| | |
|---|---|
| $X_1(0) = 1610.44$ MW | $X_{29}(0) = 0.00$ |
| $X_2(0) = 1610.44$ MW | $X_{30}(0) = 0.00$ |
| $X_3(0) = 0.00$ | $X_{31}(0) = 0.00$ |
| $X_4(0) = 0.00$ | $X_{32}(0) = 1166.00$ MW |
| $X_5(0) = 0.79545$ | $X_{33}(0) = X_{32}(0)$ |
| $X_6(0) = 0.00$ | $X_{34}(0) = X_{32}(0)$ |
| $X_7(0) = X_5(0)$ | $X_{35}(0) = 583.00$ MW |
| $X_8(0) = X_5(0)$ | $X_{36}(0) = 291.50$ MW |
| $X_9(0) = X_5(0)$ | $X_{37}(0) = 874.50$ MW |
| $X_{10}(0) = X_5(0)$ | $X_{38}(0) = X_{36}(0)$ |
| $X_{11}(0) = X_5(0)$ | $X_{39}(0) = X_{32}(0)$ |
| $X_{12}(0) = 0.00$ | $X_{40}(0) = 151.58$ MW |
| $X_{13}(0) = X_5(0)$ | $X_{41}(0) = 1014.42$ MW |
| $X_{14}(0) = 0.00$ | $X_{42}(0) = 988.83$ MW |
| $X_{15}(0) = 0.00$ | $X_{43}(0) = 2003.25$ MW |
| $X_{16}(0) = 0.00$ | $X_{44}(0) = 384.81$ MW |
| $X_{17}(0) = 0.00$ | $X_{45}(0) = 1618.44$ MW |
| $X_{18}(0) = 0.00$ | $X_{46}(0) = 8.00$ MW |
| $X_{19}(0) = 1166.00$ MW | $X_{47}(0) = 3500.00$ PSI |
| $X_{20}(0) = X_{19}(0)$ | $X_{48}(0) = 0.00$ PSI |
| $X_{21}(0) = 2727.12$ MW | $X_{49}(0) = 0.79545$ |
| $X_{22}(0) = 1561.12$ MW | $X_{50}(0) = 0.00$ |
| $X_{23}(0) = 1166.00$ MW | $X_{51}(0) = X_{49}(0)$ |
| $X_{24}(0) = 0.00$ | $X_{52}(0) = X_{49}(0)$ |
| $X_{25}(0) = 1166.00$ MW | $X_{53}(0) = X_{49}(0)$ |
| $X_{26}(0) = 0.00$ | $X_{54}(0) = 3500.00$ MW |
| $X_{27}(0) = 0.00$ | $X_{55}(0) = 3500.00$ MW |
| $X_{28}(0) = 0.00$ | $X_{56}(0) = 3.57$ MW |

Table 5.3 (cont.)

| | | | |
|---|---|---|---|
| $X_{57}(0)$ | = 714.87 MW | $X_{73}(0)$ | = 1800°K |
| $X_{58}(0)$ | = 3505.37 MW | $X_{74}(0)$ | = 714.87 MW |
| $X_{59}(0)$ | = $X_{58}(0)$ | $X_{75}(0)$ | = 104.79 MW |
| $X_{60}(0)$ | = 1564.62 MW | $X_{76}(0)$ | = 0.00 |
| $X_{61}(0)$ | = not used | $X_{77}(0)$ | = 0.79545 |
| $X_{62}(0)$ | = 0.00 | $X_{78}(0)$ | = 0.00 |
| $X_{63}(0)$ | = 1938.75 MW | $X_{79}(0)$ | = 0.00 |
| $X_{64}(0)$ | = 31.29 MW | $X_{80}(0)$ | = 0.00 |
| $X_{65}(0)$ | = 1907.46 MW | $X_{81}(0)$ | = 0.00 |
| $X_{66}(0)$ | = $X_{65}(0)$ | $X_{82}(0)$ | = 0.00 |
| $X_{67}(0)$ | = 2012.25 MW | $X_{83}(0)$ | = 0.00 |
| $X_{68}(0)$ | = 344.23 MW | $X_{84}(0)$ | = 0.79545 |
| $X_{69}(0)$ | = 1908.85 MW | $X_{85}(0)$ | = 0.00 |
| $X_{70}(0)$ | = 1.27 MW/°K | TREF | = 1800°K |
| $X_{71}(0)$ | = 1500°K | Z | = 0.00 |
| $X_{72}(0)$ | = $X_{71}(0)$ | | |

Table 5.4. Model III multipliers and time constants

Constant multipliers:

Controller and feedforward constants are design parameters and are therefore not given values

$K_1$ = 1.0
$K_2$ = generation controller
$K_3$ = generation controller
$K_4$ = generation controller
$K_5$ = valve feedforward
$K_6$ = 1.0
$K_7$ = 0.1
$K_8$ = 1.0
$K_9$ = 0.87
$K_{10}$ = 0.13
$K_{11}$ = 0.87
$K_{12}$ = 1.0
$K_{13}$ = 1.0
$K_{14}$ = 1.0
$K_{15}$ = 0.25
$K_{16}$ = 0.25
$K_{17}$ = 0.5
$K_{18}$ = 0.13
$K_{19}$ = 0.192
$K_{20}$ = fuel feedforward
$K_{21}$ = firing rate controller
$K_{22}$ = firing rate controller
$K_{23}$ = firing rate controller
$K_{24}$ = 0.1
$K_{25}$ = 1.0
$K_{26}$ = 4400 MW/unit $X_{53}$
$K_{27}$ = 0.553
$K_{28}$ = 0.016
$K_{29}$ = not used
$K_{30}$ = 0.572
$K_{31}$ = $3.64 \times 10^{-4}$
n = 1.0

Time constants (seconds):

$\tau_1$ = 0.00
$\tau_2$ = generation controller
$\tau_3$ = valve feedforward
$\tau_4$ = 0.30
$\tau_5$ = 0.30
$\tau_6$ = 115.00
$\tau_7$ = 115.00
$\tau_8$ = 115.00
$\tau_9$ = 6.00
$\tau_{10}$ = 0.30
$\tau_{11}$ = 11.00
$\tau_{12}$ = 0.40
$\tau_{13}$ = fuel feedforward
$\tau_{14}$ = firing rate controller
$\tau_{15}$ = 10.00
$\tau_{16}$ = 1.00
$\tau_{17}$ = 1.00
$\tau_{18}$ = 500.00
$\tau_{19}$ = 20.00

## 5.6 System Equation Solutions

Defining computer simulation cases for model III is more difficult than for previous cases. The primary cause for this is the significant increase in number of controller design parameters in this model compared with models I and II. The first two models have only a proportional constant and an integral constant as controller parameters while model III has 12 adjustable parameters which may be identified in Figures 5.6 and 5.12.

Figure 5.6 defines the following 6 parameters associated with the generation and valve feedforward controllers:

$K_2$ = generation controller proportional multiplier

$K_3$ = generation controller integrator multiplier

$K_4$ = generation controller differentiator multiplier

$K_5$ = valve feedforward differentiator multiplier

$\tau_2$ = first-order lag time constant with generation controller differentiator

$\tau_3$ = first-order lag time constant associated with valve feedforward differentiator

Figure 5.12 defines 6 parameters associated with the firing rate and fuel feedforward controllers:

$K_{20}$ = fuel feedforward differentiator multiplier

$K_{21}$ = firing rate controller proportional multiplier

$K_{22}$ = firing rate controller integrator multiplier

$K_{23}$ = firing rate controller differentiator multiplier

$\tau_{13}$ = first-order lag time constant associated with fuel feedforward differentiator

$\tau_{14}$ = first-order lag time constant associated with firing rate controller differentiator

Thirty-two model III simulation cases have been run with the boiler-following type of control as shown in Figure 5.1. The conditions and important results of these simulations are given in Table 5.5. Values of the 12 control parameters are listed for each case. The control configuration is indicated, and four characteristics of plant output power, $X_2$, are tabulated for a 50 MW step decrease in $MW_{REF}$ $X_1$ at t = 0+. $E_1(t)$, $T_1(t)$, and Z are zero for all cases shown.

Five variations of control are considered:

1) PI generation controller, PI firing rate controller only; no feedforward control 2) PID generation controller, PI firing
2) PID generation controller, PI firing rate controller; no feedforward control
3) PI generation controller, PID firing rate controller; no feedforward control
4) PI generation controller, PID firing rate controller; both feedforward controllers operating
5) PI generation controller, PI firing rate controller; fuel feedforward controller operating

Table 5.5. System model III simulation cases.

| Case | Controller Design Parameters | | | | | | | | | | | | Control config. | $X_2$ Characteristics | | | |
|---|---|---|---|---|---|---|---|---|---|---|---|---|---|---|---|---|---|
| | $K_2$ | $K_3$ | $K_4$ | $K_5$ | $K_{20}$ | $K_{21}$ | $K_{22}$ | $K_{23}$ | $\tau_2$ | $\tau_3$ | $\tau_{13}$ | $\tau_{14}$ | | Stable | $t_1$ | $P_u$ | $\Delta P$ |
| 1 | $10^{-4}$ | $10^{-5}$ | 0.0 | 0.0 | 0.0 | $10^{-4}$ | $10^{-5}$ | 0.0 | 0.0 | 0.0 | 0.0 | 0.0 | 1 | ? | 95 | 20.3 | 27.0 |
| 2 | $10^{-4}$ | $10^{-4}$ | 0.0 | 0.0 | 0.0 | $10^{-4}$ | $10^{-5}$ | 0.0 | 0.0 | 0.0 | 0.0 | 0.0 | 1 | Yes | 24 | 13.9 | 5.1 |
| 3 | $10^{-4}$ | $10^{-3}$ | 0.0 | 0.0 | 0.0 | $10^{-4}$ | $10^{-5}$ | 0.0 | 0.0 | 0.0 | 0.0 | 0.0 | 1 | Yes | 5 | 18.6 | 0.5 |
| 4 | $10^{-4}$ | $10^{-3}$ | 0.0 | 0.0 | 0.0 | $10^{-4}$ | $10^{-4}$ | 0.0 | 0.0 | 0.0 | 0.0 | 0.0 | 1 | Yes | 5 | 30.1 | 0.0 |
| 5 | $10^{-4}$ | $10^{-3}$ | 0.0 | 0.0 | 0.0 | $10^{-4}$ | $10^{-3}$ | 0.0 | 0.0 | 0.0 | 0.0 | 0.0 | 1 | No | 4 | 146.3 | 410.6 |
| 6 | $10^{-4}$ | $10^{-3}$ | 0.0 | 0.0 | 0.0 | $10^{-3}$ | $10^{-4}$ | 0.0 | 0.0 | 0.0 | 0.0 | 0.0 | 1 | Yes | 4 | 43.5 | 0.0 |
| 7 | $10^{-4}$ | $10^{-3}$ | 0.0 | 0.0 | 0.0 | $10^{-3}$ | $10^{-3}$ | 0.0 | 0.0 | 0.0 | 0.0 | 0.0 | 1 | No | 3.5 | 111.7 | 406.3 |
| 8 | $10^{-3}$ | $10^{-5}$ | 0.0 | 0.0 | 0.0 | $10^{-4}$ | $10^{-5}$ | 0.0 | 0.0 | 0.0 | 0.0 | 0.0 | 1 | ? | 85 | 4.1 | 4.4 |
| 9 | $10^{-3}$ | $10^{-4}$ | 0.0 | 0.0 | 0.0 | $10^{-4}$ | $10^{-5}$ | 0.0 | 0.0 | 0.0 | 0.0 | 0.0 | 1 | Yes | 27 | 8.0 | 3.6 |
| 10 | $10^{-3}$ | $10^{-4}$ | 0.0 | 0.0 | 0.0 | $10^{-4}$ | $10^{-4}$ | 0.0 | 0.0 | 0.0 | 0.0 | 0.0 | 1 | No | 13.5 | 26.3 | 606.8 |
| 11 | $10^{-3}$ | $10^{-4}$ | 0.0 | 0.0 | 0.0 | $10^{-4}$ | $10^{-3}$ | 0.0 | 0.0 | 0.0 | 0.0 | 0.0 | 1 | No | 6 | 60.7 | 998.8 |
| 12 | $10^{-3}$ | $10^{-4}$ | 0.0 | 0.0 | 0.0 | $10^{-3}$ | $10^{-4}$ | 0.0 | 0.0 | 0.0 | 0.0 | 0.0 | 1 | Yes | 10 | 13.7 | 0.0 |
| 13 | $10^{-3}$ | $10^{-4}$ | 0.0 | 0.0 | 0.0 | $10^{-3}$ | $10^{-3}$ | 0.0 | 0.0 | 0.0 | 0.0 | 0.0 | 1 | No | 5 | 47.3 | 946.9 |
| 14 | $10^{-3}$ | $10^{-3}$ | 0.0 | 0.0 | 0.0 | $10^{-4}$ | $10^{-5}$ | 0.0 | 0.0 | 0.0 | 0.0 | 0.0 | 1 | Yes | 5 | 11.5 | 0.2 |
| 15 | $10^{-4}$ | $10^{-3}$ | $10^{-3}$ | 0.0 | 0.0 | $10^{-4}$ | $10^{-4}$ | 0.0 | 0.5 | 0.0 | 0.0 | 0.0 | 2 | Yes | 5 | 30.2 | 0.0 |
| 16 | $10^{-4}$ | $10^{-3}$ | $5\times10^{-3}$ | 0.0 | 0.0 | $10^{-4}$ | $10^{-4}$ | 0.0 | 0.5 | 0.0 | 0.0 | 0.0 | 2 | Yes | 6 | 31.0 | 0.0 |
| 17 | $10^{-4}$ | $10^{-3}$ | $10^{-2}$ | 0.0 | 0.0 | $10^{-4}$ | $10^{-4}$ | 0.0 | 0.5 | 0.0 | 0.0 | 0.0 | 2 | Yes | 7 | 31.3 | 0.0 |
| 18 | $10^{-4}$ | $10^{-3}$ | 0.0 | 0.0 | 0.0 | $10^{-4}$ | $10^{-4}$ | $10^{-4}$ | 0.5 | 0.0 | 0.0 | 0.5 | 3 | Yes | 5 | 29.5 | 0.0 |

Table 5.5 (cont.)

| Case | Controller Design Parameters | | | | | | | | | | | | Control config. | $X_2$ Characteristics | | | |
|---|---|---|---|---|---|---|---|---|---|---|---|---|---|---|---|---|---|
| | $K_2$ | $K_3$ | $K_4$ | $K_5$ | $K_{20}$ | $K_{21}$ | $K_{22}$ | $K_{23}$ | $\tau_2$ | $\tau_3$ | $\tau_{13}$ | $\tau_{14}$ | | Stable | $t_1$ | $P_u$ | $\Delta P$ |
| 19 | $10^{-4}$ | $10^{-3}$ | 0.0 | 0.0 | 0.0 | $10^{-4}$ | $10^{-4}$ | $5\times10^{-4}$ | 0.5 | 0.0 | 0.0 | 0.5 | 3 | Yes | 4.5 | 26.8 | 0.0 |
| 20 | $10^{-4}$ | $10^{-3}$ | 0.0 | 0.0 | 0.0 | $10^{-4}$ | $10^{-3}$ | $10^{-3}$ | 0.5 | 0.0 | 0.0 | 0.5 | 3 | Yes | 4.5 | 24.5 | 0.0 |
| 21 | $10^{-4}$ | $10^{-3}$ | 0.0 | 0.0 | 0.0 | $10^{-4}$ | $10^{-4}$ | $10^{-3}$ | 0.0 | 0.0 | 0.0 | 0.1 | 3 | Yes | 4.5 | 24.4 | 0.0 |
| 22 | $10^{-4}$ | $10^{-3}$ | 0.0 | 0.0 | 0.0 | $10^{-4}$ | $10^{-4}$ | $10^{-2}$ | 0.0 | 0.0 | 0.0 | 0.1 | 3 | Yes | 3.5 | 36.6 | 0.2 |
| 23 | $10^{-4}$ | $10^{-3}$ | 0.0 | 0.0 | 0.0 | $10^{-4}$ | $10^{-4}$ | $10^{-1}$ | 0.0 | 0.0 | 0.0 | 0.1 | 3 | No | 3.5 | 55.9 | 61.2 |
| 24 | $10^{-4}$ | $10^{-3}$ | 0.0 | 0.0 | 0.0 | $10^{-4}$ | $10^{-4}$ | 1.0 | 0.0 | 0.0 | 0.0 | 0.1 | 3 | No | 3.5 | 60.4 | 92.6 |
| 25 | $10^{-3}$ | $10^{-4}$ | 0.0 | 0.0 | 0.0 | $10^{-4}$ | $10^{-5}$ | $10^{-3}$ | 0.0 | 0.0 | 0.0 | 0.1 | 3 | Yes | 28 | 8.1 | 5.1 |
| 26 | $10^{-3}$ | $10^{-3}$ | 0.0 | 0.0 | 0.0 | $10^{-4}$ | $10^{-5}$ | $10^{-3}$ | 0.0 | 0.0 | 0.0 | 0.1 | 3 | Yes | 4.5 | 8.0 | 0.2 |
| 27 | $10^{-4}$ | $10^{-3}$ | 0.0 | $10^{-4}$ | $10^{-4}$ | $10^{-4}$ | $10^{-3}$ | $10^{-3}$ | 0.0 | 0.2 | 0.2 | 0.1 | 4 | Yes | 4.5 | 23.9 | 0.0 |
| 28 | $10^{-4}$ | $10^{-3}$ | 0.0 | $10^{-2}$ | $10^{-2}$ | $10^{-4}$ | $10^{-4}$ | $10^{-3}$ | 0.0 | 0.2 | 0.2 | 0.1 | 4 | Yes | 4.5 | 15.1 | 0.0 |
| 29 | $10^{-4}$ | $10^{-3}$ | 0.0 | 0.0 | $9\times10^{-4}$ | $10^{-4}$ | $10^{-4}$ | 0.0 | 0.0 | 0.0 | 1.0 | 0.0 | 5 | Yes | 4.5 | 27.2 | 0.0 |
| 30 | $10^{-4}$ | $10^{-3}$ | 0.0 | 0.0 | $1.3\times10^{-3}$ | $10^{-4}$ | $10^{-4}$ | 0.0 | 0.0 | 0.0 | 3.0 | 0.0 | 5 | Yes | 4.5 | 27.4 | 0.0 |
| 31 | $10^{-3}$ | $10^{-4}$ | 0.0 | 0.0 | $5\times10^{-3}$ | $10^{-4}$ | $10^{-5}$ | 0.0 | 0.0 | 0.0 | 12.0 | 0.1 | 5 | Yes | 35 | 6.5 | 4.0 |
| 32 | $10^{-3}$ | $10^{-4}$ | 0.0 | 0.0 | $5\times10^{-2}$ | $10^{-4}$ | $10^{-5}$ | 0.0 | 0.0 | 0.0 | 12.0 | 0.1 | 5 | Yes | 3.5 | 41.8 | 10.5 |

The control configuration for each case given in Table 5.5 is identified by the number 1 through 5 corresponding to the above list.

Plant output power characteristics included in Table 5.5 are:

stability: yes = stable, no = unstable,

? = insufficient information (borderline case)

$t_1$ (seconds) = time required for $X_2$ to change from initial value (1610.44 MW) to the first crossing of the new steady-state value (1560.44 MW)

$P_u$ (megawatts) = undershoot of $X_2$

$= 1560.44 - X_{2(\text{minimum})}$

$\Delta P$ (megawatts) = last peak value of $X_2$ relative to 1560.44 MW before $t = 400$ seconds (within the last half-period of $X_2$)

$t_1$ is a measure of the rate of response of $X_2$. $P_u$ determines the amount of undershoot, and $\Delta P$ indicates how closely the system approaches steady state within 400 seconds.

As an example, consider case 4 of Table 5.5. Control configuration 1 implies a PI generation controller and a PI firing rate controller only. Thus, $K_2$, $K_3$, $K_{21}$, and $K_{22}$ are the only non-zero controller parameters. The system is stable for this condition. It takes $X_2$ five seconds to reach 1560.44 MW, starting from 1610.44 MW at $t = 0+$. $X_2$ then undershoots the new steady-state value of 1560.44 MW by 30.1 MW but has settled to the new steady-state value before $t = 400$ seconds.

Several interesting observations may be made with the aid of Table 5.5.

1) It is possible to make the overall system unstable. This was not possible with models I and II for the cases considered.

2) Using derivative control with the generation controller degrades system performance for the cases considered. This may be seen by comparing cases 15, 16, and 17 with case 4 which lacks derivative control but is otherwise identical to cases 15, 16, and 17. Cases 15, 16, and 17 have equal or slower response and greater undershoot than case 4.

3) Using derivative control with the firing rate controller improves system performance in several cases. For example, cases 18, 19, 20, and 21 all have the same or faster response time and less undershoot than case 4. However, if differentiation constant $K_{23}$ becomes too large, undershoot increases and system instability results as in cases 22, 23 and 24.

4) Feedforward control is beneficial in several instances: Cases 27 and 28, with two feedforward controllers operating, have less undershoot than case 21 with no loss in response time. Cases 29 and 30 are the same as case 4 except that fuel feedforward control is added. Both cases have faster response and somewhat less undershoot than case 4.

Plots of five model III variables are given as functions of time in Figures 5.16 through 5.44. The variables are:

$X_2$ (net plant output power)

$X_{41}$ (net steam turbine output power)

$X_{42}$ (net MHD electrical output power)

$X_{55}$ (thermal power of fuel in combustor)

$X_{73}$ (preheated air temperature)

Each variable is described by six figures except that $X_{73}$ is described by five figures. The first figure consists of three curves, corresponding to cases 4, 9, and 14 of Table 5.5, drawn on a single set of axes. This allows comparison of the effects caused by varying PI controller constants $K_2$, $K_3$, and $K_{22}$ for the three selected cases. The second figure contains two plots, corresponding to cases 4 and 21, drawn on a single set of axes to illustrate the effect of derivative control used in the firing rate controller. The third figure compares cases 14 and 26, thus repeating the second figure for different values of controller constants $K_2$ and $K_{22}$. The fourth figure compares cases 21 and 28, showing the improvement in system response due to the addition of feedforward control to both the governor and the firing system. The fifth figure repeats case 4 with time functions $E_1(t)$ and $T_1(t)$ functioning. $E_1(t)$ is the variation in thermal power available to the steam plant, and $T_1(t)$ is the variation in preheated air temperature due to air preheater cycling. Temperature controller Z is

also operating. The sixth figure repeats case 14 with $E_1(t)$, $T_1(t)$, and Z all functioning.

### 5.6.1 Net plant output power $X_2$

Figure 5.16 gives three plots of $X_2$ as functions of time corresponding to cases 4, 9, and 14 of Table 5.5. Initial response, maximum undershoot, and steady-state error are all tabulated in the table. $MW_{REF}$ $X_1$ changes from 1610.44 MW to 1560.44 MW at t = 0+ for all cases considered. $E_1(t) = T_1(t) = Z = 0$.

Figure 5.17 shows two plots of $X_2$ operating under the conditions of cases 4 and 21. Case 21 repeats case 4 with the addition of derivative control in the firing rate controller. The remaining remarks for Figure 5.16 are applicable to Figures 5.17, 5.18, and 5.19.

Figure 5.18 repeats Figure 5.17 for cases 14 and 26. Different values of controller constants $K_2$ and $K_{22}$ are used.

Figure 5.19 presents two plots of $X_2$ corresponding to cases 21 and 28. Feedforward control to both the governor and the firing system is added to case 21 to form case 28.

Figure 5.20 repeats case 4 of Figure 5.16 with the addition of $E_1(t)$, $T_1(t)$, and Z. The magnitude jump in $X_2$ at t = 225 seconds, due to $E_1(t)$ and $T_1(t)$ is 5.60 MW.

Figure 5.21 repeats case 14 of Figure 5.16 with $E_1(t)$, $T_1(t)$, and Z all functioning. The magnitude step in $X_2$ at t = 225 seconds, due to $E_1(t)$ and $T_1(t)$, is 4.95 MW.

5.6.2 Net steam turbine output power $X_{41}$

Figure 5.22 shows three plots of $X_{41}$ as a function of time corresponding to cases 4, 9, and 14 of Table 5.5. $MW_{REF}$ $X_1$ changes from 1610.44 MW to 1560.44 MW at t = 0+. $E_1(t) = T_1(t) = Z = 0$ for Figures 5.22, 5.23, 5.24, and 5.25. In case 4, $X_{41}$ starts from an initial value of 1014.42 MW at t = 0, undershoots the steady-state value of 990.6 MW by 47.0 MW at t = 8 seconds, and then overshoots steady-state, reaching 1060.5 MW at t = 22 seconds. The $X_{41}$ oscillations reduce significantly after the initial cycle. The maximum value of the second cycle is 996.7 MW at t = 99 seconds. In case 9, $X_{41}$ starts at the same initial value as before, never stabilizes at a steady-state value within 400 seconds, and reaches a first minimum value of 972.8 MW at t = 22 seconds. In case 14, $X_{41}$ reaches a minimum value of 947.9 MW in 8 seconds, a maximum value of 1018.4 MW at t = 84 seconds, and does not stabilize within 400 seconds.

Figure 5.23 gives two plots of $X_{41}$ for cases 4 and 21. In case 21, where derivative control has been added, the maximum undershoot of $X_{41}$ is 40.3 MW at t = 7 seconds, compared with 47.0 MW undershoot in case 4.

Figure 5.24 illustrates plots of $X_{41}$ corresponding to cases 14 and 26. Case 26 has derivative control added, resulting in a minimum value of 956.5 MW for $X_{41}$ at t = 8 seconds. This compares favorably with a minimum value of 947.9 MW given in case 14. That is, derivative control reduces undershoot by 8.6 MW.

Figure 5.25 compares cases 21 and 28 for $X_{41}$. Case 28 has two feedforward controllers operating. The maximum undershoot of $X_{41}$ is 23.7 MW at t = 7 seconds compared with a corresponding undershoot of 40.3 MW for case 21 and 47.0 MW undershoot for case 4.

Figure 5.26 repeats case 4 of Figure 5.22 with $E_1(t)$, $T_1(t)$, and Z all functioning. No discontinuities exist in steam turbine output power, $X_{41}$, due to $E_1(t)$ and $T_1(t)$, but a steady-state ripple does occur. The peak value of the ripple is 7.59 MW.

Figure 5.27 repeats case 14 of Figure 5.22 with $E_1(t)$, $T_1(t)$, and Z all functioning. Disturbances due to $E_1(t)$ and $T_1(t)$ are apparent in $X_{41}$. The peak value of the fluctuation at t = 225 seconds is 2.13 MW.

### 5.6.3 Net MHD electrical output power $X_{42}$

Figure 5.28 shows three plots of $X_{42}$ as a function of time corresponding to cases 4, 9, and 14 of Table 5.5. $MW_{REF}$ $X_1$ experiences a 50 MW step decrease at t = 0+. $E_1(t)$, $T_1(t)$, and Z are all zero for Figures 5.28, 5.29, 5.30, and 5.31. In case 4, $X_{42}$ starts

from an initial value of 988.8 MW at t = 0 and reaches a minimum value of 896.3 MW at t = 21 seconds before settling at a steady-state value of 950.7 MW. In case 9, $X_{42}$ starts from the same initial value, reaches a minimum value of 915.9 MW at t = 94 seconds, and never stabilizes at steady-state within 400 seconds. In case 14, $X_{42}$ reaches a minimum value of 922.7 MW at t = 84 seconds and does not stabilize within 400 seconds.

Figure 5.29 illustrates two plots of $X_{42}$ for cases 4 and 21. Derivative control reduces undershoot so that at t = 25 seconds, $X_{42}$ reaches a minimum value of 902.6 MW compared with a minimum value of 896.3 MW without derivative control.

Figure 5.30 compares cases 14 and 26 for $X_{42}$. With derivative control in case 26, $X_{42}$ attains a minimum value of 924.8 MW at t = 88 seconds, compared with a minimum value of 922.7 MW at t = 84 seconds without derivative control.

Figure 5.31 displays cases 21 and 28, showing the effect of two feedforward controllers operating. Feedforward control reduces the undershoot of $X_{42}$ so that at t = 25 seconds the minimum value of $X_{42}$ is 909.8 MW compared with 902.6 MW without feedforward control.

Figure 5.32 shows the effect of $E_1(t)$, $T_1(t)$, and Z on $X_{42}$ with the system operating as in case 4. The magnitude jump in $X_{42}$ at t = 225 seconds due to $T_1(t)$ is 7.54 MW.

Figure 5.33 repeats Figure 5.32 for case 14. The magnitude jump in $X_{42}$ at t = 225 seconds in this case is 7.1 MW.

### 5.6.4 Thermal power of fuel in combustor $X_{55}$

Figure 5.34 illustrates three plots of $X_{55}$ as a function of time corresponding with cases 4, 9, and 14 of Table 5.5. The conditions for Figure 5.28 apply. In case 4, $X_{55}$ starts at an initial value of 3500 MW at t = 0, reaches a minimum value of 3265.6 MW at t = 21 seconds, and ends at a steady-state value of 3405.8 MW. In case 9, $X_{55}$ starts at 3500 MW, reaches a minimum of 3316.3 MW at t = 94 seconds, and does not stabilize at steady-state within 400 seconds. In case 14, $X_{55}$ reaches a minimum value of 3333.5 MW at t = 83 seconds, and does not stabilize within 400 seconds.

Figure 5.35 shows $X_{55}$ plotted for cases 4 and 21. Derivative control in the firing rate controller reduces undershoot so that the minimum value of $X_{55}$ becomes 3281.8 MW at t = 25 seconds, compared with 3265.6 MW at t = 21 seconds without derivative control.

Figure 5.36 compares case 14 and 26 for $X_{55}$. With derivative control in case 26, undershoot of $X_{55}$ is reduced by 5.3 MW.

Figure 5.37 compares cases 21 and 28 with respect to $X_{55}$. Feedforward control reduces undershoot of $X_{55}$ by 18.6 MW compared with case 21.

Figure 5.38 repeats case 4 with $E_1(t)$, $T_1(t)$, and Z all operating. $X_{55}$ does not experience discontinuities as a result of $E_1(t)$ and $T_1(t)$ functioning. The peak value of ripple noted in Figure 5.38 is 11.42 MW.

Figure 5.39 repeats Figure 5.38 for case 14. A slight disturbance of approximately 0.5 MW peak value is observed in $X_{55}$ due to $E_1(t)$ and $T_1(t)$.

### 5.6.5 Preheated air temperature $X_{73}$

Figure 5.40 shows three plots of $X_{73}$(°K) as a function of time. The conditions of Figure 5.28 apply. In case 4, $X_{73}$ starts at an initial value of 1800°K and decreases without oscillation to a value of 1798.17°K at t = 400 seconds. In case 9, $X_{73}$ behaves as in case 4, having a value of 1798.08°K at t = 400 seconds. In case 14, $X_{73}$ again corresponds to case 4, having a value of 1798.10°K at t = 400 seconds.

Figure 5.41 compares $X_{73}$ for cases 4 and 21. The plots are essentially identical.

Figure 5.42 compares $X_{73}$ for cases 14 and 26. Again, the results are nearly the same for both cases.

Figure 5.43 compares $X_{73}$ for cases 21 and 28. There is almost no variation between the two cases.

Figure 5.44 shows the effect of $T_1(t)$ on $X_{73}$. The result is the superposition of $T_1(t)$ on $X_{73}$ plotted in Figure 5.42 for case 14. $T_1(t)$ is defined in Figure 4.3.

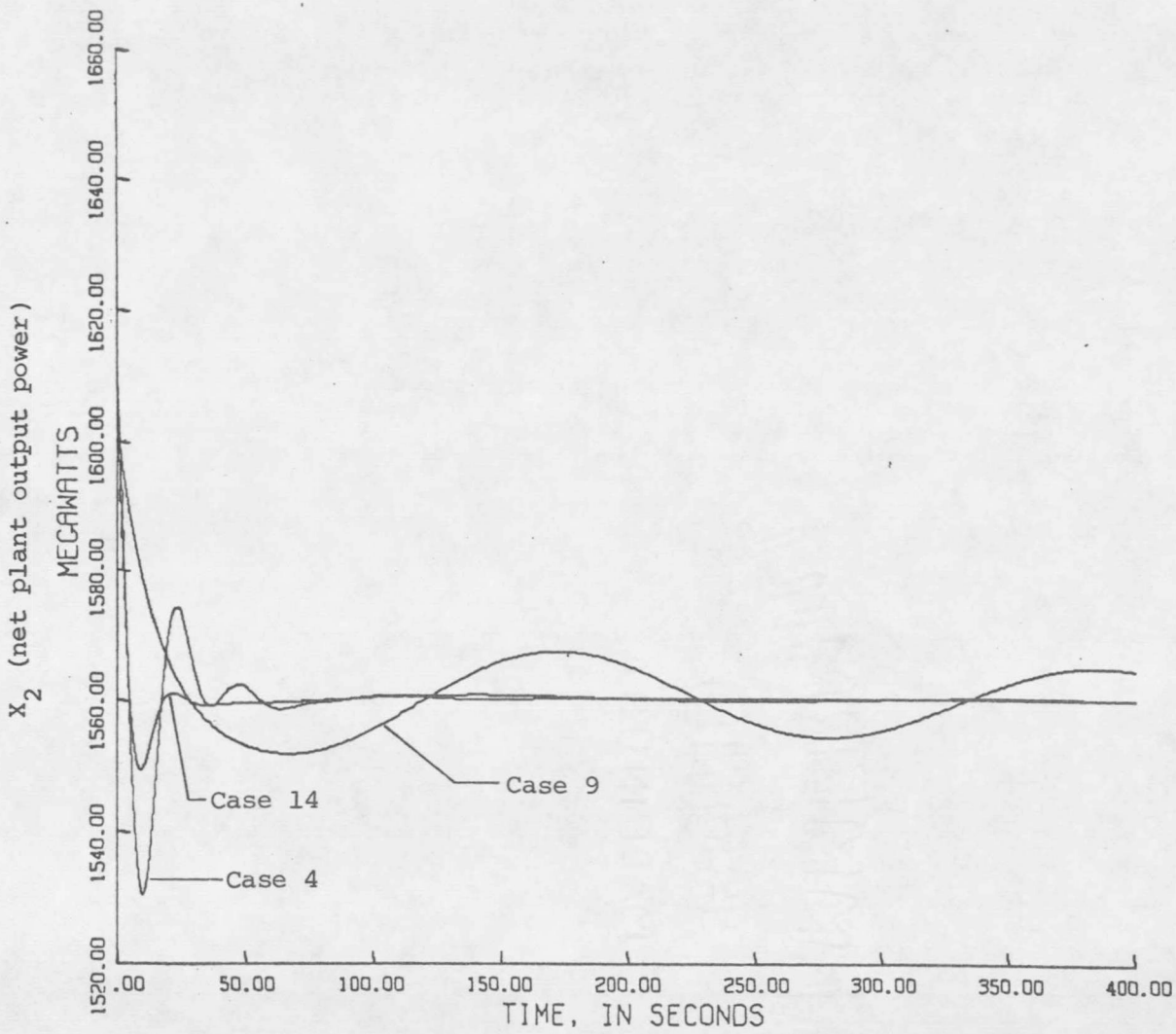



Figure 5.16. $MW_{REF}$ $X_1$ changes from 1610.44 MW to 1560.44 MW at t = 0+; cases are defined in Table 5.5

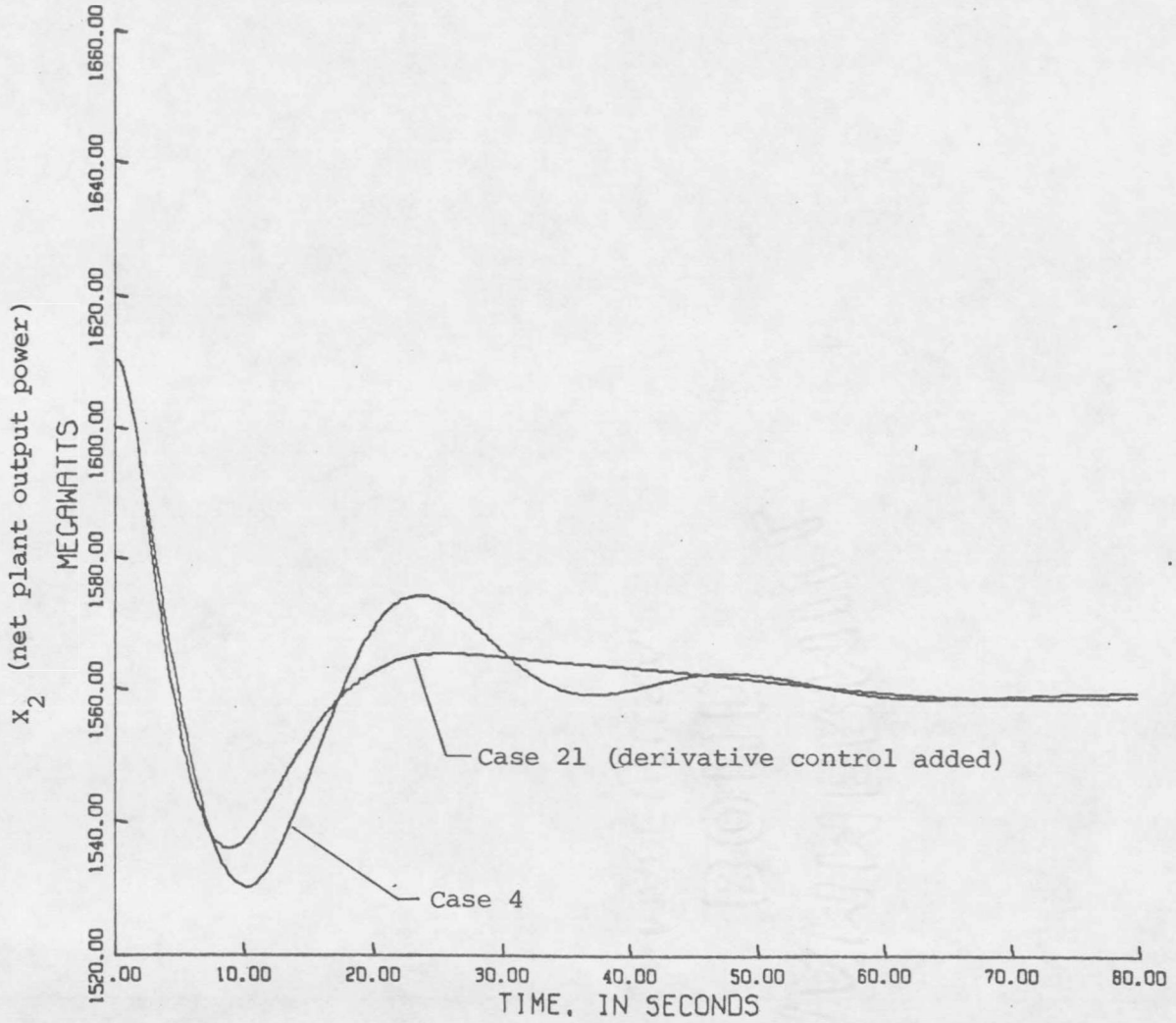



Figure 5.17. $MW_{REF}$ $X_1$ changes from 1610.44 MW to 1560.44 MW at t = 0+; cases are defined in Table 5.5

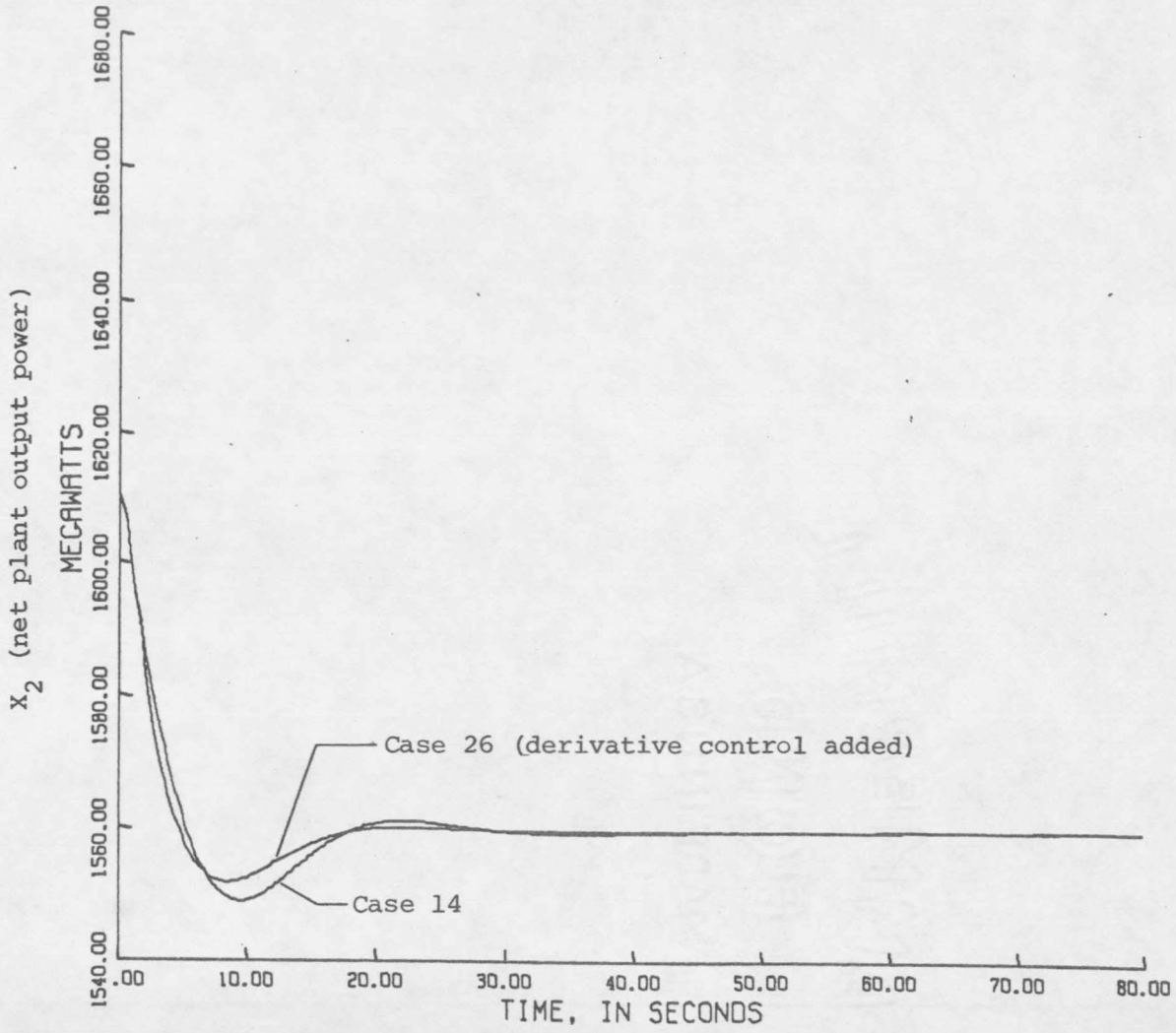



Figure 5.18. $MW_{REF}$ $X_1$ changes from 1610.44 MW to 1560.44 MW at t = 0+; cases are defined in Table 5.5

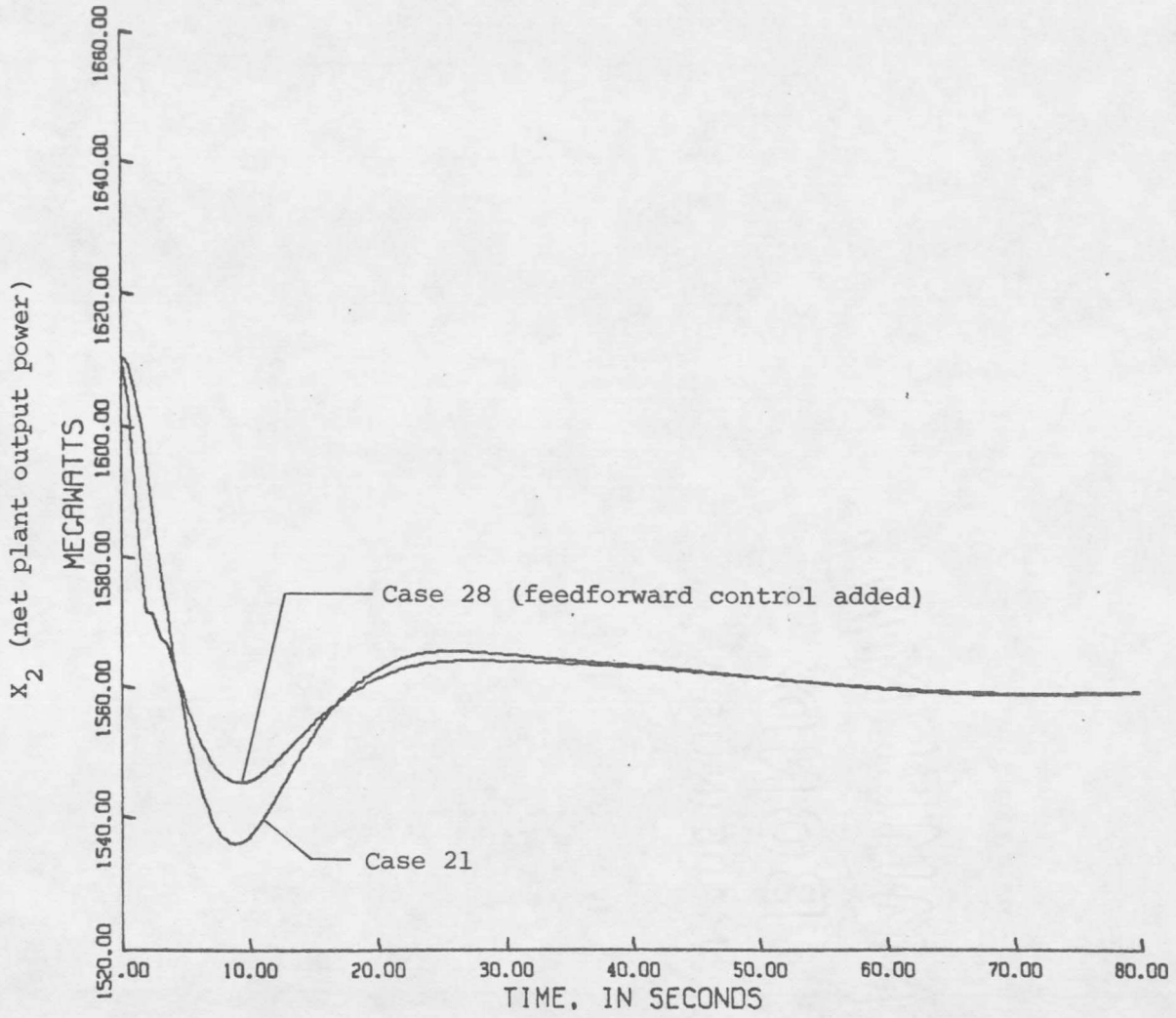



Figure 5.19. $MW_{REF}$ $X_1$ changes from 1610.44 MW to 1560.44 MW at t = 0+; cases are defined in Table 5.5

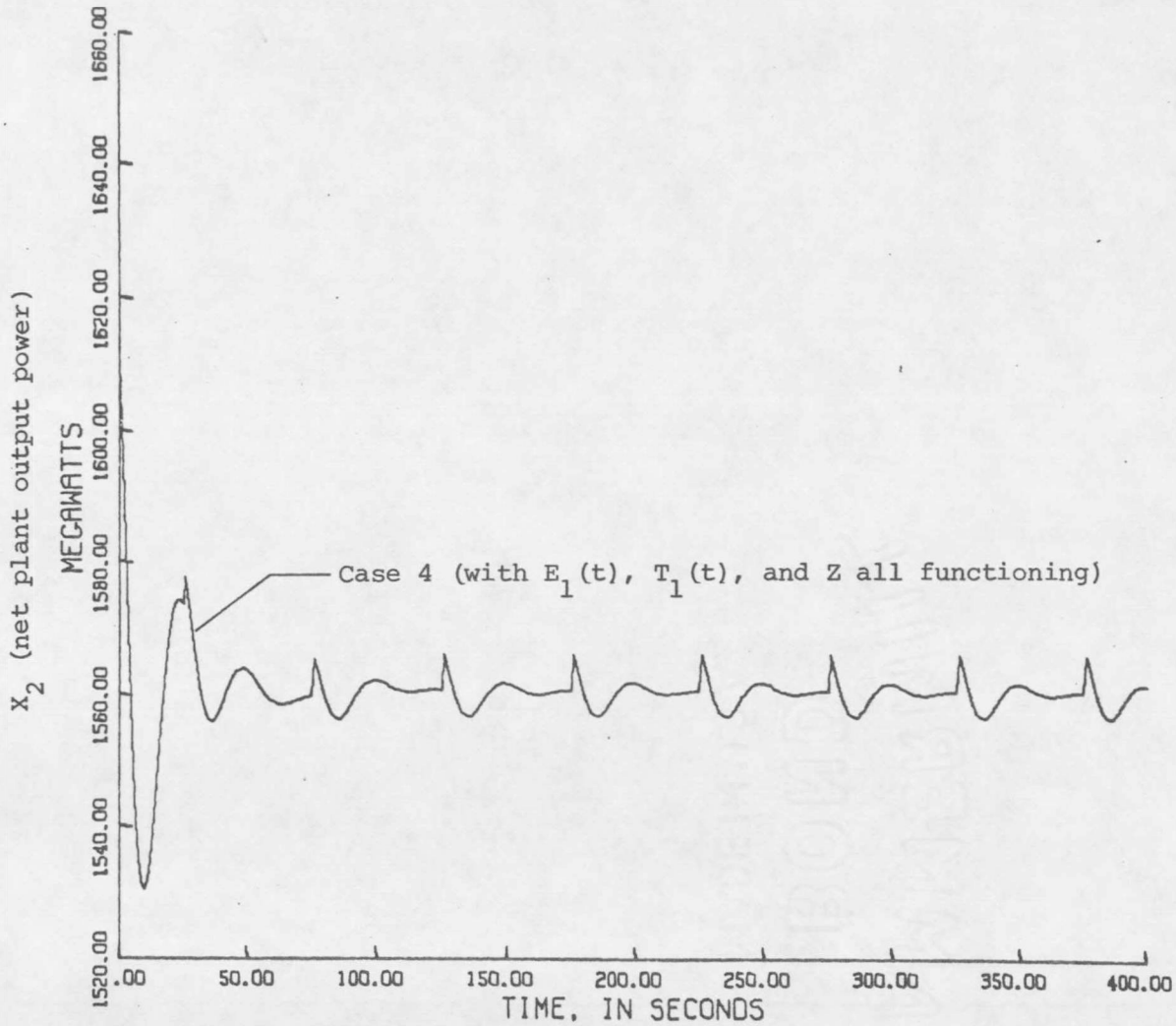



Figure 5.20. $MW_{REF}$ $X_1$ changes from 1610.44 MW to 1560.44 MW at t = 0+; cases are defined in Table 5.5

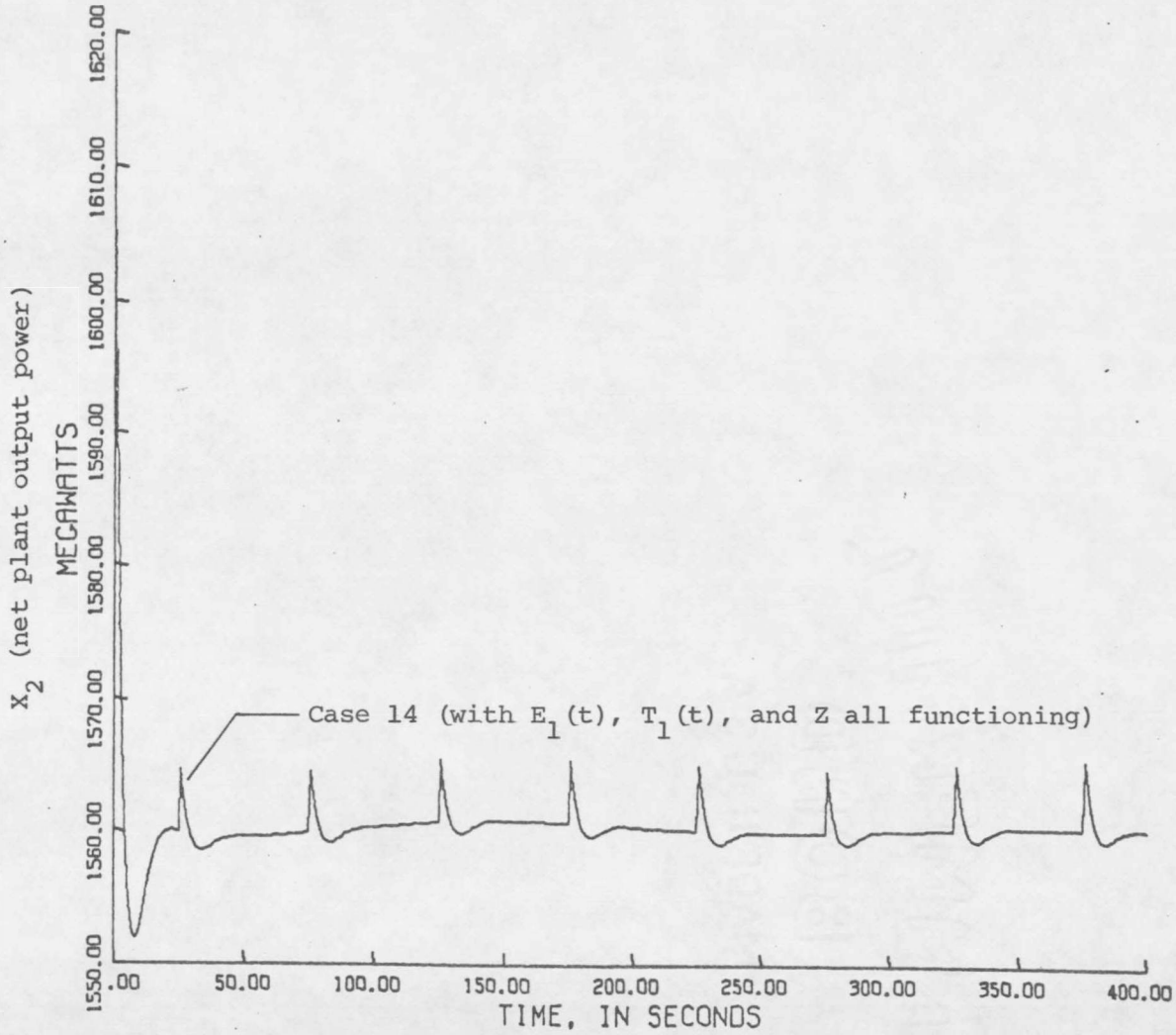



Figure 5.21. $MW_{REF}$ $X_1$ changes from 1610.44 MW to 1560.44 MW at t = 0+; cases are defined in Table 5.5

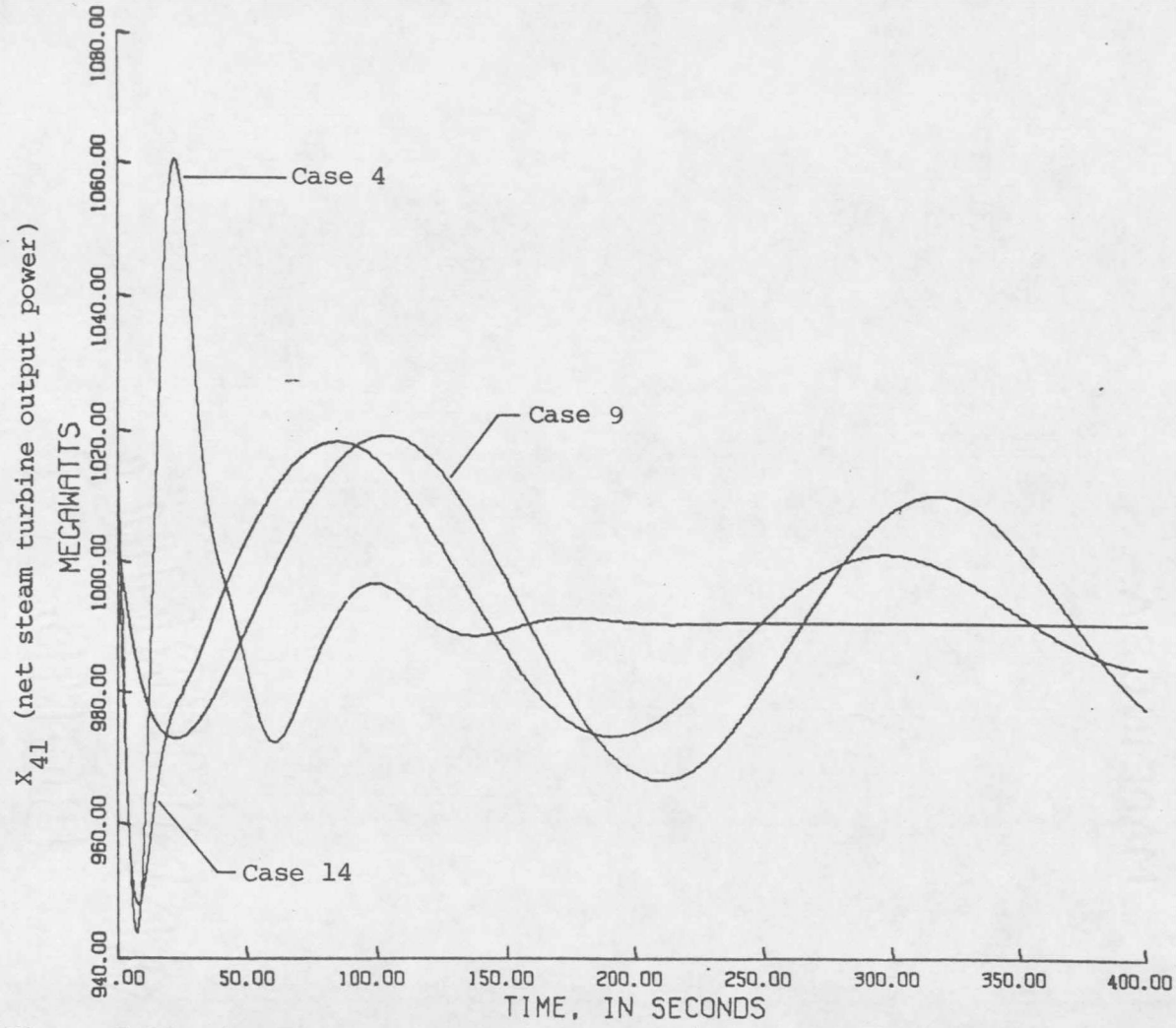



Figure 5.22. $MW_{REF}$ $X_1$ changes from 1610.44 MW to 1560.44 MW at t = 0+; cases are defined in Table 5.5

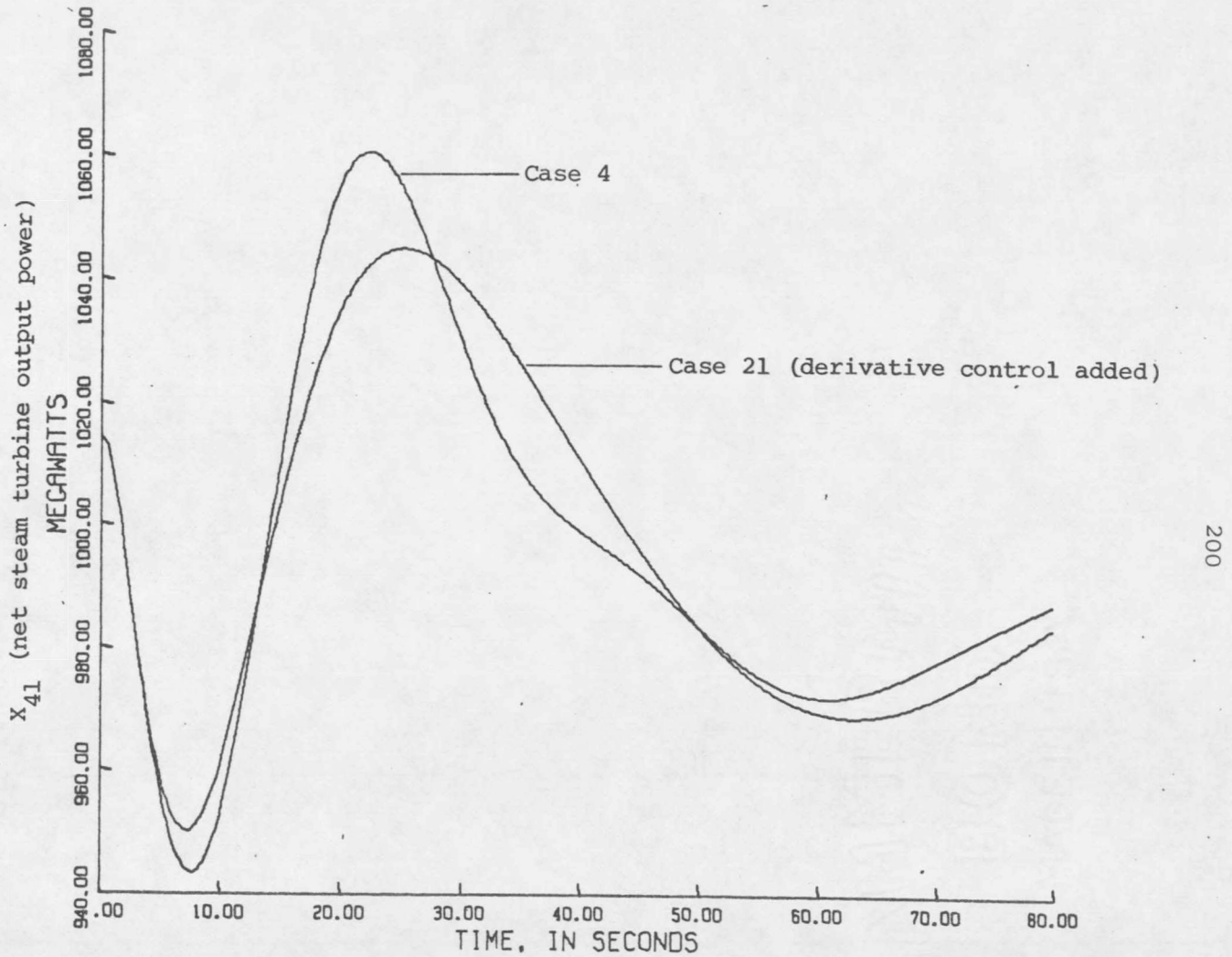



Figure 5.23. $MW_{REF}$ $X_1$ changes from 1610.44 MW to 1560.44 MW at t = 0+; cases are defined in Table 5.5

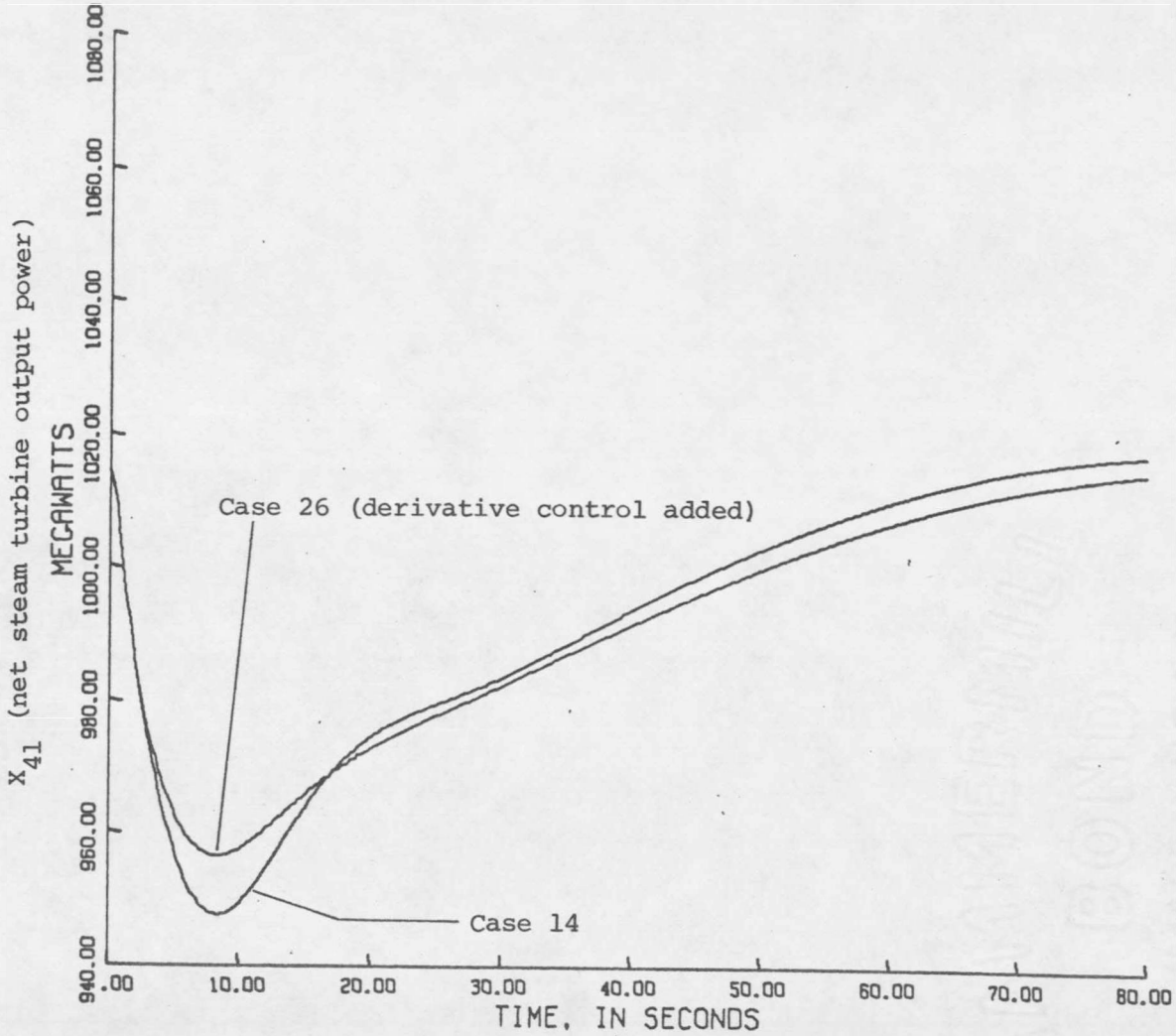



Figure 5.24. $MW_{REF}$ $X_1$ changes from 1610.44 MW to 1560.44 MW at t = 0+; cases are defined in Table 5.5

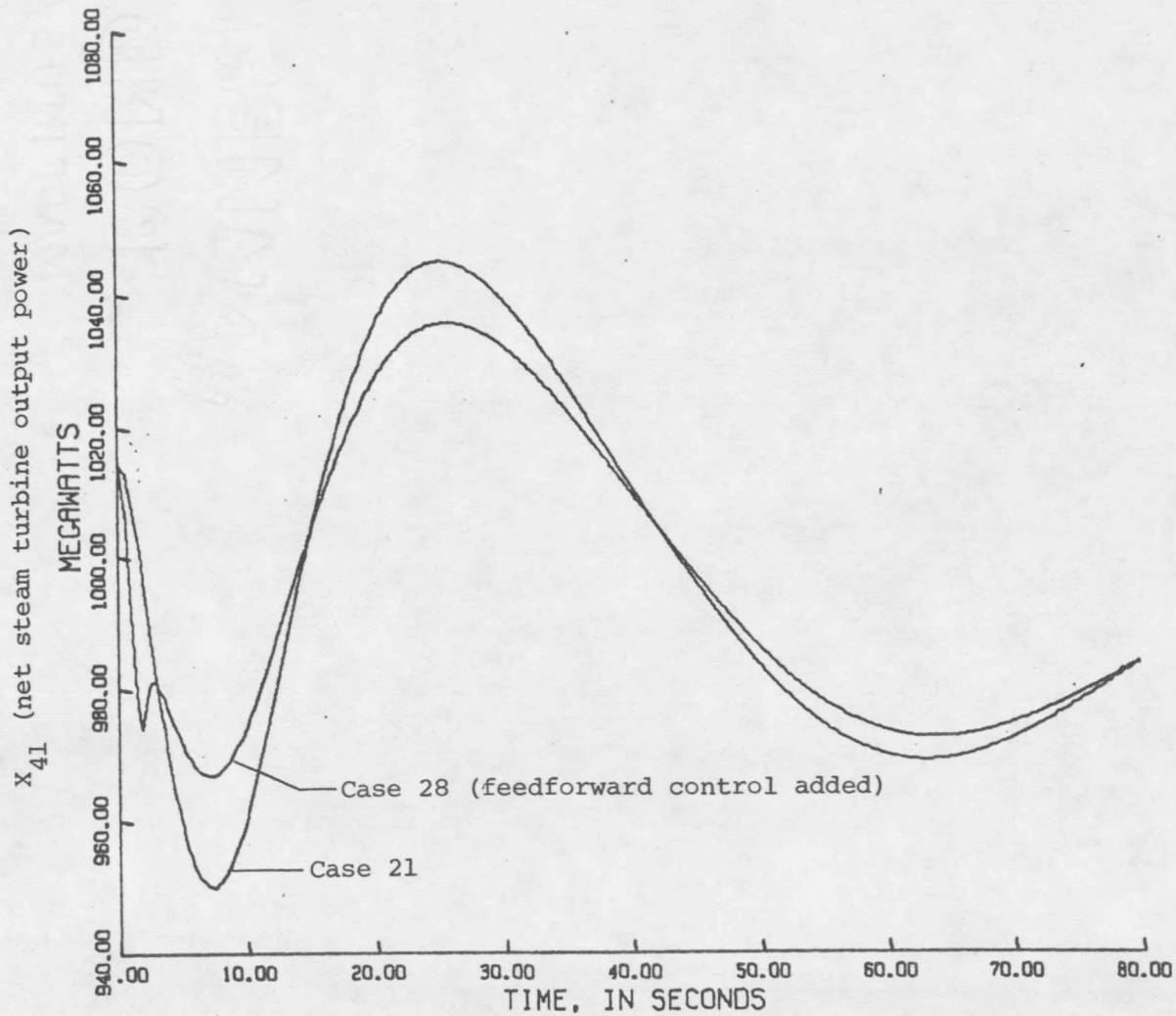



Figure 5.25. $MW_{REF}$ $X_1$ changes from 1610.44 MW to 1560.44 MW at t = 0+; cases are defined in Table 5.5

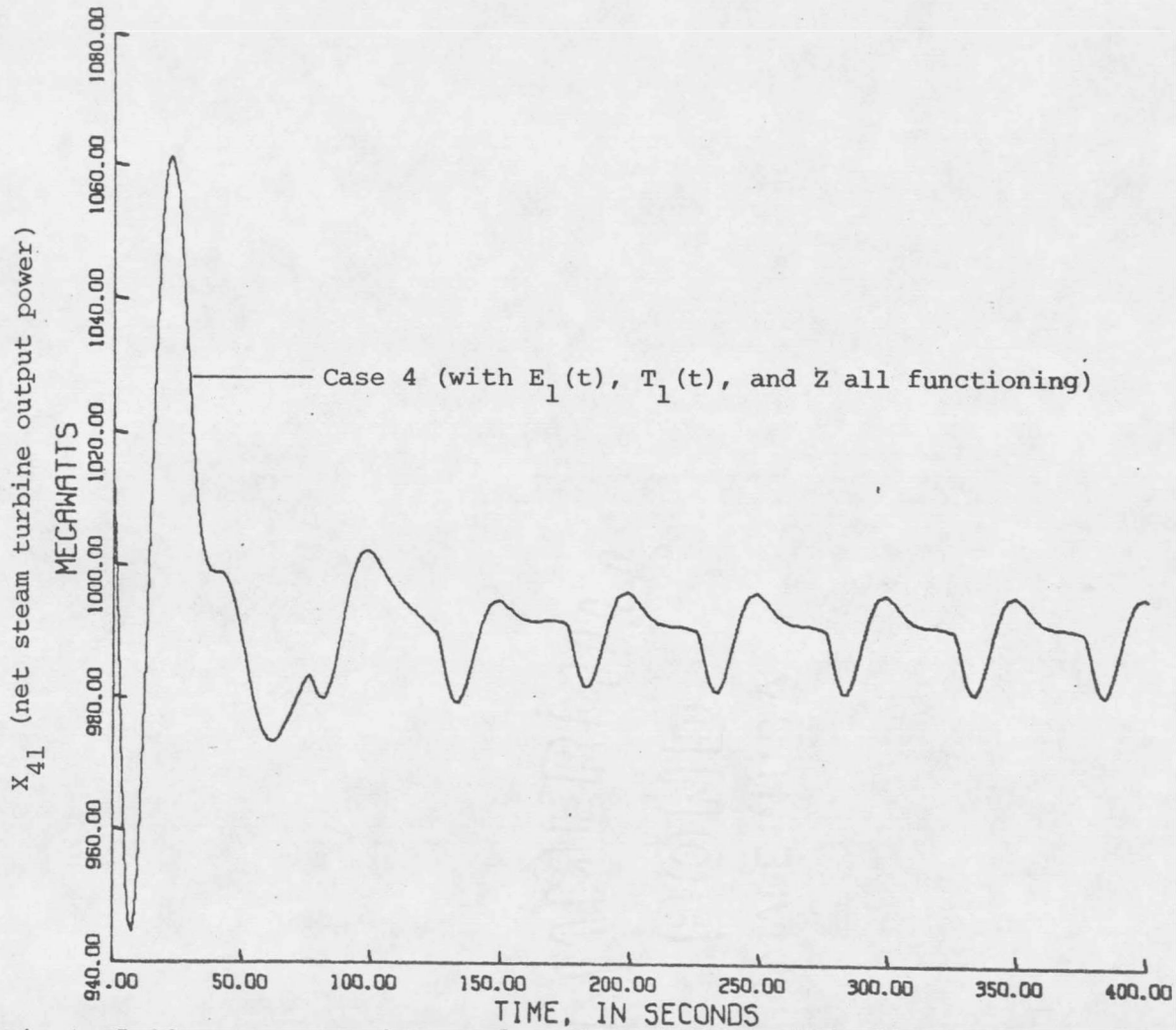



Figure 5.26. $MW_{REF}$ $X_1$ changes from 1610.44 MW to 1560.44 MW at t = 0+; cases are defined in Table 5.5

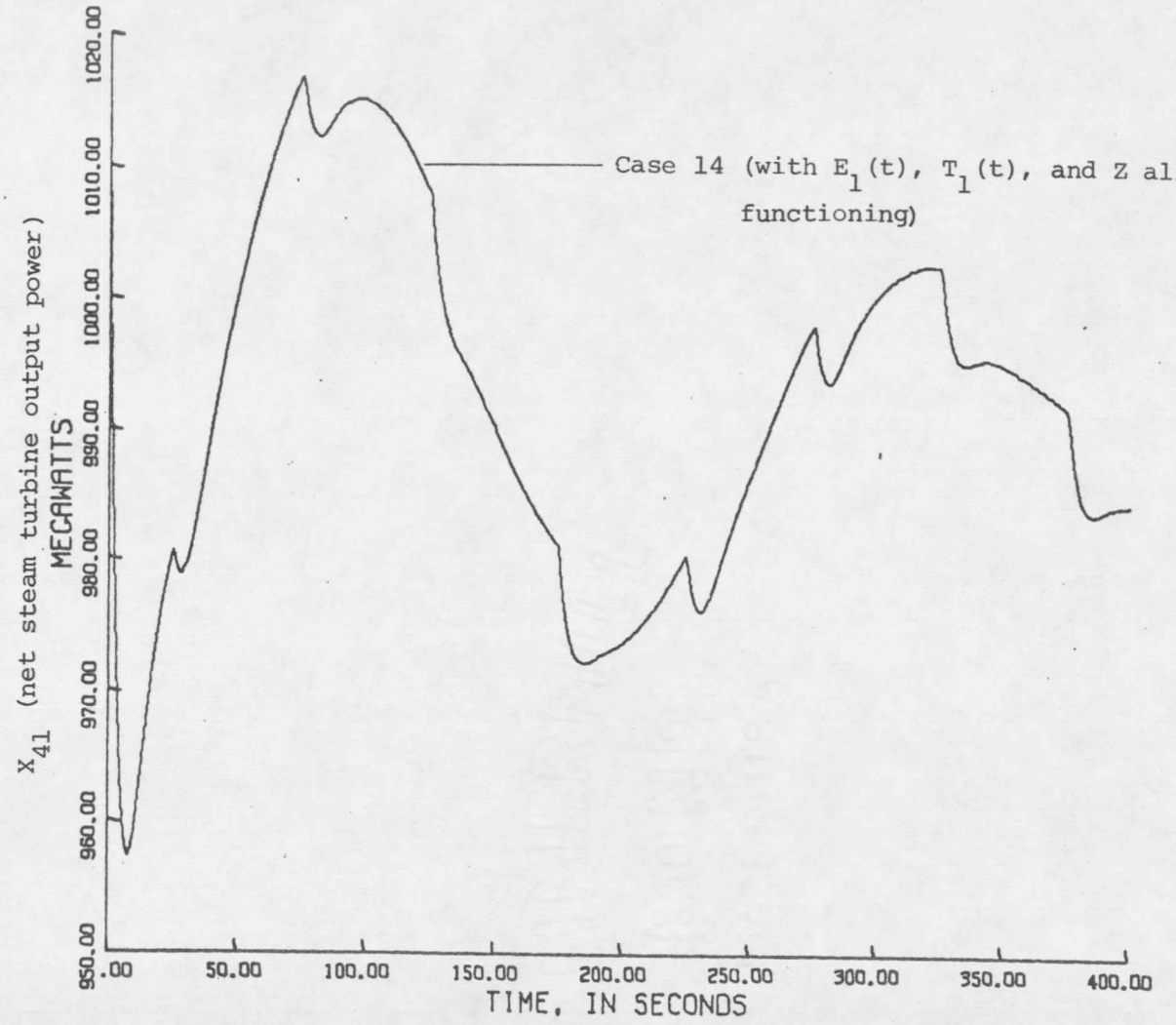



Figure 5.27. $MW_{REF}$ $X_1$ changes from 1610.44 MW to 1560.44 MW at t = 0+; cases are defined in Table 5.5

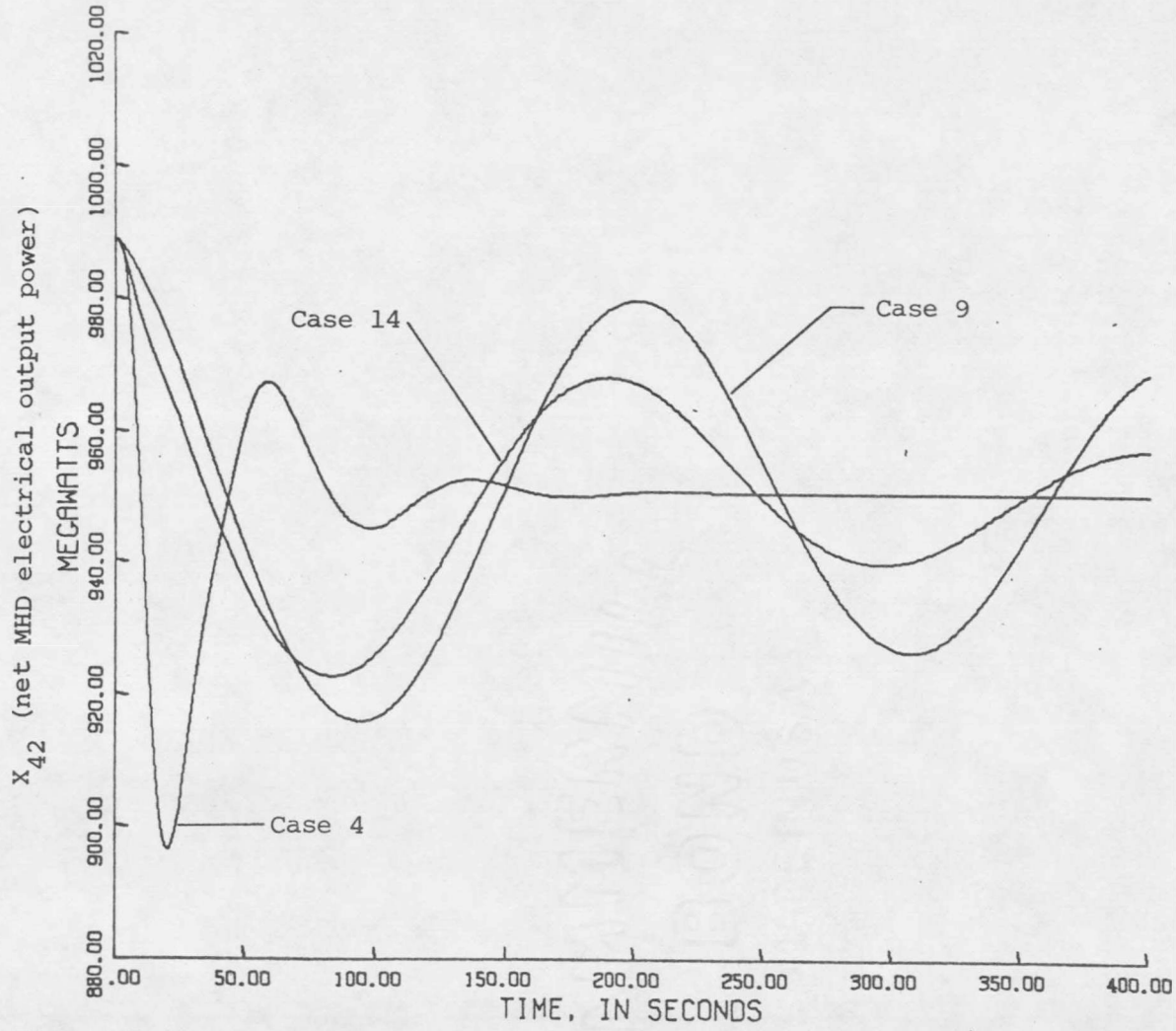



Figure 5.28. $MW_{REF}$ $X_1$ changes from 1610.44 MW to 1560.44 MW at t = 0+; cases are defined in Table 5.5

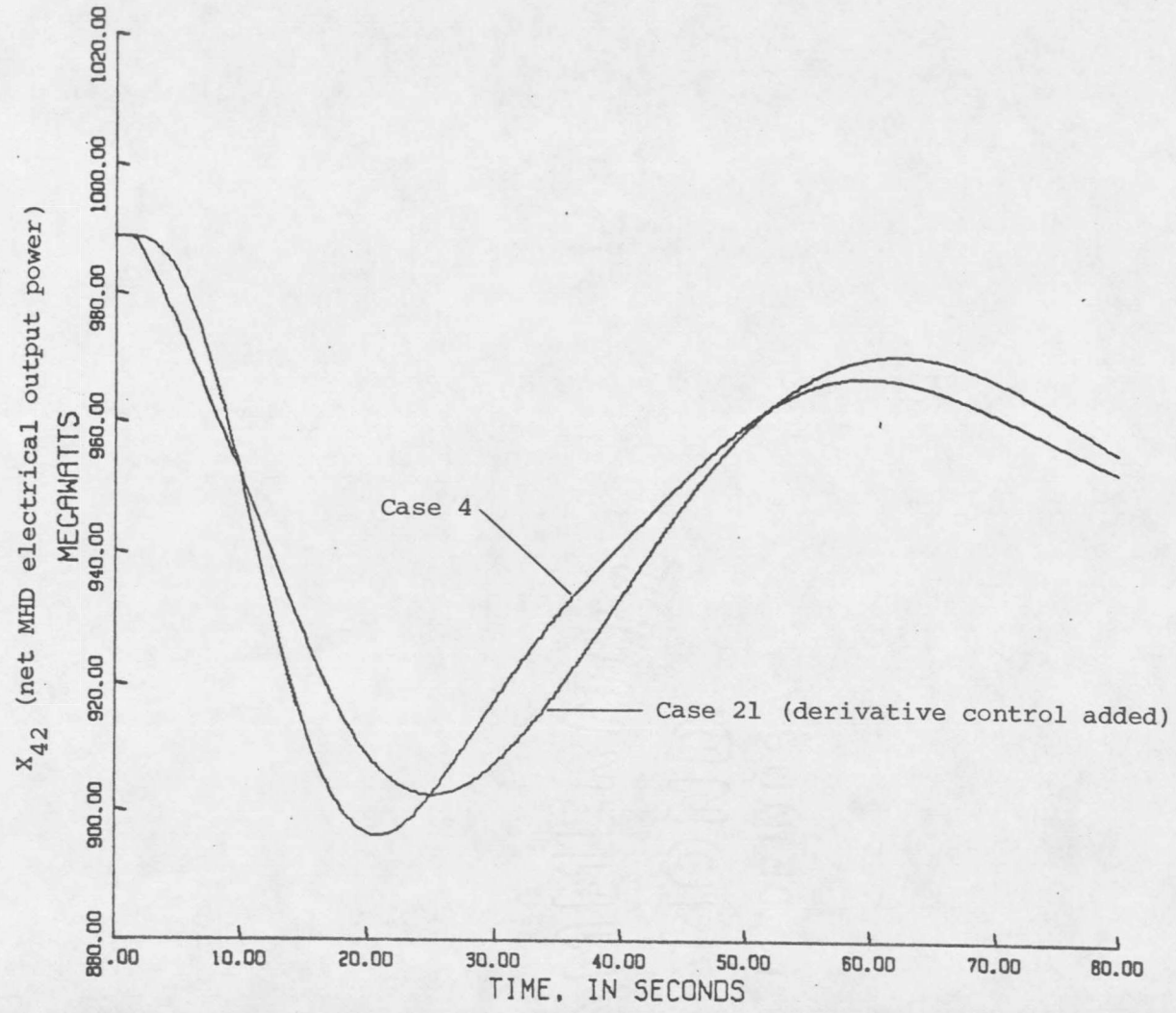



Figure 5.29. $MW_{REF}$ $X_1$ changes from 1610.44 MW to 1560.44 MW at t = 0+; cases are defined in Table 5.5

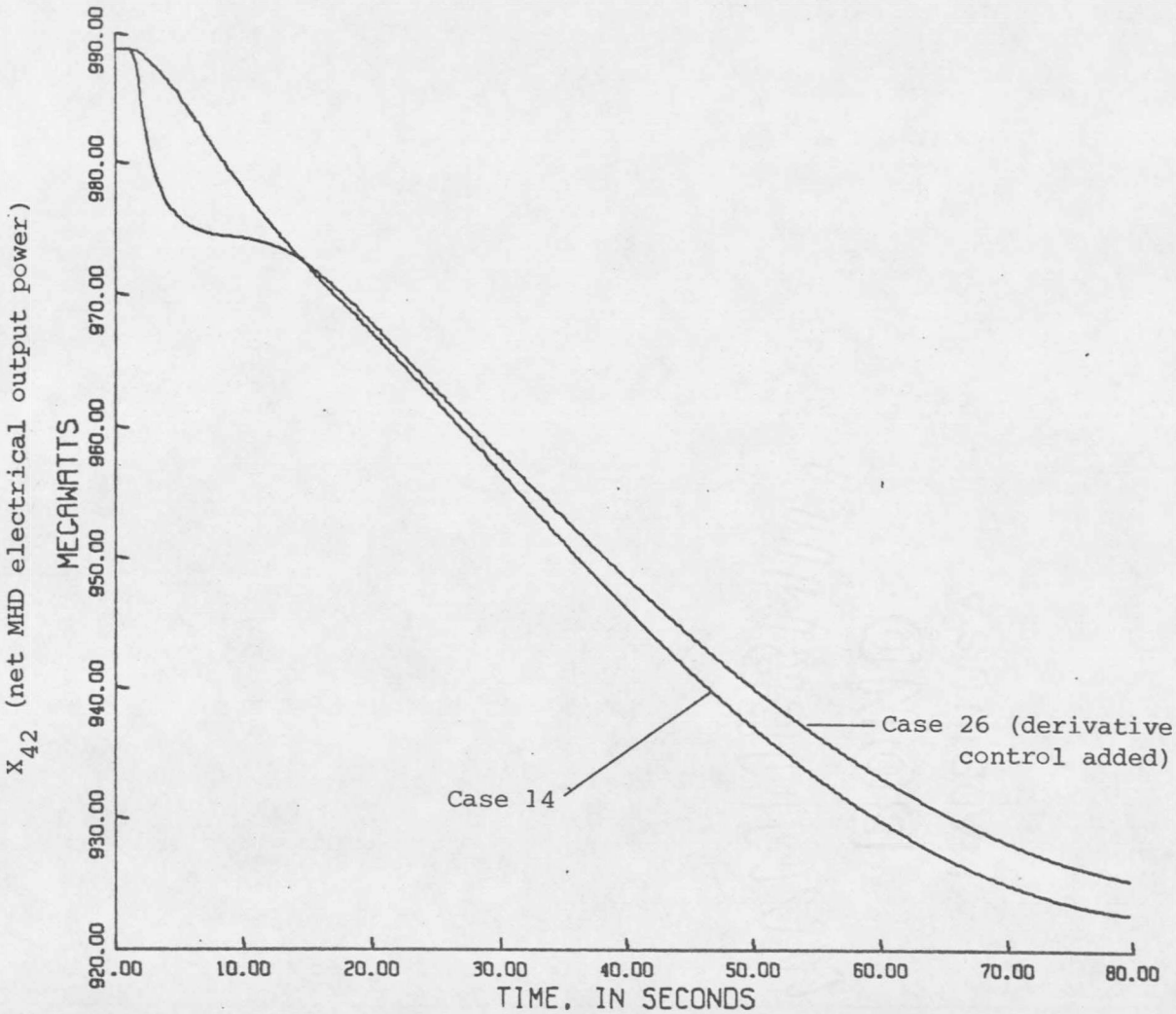



Figure 5.30. $MW_{REF}$ $X_1$ changes from 1610.44 MW to 1560.44 MW at t = 0+; cases are defined in Table 5.5

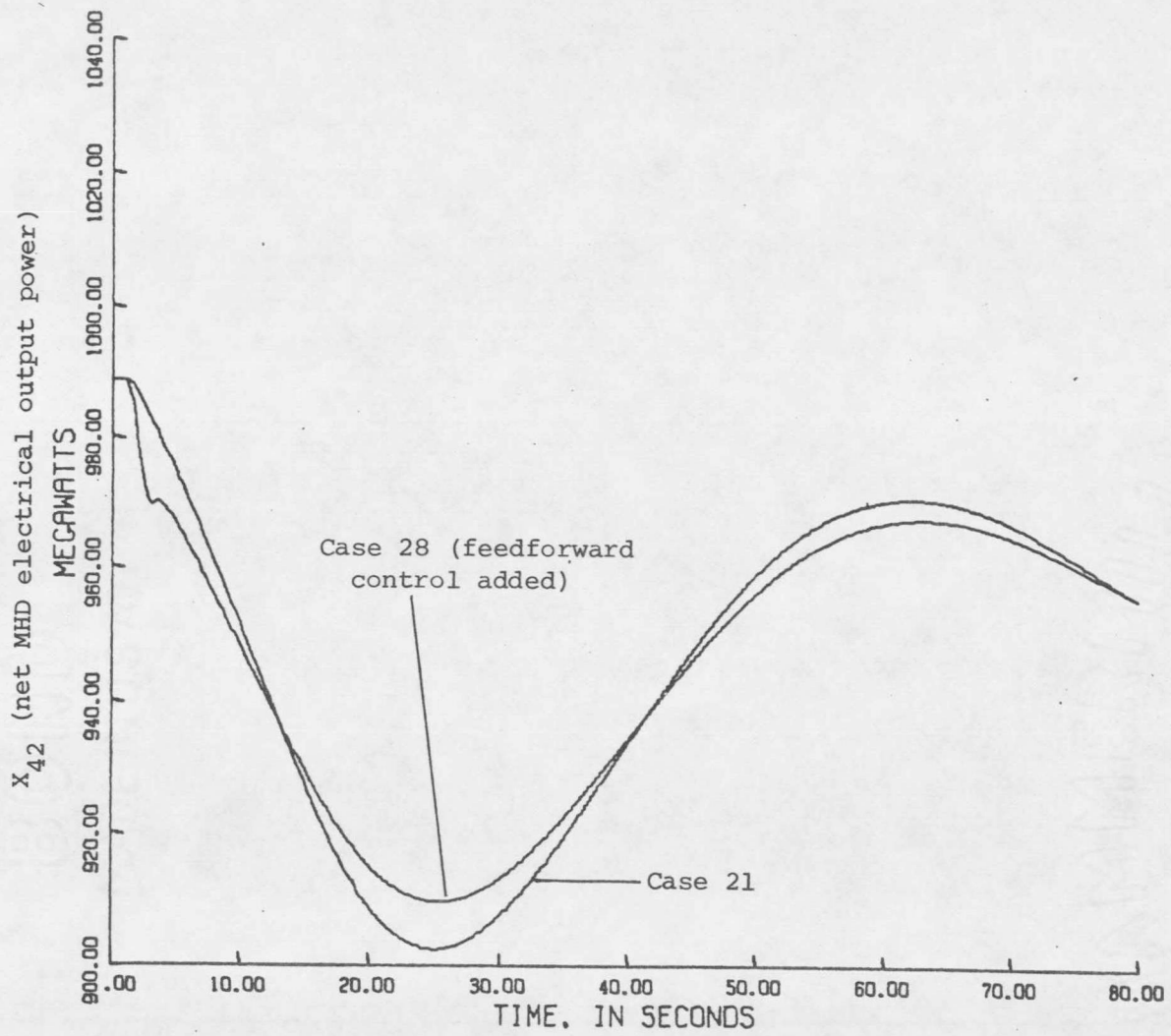



Figure 5.31. $MW_{REF}$ $X_1$ changes from 1610.44 MW to 1560.44 MW at t = 0+; cases are defined in Table 5.5

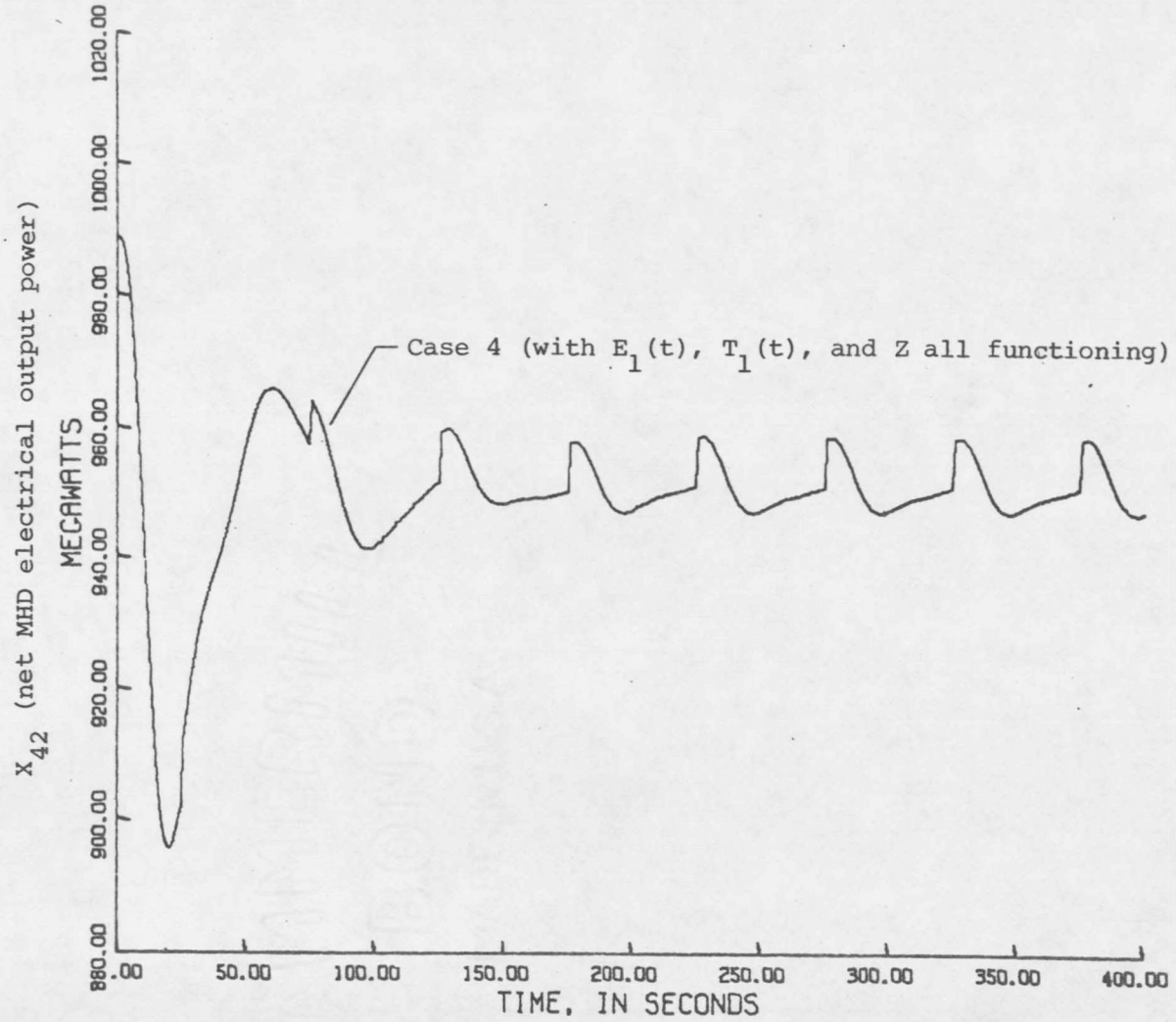



Figure 5.32. $MW_{REF}$ $X_1$ changes from 1610.44 MW to 1560.44 MW at t = 0+; cases are defined in Table 5.5

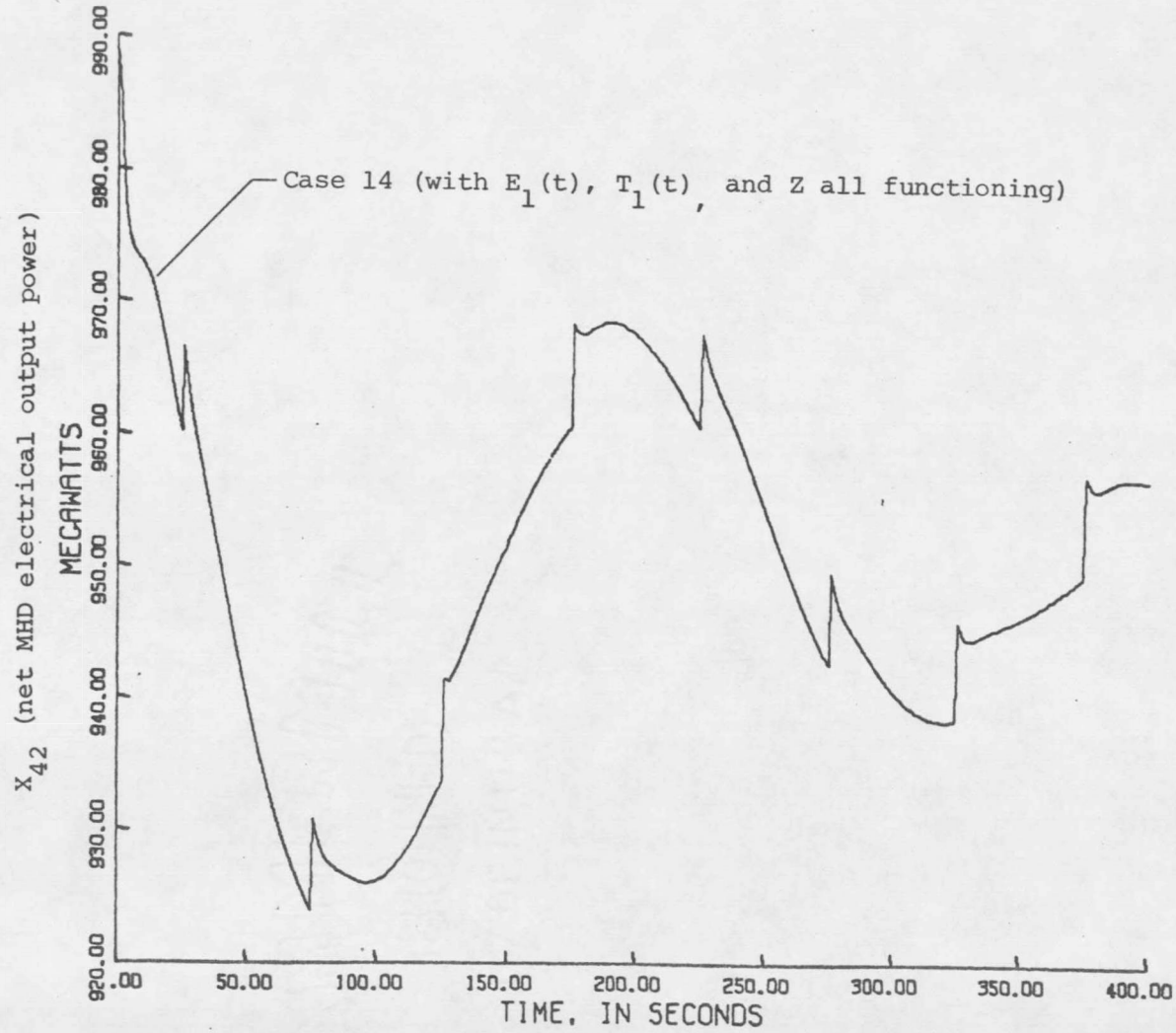



Figure 5.33. $MW_{REF}$ $X_1$ changes from 1610.44 MW to 1560.44 MW at t = 0+; cases are defined in Table 5.5

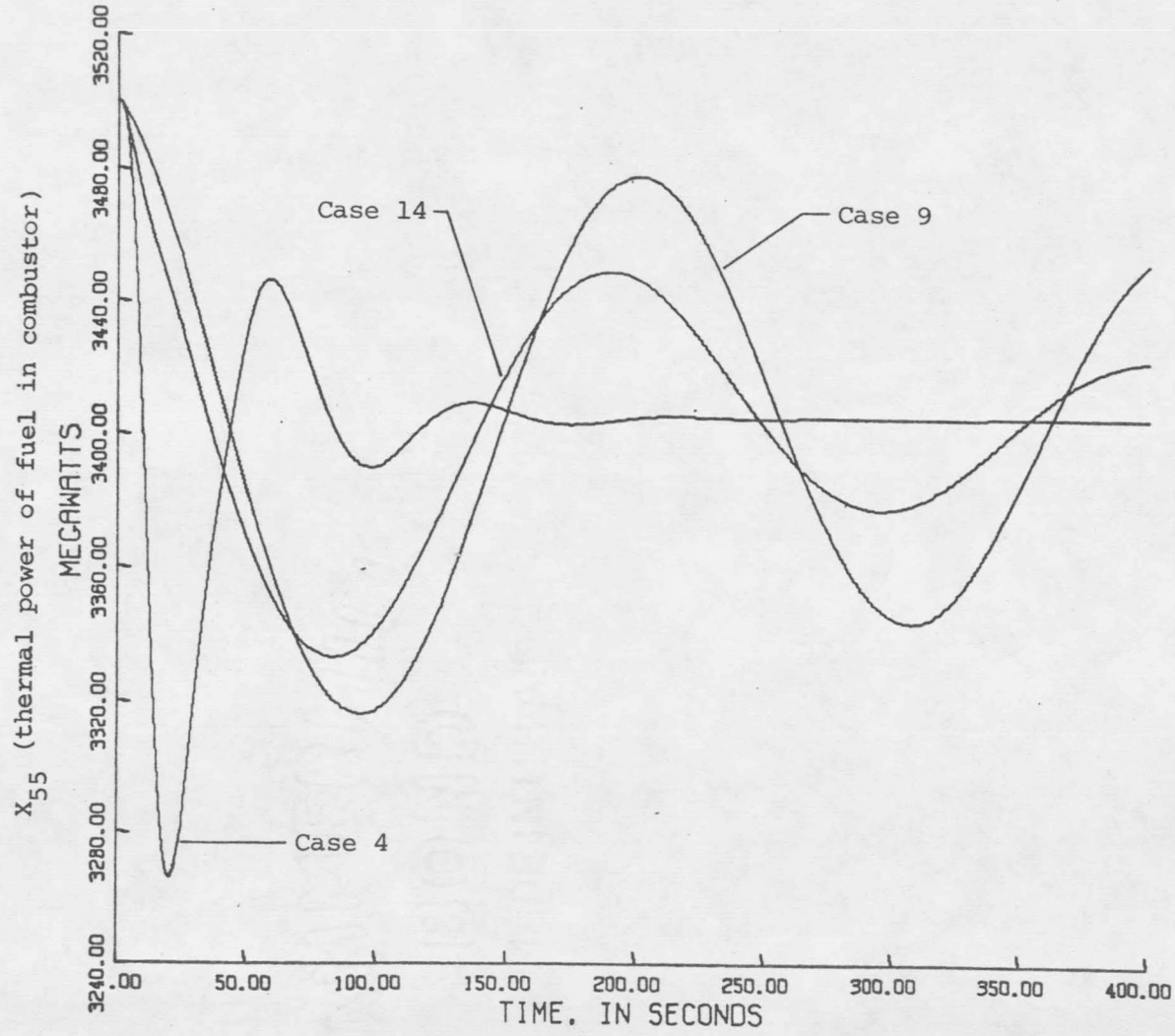



Figure 5.34. $MW_{REF}$ $X_1$ changes from 1610.44 MW to 1560.44 MW at t = 0+; cases are defined in Table 5.5

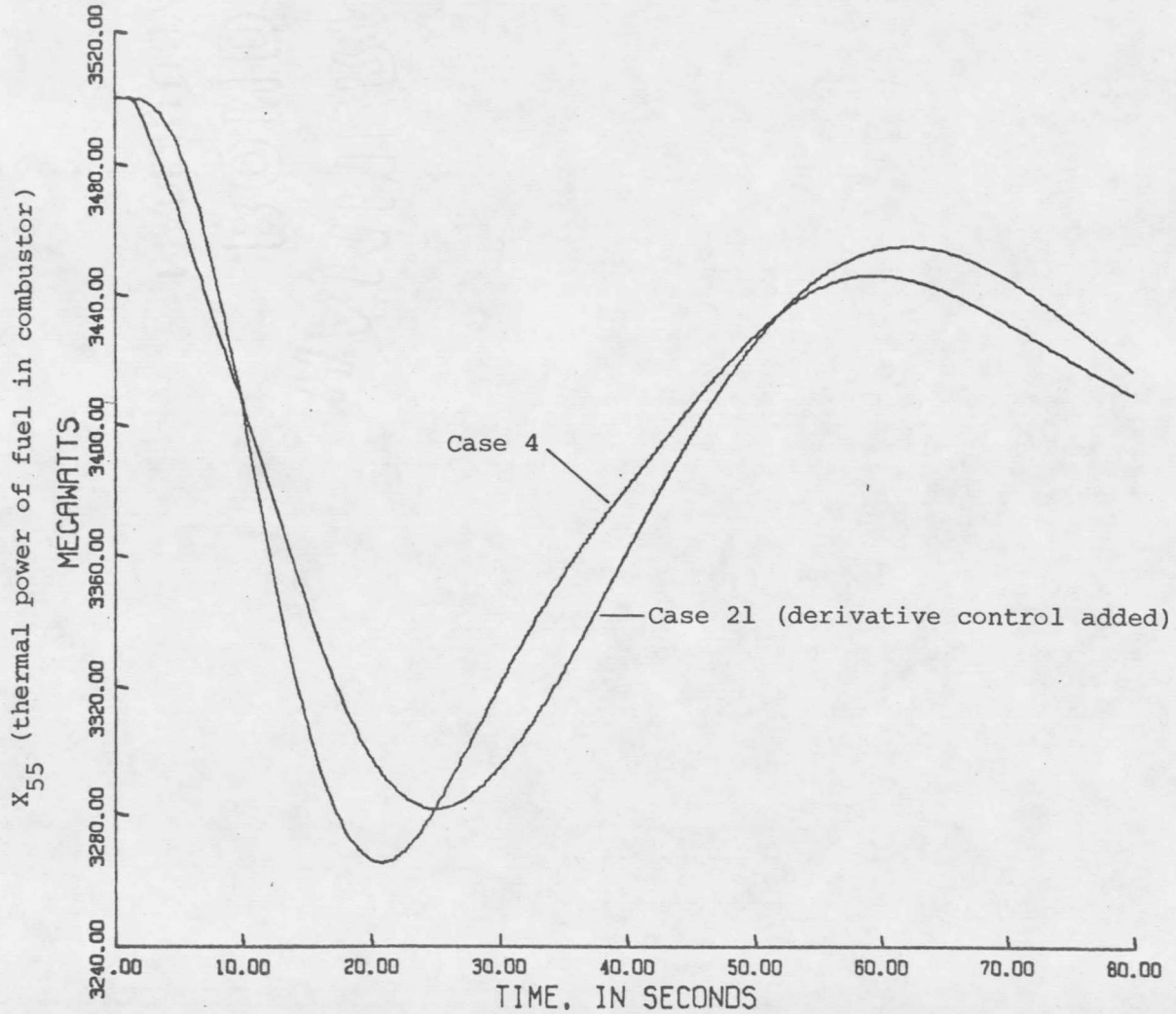



Figure 5.35. $MW_{REF}$ $X_1$ changes from 1610.44 MW to 1560.44 MW at t = 0+; cases are defined in Table 5.5

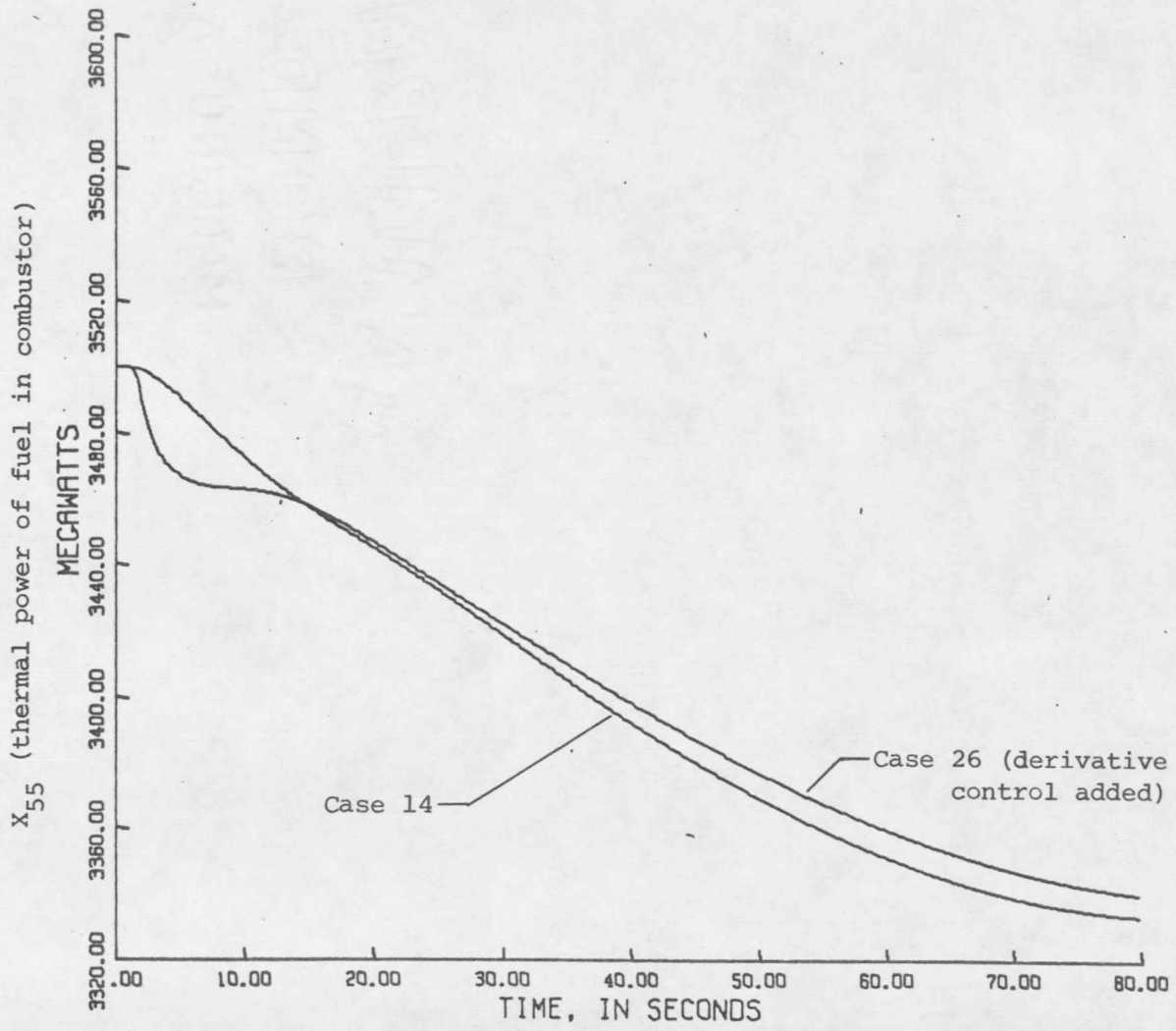



Figure 5.36. $MW_{REF}$ $X_1$ changes from 1610.44 MW to 1560.44 MW at t = 0+; cases are defined in Table 5.5

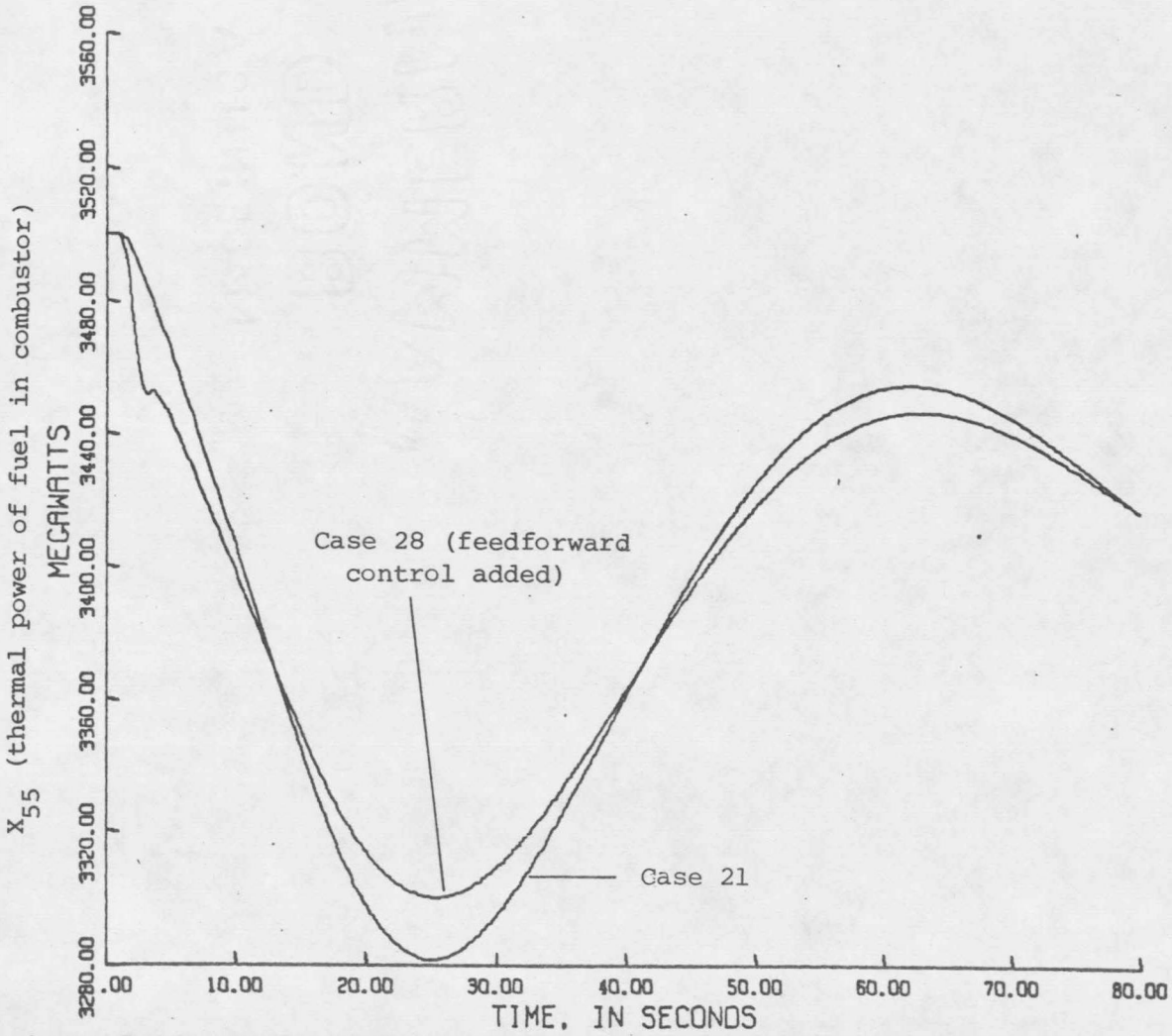



Figure 5.37. $MW_{REF}$ $X_1$ changes from 1610.44 MW to 1560.44 MW at t = 0+; cases are defined in Table 5.5

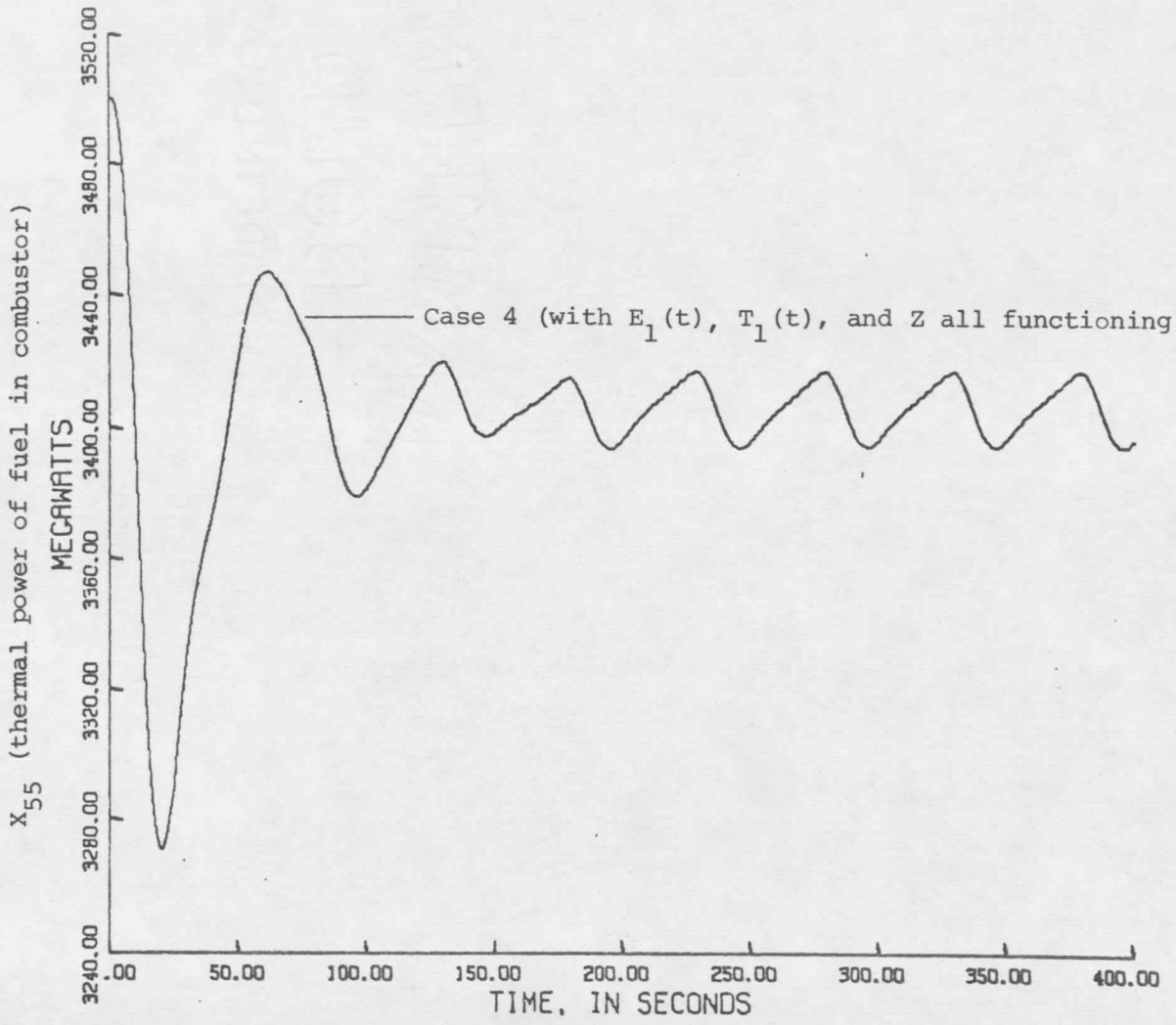



Figure 5.38. $MW_{REF} \cdot X_1$ changes from 1610.44 MW to 1560.44 MW at t = 0+; cases are defined in Table 5.5

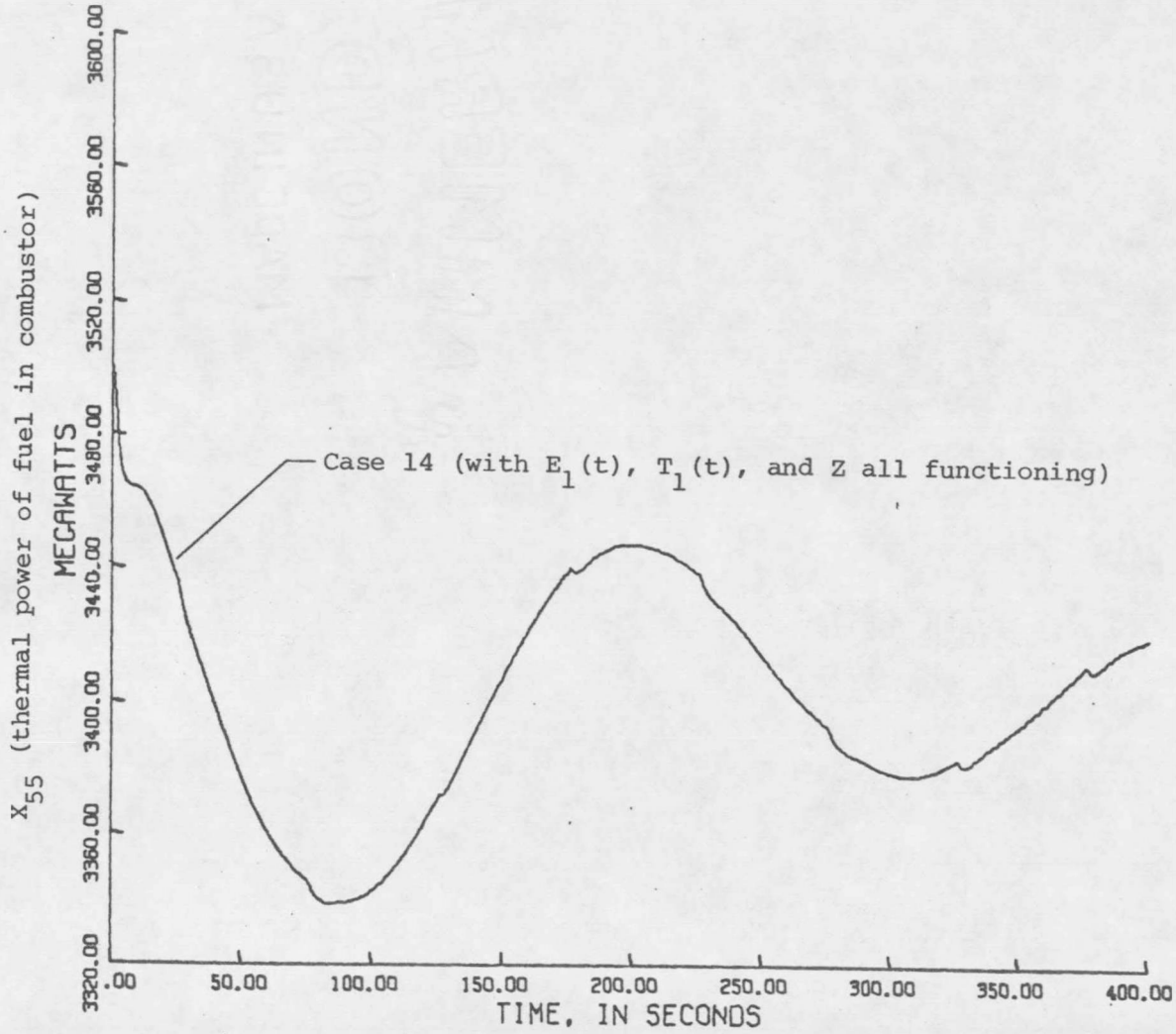



Figure 5.39. $MW_{REF}$ $X_1$ changes from 1610.44 MW to 1560.44 MW at t = 0+; cases are defined in Table 5.5

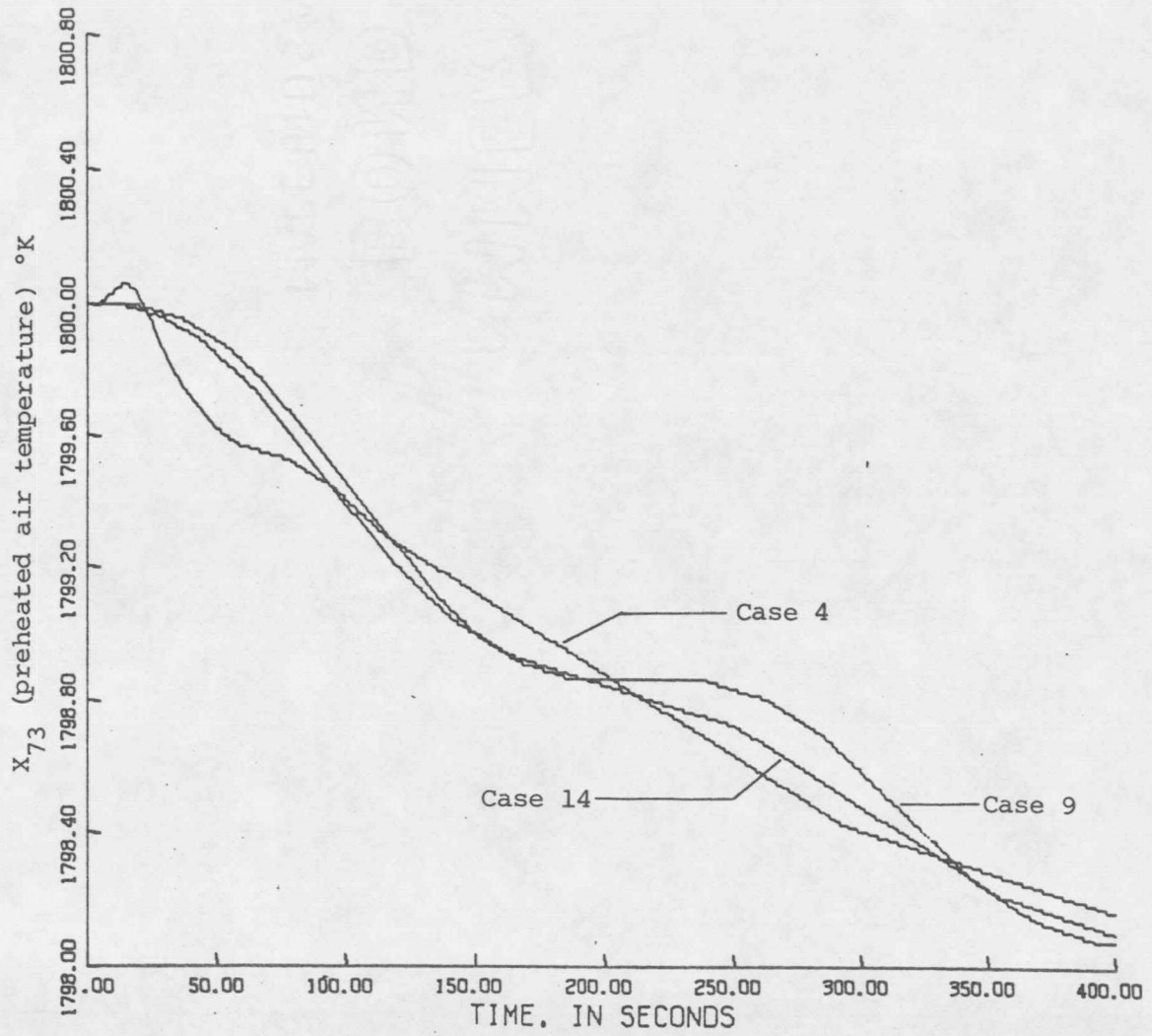



Figure 5.40. $MW_{REF}$ $X_1$ changes from 1610.44 MW to 1560.44 MW at t = 0+; cases are defined in Table 5.5

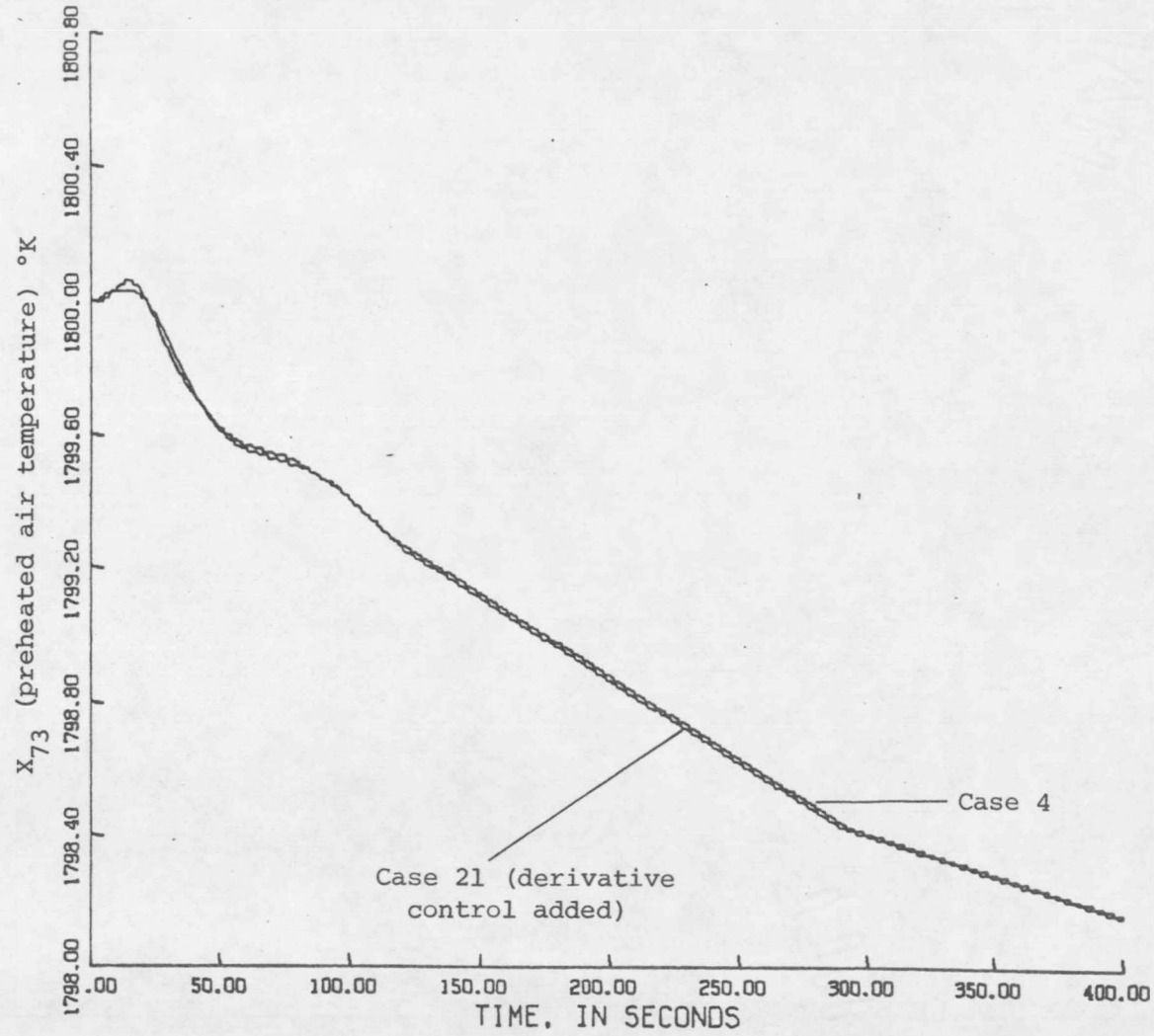



Figure 5.41. $MW_{REF}$ $X_1$ changes from 1610.44 MW to 1560.44 MW at t = 0+; cases are defined in Table 5.5

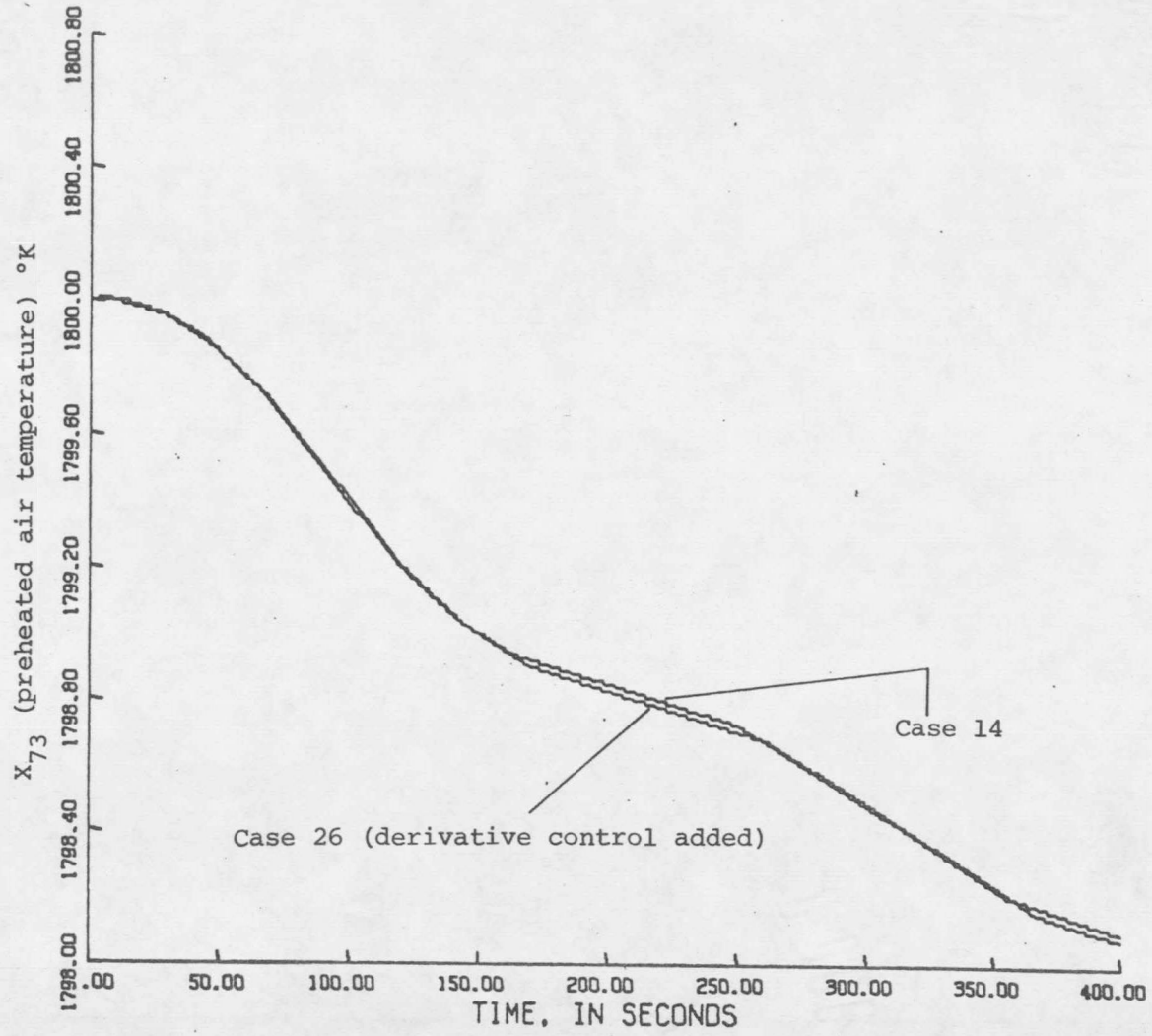



Figure 5.42. $MW_{REF}$ $X_1$ changes from 1610.44 MW to 1560.44 MW at t = 0+; cases are defined in Table 5.5

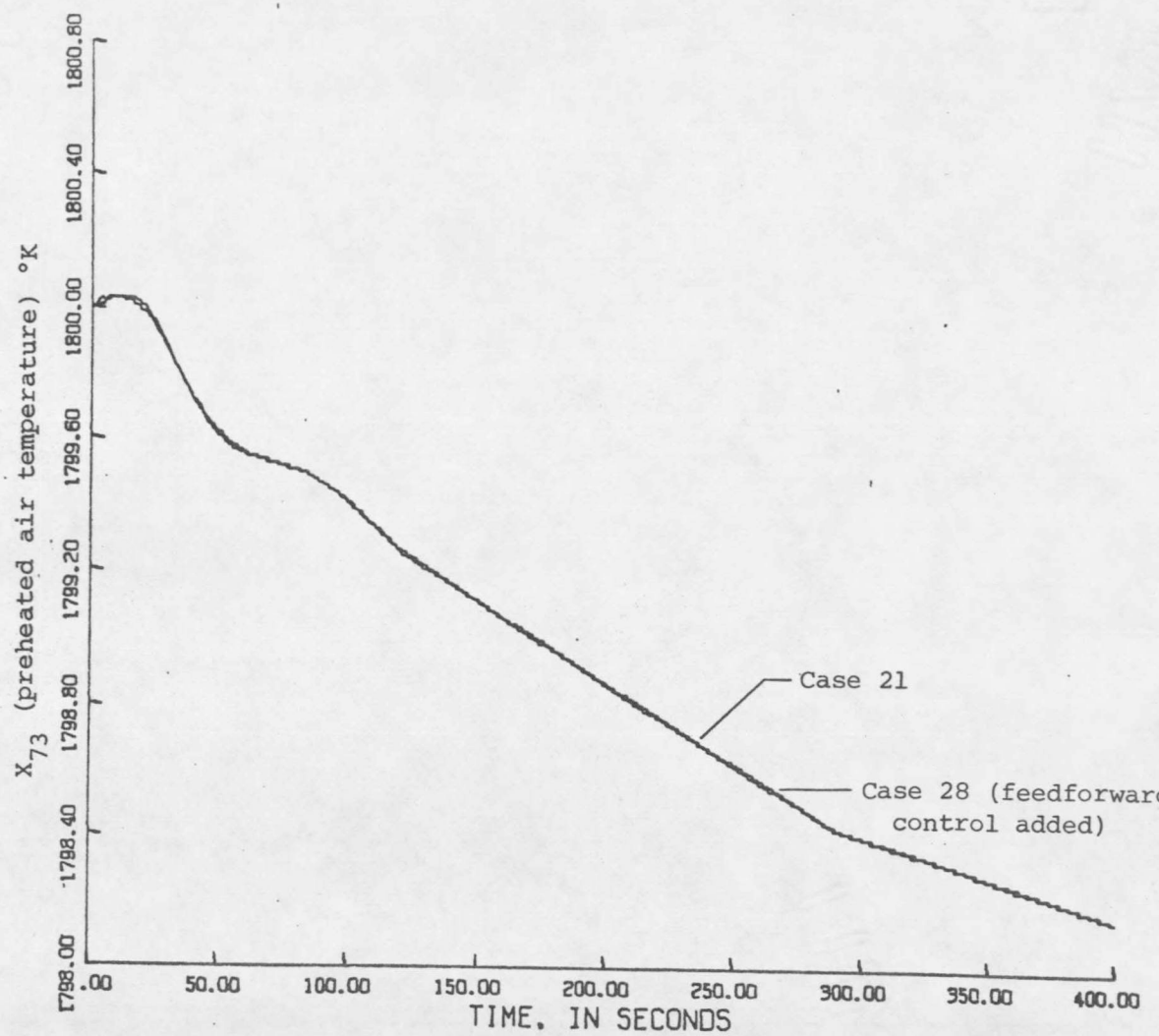



Figure 5.43. $MW_{REF}$ $X_1$ changes from 1610.44 MW to 1560.44 MW at t = 0+; cases defined in Table 5.5

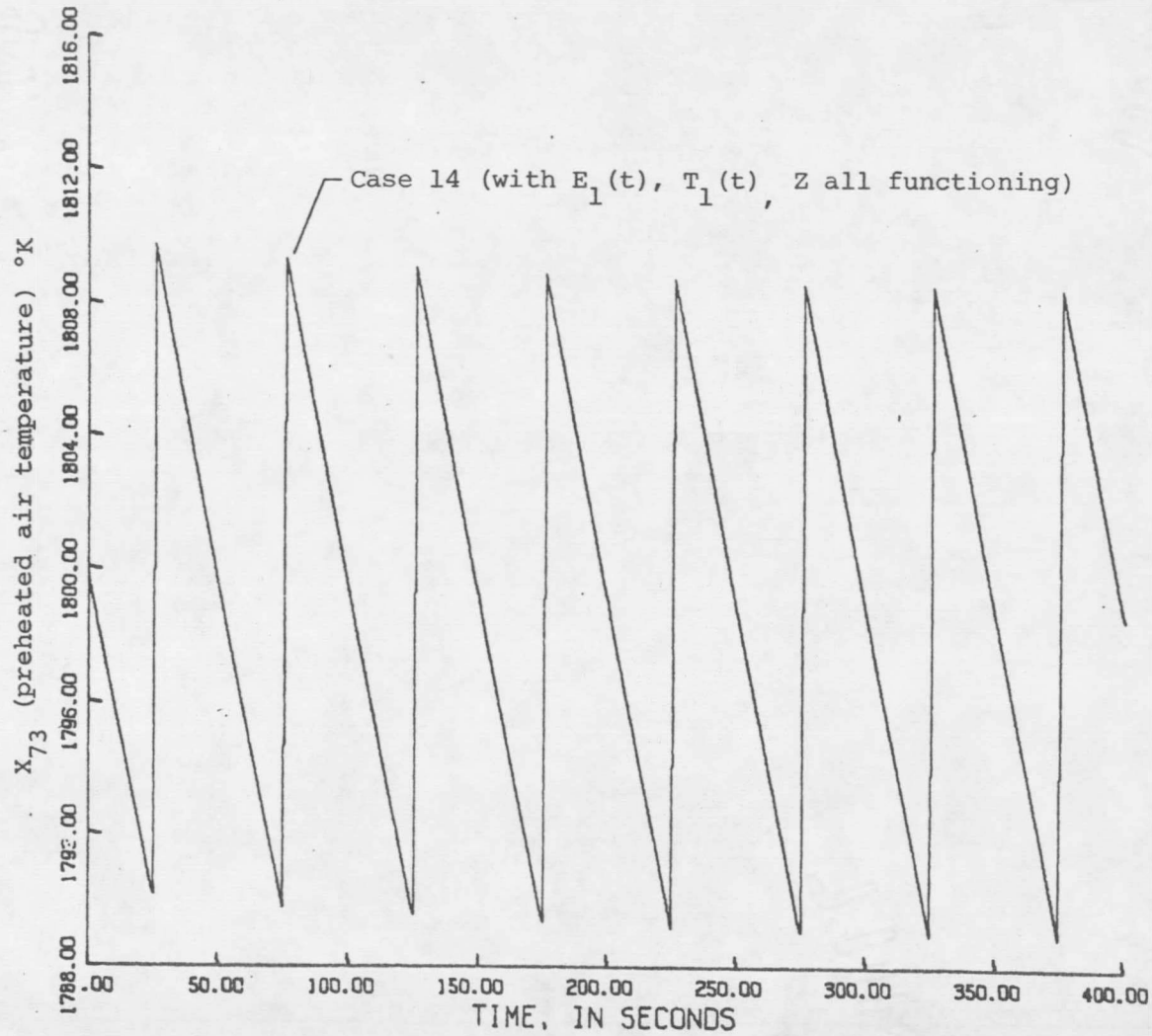



Figure 5.44. $MW_{REF}$ $X_1$ changes from 1610.44 MW to 1560.44 MW at t = 0+; cases are defined in Table 5.5

# Chapter VI

# SUMMARY OF RESULTS

## 6.1 Introduction

The purpose of Chapter VI is to summarize and evaluate the results of computer simulations of the three system models developed in Chapters III, IV, and V. Suggestions for future research are included in Section 6.5.

## 6.2 System Model I

System model I, shown in Figure 3.3, represents the initial dynamic modeling effort described in this paper. The basis for the model is an idealized heat balance diagram given in Figure 3.1 [143]. Proportional-plus-integral control is used. Generation error is the controller input. The fuel system is characterized by a limiter and a first-order lag in cascade. The MHD channel is described by enthalpy extraction in the form of electrical output power and by a negligible time constant compared with the remainder of the system. Heat exchangers or air preheaters are regenerative and are described by a first-order lag with a 360 second time constant. Inputs to the preheaters are air compressor power and thermal power from combustion gases. Air preheater output is thermal power in preheated air available to the combustor. The steam plant, described by a cascade of two first-order lags, has thermal power of combustion gases as the input

and gross electrical power as the output. Net plant generated power is the sum of inverter output power and steam plant output power less in-house load requirements.

Numerous computer simulations of system dynamic response are illustrated in Figures 3.4 through 3.23. Figures 3.4 and 3.5 show the effect of variations in MHD channel enthalpy extraction efficiency for several system variables. Figures 3.6 through 3.23 describe the result of perturbing the system with a 50 MW step decrease in $MW_{REF}$ $X_1$ at t = 0+. Several combinations of controller parameter values are represented. A wide variation in overall plant response is possible, as shown in Figures 3.21 through 3.23, ranging from highly damped to underdamped cases. System response time to the -50 MW step ranges from 1.5 seconds to 270 seconds for the cases considered.

A very interesting observation is that the system described by model I is stable for all cases considered. This is verified by a classical stability analysis detailed in Section 3.7.

## 6.3 System Model II

System model II, discussed in Chapter III, was developed as the first phase in an orderly extension of model I complexity. The idealized heat balance of Figure 3.1 is retained, as is the basic PI control and steam plant representation.

Model II extends model I in the following ways:

1) Transport delays are included between the fuel valve and the MHD channel ($\tau_1$), between the radiant boiler and steam plant ($\tau_4$), and between the MHD channel and heat exchangers ($\tau_5$).

2) $T_1(t)$ and $E_1(t)$ describe time variations in preheated air temperature and variations in input power to the steam bottoming plant due to air preheater cycling.

3) A feedback path, denoted by the variable Z, has been introduced to reduce variations in air preheat temperature.

4) A radiant boiler in the diffuser has been added.

5) A nonlinear block ($f_1$) is used to implement the combustion air preheat temperature control.

6) A nonlinear block ($f_2$) describes compressor power.

Computer simulations of model II dynamic response are shown in Figures 4.4 through 4.24. The essential response characteristics of model II are similar to model I. No instabilities exist in any cases considered. Of particular interest is the effect of time functions $E_1(t)$ and $T_1(t)$ on system performance. $E_1(t)$ and $T_1(t)$, used to model air preheater cycling, have no effect on steam plant output power (Figures 4.17 through 4.20), but have a significant effect on many important system variables, such as fuel thermal input power, inverter output power, and net plant output power. For example, net plant output power, $X_{28}$, shown in Figures 4.21 through 4.24, exhibits 4 MW

perturbations due to air preheater cycling for the cases investigated. Four MW is 0.254% of the 1577.5 MW nominal plant output power. An increase of 0.25% in plant output power corresponds to an increase in line voltage of 0.127%. This disturbance occurs too rapidly to be eliminated by the existing controller. The most promising way to reduce the transients to an acceptable level is to control some parameter associated with the MHD channel which affects enthalpy extraction. The MHD channel is the only system component that has sufficiently short response times to be affected by the variations in preheated air temperature. Because of this, it is the most likely candidate to effect a solution to the output transient problem. Tempering combustion air temperature with air from a secondary source is one possible solution. Introducing seed flow variations to alter gas conductivity is another means of approaching the problem. Still another is fast control of the inverters.

The existing air temperature controller (feedback variable Z) only affects long-term variations in air temperature. This may be noted by examining Figures 4.8 through 4.12. The control used is proportional type, and steady-state error could certainly be improved by the addition of more gain and/or integral type control. However, the extremely long time lag due to preheater cycling is still in the control loop, making it impossible to cause any rapid changes in the preheated air temperature with air temperature control which adjusts

thermal input power to the preheaters. Thus, model II indicates that temperature variations due to air preheater cycling may be a problem and that fast acting control of appropriate MHD channel parameters may be necessary.

## 6.4 System Model III

System model III is the second and final extension of model I complexity described in this paper. It is considerably more detailed than either model I or model II. An overall block diagram of model III is given in Figure 5.1, and detailed block diagrams of system components are shown in Figures 5.6 through 5.15.

The added complexity of model III is particularly evident in the characterization of the steam plant, the steam turbines, the Combustor/Nozzle/Channel/Diffuser (CNCD), and the control system. The boiler and turbine valve model, which was previously described as a pair of cascaded first-order lags, is now a two-input, three-output model [81]. Inputs are turbine valve area and power available to generate steam. Outputs are throttle pressure, power to the turbines, and boiler and stack loss. The steam turbines are modeled assuming a reheat system with high-pressure, reheat, and low-pressure turbines represented with appropriate time constants and losses [65]. The CNCD is much more sophisticated than in previous models. It is an input-output model resulting from polynomial approximations of data

obtained from the solution of energy balance, state, and continuity equations for the combustor, and the quasi one-dimensional MHD equations for the nozzle, channel, and diffuser [114]. CNCD inputs are fuel thermal input power and preheated combustion air temperature. Outputs are thermal power loss, power absorbed by the cooling water, thermal power in the combustion gases leaving the diffuser, and inverter electrical output power. The control system is essentially boiler following type (Figure 5.2) with additional feedforward controllers available. A wide variety of control possibilities are available with twelve adjustable control parameters included in two proportional-integral-derivative controllers and two feedforward controllers.

A large number of computer simulations of system dynamic response are tabulated in Table 5.5. In all cases the boiler-following type of control shown in Figure 5.1 is used. The values of the 12 controller parameters are given, as are important characteristics of net plant output power $X_2$. Graphical displays of the behavior of several model III variables as a function of time are given for several different controller conditions in Figure 5.16 through 5.44.

Many interesting aspects of the dynamic behavior of model III are apparent in Table 5.5. First, it is possible to make the overall system described by model III unstable. This was not possible with models I and II for all cases considered. Second, derivative control

added to the generation controller degrades system performance for the case considered. This may be seen by comparing cases 15, 16, and 17, all with derivative control, with case 4 which lacks derivative control but is otherwise identical. Cases 15, 16, and 17 have equal or slower response and greater undershoot than case 4. Third, using derivative control with the firing rate controller improves system performance in cases 18, 19, 20, and 21, compared with case 4. Cases 18 through 21 all have the same or faster response time and less undershoot than case 4. However, if differentiator constant $K_{23}$ becomes too large, undershoot increases and system instability results as in cases 22, 23, and 24. Fourth, feedforward control is beneficial in several cases. For example, cases 27 and 28, with two feedforward controllers operating, have less undershoot than case 21 with no loss in response time. Case 21 is identical to cases 27 and 28 except that it has no feedforward control. Cases 29 and 30 are the same as case 4 except that fuel feedforward control is added in 29 and 30. Both cases have faster response and somewhat less undershoot than case 4.

Plots of several system variables are given as functions of time for cases 4, 9, 14, 21, 26, and 28 as defined in Table 5.5. Also shown are cases 4 and 14 with $E_1(t)$, $T_1(t)$, and Z all functioning. These plots are shown in Figures 5.16 through 5.44. The cases are chosen to illustrate the effect of various PI controller parameter

values, derivative control, feedforward control, and the effect of air preheater cycling. The magnitude jump in net plant output power noted in Figure 5.20 due to air preheater cycling is 5.6 MW. This corresponds to a 0.36% increase in plant output power and to a 0.18% increase in line voltage.

## 6.5 Comparison Between Model Simulations

A comparison between the results of the computer simulations for each of the three models developed is appropriate.

First, the primary difference between model I and model II is the air preheater detail. In particular, the effect of preheater cycling is accounted for in model II by the presence of time functions $E_1(t)$ and $T_1(t)$. $E_1(t)$ represents the variation of power available to the steam plant, and $T_1(t)$ describes the fluctuation in air preheat temperature due to air preheater cycling. Both models are stable for all cases considered. The overall system response of models I and II are very similar except for the effect of $E_1(t)$ and $T_1(t)$.

Second, the computer simulation of model III, which represents a substantial advance in modeling complexity, have one major characteristic which is notably different from the simulations of models I and II. That is, model III is unstable for several controller design parameter cases as may be seen in Table 5.5. Another property is that, for all cases considered using the boiler-following control, the plant

output power always exhibits undershoot ranging from 3.5 MW to 43.5 MW.

As a supplement to the boiler-following simulations of Chapter V, six simulation cases were run for turbine-following control as shown in Figure 5.3. The model III system equations were changed so that the firing system was operated by a signal related to generation error $X_3$ and the turbine governor was operated by a signal related to throttle pressure error $X_{48}$. The only changes required in the system equations are:

$$X_7 = X_{49} + X_{50} \tag{6.1}$$

$$X_{51} = X_5 + X_6 \tag{6.2}$$

Two PI controllers were used with no derivative or feedforward control considered. The cases are defined in Table 6.1

Table 6.1. Simulation cases for turbine-following control

| Case | $K_2$ | $K_3$ | $K_{21}$ | $K_{22}$ |
|---|---|---|---|---|
| 1 | $10^{-3}$ | $10^{-3}$ | $10^{-3}$ | $10^{-4}$ |
| 2 | $10^{-3}$ | $10^{-3}$ | $10^{-4}$ | $10^{-5}$ |
| 3 | $10^{-3}$ | $10^{-4}$ | $10^{-3}$ | $10^{-4}$ |
| 4 | $10^{-3}$ | $10^{-4}$ | $10^{-4}$ | $10^{-5}$ |
| 5 | $10^{-3}$ | $10^{-5}$ | $10^{-3}$ | $10^{-4}$ |
| 6 | $10^{-3}$ | $10^{-5}$ | $10^{-4}$ | $10^{-5}$ |

In all cases $MW_{REF}$ $X_1$ changes from 1610.44 MW to 1560.44 MW at t = 0+. $E_1(t) = T_1(t) = Z = 0$. Cases 5 and 6 exhibit overdamped characteristics. $X_2$ has oscillations with a 16 second period in cases 1 and 2. The oscillations disappear in 200 seconds for case 1 and 356 seconds for case 2. In both cases the new steady-state value of 1560.44 MW is reached at the end of the oscillation period. Cases 3 and 4 are both underdamped. In case 3, $X_2$ takes 20 seconds to drop 50 MW and reaches a maximum undershoot of 4.14 MW at t = 41 seconds. In case 4, $X_2$ requires 23 seconds to drop 50 MW and reaches a maximum undershoot of 2.55 MW at t = 57 seconds. In case 5, net plant output power, $X_2$, equals 1610.44 MW at t = 0 seconds, 1569.63 MW at t = 50 seconds, and 1566.8 MW at t = 100 seconds. In case 6, $X_2$ equals 1610.44 MW at t = 0 seconds, 1572.19 MW at t = 50 seconds, and 1565.35 MW at t = 100 seconds.

A comparison between the results of turbine-following and boiler-following control modes is in order. Considering the cases investigated, both types of control can give stable system response to a disturbance. Boiler-following control is somewhat faster than turbine-following control in terms of overall plant response, but this could be altered if MHD channel and inverter controls were applied. Turbine-following control makes overdamped system response possible, although for the cases considered, response was very slow. Based on available results, either type of control mode could be used, but

neither type would respond sufficiently rapidly to eliminate transients caused by air preheater cycling. It is likely that only fast-acting channel or inverter controls could reduce or eliminate the effect of these transients.

A -50 MW step input disturbance of $MW_{REF}$, $X_1$, was chosen as a standard perturbation of all three system models. This was done to allow comparison of step responses of the models. A step change in $MW_{REF}$ is not a realistic variation from a normal operational point of view. Standard practice is to vary desired generation by introducing a ramp change in $MW_{REF}$. A step function perturbation of the system might, however, be appropriate in determining system response to a network fault.

## 6.6 Conclusions

Several important conclusions may be drawn from the results derived in this paper.

The fast response of system models I and II for cases typified by Figure 3.11, page 66, is unrealistic. If the controller proportional multiplier $K_1$ = 0.1, 1.0, or 10.0, and integrator multiplier $K_2$ = 10.0, nonlinear system behavior results, due to the magnitude limiter in the fuel valve. The valve passes through its dynamic range, from fully off to fully on, in approximately 0.03 seconds. This is clearly not feasible in practice. System model III

incorporates rate limits, as well as magnitude limits, in the governor and firing system. It therefore gives more realistic behavior in regions of fast system response. The rate limiter values are important in such regions.

System model III exhibits unstable behavior for certain values of controller constants. This represents a significant departure from results obtained with models I and II. As model III is a more realistic description of the MHD/steam combined-cycle system, it is probable that regions of instability may be found in actual plant operation. These unstable regions must, of course, be carefully avoided.

Several significant characteristics of the control configurations studied were identified. First, both boiler-following (Figure 5.2, page 136) and turbine-following (Figure 5.3, page 137) control modes were simulated. Both types of control allowed stable system response with boiler-following control being somewhat faster. The only simulation cases exhibiting overdamped response were for turbine-following control. Very interesting simulation results appear in Figures 5.16, 5.22, and 5.28 on pages 193, 199, and 205, respectively. Net plant output power, $X_2$, is plotted in Figure 5.16 for three different cases defined in Table 5.5. Case 14 appears to give a significantly better plant response than either cases 4 or 9. It exhibits the least undershoot and the fastest settling time. From the steam plant or MHD channel point of view, however, case 14 does not look as

good as case 4. The steam turbine and MHD channel outputs, which add together to form plant output power, both display lightly damped response characteristics 180° out of phase from each other. Therefore, it is not sufficient to evaluate controller performance only on the basis of plant ouput. Derivative control used with the firing rate controller improves system performance in cases 18, 19, 20, and 21, compared with case 4. Derivative control may, however, cause system instability as seen in cases 22, 23, and 24. Feedforward control may be definitely beneficial as shown in Figure 5.19, page 196. Feedforward control reduces system undershoot while maintaining rate of response.

The input-output model of the Combustor/Nozzle/Channel/Diffuser (CNCD), described in Section 5.3.7, provides a more accurate description of MHD system steady-state effects than was possible in models I and II where only enthalpy extraction was considered. This more detailed model of the CNCD did not, however, substantially change the overall MHD/steam system dynamic response. Although quadratic polynomial approximations of steady-state data were used to formulate the CNCD model, linear curve-fits were very good, thereby adding confidence to the validity of models I and II.

As a final conclusion, air preheater cycling does affect several important system variables as may be seen in Figures 5.20, 5.21, 5.26, 5.27, 5.32, 5.33, 5.38, and 5.44, for example. If these

fluctuations prove to be a problem in system operation, the most appropriate means of reducing or eliminating the effect of these transients is via fast-acting channel or inverter controls.

## 6.7 Recommendations for Future Research

There are many areas which are suitable for future work. A number of these are enumerated in [113] and are included in the following comments.

First, consider the steam plant. It is characterized in system model III by a linear, time-invariant, black-box model. This model is very adequate for investigating system dynamic response about some quiescent operating point, but it will prove useful in future work to increase the range of applicability. One means of achieving this is by deductive modeling [92]. Deductive modeling involves developing a system model from basic physical laws such as the conservation of energy, mass, and momentum. The state properties of materials such as water and steam are defined by empirical relationships such as given by steam tables [94]. Deductive modeling is considered to have the following advantages:

1) Values of equation coefficients may be determined by plant design and steady-state data
2) Minimum-order models may be logically determined
3) The model is independent of transient response data

4) Nonlinear models should be used, if applicable, because they are valid over a wider operating range than linearized models and may be validated using steady-state data

It will also be useful to have models available to describe the steam plant during start-up.

Much additional work can be done with the Combustor/Nozzle/Channel/Diffuser (CNCD) model. It currently has two independent, time variable inputs; fuel thermal input power and preheated air temperature. Additional inputs are necessary in order that advanced control of the CNCD may be modeled. Possible inputs include loading parameter, seed density, oxygen enrichment, and the distribution of inverter voltage characteristics. The transient characteristics of the CNCD must also be known to determine its effect on system behavior. A more accurate combustor model is currently being developed.

The control system should be expanded and refined to include:

1) Control of additional time-variable CNCD inputs
2) Separate firing of the steam plant
3) Inverter control of electrical output and other channel characteristics
4) Throttle-pressure setpoint control
5) Rate limits on MW reference variations
6) Pressure limits
7) Feedwater and airflow controls

Continued work in the cycle analysis and control area will make evident appropriate research activities which will undoubtedly go beyond those outlined above.

# APPENDICES

# APPENDIX A

## DIGITAL COMPUTER SIMULATION PROGRAM FOR SYSTEM MODEL I

The digital computer program used to simulate model I is given in this Appendix. The program was adapted from Franks [51] by William Crane.

Algebraic and differential equations for model I are listed in the program under headings "calculate algebraic quantities" and "calculate the derivatives of the state variables."

Subroutines required for the program are included. The same set of subroutines is used for the programs listed in Appendix B and Appendix C.

```
C-----------------------------------------------------------------------
C
C        PROGRAM TO SIMULATE MHD/STEAM COMBINED CYCLE
C     OPERATION USING MODEL I.  REFER TO MODEL I BLOCK DIAGRAM.
C
C-------------------------
C
C     VARIABLES USED:
C
C        DT  : TIME INCREMENT, IN SECONDS.
C        DTA : ARRAY TO HOLD TIME INCREMENT INTERVALS.
C        DXI : TIME DERIVATIVE OF VARIABLE X(I)
C        HDR : 132 CHARACTERS READ FROM CARD READER CONTAINING ANY
C              DESIRED INFORMATION.  THIS IS PRINTED OUT ON THE OUTPUT.
C        K   : ALL CONSTANTS AS NUMBERED ON MODEL DIAGRAM.
C        NF  : VARIABLE SET BY SUBROUTINE PRTFIN.  EQUALS 1 IF
C              CALCULATION DONE ; EQUALS 0 OTHERWISE.
C        NPR : SET BY SUBROUTINE PRTFIN. EQUALS 1 WHEN TIME TO PRINT
C              RESULTS.  EQUAL 0 OTHERWISE.
C        T   : TIME VARIABLE, IN SECONDS.
C        TAU : TIME CONSTANTS AS NUMBERED ON MODEL DIAGRAM.
C        X   : VARIABLES AS NUMBERED ON MODEL DIAGRAM.
C
C-------------------------
C
C        VALUES FOR K(I) AND TAU(I) ARE INPUT VIA THE CARD READER.
C        THE INITIAL VALUES OF X(I) ARE ENTERED DIRECTLY INTO THE
C     PROGRAM.  ANY STABLE OR UNSTABLE INITIAL CONDITIONS MAY BE
C     ENTERED.
C
C-------------------------
C
C     SUBROUTINES NEEDED:
C        PRTFIN ( MODSIM ROUTINE )
C        INTI   ( MODSIM ROUTINE )
C        INT    ( MODSIM ROUTINE )
C        TIMDAT ( TO OBTAIN TIME AND DATE )
C
C-------------------------
C
C       MODEL DEVELOPED BY JOHN ASPNES.
C       PROGRAM WRITTEN BY WILLIAM CRANE.
C       BOTH OF MONTANA STATE UNIVERSITY
C       BOZEMAN, MONTANA.
C       JULY 1975
C
C-----------------------------------------------------------------------
C
      IMPLICIT DOUBLE PRECISION (A-H,O-Z)
      REAL K
      DIMENSION X(20), DTA(3), TAU(5), K(12), TDATE(4), HDR(33)
      DATA DTA / 0.5, 0.2, 0.1 /
C-----------------------------------------------------------------------
C        READ VALUES OF MULTIPLIERS (K), TIME CONSTANTS (TAU), THE
C     HEADER LINE, AND CALL TIMDAT TO GET THE TIME AND DATE.
C-----------------------------------------------------------------------
 50   READ ( 105,10,END=51 ) K, TAU
```

```
 10   FORMAT ( 8F10.5,/,4F10.5,/,5F10.5 )
      READ ( 105,11 ) HDR
 11   FORMAT ( 20A4 )
      CALL TIMDAT ( TDATE)
C-----------------------------------------------------------------------
C         DO LOOP TO TRY SEVERAL STEP SIZES.  MAY BE OMITTED IF
C      ONLY ONE STEP SIZE IS DESIRED BY SETTING THE STEP IN STATEMENT 1.
C-----------------------------------------------------------------------
      DO 8 J = 1, 3
C-----------------------------------------------------------------------
C         INITIAL VALUES OF STATE VARIABLES
C-----------------------------------------------------------------------
      X(6) = 3495.93506
      X(9) = 1224.97607
      X(14) = 968.83984
      X(15) = 968.83984
      X(20) = 0.86534
C-----------------------------------------------------------------------
C         MISC.  VALUES
C-----------------------------------------------------------------------
      X(1) = 1570.0
      T = 0.0
 1    DT = DTA(J)
C-----------------------------------------------------------------------
C         HEADERS FOR PRINTED OUTPUT
C-----------------------------------------------------------------------
      WRITE(108,30)TDATE,K,TAU,X(6),X(9),X(14),X(15),X(20),DT,HDR
 30   FORMAT ( '1',90X,4A4,///,' ','COMBINED MHD - STEAM BOTTOMING ',
     1        'PLANT SIMULATION,  MODEL I',///,' ','MULTIPLIER VALUES',
     2        //,' ',10X,'K  - K',  6F12.5,/,' ',11X,'1     6',//,
     3        ' ',10X,'K  - K',6F12.5,/,' ',11X,'7     12',///,' ',
     4        'TIME CONSTANTS',//,  ' ',  10X,  'TAU  - TAU',  5F12.5,
     5        /,  ' ',  13X,  '1       5',  ///,  ' ',  'INITIAL VALUES OF'
     6        ' STATE VARIABLES',  //,  ' ',  10X,  'X',  15X,  5F12.5,
     7        /,  ' ',  11X,  '6,9,14,15,20',  ///,  ' ',  'TIME STEP = ',
     8        F12.4,  ' SEC.',  ///,  ' ',  'SPECIAL CONDITIONS FOR THIS ',
     9        'ARE:',  //,  ' ',  33A4 )
      WRITE ( 108,31 )
 31   FORMAT ( '1',  '  TIME,  SEC',  8X,  'X(2)',  9X,  'X(4)',
     1        9X,  'X(6)',  9X,  'X(9)',  9X,  'X(10)',  8X,  'X(12)',
     2        8X,  'X(15)',  8X,  'X(17)',  8X,  'X(19)',  // )
C-----------------------------------------------------------------------
C         CALCULATE ALGEBRAIC QUANTITIES
C-----------------------------------------------------------------------
 7    X(7) = K(5) * X(6)
      X(10) = X(6) + X(9)
      X(12) = ( 1.0 - K(7) ) * X(10)
      X(13) = K(10) * ( 1.0 - K(9) ) * X(12)
      X(16) = K(11) * X(12)
      X(17) = K(7) * K(8) *X(10)
      X(18) = X(15) + X(17)
      X(19) = K(12) * X(18)
      X(2) = X(1) - X(19)
      X(3) = K(1) * X(2)
      X(4) = X(3) + X(20)
      X(5) = X(4)
      X(8) = X(7) + K(9) * X(12)
```

```
C-----------------------------------------------------------------------
C         LIMITER FOR X(5)
C-----------------------------------------------------------------------
      IF ( X(5) - K(3) ) 20, 20, 21
 21   X(5) = K(3)
      GO TO 23
 20   IF ( X(5) ) 22, 23, 23
 22   X(5) = 0.0
C-----------------------------------------------------------------------
C         CALCULATE THE DERIVATIVES OF THE STATE VARIABLES
C-----------------------------------------------------------------------
 23   DX6 = ( K(4) * X(5) - X(6) ) / TAU(1)
      DX9 = ( K(6) * X(8) - X(9) ) / TAU(2)
      DX14 = ( X(13) - X(14) ) / TAU(4)
      DX15 = ( X(14) - X(15) ) / TAU(5)
      DX20 = X(3) * K(2)
C-----------------------------------------------------------------------
C         CHECK TO SEE IF READY TO PRINT VALUES AND/OR IF
C     CALCULATIONS ARE DONE
C-----------------------------------------------------------------------
      CALL PRTFIN ( 2.0, 500.0,  NF, NPR )
      IF ( NPR ) 25, 24, 25
C-----------------------------------------------------------------------
C         PRINT RESULTS : UNIT 108 = LP, UNIT 109 = DISK OR OTHER DEVICE.
C     UNIT 109 IS FOR TEMPORARY STORAGE OF VALUES FOR POSSIBLE
C     LATER USE.
C-----------------------------------------------------------------------
 25   WRITE ( 108,32 ) T, X(2),X(4),X(6),X(9),X(10),X(12),
     1                  X(15),X(17),X(19)
      WRITE ( 109,32 ) T,X(4),X(6),X(10),X(15),X(17),X(19)
 32   FORMAT ( ' ', 10(1PE13.5) )
      IF ( NF ) 8,  24, 8
C-----------------------------------------------------------------------
C         INTEGRATE THE STATE VARIABLES
C-----------------------------------------------------------------------
 24   CALL INTI ( T, DT, 4 )
      CALL INT ( X(6), DX6 )
      CALL INT ( X(9), DX9 )
      CALL INT ( X(14), DX14 )
      CALL INT ( X(15), DX15 )
      CALL INT ( X(20), DX20 )
      GO TO 7
 8    CONTINUE
      GO TO 50
 51   END FILE 109
      REWIND 109
      STOP
      END
```

```
      SUBROUTINE PRTFIN ( PRTINT, FINISH, NOTFIN, NOPRT )
C
C-----------------------------------------------------------------------
C
C        SUBROUTINE TO CONTROL THE FREQUENCY OF PRINTING THE SOLUTION
C     VALUES AND TO INDICATE WHEN COMPUTATION IS COMPLETE.
C        THIS SUBROUTINE IS PART OF THE MODSIM SYSTEM.
C
C-------------------------
C
C     USAGE  : CALL PRTFIN ( PRTINT, FINISH, NOTFIN, NOPRT )
C
C      WHERE
C
C        PRTINT : PRINT INTERVAL.  THIS GIVES THE INTERVAL DESIRED
C                 BETWEEN PRINTING OF SOLUTION VALUES.  THIS VALUE
C                 IS SUPPLIED BY THE CALLING ROUTINE, AND IS IN THE
C                 SAME UNITS AS THE INDEPENDENT VARIABLE USED IN THIS
C                 SIMULATION.  IT IS NOT MODIFIED BY THIS ROUTINE.
C
C        FINISH : THE UPPER VALUE DESIRED OF THE INDEPENDENT VARIABLE.
C                 WHEN THE INDEPENDENT VARIABLE REACHES OR EXCEEDS
C                 FINISH, NOTFIN IS SET TO THE VALUE 1.  THE VALUE OF
C                 FINISH IS SUPPLIED BY THE CALLING ROUTINE IN THE
C                 SAME UNITS AS THE INDEPENDENT VARIABLE, AND IS
C                 NOT MODIFIED BY THIS ROUTINE.
C
C        NOTFIN : FLAG TO INDICATE IF COMPUTATION HAS BEEN COMPLETED.
C                 IF THE INDEPENDENT VARIABLE EQUALS OR EXCEEDS FINISH
C                 NOTFIN IS SET TO THE VALUE 1.  IT IS SET TO 0 OTHER-
C                 WISE.
C
C        PRINT  : FLAG TO INDICATE WHEN TO PRINT SOLUTION VALUES.
C                 IT IS SET TO THE VALUE 1 AT THE END OF EVERY PRINT
C                 INTERVAL, WHEN THE INDEPENDENT VARIABLE IS ZERO,
C                 AND WHEN COMPUTATION IS COMPLETE.  IT HAS THE VALUE
C                 0 OTHERWISE.  THIS ALLOWS EVERY N'TH SOLUTION
C                 VALUE TO BE PRINTED, RATHER THAN EVERY VALUE.
C
C-------------------------
C
C     SUBROUTINES REQUIRED:
C
C        NONE.
C
C-------------------------
C
C     WRITTEN BY WILLIAM CRANE
C     MONTANA STATE UNIVERSITY, BOZEMAN, MONTANA
C     JULY 1975
C
```

```
C-----------------------------------------------------------------------
C
      COMMON /MODSIM/ T, DT, JS, JN, DXA(50), XA(50), IO, JS4, MAXJN,
     1                NTD, MAXNTD
      IMPLICIT DOUBLE PRECISION (A-H,O-Z)
      DATA TPRNT / 0.0 /
      NOPRT = 0
C-----------------------------------------------------------------------
C         CHECK TO SEE IF IT IS TIME TO PRINT SOLUTION VALUES.
C      VALUES WILL BE PRINTED ONLY AT THE END OF AN
C      INTEGRATION STEP ( WHEN JS = 2 OR JS4 = 4 )
C-----------------------------------------------------------------------
      IF ( TPRNT - PRTINT ) 20, 21, 21
 21   IF ( T - ( FINISH - DT / 2.0 ) ) 26, 27, 27
 27   IF ( JS - 2 ) 28, 29, 28
 28   IF ( JS4 - 4 ) 26, 29, 26
 26   IF ( T - ( TPRNT - DT / 2.0 ) ) 22, 23, 23
 23   IF ( JS - 2 ) 24, 25, 24
 24   IF ( JS4 - 4 ) 22, 25, 22
 22   RETURN
C-----------------------------------------------------------------------
C         SET COMPUTATION FINISHED FLAG OFF
C-----------------------------------------------------------------------
 20   NOTFIN = 0
C-----------------------------------------------------------------------
C         SET PRINT FLAG ON AND INCREMENT TPRNT
C-----------------------------------------------------------------------
 25   NOPRT = 1
      TPRNT = TPRNT + PRTINT
      RETURN
C-----------------------------------------------------------------------
C         FOR T >= FINISH
 RESET PARAMETERS AND INDICATE RUN IS DONE
C-----------------------------------------------------------------------
 29   TPRNT = 0.0
      NOTFIN = 1
      NOPRT = 1
      T = 0.0
      JS = 0
      JN = 0
      JS4 = 0
      NTD = 0
      RETURN
      END
```

```
      SUBROUTINE INTI ( TX, DTX, IOX )
C
C-------------------------------------------------------------------------
C
C        BASIC CONTROL SUBROUTINE FOR THE MODSIM SYSTEM OF SUBROUTINES.
C     THIS SUBROUTINE CONTROLS CERTAIN PARAMETER VALUES, INCREMENTS
C     THE DEPENDENT VARIABLE, AND INFORMS THE OTHER SUBROUTINES OF THE
C     METHOD CHOSEN FOR SOLUTION OF THE DIFFERENTIAL EQUATIONS.
C     A FIRST ORDER EULER METHOD, A SECOND ORDER MODIFIED EULER
C     METHOD, AND A 4TH ORDER RUNGE - KUTTA METHOD ARE AVAILABLE.
C        THIS SUBROUTINE MUST BE CALLED PRIOR TO ALL CALLS TO INT
C     FOR A GIVEN INTEGRATION STEP.
C
C-------------------------
C
C     USAGE : CALL INTI ( TX, DTX, IOX )
C
C      WHERE
C
C        TX   : THE VALUE OF THE INDEPENDENT VARIABLE.  IT SHOULD BE SET
C               TO 0.0 BY THE CALLING ROUTINE BEFORE ANY CALLS TO INTI
C               AND LEFT ALONE AFTER THAT.  IT IS INCREMENTED BY THIS
C               SUBROUTINE.  AT THE COMPLETION OF ANY INTEGRATION STEP
C               TX  WILL HAVE THE PROPER VALUE.
C
C        DTX  : THE INTEGRATION STEP SIZE.  THIS IS GIVEN IN THE
C               SAME  UNITS AS TX.  THIS VALUE CAN BE MODIFIED BY THE
C               CALLING  ROUTINE DURING A PROGRAM RUN.  SEE NOTE BELOW.
C
C        IOX  : THE INTEGRATION ORDER.  THIS SELECTS THE METHOD OF
C               INTEGRATION  WHICH WILL BE USED WITH VALUES OF
C               1,  2, OR 4 TO SPECIFY 1ST, 2ND, OR 4TH ORDER METHOD.
C               THIS  VALUE MAY BE CHANGED DURING A PROGRAM RUN.
C               SEE  NOTE BELOW.
C
C-------------------------
C
C    SUBROUTINES REQUIRED :
C
C         NONE.
C
C-------------------------
C
C         IT IS POSSIBLE TO CHANGE THE VALUES OF DTX AND IOX DURING
C     A PROGRAM RUN.  HOWEVER, ANY CHANGE MUST TAKE PLACE AT THE END
C     OF ALL CALCULATIONS FOR A GIVEN INTEGRATION STEP.  THE EASIEST
C     WAY TO INSURE THIS IS TO CHANGE VALUES WHEN SOLUTION VALUES ARE
C     PRINTED OUT, AS SPECIFIED BY SUBROUTINE PRTFIN.
C
C-------------------------
C
C     WRITTEN BY WILLIAM CRANE
C     MONTANA STATE UNIVERSITY, BOZEMAN, MONTANA
C     JULY 1975
C
```

```
C-----------------------------------------------------------------------
C
      COMMON /MODSIM/ T, DT, JS, JN, DXA(50), XA(50), IO, JS4, MAXJN,
     1                NTD, MAXNTD
      IMPLICIT DOUBLE PRECISION (A-H,O-Z)
      IO = IOX
      JN = 0
      NTD = 0
C-----------------------------------------------------------------------
C          CHECK FOR IO = 1, 2, 3, OR 4.  IO = 3 IS TREATED AS IO = 2.
C-----------------------------------------------------------------------
      IF ( IO ) 20, 20, 21
 21   IF ( IO - 4 ) 22, 22, 20
 22   GO TO ( 23, 24, 24, 25 ), IO
C-----------------------------------------------------------------------
C          1ST ORDER SOLUTION - EULER'S METHOD
C-----------------------------------------------------------------------
 23   JS = 2
      GO TO 26
C-----------------------------------------------------------------------
C          2ND ORDER SOLUTION - MODIFIED EULER METHOD
C-----------------------------------------------------------------------
 24   JS = JS + 1
      IF ( JS - 3 ) 40, 41, 40
 40   IF ( JS - 2 ) 26, 42, 26
 42   RETURN
 41   JS = 1
 26   DT = DTX
      T = T + DT
      TX = T
      RETURN
C-----------------------------------------------------------------------
C          4TH ORDER SOLUTION - RUNGE - KUTTA METHOD
C-----------------------------------------------------------------------
 25   JS4 = JS4 + 1
      IF ( JS4 - 5 ) 44, 43, 44
 44   IF ( JS4 - 3 ) 45, 29, 45
 45   IF ( JS4 - 1 ) 46, 28, 46
 46   RETURN
 43   JS4 = 1
 28   DT = DTX / 2.0
      T = T + DT
      TX = T
      RETURN
 29   T = T + DT
      TX = T
      DT = DT * 2.0
      RETURN
C-----------------------------------------------------------------------
C          ERROR MESSAGE FOR IO NOT IN RANGE OF 1 TO 4
C-----------------------------------------------------------------------
 20   WRITE ( 108,30 )
 30   FORMAT ( '0', '*** INTEGRATION ORDER OUT OF RANGE OF 1 TO 4',
     1        ' IN SUB.  INTI.  PROGRAM TERMINATED. ' )
      STOP
      END
```

```
      SUBROUTINE INT ( X, DX )
C
C-------------------------------------------------------------------------
C
C        SUBROUTINE TO PERFORM THE ACTUAL INTEGRATION OF DIFFERENTIAL
C     EQUATIONS.  THE METHOD USED IS CHOSEN BY THE PREVIOUS CALL TO
C     SUBROUTINE INTI, AND MAY BE THE 1ST ORDER EULER METHOD, THE 2ND
C     ORDER MODIFIED EULER METHOD, OR THE 4TH ORDER RUNGE - KUTTA
C     METHOD.  A SYSTEM OF UP TO 50 FIRST ORDER EQUATIONS MAY
C     BE SOLVED BY THIS SUBROUTINE, ONE EQUATION PER CALL OF THIS
C     SUBROUTINE.
C
C-------------------------
C
C     USAGE : CALL INT ( X, DX )
C
C      WHERE
C
C        X  : THE VALUE OF THE FUNCTION AT SOME VALUE OF THE INDEPENDENT
C             VARIABLE.  THE INITIAL VALUE OF THE SOLUTION MUST BE
C             SUPPLIED AS A BOUNDARY CONDITION BY THE CALLING ROUTINE.
C             AFTER THAT, X IS ALWAYS CALCULATED BY THIS SUBROUTINE
C             AND SHOULD NOT BE MODIFIED BY THE CALLING ROUTINE.
C
C        DX : THE DERIVATIVE OF THE FUNCTION BEING INTEGRATED AT SOME
C             VALUE OF THE INDEPENDENT VARIABLE.  THIS VALUE IS
C             ALWAYS CALCULATED  BY THE CALLING ROUTINE.
C
C-------------------------
C
C     SUBROUTINES REQUIRED :
C        NONE.
C
C-------------------------
C
C     WRITTEN BY WILLIAM CRANE
C     MONTANA STATE UNIVERSITY, BOZEMAN, MONTANA
C     JULY 1975
C
C-------------------------------------------------------------------------
C
      COMMON /MODSIM/ T, DT, JS, JN, DXA(50), XA(50), IO, JS4, MAXJN,
     1                NTD, MAXNTD
      IMPLICIT DOUBLE PRECISION (A-H,O-Z)
C-------------------------------------------------------------------------
C        INCREMENT THE CALL INDEX JN AND SEE IF IT IS LE THE MAXIMUM
C     VALUE ALLOWED ( MAXJN ).  BRANCH TO CHOSEN SOLUTION METHOD.
C-------------------------------------------------------------------------
      JN = JN + 1
      IF ( JN - MAXJN ) 28, 28, 29
 28   GO TO ( 20, 21, 21, 22 ), IO
C-------------------------------------------------------------------------
C        1ST ORDER INTEGRATION METHOD ( EULER METHOD )
C-------------------------------------------------------------------------
 20   X = X + DX * DT
      RETURN
```

```
C-----------------------------------------------------------------------
C         2ND ORDER METHOD ( MODIFIED EULER )
C-----------------------------------------------------------------------
 21   GO TO ( 23, 24 ), JS
 23   DXA(JN) = DX
      X = X + DX * DT
      RETURN
 24   X = X + ( DX - DXA(JN) ) * DT / 2.0
      RETURN
C-----------------------------------------------------------------------
C         4TH ORDER METHOD ( RUNGE - KUTTA )
C-----------------------------------------------------------------------
 22   GO TO ( 25, 26, 26, 27 ), JS4
 25   XA(JN) = X
      DXA(JN) = DX
      X = X + DX * DT
      RETURN
 26   DXA(JN) = DXA(JN) + DX + DX
      X = XA(JN) + DX * DT
      RETURN
 27   X = XA(JN) + ( DXA(JN) + DX ) * DT / 6.0
      RETURN
C-----------------------------------------------------------------------
C      ERROR MESSAGE FOR JN > MAXJN
C-----------------------------------------------------------------------
 29   WRITE ( 108,30 ) MAXJN
 30   FORMAT ( '0', '*** MORE THAN ',I5,' EQUATIONS IN THIS ',
     1          'SYSTEM.  PROGRAM TERMINATED.' )
      STOP
      END
```

```
*************************************************************************
*
*         SUBROUTINE TO OBTAIN THE TIME AND DATE FROM THE MONITOR
*    WRITTEN BY WILLIAM CRANE
*    MONTANA STATE UNIVERSITY, BOZEMAN, MONTANA
*    JULY 1975
*
*    VARIABLES :
*
*         TIMEDATE : ADDRESS OF THE 4 WORD LOCATION INTO WHICH THE
*                    TIME AND DATE WILL BE PLACED.
*
*
*    SUBROUTINE USAGE :
*
*         CALL TIMDAT ( TD )
*
*       WHERE TD IS AN ARRAY CONTAINING 4 WORDS OF STORAGE.
*
*
*         THE TIME AND DATE ARE RETURNED IN THE FORM :
*
*                         HH:MM DD MON 'YY
*
*************************************************************************
*
          SYSTEM    BPM
         SYSTEM    FORTLIB
          SYSTEM    SIG7F
TIMDAT    BAL,6     %SETUP1
          EVRY      TIMEDATE
          M:TIME    *TIMEDATE
          B         *15
TIMEDATE  RES       1
          REF       %SETUP1
          DEF       TIMDAT
          END
```

```
      BLOCK DATA
C
C-----------------------------------------------------------------------
C
C        SUBROUTINE TO INITIALIZE COMMON DATA VALUES.
C
C        ALL COUNTERS ARE SET TO ZERO.  THE INDEPENDENT VARIABLE T IS
C     SET TO 0.0.  MAXJN IS SET TO THE NUMBER OF LOCATIONS IN DXA AND
C     XA.  MAXNTD IS SET TO THE MAXIMUM NUMBER OF TIME DELAYS ALLOWED
C     PER SIMULATION ( SEE SUBROUTINE DELAY ).
C        THIS SUBROUTINE IS PART OF THE MODSIM SYSTEM.
C
C-------------------------
C
C     WRITTEN BY WILLIAM CRANE
C     MONTANA STATE UNIVERSITY, BOZEMAN, MONTANA
C     JULY 1975
C
C-----------------------------------------------------------------------
C
      COMMON /MODSIM/ T, DT, JS, JN, DXA(50), XA(50), IO, JS4, MAXJN,
     1                NTD, MAXNTD
      IMPLICIT DOUBLE PRECISION (A-H,O-Z)
      DATA JS /0/, JN /0/, JS4 /0/, T /0.0/, MAXJN /50/
      DATA NTD /0/, MAXNTD /25/
      END
```

# APPENDIX B

## DIGITAL COMPUTER SIMULATION PROGRAM FOR SYSTEM MODEL II

The digital computer program used to simulate model II is given in this Appendix. The program was adapted from Franks [51] by William Crane. Subroutines required for this program are given in Appendix A. An additional subroutine DELAY is required and follows the model II program. This subroutine was written by William Crane and modified by Robert Uhlrich.

Algebraic and differential equations for model II are listed in the program under the heading "calculate algebraic quantities."

```
C-----------------------------------------------------------------------
C
C       PROGRAM TO SIMULATE MHD/STEAM COMBINED CYCLE OPERATION
C     USING MODEL II.   REFER TO MODEL II BLOCK DIAGRAM.
C
C-------------------------
C
C         VARIABLES USED :
C
C           DLINEI :  DELAY LINE ARRAYS FOR DELAY UNIT I.
C           DT     :  TIME INCREMENT, IN SECONDS.
C           DXI    :  TIME DERIVATIVE OF VARIABLE X(I).
C           HDR    :  ONE PRINTER LINE ( 132 CHARACTERS ) OF INFORMATION
C                     READ FROM THE CARD READER.   THIS IS PRINTED ON THE
C                     OUTPUT.
C           K      :  MULTIPLICATIVE CONSTANTS, AS NUMBERED ON THE MODEL
C                     DIAGRAM.
C           NF     :  SET BY SUBROUTINE PRTFIN.  EQUALS 1 IF CALCULATIONS
C                     ARE DONE.  OTHERWISE EQUALS 0.
C           NPR    :  SET BY PRTFIN.  EQUALS 1 WHEN IT IS TIME TO PRINT
C                     RESULTS, AND IS 0 OTHERWISE.
C           T      :  TIME, IN SECONDS.
C           TAU    :  TIME CONSTANTS AND DELAY TIMES, AS NUMBERED ON THE
C                     MODEL DIAGRAM.
C           X      :  VARIABLES AS NUMBERED ON MODEL DIAGRAM.
C
C-------------------------
C
C         VALUES FOR K(I) AND TAU(I) ARE ENTERED VIA THE CARD READER.
C       THE INITIAL VALUES OF X(I) ARE ENTERED DIRECTLY INTO THE
C     PROGRAM.   ANY STABLE OR UNSTABLE INITIAL CONDITIONS MAY BE
C     ENTERED.
C
C-------------------------
C
C
C     SUBROUTINES REQUIRED :
C
C          PRTFIN ( MODSIM ROUTINE )
C          INTI   ( MODSIM ROUTINE )
C          INT    ( MODSIM ROUTINE )
C          DELAY  ( MODSIM ROUTINE )
C          TIMDAT ( TO OBTAIN THE TIME AND DATE )
C
C-------------------------
C
C     MODEL DEVELOPED BY JOHN ASPNES.
C     PROGRAM WRITTEN BY WILLIAM CRANE.
C     BOTH OF MONTANA STATE UNIVERSITY, BOZEMAN, MONTANA.
C     AUGUST 1975
C
C-------------------------
      IMPLICIT DOUBLE PRECISION (A-H,O-Z)
      REAL K
      INTEGER TDATE
      DIMENSION X(36), K(19), TAU(8), DLINE1(50), DLINE4(50), DLINE5(50)
      DIMENSION HDR(33), TDATE(4)
```

```
C-----------------------------------------------------------------------
C         GET TIME AND DATE.   READ K, TAU, AND HDR FROM CARD READER.
C-----------------------------------------------------------------------
      CALL TIMDAT ( TDATE )
 50   READ ( 105,10,END=51 ) K, TAU, DT, HDR
 10   FORMAT ( 2( 8F10.5, / ), 3F10.5, /, 8F10.5, /, 1F10.5,
     & /, ( 20A4 ))
C-----------------------------------------------------------------------
C         INITIAL VALUES OF STATE VARIABLES.
C-----------------------------------------------------------------------
      X(6) = 3500.002
      X(11) = 1173.15
      X(26) = X(27) = 2744.3774
      X(36) = .795455
C-----------------------------------------------------------------------
C         MISC. INITIAL VALUES.
C-----------------------------------------------------------------------
      X(1) = 1577.5
      KNT = 9
      T = 0.0
      X(7) = X(6)
      X(18) = X(19) = 595.0
      X(20) = X(21) = 3311.4
      TREF = 1473.15
C-----------------------------------------------------------------------
C         CALCULATE THE NUMBER OF LOCATIONS NEEDED FOR THE DESIRED
C      TIME DELAYS.   THIS NUMBER MUST BE NO GREATER THAN THE MAXIMUM
C      NUMBER OF LOCATIONS AVAILABLE ( MAXLOC ).
C-----------------------------------------------------------------------
      NTD1 = IFIX( TAU(1) / DT )
      NTD4 = IFIX( TAU(4) / DT )
      NTD5 = IFIX( TAU(5) / DT )
      MAXLOC = 50
      IF ( NTD1 - MAXLOC ) 28, 28, 29
 28   IF ( NTD4 - MAXLOC ) 40, 40, 29
 40   IF ( NTD5 - MAXLOC ) 41, 41, 29
C-----------------------------------------------------------------------
C         WRITE OUTPUT HEADINGS
C-----------------------------------------------------------------------
 41   WRITE ( 108,30 ) TDATE, K, TAU, X(6), X(11), X(26), X(27), X(36),
     1                 X(1), DT, HDR
 30   FORMAT ( '1', 'COMBINED MHD - STEAM PLANT CONTROL SIMULATION,',
     1          ' MODEL II', T90, 4A4, ///, ' ', 'MULTIPLIER VALUES',
     2          //, ' ', 10X, 'K   - K', 7X, 6E12.5, /, ' ', 11X,
     3          '1    6', //, ' ', 10X, 'K   - K', 7X, 6E12.5, /, ' ',11X,
     4          '7    12', //, ' ', 10X, 'K   - K', 7X, 6E12.5, /, ' ',
     5          11X, '13    18', //, ' ', 10X, 'K', 12X, E12.5, /, ' ',
     6          11X, '19', ///, ' ', 'TIME CONSTANTS AND DELAY TIMES',
     7          //, ' ', 10X, 'TAU  - TAU', 3X, 6E12.5, /, ' ',
     8          13X, '1     6', //, ' ', 10X, 'TAU  - TAU', 3X,
     9          2E12.5, /, ' ', 13X, '7     8', ///, ' ',
     A          'INITIAL VALUES OF STATE VARIABLES', //, ' ',
     B          10X, 'X', 15X, 5F12.5, /, ' ', 11X, '6,11,26,27,36',
     C          ///, ' ', 'DEMAND REFERENCE IS X(1) = ', F12.5,
     D          ' MEGAWATTS', ///, ' ', 'TIME STEP = ', F7.5,
     E          ' SECONDS', ///, ' ', 'REMARKS:',/, ' ', 33A4 )
```

```
      WRITE ( 108,31 )
 31   FORMAT ( '1', '  TIME, SEC', 8X, 'X(2)', 9X, 'X(4)', 9X,
     1          'X(7)', 9X, 'X(12)', 8X, 'X(14)', 8X, 'X(16)', 8X,
     2          'X(28)', 8X, 'X(30)', 10X, 'Z', // )
C-------------------------------------------------------------------
C         CALCULATE ALGEBRAIC QUANTITIES
C-------------------------
 20   CALL DELAY (DLINE1, NTD1, X(6), X(7), 1)
      X(12) = X(11) + T1(T)
      X(8)  = K(5) * X(7)
      X(31) = X(8) * X(12)
      X(14) = X(7) + X(31)
      X(34) = (1.0 - K(9)) * X(14)
      X(15) = X(34)
      X(16) = K(11) * K(12) * X(15)
      X(28) = (1.0 - K(16) - K(17)) *X(27)
      X(29) = X(16) + X(28)
      X(30) = K(18) * X(29)
      X(32) = K(19) * X(30)
      X(2)  = X(1) - X(32)
      X(3)  = K(1) * X(2)
      X(4)  = X(3) + X(36)
      X(5)  = X(4)
      Z = (X(12) - (TREF -300)) * K(7)
      X(33) = (1.0 - K(11)) * X(15)
      X(20) = X(33) * (1.0 - K(10))
      CALL DELAY (DLINE4, NTD4, X(20), X(21), 2)
      X(22) = (1 - K(13)) * X(21) - Z * X(8)
      X(9) = (239+.029*(X(7)-3500)) * (.0003555*X(7)) + X(22)
      X(10) = X(9) / X(8)
      X(18) = K(10) * X(33)
      CALL DELAY (DLINE5, NTD5, X(18), X(19), 3 )
      X(35) = K(13) * X(21)
      X(23) = X(35) + E1(T)
      X(24) = Z * X(8)
      X(25) = X(19) + X(23) + X(24)
      X(17) = K(9) * X(14)
C-------------------------------------------------------------------
C         LIMITER FOR X(5),   0 <= X(5) <= 1.0
C-------------------------------------------------------------------
      IF (X(5)) 24, 24, 25
 24   X(5)  = 0.0
      GO TO 26
 25   IF (X(5) - 1.0) 26, 26, 27
 27   X(5)  = 1.0
 26   DX6 = (X(5) * K(3) - X(6)) / TAU(8)
      DX11 = (X(10) - X(11)) / TAU(2)
      DX26 = (X(25) * K(15) - X(26)) / TAU(7)
      DX27 = (X(26) - X(27)) / TAU(6)
      DX36 = K(2) * X(3)
```

```
C-----------------------------------------------------------------------
C        CHECK TO SEE IF READY TO PRINT VALUES ( NPR = 1 ) AND IF
C     CALCULATIONS ARE DONE ( NF = 1 ).  UNIT 108 = LINE PRINTER.
C     UNIT 109 = DISK OR OTHER SECONDARY STORAGE TO HOLD DATA FOR
C     POSSIBLE LATER USE.
C-----------------------------------------------------------------------
      CALL PRTFIN ( 0.1, 400.0,   NF, NPR )
      IF ( NPR ) 21, 22, 21
 21   WRITE ( 109,32 ) T, X(2), X(4), X(7), X(12), X(14), X(16),
     1                 X(28), X(30), Z
      KNT = KNT + 1
 32   FORMAT ('   ',1PE11.3, 9 (1PE13.5) )
      IF (KNT.NE.10) GO TO 35
      WRITE ( 108,32 ) T, X(2), X(4), X(7), X(12), X(14), X(16),
     1                 X(28), X(30), Z
      KNT = 0
 35   IF ( NF ) 23, 22, 23
C-----------------------------------------------------------------------
C        INTEGRATE THE STATE VARIABLES
C-----------------------------------------------------------------------
 22   CALL INTI ( T, DT, 4 )
      CALL INT ( X(6), DX6 )
      CALL INT ( X(11), DX11 )
      CALL INT ( X(26), DX26 )
      CALL INT ( X(27), DX27 )
      CALL INT ( X(36), DX36 )
      GO TO 20
 23   CONTINUE
      GO TO 50
 51   STOP
C-----------------------------------------------------------------------
C        ERROR MESSAGE FOR TOO LONG A DELAY.
C-----------------------------------------------------------------------
 29   WRITE ( 108,33 )
 33   FORMAT ( ' ', '*** TOO LONG A TIME DELAY DESIRED FOR GIVEN ARRAY '
     1         'SIZE.  PROGRAM TERMINATED. ' )
      STOP
      END
      FUNCTION T1(T)
C-----------------------------------------------------------------------
C
C        FUNCTION SUBROUTINE TO GENERATE THE TEMPERATURE RIPPLE
C     FUNCTION FOR THE MHD/STEAM CYCLE, MODEL II.
C
C-----------------------------------------------------------------------
      PERD = 50.0
      TIME = T + 25
      T1 = 10 - (TIME/PERD  - INT(TIME/PERD))  * 20
      RETURN
      END
      FUNCTION E1(T)
C-----------------------------------------------------------------------
C
C        FUNCTION SUBROUTINE TO GENERATE THE POWER RIPPLE FUNCTION
C     FOR THE MHD/STEAM CYCLE, MODEL II.
C
C-----------------------------------------------------------------------
      PERD = 50.0
      TIME = T + 25
      E1 = -12.44 + (TIME/PERD - INT(TIME/PERD)) * 24.88
      RETURN
      END
```

```
      SUBROUTINE DELAY      (DLINE,NUNITS,VALIN,VALOUT,KNT)
C-------------------------------------------------------------------------
C
C          SUBROUTINE TO SIMULATE A PURE TIME DELAY.   THIS SUBROUTINE
C     WILL WORK ONLY FOR THE FIRST ORDER EULER METHOD OR THE FOURTH
C     ORDER RUNGE-KUTTA METHOD.  IT IS PART OF THE MODSIM SYSTEM.
C
C-------------------------
C
C     USAGE :   CALL DELAY (DLINE, NUNITS, VALIN, VALOUT, KNT)
C
C      WHERE:
C
C        DLINE   : AN ARRAY TO HOLD DELAYED VALUES.   ON THE FIRST CALL
C                  TO DELAY (T = 0.0) THE ARRAY IS INITIALIZED TO THE
C                  VALUE OF VALOUT.
C
C        KNT     : AN INDEX TO INDICATE A PARTICULAR DELAY IN THE SYSTEM.
C                  THERE ARE 25 POSSIBLE DELAYS, NUMBERED 1 TO 25.
C
C        NUNITS  : THE NUMBER OF LOCATIONS IN DLINE.   NUNITS MUST BE
C                  EQUAL TO THE TIME DELAY DESIRED DIVIDED BY THE STEP
C                  SIZE, AND MUST BE AN INTEGER MULTIPLE OF THE STEP
C                  SIZE.
C
C        VALIN   : THE VALUE BEING PUT INTO THE DELAY LINE.
C
C        VALOUT  : THE VALUE RETURNED FROM THE DELAY UNIT.
C
C-------------------------
C
C     NOTE:  UPON THE FIRST CALL TO RKDELAY, THE VALUE OF VALOUT IS USED
C      TO INITIALIZE THE ARRAY DELAY LINE.   IT IS ASSUMED THAT VALOUT
C      HAS REACHED EQUILIBRIUM FOR T<=0.
C
C-------------------------
C
C     WRITTEN BY WILLIAM CRANE
C     AUGUST 1975
C     REVISED BY ROB UHLRICH
C     BOTH OF MONTANA STATE UNIVERSITY, BOZEMAN, MONTANA
C     APRIL 1976
C
C-------------------------------------------------------------------------
C
      COMMON /MODSIM/ T, DT, JS, JN, DXA(50), XA(50), IO, JS4, MAXJN,
     & NTD, MAXNTD
      IMPLICIT DOUBLE PRECISION (A-H,O-Z)
      DIMENSION DLINE(1), IPOINT(25), PREV(25)
C-------------------------------------------------------------------------
C          SEE IF INITIALIZATION IS NEEDED (T=0.0) AND INSURE THAT KNT
C          IS IN THE RANGE OF 1 TO 25
C-------------------------------------------------------------------------
      IF (T) 27, 27, 28
   28 IF ((KNT.LT.1).OR.(KNT.GT.25)) GO TO 25
```

```
C-----------------------------------------------------------------------
C           CHECK FOR VALID INTEGRATION ORDER.
C           BRANCH FOR EULER OR RUNGE-KUTTA METHOD OF INTEGRATION.
C-----------------------------------------------------------------------
      IF (IO.EQ.1) GO TO 35
      IF (IO.EQ.4) GO TO 29
      GO TO 50
C-----------------------------------------------------------------------
C           BRANCH FOR THE NUMBER OF THE PASS (INDICATED BY JS4)
C           IN THE RUNGE KUTTA INTEGRATION ROUTINE.   IF JS4 IS OUT OF
C           THE RANGE 1 TO 4, OUTPUT AN ERROR MESSAGE AND STOP EXECUTION.
C-----------------------------------------------------------------------
 29   GO TO (33,33,34,35) JS4
      GO TO 32
C-----------------------------------------------------------------------
C           (JS4 = 1 OR 2) INTERPOLATE MIDPOINT BETWEEN LAST TWO VALUES
C           IN THE DELAY LINE.
C-----------------------------------------------------------------------
 33   VALOUT = (DLINE(IPOINT(KNT)) + PREV(KNT))/2.0
      RETURN
C-----------------------------------------------------------------------
C           (JS4 = 3).  TAKE THE LAST VALUE OUT OF THE DELAY LINE.
C           NO NEW VALUE IS INSERTED.
C-----------------------------------------------------------------------
 34   VALOUT = DLINE(IPOINT(KNT))
      RETURN
C-----------------------------------------------------------------------
C           (JS4 = 4 OR EULER METHOD)
C           SWAP VALUES INTO AND OUT OF DELAY LINE AND INCREMENT POINTER
C-----------------------------------------------------------------------
 35   VALOUT = DLINE(IPOINT(KNT))
      PREV(KNT) = VALOUT
      DLINE(IPOINT(KNT)) = VALIN
      IPOINT(KNT) = IPOINT(KNT) + 1
      IF (IPOINT(KNT).GT.NUNITS) IPOINT(KNT) = 1
      RETURN
C-----------------------------------------------------------------------
C           INITIALIZE THE DELAY
C-----------------------------------------------------------------------
 27   DO 29 I = 2, NUNITS
 29   DLINE(I) = VALOUT
      DLINE(1) = VALIN
      IPOINT(KNT) = 1
      PREV(KNT) = VALOUT
      RETURN
C-----------------------------------------------------------------------
C           ERROR MESSAGES
C-----------------------------------------------------------------------
 25   WRITE (108,31) KNT
 31   FORMAT ('0', '***DELAY INDEX OUT OF RANGE OF 1 TO 25  ',
     &  'VALUE IS ',I15, '.  PROGRAM TERMINATED')
      STOP
 32   WRITE (108,41) KNT
 41   FORMAT('0','***INTEGRATION INDEX (JS4) OUT OF RANGE FROM 1 TO 4. '
     & 'VALUE IS ',I15,'.  PROGRAM TERMINATED.')
      STOP
 50   WRITE (108,51)
 51   FORMAT ('0','***DELAY LINE WORKS ONLY FOR 1ST ORDER EULER OR ',
     1 'FOURTH ORDER RUNGE-KUTTA INTEGRATION METHOD.' ,
     2 'PROGRAM TERMINATED.'
      STOP
      END
```

# APPENDIX C

## DIGITAL COMPUTER SIMULATION PROGRAM FOR SYSTEM MODEL III

The digital computer program used to simulate model III is given in this Appendix. The program was adapted from Franks [51] by Robert Uhlrich. Subroutines required for this program are given in Appendix A and Appendix B.

Algebraic and differential equations for model III are listed under the headings "calculate algebraic quantities" and "calculate derivatives."

```
C-----------------------------------------------------------------------
C
C        PROGRAM TO SIMULATE MHD/STEAM COMBINED CYCLE OPERATION
C     USING MODEL III.  REFER TO MODEL III BLOCK DIAGRAMS.
C
C-------------------------
C
C        VARIABLES USED :
C
C          DLINEI  : DELAY LINE ARRAYS FOR DELAY UNIT I.
C          DT      : TIME INCREMENT, IN SECONDS.
C          DXI     : TIME DERIVATIVE OF VARIABLE X(I).
C          HDR     : ONE PRINTER LINE ( 132 CHARACTERS ) OF INFORMATION
C                    READ FROM THE CARD READER.  THIS IS PRINTED ON THE
C                    OUTPUT.
C          K       : MULTIPLICATIVE CONSTANTS, AS NUMBERED ON THE MODEL
C                    DIAGRAMS.
C          NF      : SET BY SUBROUTINE PRTFIN.  EQUALS 1 IF CALCULATIONS
C                    ARE DONE.  OTHERWISE EQUALS 0.
C          NPR     : SET BY PRTFIN.  EQUALS 1 WHEN IT IS TIME TO PRINT
C                    RESULTS, AND IS 0 OTHERWISE.
C          T       : TIME, IN SECONDS.
C          TAU     : TIME CONSTANTS AND DELAY TIMES, AS NUMBERED ON THE
C                    MODEL DIAGRAMS.
C          X       : VARIABLES AS NUMBERED ON MODEL DIAGRAMS.
C
C-------------------------
C
C        VALUES FOR K(I) AND TAU(I) ARE ENTERED VIA THE CARD READER.
C        THE INITIAL VALUES OF X(I) ARE ENTERED DIRECTLY INTO THE
C     PROGRAM.  ANY STABLE OR UNSTABLE INITIAL CONDITIONS MAY BE
C     ENTERED.
C
C--------------------
C
C
C    SUBROUTINES REQUIRED :
C         PRTFIN ( MODSIM ROUTINE )
C         INTI   ( MODSIM ROUTINE )
C         INT    ( MODSIM ROUTINE )
C         DELAY  ( MODSIM ROUTINE )
C         TIMDAT ( TO OBTAIN THE TIME AND DATE )
C
C-----------------
C
C     MODEL DEVELOPED BY JOHN ASPNES.
C     PROGRAM WRITTEN BY ROB UHLRICH
C     BOTH OF MONTANA STATE UNIVERSITY, BOZEMAN, MONTANA.
C     APRIL 1976
C
C-------------------------
      IMPLICIT DOUBLE PRECISION (A-H,O-Z)
      REAL K
      INTEGER TDATE
      DIMENSION X(85),  K(31), TAU(19), DLINE1(50), DLINE2(50)
      DIMENSION HDR(33), TDATE(4)
```

```
C-------------------------------------------------------------------------
C          GET TIME AND DATE,  READ K, TAU, DT, AND HDR FROM CARD READER.
C-------------------------------------------------------------------------
      CALL TIMDAT ( TDATE )
 50   READ ( 105,10,END=51 ) K, TAU, DT,  HDR
 10   FORMAT (3(8F10.5,/), 7F10.5,/, 2(8F10.5,/), 3F10.5,/,
     &  1F10.5,/, (20A4))
C-------------------------------------------------------------------------
C        INITIAL VALUES OF STATE VARIABLES.
C-------------------------------------------------------------------------
      X(8) = X(9) = .795455
      X(27) = 0.0
      X(28) = 0.0
      X(32) = X(33) = X(34) = 1165.9988
      X(54) = 3500.0
      X(72) = 1500.0
      X(74) = 714.86834
      X(77) = .795455
      X(78) = 0.0
      X(80) = 0.0
      X(82) = 0.0
      X(84) = -.795455
      X(85) = 0.0
C-------------------------------------------------------------------------
C         MISC.  INITIAL VALUES.
C-------------------------------------------------------------------------
      X(1) = 1560.4418
      PREV4 = X(4) = 0.0
      X(9) = X(11) = .795455
      X(13) = .795455
      X(19) = 1165.9988
      X(25) = 1165.9988
      X(46) = 8.0
      X(47) = 3500.0
      PREV48 = X(48) = 0.0
      X(53) = .795455
      X(54) = X(55) = 3500.0
      X(58) = X(59) = 3503.372
      KNT = 9
      A = -50.0
      TREF = 1800
      T = 0.0
C-------------------------------------------------------------------------
C         CALCULATE THE NUMBER OF LOCATIONS NEEDED FOR THE DESIRED
C      TIME DELAYS.   THIS NUMBER MUST BE NO GREATER THAN THE MAXIMUM
C      NUMBER OF LOCATIONS AVAILABLE ( MAXLOC ).
C-------------------------------------------------------------------------
      NTD1 = IFIX( TAU(16) / DT )
      NTD2 = IFIX( TAU(17) / DT )
      MAXLOC = 50
      IF ( NTD1 - MAXLOC ) 40, 40, 29
 40   IF ( NTD2 - MAXLOC ) 41, 41, 29
```

```
C-----------------------------------------------------------------------
C         WRITE OUTPUT HEADINGS
C-----------------------------------------------------------------------
 41    WRITE (108,30) TDATE, K,TAU,X(4), X(8), X(9), X(27), X(28),X(32),
     &  X(33), X(34), X(54), X(72), X(74), X(77), X(78), X(80), X(82),
     &  X(84),X(85), X(1), DT, HDR
 30    FORMAT ( '1', 'COMBINED MHD - STEAM PLANT CONTROL SIMULATION,',
     1          ' MODEL III', T90, 4A4, ///, ' ', 'MULTIPLIER VALUES',
     2          //, ' ', 10X, 'K - K',   7X, 6(1PE12.5), /, ' ', 11X,
     3          '1    6',//,' ',10X,'K - K',7X,6(1PE12.5),/,' ',11X,
     4          '7    12', //, ' ', 10X, 'K - K',  7X, 6(1PE12.5), /, ' ',
     5           11X,'13    18',//,' ',10X,'K - K',7X,6(1PE12.5),/,' ',
     6          11X,'19    24',//,' ',10X,'K - K',7X,6(1PE12.5),/,' ',11X,
     7          '25    30',//,' ',10X,'K',12X,(1PE12.5),/,' ',11X,'31',
     8          6/, ' ', 'TIME CONSTANTS AND DELAY TIMES',
     9          //, ' ', 10X, 'TAU  - TAU', 3X, 6(1PE12.5), /, ' ',
     A          13X, '1     6', //, ' ', 10X, 'TAU - TAU', 3X, 6(1PE12.5),
     B          /,13X,'7     12',//,' ',10X,'TAU - TAU',3X,6(1PE12.5),
     C          /, 13X, '13     18', //, ' ',10X, 'TAU', 9X, 1(1PE12.5),
     D          /, 13X, '19', ///, ' ',
     E          'INITIAL VALUES OF STATE VARIABLES', //, ' ',
     F          10X, 'X', 15X, 6(1PE12.5), /, ' ', 11X, '8,9,27,28,32',
     G          //, ' ', 10X, 'X', 15X, 5(1PE12.5), /, ' ', 11X,
     H          '33,34,54,72,74,77', //, ' ', 10X, 'X', 15X, 5(1PE12.5),
     I          /, ' ', 11X, '78,80,82,84,85',
     J          ///, ' ', 'DEMAND REFERENCE IS X(1) = ', (1PE12.5),
     K          ' MEGAWATTS', ///, ' ', 'TIME STEP = ', (1PE11.3),
     L          ' SECONDS', ///, ' ', 'REMARKS:',/, ' ', 33A4 )
       WRITE ( 108,31 )
 31    FORMAT ( '1', '  TIME, SEC', 6X, 'X(2)', 9X, 'X(3)', 9X,
     1          'X(7)', 9X, 'X(41)', 8X, 'X(42)', 8X, 'X(48)', 8X,
     2          'X(51)', 8X, 'X(55)', 8X,  'X(14)', // )
C-----------------------------------------------------------------------
C         CALCULATE ALGEBRAIC QUANTITIES
C-----------------------------------------------------------------------
 20    X(6) = ( A*K(5)/TAU(3)) * EXP (-T/TAU(3))
       X(50) = ( A*K(20)/TAU(13)) * EXP(-T/TAU(13))
       X(76) = K(2) * X(4)
       X(5) = X(76) + X(77) + X(78)
       X(7) = X(5) + X(6)
C      **** RATE AND MAGNITUDE LIMITERS FOR X(11)
            PREV11 = X(11)
            X(11) = X(9)
            CNGMAX = K(7) * K(8) * DT / 4.0
            IF (X(11) .GT. (PREV11 + CNGMAX)) X(11) = PREV11 + CNGMAX
            IF (X(11) .LT. (PREV11 - CNGMAX)) X(11) = PREV11 - CNGMAX
            IF (X(11) .LT. 0.0) X(11) = 0.0
            IF (X(11) .GT. K(8)) X(11) = K(8)
       X(12) = X(11) - X(13)
       X(14) = X(12)/X(13)
       X(79) = K(9) * X(14)
       X(15) = X(79) - X(80)
       X(16) = K(12) * X(28)
       X(17) = X(15) + X(16)
       X(18) = X(17) * X(19)
       X(20) = X(18) + X(19)
       X(38) = K(15) * X(32)
```

```
      X(36) = K(16) * X(33)
      X(35) = K(17) * X(34)
      X(37) = X(35) + X(36)
      X(39) = X(37) + X(38)
      X(40) = K(18) * X(39)
      X(41) = (1.0-K(18)) * X(39)
      X(29) = K(13) * X(28)
      X(81) = K(10) * X(14)
      X(30) = X(81) + X(82)
      X(31) = X(29) - X(30)
      X(48) = X(31) * X(47)
      X(83) = K(21) * X(48)
      X(49) = X(83) + X(84) + X(85)
      X(51) = X(50) - X(49)
C     **** RATE AND MAGNITUDE LIMITERS FOR X(53)
      PREV53 = X(53)
      X(53) = X(51)
      CNGMAX = K(24) * K(25) * DT / 4.0
      IF (X(53) .GT. (PREV53 + CNGMAX)) X(53) = PREV53 + CNGMAX
      IF (X(53) .LT. (PREV53 - CNGMAX)) X(53) = PREV53 - CNGMAX
      IF (X(53) .LT. 0.0) X(53) = 0.0
      IF (X(53) .GT. K(25)) X(53) = K(25)
      CALL DELAY (DLINE1, NTD1, X(54), X(55), 1)
      X(73) = X(72) + T1(T) + 300
C     Z = X(73) -TREF
      Z = 0
      X(42) = -470.83184 + .30481901 * X(73) + .08256244 * X(55)
     & -(9.3459595E-5) * (X(73) ** 2) + 1.180927E-4 * X(55) * X(73)
     & + (1.4762662E-5) * (X(55) ** 2)
      X(57) = -3.4977822 + .087958017 * X(73) - .048262178 * X(55)
     & + 3.132002E-5 * (X(73)**2) + 1.2341633E-4 * X(55) * X(73)
     & - (1.2248198E-5) * (X(55) ** 2)
      X(58) = X(55) + 3.6359E-4 * X(55) * (X(73) -300) - 1.0099748 *
     & X(42) - 1.005 * X(57) - 5.3811701E-2 * X(55)
      X(56) = .005 * X(57)
      X(75) = 2.9938733E-2 * X(55)
      CALL DELAY (DLINE2, NTD2, X(58), X(59), 2)
      X(70) = K(31) * X(55)
      X(61) = X(70)
      X(62) = Z * X(61)
      X(60) = (1.0 - K(27)) * X(59) - X(62)
      X(68) = (270.5 + 0.029 * (X(55) - 3500)) * .00036359 * X(55)
      X(69) = X(60) + X(68)
      X(71) = X(69) / X(70)
      X(63) = K(27) * X(59)
      X(64) = K(28) * X(63)
      X(65) = (1.0 - K(28)) * X(63)
      X(66) = X(65) + E1(T)
      X(67) = X(66) + X(62) + X(75)
      X(21) = X(67) + X(74)
      X(22) = K(30) * X(21)
      X(23) = (1.0 - K(30)) * X(21)
      X(24) = X(23) - X(25)
      X(26) = X(24) / X(25)
      X(43) = X(41) + X(42)
      X(44) = K(19) * X(43)
      X(45) = (1.0 - K(19)) * X(43)
```

```
      X(2) = X(45) - X(46)
      X(3) = X(1) - X(2)
      X(4) = K(1) * X(3)
C-----------------------------------------------------------------------
C           CALCULATE DERIVATIVES
C-----------------------------------------------------------------------
C     **** APPROXIMATE DX4 BY NUMERICAL DIFFERENTIATION
                DX4 = (X(4) - PREV4) * 4.0 / DT
                PREV4 = X(4)
      DX8 = (X(7) - X(8)) / TAU (4)
      DX9 = (K(6) * X(8) - X(9)) / TAU(5)
      DX27 = (K(14) * X(26) - X(27)) / TAU(9)
      DX28 = (X(27) - X(28)) / TAU(8)
      DX32 = (X(20) - X(32)) / TAU(10)
      DX33 = (X(32) - X(33)) / TAU (11)
      DX34 = (X(33) - X(34)) / TAU(12)
C     ****  APPROXIMATE DX48 BY NUMERICAL DIFFERENTIATION
      DX48 = (X(48) - PREV48) * 4.0 / DT
      PREV48 = X(48)
      DX54 = (K(26) * X(53) - X(54)) / TAU(15)
      DX72 = (X(71) - X(72)) / TAU(18)
      DX74 = (X(57) - X(74)) / TAU(19)
      DX77 = K(3) * X(4)
      DX78 = (K(4) * DX4 - X(78)) / TAU(2)
      DX80 = (K(9) * X(14) - X(80)) / TAU(6)
      DX82 = (K(11) * X(14) - X(82)) / TAU(7)
      DX84 = K(22) * X(48)
      DX85 = (K(23) * DX48 - X(85)) / TAU(14)
C-----------------------------------------------------------------------
C        CHECK TO SEE IF READY TO PRINT VALUES ( NPR = 1 ) AND IF
C     CALCULATIONS ARE DONE ( NF = 1 ).  UNIT 108 = LINE PRINTER.
C     UNIT 109 = DISK OR OTHER SECONDARY STORAGE TO HOLD DATA FOR
C     POSSIBLE LATER USE.
C-----------------------------------------------------------------------
      CALL PRTFIN ( 0.1, 400.0,   NF, NPR )
      IF ( NPR ) 21, 22, 21
 21   WRITE (109,32)   T, X(2), X(3), X(7), X(41), X(42), X(48),
     &     X(51), X(55), X(73)
      WRITE (109,32) T, X(14), X(20), X(21), X(31), X(58), X(60), X(67),
     &  X(11), X(53)
C     X(5) & X(49) WHEN X(6) AND X(50) .NE. 0 ; X(11), X(53) OTHERWISE
 32   FORMAT ( ' ', 1(1PE11.3), 9(1PE13.5))
      KNT = KNT + 1
      IF (KNT.NE.10) GO TO 34
      KNT = 0
      WRITE (108,32) T, X(2), X(3), X(7), X(41), X(42), X(48), X(51),
     &     X(55), X(14)
 34   IF ( NF ) 50, 22, 50
```

```
C-----------------------------------------------------------------------
C         INTEGRATE THE STATE VARIABLES
C-----------------------------------------------------------------------
 22    CALL INTI ( T, DT, 4 )
       CALL INT (X(8), DX8)
       CALL INT (X(9), DX9)
       CALL INT (X(27), DX27)
       CALL INT (X(28), DX28)
       CALL INT (X(32), DX32)
       CALL INT (X(33), DX33)
       CALL INT (X(34), DX34)
       CALL INT (X(54), DX54)
       CALL INT (X(72), DX72)
       CALL INT (X(74), DX74)
       CALL INT (X(77), DX77)
       CALL INT (X(78), DX78)
       CALL INT (X(80), DX80)
       CALL INT (X(82), DX82)
       CALL INT (X(84), DX84)
       CALL INT (X(85), DX85)
       GO TO 20
51     STOP
C-----------------------------------------------------------------------
C         ERROR MESSAGE FOR TOO LONG A DELAY.
C-----------------------------------------------------------------------
 29    WRITE ( 108,33 )
 33    FORMAT ( ' ', '*** TOO LONG A TIME DELAY DESIRED FOR GIVEN ARRAY ',
     1           'SIZE.  PROGRAM TERMINATED.' )
       STOP
       END
       FUNCTION T1(T)
C-----------------------------------------------------------------------
C
C         FUNCTION SUBROUTINE TO GENERATE THE TEMPERATURE RIPPLE
C      FUNCTION FOR THE MHD/STEAM CYCLE, MODEL III.
C
C-----------------------------------------------------------------------
       PERD = 50.0
       TIME = T + 25
       T1 = 10 - ((TIME/PERD - INT(TIME/PERD))) * 20
       T1 = 0
       RETURN
       END
       FUNCTION E1(T)
C-----------------------------------------------------------------------
C
C         FUNCTION SUBROUTINE TO GENERATE THE POWER RIPPLE FUNCTION
C      FOR THE MHD/STEAM CYCLE, MODEL III.
C
C-----------------------------------------------------------------------
       PERD = 50.0
       TIME = T + 25.0
       E1 = -12.726 + (TIME/PERD - INT (TIME/PERD)) * 25.452
       E1 = 0.0
       RETURN
       END
```

# REFERENCES

REFERENCES


1. Adams, J., et al. "Mathematical Modeling of Once-Through Boiler Dynamics," IEEE Transactions on Power Apparatus and Systems, Vol. PAS-84, February, 1965, pp. 146-156.

2. Anderson, J.H., and G.H. Qualtrough. "Dynamic Optimization of a Boiler-Turboalternator Model," Proceedings IEE, Vol. 113, No. 10, October, 1966, pp. 1680-1682.

3. _____. "Dynamic Control of a Power Boiler," Proceedings IEE, Vol. 116, No. 7, July, 1969, pp. 1257-1268.

4. Anderson, P.M. "An Annotated Bibliography on Power Plant Control and Modeling of Energy Source Systems 1957-1971," Engineering Planning Department, Pacific Gas and Electric Co., March, 1972.

5. _____. "Mathematical Modeling of Boilers for Dynamic Stability Simulation," Proceedings of the First Power Plant Dynamics, Control and Testing Symposium, Knoxville, Tennessee, 1973, pp. 7-1 to 7-39.

6. _____. "Modeling Thermal Power Plants for Dynamic Stability Studies," Ames, Iowa: Cyclone Copy Center, 1974.

7. _____, and S. Nanakorn. "An Analysis and Comparison of Certain Low-Order Boiler Models," ISA Transactions, Vol. 14, No. 1, 1975, pp. 17-23.

8. Aspnes, J. "Cycle Analysis and Control, Summer, 1975" ERL Report No. 3675, Montana State University, September, 1975.

9. Astrom, K.J., and K. Eklund. "A Simplified Non-linear Model of a Drum Boiler-Turbine Unit," International Journal of Control, Vol. 16, No. 1, July, 1972, pp. 145-169.

10. _____. "Modeling and Identification of Power System Components," Handschin, E. (Ed.) Real-Time Control of Electric Power Systems, New York: Elsevier Publishing Co., 1972, pp. 1-28.

11. Babcock and Wilcox Co. Steam/its generation and use. 38th edition, New York: Babcock and Wilcox, 1972.

12. Bailey, J.M., and G.F. Pierce. "Modeling of Operating Fossil Fired Power Plants--An Application Approach," Proceedings of the Second Power Plant Dynamics, Control and Testing Symposium, Knoxville, Tennessee, 1975, paper No. 7.

13. _____. "Properties of Coal Pulverizers," Proceedings of the Seminar on Boiler Modeling. D.A. Berkowitz (ed.). Bedford, Massachusetts: The MITRE Corporation, October, 1975, pp. 169-176.

14. Bailey, S.J. "Control Practice in the Electric Power Industry--A Special Report," Control Engineering, Vol. 18, No. 9, September, 1971, pp. 41-53

15. Baylis, J.A., et al. "Duct Physics," in Open Cycle M.H.D. Power Generation. J.B. Heywood, and G.J. Womack (eds.) Oxford: Pergamon Press, 1969, pp. 393-465.

16. Bekey, G.A. "System Identification--an Introduction and a Survey," Simulation, Vol. 9, No. 5, October, 1970, pp. 151-166.

17. Berg, G.J., and A.K. Kar. "Model Representation of Power System Loads," IEEE 1971 Power Industry Computer Applications Conference Proceedings, 1971, pp. 153-162.

18. Bergman, P.D., et al. "Conceptual Design and Economics of an MHD Pilot Plant," presented at the Intersociety Conference on Energy Conversion, Newark, Delaware, August, 1975.

19. Berkowitz, D.A., R.T. Jones, and A.L. Markunas. "Dynamic Model for Mystic No. 4," Proceedings of the Seminar on Boiler Modeling. D.A. Berkowitz (ed.). Bedford, Massachusetts: The MITRE Corporation, October, 1975, pp. 53-66.

20. Bethune, J.L. III. "Use of the Computer for Dynamic Analysis of a Power Plant's Performance," ISA Transactions, Vol. 14, No. 1, 1975, pp. 1-16.

21. Bienstock, D., et al. "Air Pollution Aspects of MHD Power Generation," Proceedings of the 13th Symposium on Engineering Aspects of MHD, Stanford University, March, 1973, pp. VII.1.1-VII.1.10.

22. Bloethe, W.G., and P.M. Anderson. "Application of a Low-Order Boiler Model to Transient Stability Studies," presented at the IEEE Power Engineering Society Winter Meeting, 1976, paper A 76 149-5.

23. Brown, P.G., et al. "Effects of Excitation, Turbine Energy Control, and Transmission on Transient Stability," IEEE Transactions on Power Apparatus and Systems, Vol. PAS-89, No. 4, July/August, 1970, pp. 1247-1252.

24. Buntzel, H., Jr. "Calibrating Boiler Control Systems," Instrumentation Technology, Vol. 21, No. 1, January, 1974, pp. 39-42.

25. Carnahan, B., H.A. Luther, and J.O. Wilkes. Applied Numerical Methods. New York: John Wiley and Sons, 1969.

26. Carter, C., and J.B. Heywood. "Optimization Studies on Open-Cycle MHD Generators," Proceedings IEEE, Vol. 56, No. 9, September, 1968, pp. 1409-1419.

27. Caseau, P., R. Chaussard, and P. Godin. "Representation of Thermal Power Stations by Models and Operating Studies," Proceedings of the 5th World Congress (IFAC), Paris, June 12-17, 1972, paper No. 5.2

28. Chen, T., and K.R. Galle. "Transfer Functions for Steam-Generating Heat Exchangers," ISA Transactions, Vol. 3, No. 2, April, 1964, pp. 175-183.

29. Chidambara, M.R. "Two Simple Techniques for the Simplification of Large Dynamic Systems," Proceedings of the 1969 Joint Automatic Control Conference of the American Control Council, August, 1969, pp. 669-674.

30. Chien, K.L., et al. "Dynamic Analysis of a Boiler," Trans. ASME, Vol. 80, November, 1958, pp. 1809-1819.

31. Chojnowski, B., D.E. Fussey, and P.E. Chew. "Checker Brick Regenerator," in Open Cycle M.H.D. Power Generation. J.B. Heywood, and G.J. Womack (eds.). Oxford: Pergamon Press, 1969, pp. 28-44.

32. Choung, K.C., and D.J. Dziubakowski. "Modeling of a Boiler at Start-up," Proceedings of the Second Power Plant Dynamics, Control and Testing Symposium, Knoxville, Tennessee, 1975, paper No. 8.

33. Concordia, C. "Effect of Steam-Turbine Reheat on Speed-Governor Performance," ASME Journal of Engineering for Power, Vol. 81, April, 1959, pp. 201-207.

34. _____, et al. "Effect of Prime-Mover Response and Governing Characteristics on System Dynamics Performance," Proceedings of the American Power Conference, Vol. 28, 1966, pp. 1074-1085. (Also IEEE Spectrum, October, 1966, pp. 106-111.

35. _____, and P.G. Brown. "Effects of Trends in Large Steam Turbine Driven Generator Parameters on Power System Stability," IEEE Transactions on Power Apparatus and Systems, Vol. PAS-90, No. 5, September/October, 1971, pp. 2211-2218.

36. Crevier, D., and F.C. Schweppe. "The Use of Laplace Transforms in the Simulation of Power System Frequency Transients," IEEE Transactions on Power Apparatus and Systems, Vol. PAS-94, No. 2, March/April, 1975, pp. 236-241.

37. Cushing, E.W., et al. "Fast Valving as an Aid to Power System Transient Stability and Prompt Resynchronization and Rapid Reload After Full Load Rejection," IEEE Transactions on Power Apparatus and Systems, Vol. PAS-91, No. 4, July/August, 1972, pp. 1624-1636.

38. Davis, G.E., Jr. "Hybrid Digital-Analog Power Plant Control," ISA Transactions, Vol. 9, No. 4, 1970, pp. 298-308.

39. Davison, E.J. "A Method for Simplifying Linear Dynamic Systems," IEEE Transactions on Automatic Control, Vol. AC-11, No. 1, January, 1966, pp. 93-101.

40. deMello, F.P., R.J. Mills, and W.F. B'Rells. "Automatic Generation Control; Part I: Process Modeling; Part II; Digital Control Techniques," presented at the IEEE Summer Power Meeting, San Francisco, July, 1972.

41. _____, and R.J. Mills. "Discussion of Part II: A Manufacturer's Viewpoint in Utilizing Boiler Dynamic Modeling," IEEE Transactions on Power Apparatus and Systems, Vol. PAS-90, No. 4, July/August, 1971, pp. 1732-1733.

42. Durrant, O.W. "Operation and Control of Once-Through Boilers During Electric Power System Emergencies," Proceedings of the 13th International ISA Instrumentation in the Power Industry Conference, Kansas City, Missouri, Vol. 13, May 19-21, 1970, pp. 1-14.

43. Eklund, K. "A Comparison of a Drum Boiler-Turbine Model to Measurements and Models Obtained by Identification," Proceedings of the 5th World Congress (IFAC), Paris, June 12-17, 1972, paper No. 5.3.

44. El-Abiad, A., and A. Keyhani. "Optimal Dynamic Generation Control Using Variable Pressure Steam Generators," Proceedings of the Seminar on Boiler Modeling. D.A. Berkowitz (ed.). Bedford, Massachusetts: The MITRE Corporation, October, 1975, pp. 143-168.

45. El'kin, A.I., and E.I. Yantovskii. "The Volt-Ampere Characteristics of an MHD Generator with a Fixed Direction for the Electric Field and a Single Load," Magnitnaya Gidrodinamika, Vol. 5, No. 3, 1969, pp. 74-80. (Also MHD Russian Original, Vol. 5, No. 3, July/September, 1969, pp. 47-51.)

46. Enns, M. "Comparison of Dynamic Models of a Superheater," ASME paper 61-WA-171, 1961. ASME J. Heat Transfer, Vol. 84, November, 1962, pp. 375-385.

47. Fenton, F.H., Jr., and J.V. Pigford. "Rapid Response and Maneuverability are Obtainable from Supercritical Plants," ISA Transactions, Vol. 9, No. 4, 1970, pp. 270-283.

48. _____. "Part II: A Manufacturer's Viewpoint in Utilizing Boiler Dynamic Modeling," Proceedings of the Seminar on Boiler Modeling. D.A. Berkowitz (ed.). Bedford, Massachusetts: The MITRE Corporation, October, 1975, pp. 110-128.

49. Fink, L.H. "Evolution of a Successful Modeling Program," Proceedings of the Seminar on Boiler Modeling. D.A. Berkowitz (ed.). Bedford, Massachusetts: The MITRE Corporation, October, 1975, pp. 5-30.

50. Ford, R.L. "Electrical Analogues for Heat Exchangers," Proceedings IEE, Vol. 103, Part B, January 1956, pp. 65-82.

51. Franks, R.G.E. Modeling and Simulation in Chemical Engineering. New York: Wiley Interscience, 1972.

52. Fryling, G.R. (ed.). Combustion Engineering; a Reference Book on Fuel Burning and Steam Generation. New York: Combustion Engineering, Inc., 1966.

53. Gigauri, K.V. "External Characteristics of an MHD Generator With Series-Connected Segments," Magnitnaya Gidrodinamika, Vol. 6, No. 3, 1970, pp. 99-102. (Also MHD Russian Original, Vol. 6, No. 3, July/September, 1970, pp. 385-388.)

54. Giras, T.C., and M. Birnbaum. "Digital Control for Large Steam Turbine-Generators," Proceedings of the American Power Conference, Vol. 30, 1969, pp. 1275-1284.

55. _____, and P.N. Papas. "Power Plant Simulation Facilitates Dynamic Factory Operational Testing of Plant Automation and Control Systems," Westinghouse ENGINEER, Vol. 33, No. 3, May, 1973, pp. 72-75.

56. _____, and P.A. Berman. "PACE Power-Plant Control System Provides Operating Flexibility and High Plant Availability," Westinghouse ENGINEER, Vol. 34, No. 2, April, 1974, pp. 46-52.

57. Hals, F.A., and W.D. Jackson. "Systems Analysis of Central Stations MHD Power Plants," Proceedings of the 5th International Conference on MHD Electrical Power Generation, Vol. V, April 19-23, 1971, pp. 159-178.

58. Harrowell, R.V., J.B. Heywood, and G.J. Womack. "Cycle Analysis and Appraisal," in Open Cycle M.H.D. Power Generation. J.B. Heywood and G.J. Womack (eds.). Oxford: Pergamon Press, 1969, pp. 752-784.

59. Hastings, G., and J. Louis. "Control Design Development for a HTGR Power Plant by Digital Computer Simulation," IEEE 1971 Power Industry Computer Applications Conference Proceedings, 1971, pp. 463-470.

60. Hayes, R.H., and W. Crawford. "Automatic Controls Excel in Startups on Generating Unit With Once-Through Boiler," Power Engineering, Vol. 79, No. 6, June, 1975, pp. 49-53.

61. Herbrick, R., and M. Jamshidi. "Design of an Optimum State Regulator for a Once-Through Boiler," Proceedings of the 5th World Congress (IFAC), Paris, June 12-17, 1972, paper No. 5.4.

62. Herget, C.J., and C.U. Park. "Parameter Identification and Verification of Low Order Boiler Models," presented at the IEEE Power Engineering Society Winter Meeting, 1976, paper F 76 223-8.

63. Hsu, J.C., and A.U. Meyer. Modern Control Principles and Applications. New York: McGraw-Hill Book Co., 1968.

64. Hughes, W.F., and F.J. Young. The Electromagnetodynamics of Fluids. New York: John Wiley and Sons, 1966.

65. IEEE Committee Report. "Dynamic Models for Steam and Hydro Turbines in Power System Studies," IEEE Transactions on Power Apparatus and Systems, Vol. PAS-92, No. 6, November/December, 1973, pp. 1904-1915.

66. _____. "Power Plant Response," IEEE Transactions on Power Apparatus and Systems, Vol. PAS-86, No. 3, March, 1967, pp. 384-392.

67. IEEE Working Group on Power Plant Response to Load Changes. "MW Response of Fossil Fueled Steam Units," IEEE Transactions on Power Apparatus and Systems, Vol. PAS-92, No. 2, March/April, 1973, pp. 455-463.

68. Ivanov, V.A., et al. "Mathematical Model of Once-through Boiler-Turbine Unit," Izvestia V.U.Z., Energetika, No. 8, August, 1968, pp. 56-61.

69. Jackson, W.D., et al. "Considerations in the Development of Open Cycle MHD Systems for Commercial Service," Sixth International Conference on Magnetohydrodynamic Electrical Power Generation, Vol. V - Late Papers, June 9-13, 1975, pp. 21-42.

70. Johansson, K., and L. Carlsson. "Simulation of Transients in AC Networks With an Accurate Machine and Network Representation," IEEE 1971 Power Industry Computer Applications Conference Proceedings, 1971, pp. 255-256.

71. Kazachkov, Yu. A., and I.I. Shipulin. "Effect of the Method of Automatic Regulation of an Inverter on a Faraday Segmented MHD Generator," Magnitnaya Gidrodinamika, Vol. 5, No. 3, 1969, pp. 122-126. (also MHD Russian Original, Vol. 5, No. 3, July/September, 1969, pp. 80-83.)

72. Kenny, P.L. "Once-Through Boiler Control," Power Engineering, Vol. 72, No. 1,2, January, 1968, pp. 36-39, & February, 1968, pp. 58-61.

73. Kerlin, T.W. "Dynamic Testing in Nuclear Reactors for Model Verification," Proceedings of the Seminar on Boiler Modeling. D.A. Berkowitz (ed.) Bedford, Massachusetts: The MITRE Corporation, October, 1975, pp. 69-90.

74. Kirchmayer, L.K. Economic Control of Interconnected Systems. New York: John Wiley & Sons, 1959.

75. Koekebakker, J. "Canadian Experience in Direct Digital Control of Nuclear Power Stations," Power Engineering, Vol. 79, No. 5, May, 1975, pp. 42-44.

76. Kundur, P., and J.P. Bayne. "A Study of Early Valve Actuation Using Detailed Prime Mover and Power System Simulation," IEEE Transactions on Power Apparatus and Systems, Vol. PAS-94, No. 4, July/August, 1975, pp. 1275-1287.

77. Kwan, H.W., and J.H. Anderson. "A Mathematical Model of a 200 MW Boiler," International Journal of Control, Vol. 12, No. 6, June, 1970, pp. 977-998.

78. Kwatny, H.G., J.P. McDonald, and J.H. Spare. "A Nonlinear Model for Reheat Boiler-Turbine-Generator Systems, Part II - Development," Joint Automatic Control Conference Proceedings, 1971, pp. 227-236.

79. _____, L.H. Fink, J.P. McDonald, and P.J. Clelland. "Control Strategies for Power Plants--An Optimal Regulator Approach," Proceedings of the Power Plant Dynamics, Control, and Testing Symposium, Knoxville, Tennessee, October 8-10, 1973, pp. 6-1 to 6-24.

80. _____. "Power Plant Control System Design: The Application of Analytical Techniques," Proceedings of the Seminar on Boiler Modeling. D.A. Berkowitz (ed.). Bedford, Massachusetts: The MITRE Corporation, October, 1975, pp. 289-313.

81. Laubli, F., and F.H. Fenton, Jr. "The Flexibility of the Supercritical Boiler as a Partner in Power System Design and Operation; Part I: Theoretical Relationships; Part II: Application and Field Test Results," IEEE Transactions on Power Apparatus and Systems, Vol. PAS-90, No. 4, July-August, 1971, pp. 1719-1733.

82. _____. "Large Scale Boiler Simulation," Proceedings of the Seminar on Boiler Modeling, D.A. Berkowitz (ed.). Bedford, Massachusetts: The MITRE Corporation, October, 1975, pp. 207-263.

83. Laxton, J.W., and C.G. Stevens. "Steam Plant Equipment," in Open Cycle M.H.D. Power Generation. J.B. Heywood, and G.J. Womack (eds.). Oxford: Pergamon Press, 1969, pp. 716-751.

84. Lee, T.H., G.E. Adams, and W.M. Gaines. Computer Process Control: Modeling and Optimization. New York: John Wiley and Sons, 1968.

85. Lindorff, D.P. Theory of Sampled-Data Control Systems. New York: John Wiley and Sons, 1965.

86. Littman, B., and T.S. Chen. "Simulation of Bull Run Supercritical Generation Unit," IEEE Transactions on Power Apparatus and Systems, Vol. PAS-85, July, 1966, pp. 711-722.

87. Louis, J.R. "Controls for a Once-Through Boiler," Instruments and Control Systems, Vol. 44, No. 1, January, 1971, pp. 77-80.

88. Masubuchi, M. "Dynamic Response and Control of Multipass Heat Exchangers," ASME Journal of Basic Engineering, Vol. 82, March, 1960, pp. 51-65.

89. McDonald, J.P., and H.G. Kwatny. "A Mathematical Model for Reheat Boiler-Turbine-Generator Systems," IEEE paper 70 CP 221-PWR, 1970.

90. _____, H.G. Kwatny, and J.H. Spare. "A Nonlinear Model for Reheat Boiler-Turbine-Generator Systems, Part I - General Description and Evaluation," Joint Automatic Control Conference Proceedings, 1971, pp. 219-226.

91. _____, and H.G. Kwatny. "Design and Analysis of Boiler-Turbine-Generator Controls Using Optimal Linear Regulator Theory," IEEE Transactions on Automatic Control, Vol. AC-18, No. 3, June, 1973, pp. 202-209.

92. _____. "Adequacy and Philosophy of Modeling, Dynamic System Performance Representation of the Boiler-Turbine," presented at the IEEE Power Engineering Society Winter Meeting, 1975, paper 75 CHO970-4-PWR.

93. _____. "Fulton Station: Plant Dynamic Simulation," Proceedings of the Seminar on Boiler Modeling. D.A. Berkowitz (ed.). Bedford, Massachusetts: The MITRE Corporation, October, 1975, pp. 5-30.

94. Meyer, C.A., et al. 1967 ASME Steam Tables, Second Edition. New York: The American Society of Mechanical Engineers, 1967.

95. Mika, H.S. "Modern Control Theory Applied to Power Plant Analysis," Instrumentation Technology, Vol. 20, No. 7, July, 1973, pp. 53-57.

96. Mizutani, H., and T. Kitami. "On-line Real Time Identification of Parameters of Thermal Power Plant," Second IFAC Symposium on Identification, Prague, June, 1970, paper 11.3, pp. 1-6.

97. Nicholson, H. "Dynamic Optimization of a Boiler," Proceedings IEE, Vol. 111, No. 8, August, 1964, pp. 1479-1499.

98. _____. "Dual-Mode Control of a Time-Varying Boiler Model With Parameter and State Estimation," Proceedings IEE, Vol. 112, No. 2, 1965, pp. 383-395.

99. _____. "Dynamic Optimisation of a Boiler-Tuboalternator Model," Proceedings IEE, Vol. 113, No. 2, 1966, pp. 385-399.

100. _____. "Integrated Control of a Nonlinear Boiler Model," Proceedings IEE, Vol. 114, No. 10, October, 1967, pp. 1569-1576.

101. _____. "Optimal Linear Control With Input Derivatives," Proceedings IEE, Vol. 115, No. 6, June, 1968, pp. 877-878.

102. Nielsen, R.S., and D. Berkowitz. "Modeling and Testing Fossil-Fueled Generating Units," Proceedings of the Second Power Plant Dynamics, Control and Testing Symposium, Knoxville, Tennessee, 1975, paper No. 6.

103. Nikravesh, K.Y., and R.G. Hoft. "Lyapunov Stability Analysis of Thyristor Inverter System," IEEE Transactions on Industry Applications, Vol. IA-11, No. 2, March/April, 1975, pp. 158-164.

104. Ogata, K. Modern Control Engineering. Englewood Cliffs, New Jersey: Prentice-Hall, Inc., 1970.

105. Oliver, D.A., and P.H. Byer. "Physical and Economic Models of Open Cycle Coal Burning MHD Power Generation System," Gas Turbine Laboratory, MIT, GTL Report No. 107, June, 1972.

106. _____. "The Time Dependent Magnetohydrodynamic Generator," Proceedings of the 14th Symposium on Engineering Aspects of MHD, 1974, pp. V.5.1-V.5.9.

107. Park, C.U., and C.J. Herget. "Parameter Identification of Low Order Boiler Models for Dynamic Stability Analysis," Proceedings of the Second Power Plant Dynamics, Control and Testing Symposium, Knoxville, Tennessee, 1975, paper No. 19.

108. _____. "Fast Turbine Valving," IEEE Transactions on Power Apparatus and Systems, Vol. PAS-92, No. 3, May/June, 1973, pp. 1065-1073.

109. Paynter, H.M., and Y. Takahashi. "A New Method of Evaluating Dynamic Response of Counterflow and Parallel-flow Heat Exchangers," ASME Transactions, Vol. 78, May, 1956, pp. 749-758.

110. _____. "Thermofluid Process Dynamics in Boiler Modeling," Proceedings of the Seminar on Boiler Modeling. D.A. Berkowitz (ed.). Bedford, Massachusetts: The MITRE Corporation, October, 1975, pp. 143-168.

111. Peterson, D.W., and F.C. Schweppe. "Code for a General Purpose System Identifier and Evaluator (GPSIE)," IEEE Transactions on Automatic Control, Vol. AC-19, No. 6, December, 1974, pp. 852-854.

112. Pierre, D.A. Optimization Theory With Applications. New York: John Wiley and Sons, 1969.

113. _____. "PROPOSAL FOR CONTINUATION OF Task HIII Cycle Analysis and Control Under Contract E(49-18)-1811," submitted to the Energy Research and Development Administration by the Montana Energy and MHD Research and Development Institute, Inc., Box 3809, Butte, Montana 59701, February, 1976.

114. _____, C.H. Dudding, and D.J. Miller. "Polynomial Approximation for MHD CNCD," ERL Report No. 1276, Montana State University, Bozeman, June, 1976.

115. Pinnello, J.A., and J.E. Van Ness. "Dynamic Response of a Large Power System to a Cyclic Load Produced by a Nuclear Accelerator," IEEE Transactions on Power Apparatus and Systems, Vol. PAS-90, No. 6, July/August, 1971, pp. 1856-1862.

116. Profos, P. "Dynamics of Pressure and Combustion Control in Steam Generators," Combustion, Vol. 28, No. 9, March, 1957, pp. 34-44.

117. _____. "Dynamics of Superheater Control," Combustion, Vol. 31, October, 1959, pp. 34-43. (Reprinted from Sulzer Tech. Rev., April, 1958.)

118. Quazza, G., and E. Ferrari. "Role of Power Station Control in Overall System Operation," in Real-Time Control of Electric Power Systems. E. Handschin (ed.). New York: Elsevier Publishing Co., 1972, pp. 215-257.

119. Raven, F.H. Automatic Control Engineering. New York: McGraw-Hill Book Co., 1968.

120. Robles, T.C. "A Simulation Approach to a Magnetohydrodynamic-steam Electrical Power Generation System," Ph.D. Thesis, Montana State University, Bozeman, August, 1975.

121. Rosa, R.J. Magnetohydrodynamic Energy Conversion. New York: McGraw-Hill Book Co., 1968.

122. Schmidt, J.R., and D.R. Clark. "Analog Simulation Technique for Modeling Parallel-Flow Heat Exchangers," IEEE Transactions on Power Apparatus and Systems, Vol. PAS-87, No. 5, May, 1968, pp. 1300-1305.

123. Schultz, D.G., and J.L. Melsa. State Functions and Linear Control Systems. New York: McGraw-Hill Book Co., 1967.

124. Schultz, M.A. Control of Nuclear Reactors and Power Plants. New York: McGraw-Hill Book Co., 1955.

125. Schweppe, F.C. "Fitting Nonlinear Dynamic Models to Observations," Proceedings of the Seminar on Boiler Modeling. D.A. Berkowitz (ed.). Bedford, Massachusetts: The MITRE Corporation, October, 1975, pp. 91-101.

126. Scutt, E.D. "An Integrated Combustion Control System for Once-Through Boilers," Proceedings of the American Power Conference, Vol. XXI, 1959, pp. 274-283.

127. Speedy, C.B., R.D. Bell, and G.C. Goodwin. "Dynamic Modelling of a Steam Generator Using Least Squares Analysis," Joint Automatic Control Conference Proceedings, paper 16-B, 1970, pp. 365-372.

128. Stagg, G.W., and A.H. El-Abiad. Computer Methods in Power System Analysis. New York: McGraw-Hill Book Co., 1968.

129. Stevens, W.M., F.P. deMello, and D.N. Ewart. "Simulation as a Design Tool for Plant Jack McDorough Boiler Controls," 7th National Power Instrumentation Symposium, ISA, Denver, Colorado, May 18-20, 1964.

130. Sutton, G.W., and A. Sherman. Engineering Magnetohydrodynamics. New York: McGraw-Hill Book Co., 1965.

131. Takahashi, Y., M.J. Rabins, and D.M. Auslander. Control and Dynamic Systems. Reading, Massachusetts: Addison-Wesley Publishing Co., 1970.

132. Takano, K., T. Homma, and Y. Mori. "Simulation Study on Generators for the MHD Pilot Plant," Proceedings of the 6th International Conference on Magnetohydrodynamics Electrical Power Generation, Vol. I, Open Cycle, Generators and Systems, Washington, DC, June 9-13, 1975, pp. 287-300.

133. Thal-Larsen, H. "Dynamics of Heat Exchangers and Their Models," ASME Transactions, Vol. 82, ser. D, June, 1960, pp. 489-504.

134. _____, and W.V. Luscutoff. "Fluid-Temperature Transients in a Dual-Heat-Exchanger System," ASME Journal of Basic Engineering, Vol. 86, March, 1964, pp. 23-31.

135. Thompson, F.T. "A Dynamic Model of a Drum-Type Boiler System," IEEE Transactions on Power Apparatus and Systems, Vol. PAS-86, No. 5, May, 1967, pp. 625-635.

136. Townes, H.W., T.C. Reihman, and C. Moser. "Task E: Slag Flow and $NO_x$ Kinetics," Quarterly Report IV, Montana State University MHD Program of the Montana Energy and MHD Research and Development Institute, Inc., under Contract No. E(49-18)-1811, Energy Research and Development Administration, for Period January 1, 1976 to March 31, 1976.

137. Tsu, T.C., W.E. Young, and S. Way. "Optimization Studies of MHD-Steam Plants," Electricity from MHD, Vol. IV, IAEA and ENEA, Salzburg, Austria, July, 1966, pp. 899-911.

138. Undrill, J.M., and T.F. Laskowski. "Interactive Dynamic Simulation by Digital Computer," ISA Transactions, Vol. 14, No. 1, 1975, pp. 33-40.

139. Watson, W., and G. Manchur. "Experience with Supplementing Damping Signals for Generator Static Excitation Systems," IEEE Transactions on Power Apparatus and Systems, Vol. PAS-92, No. 1, January/February, 1973, pp. 199-203.

140. Watts, R.G., and R.J. Schoenhals. "Feedback Control Optimization of a Single Fluid Heat Exchanger," ASME Publication 66-WA/HT-56, 1966.

141. Womack, G.J., and J.B. Heywood. "Introduction," in Open Cycle M.H.D. Power Generation. J.B. Heywood and G.J. Womack (eds.). Oxford: Pergamon Press, 1969, pp. 1-17.

142. _____. "Types of Air Heater," in Open Cycle M.H.D. Power Generation. J.B. Heywood and G.J. Womack (eds.). Oxford: Pergamon Press, 1969, pp. 19-28.

143. Workman, K.H., and H.D. Vollmer, Jr. "Frequency Response Tests on W.H. Sammis Plant No. 6 Unit," IEEE Transactions on Power Apparatus and Systems, Vol. PAS-90, No. 4, July/August, 1971, pp. 1734-1738.

144. Yahalom, R. "On the Application of the Fundamental Conservation Equations to Steam Generator Dynamic Modeling," Proceedings of the Second Power Plant Dynamics, Control and Testing Symposium, Knoxville, Tennessee, 1975, paper No. 2.

145. Yoshie, M. "Variable Pressure Operating System of Steam Power Plant Optimized by Computer," Proceedings of the 5th World Congress (IFAC), Paris, June 12-17, 1972, paper No. 5.1.

146. Young, C.C. "Equipment and System Modeling for Large-Scale Stability Studies," IEEE Transactions on Power Apparatus and Systems, Vol. PAS-91, No. 1, January/February, 1972, pp. 99-109.

147. U.S. Energy Research and Development Administration."MAGNETO-HYDRODYNAMICS, power generation and theory--a bibliography," Publication TID-3356, National Technical Information Service, U.S. Department of Commerce, Springfield, VA 22161, November, 1975.

HH 7881 - 7801

MONTANA STATE UNIVERSITY LIBRARIES
3 1762 10005119 0

D378
As67
cop.2

Aspnes, John D
Magnetohydrodynamic/steam system dynamic modeling and control

DATE | ISSUED TO
INTERLIBRARY LOAN
INTERLIBRARY LOAN
INTERLIBRARY LOAN
MAR 23 '83
D378
As67
cop 2